LISTEN GoMex: 2010-2021

Long-term Investigations into Soundscapes, Trends, Ecosystems, and Noise in the Gulf of Mexico

Report Authors:

Macey A. Rafter[1], Kaitlin E. Frasier[1], Melissa S. Soldevilla[2], Lynne Hodge[2], Héloïse Frouin-Mouy[2], Itzel Pérez Carballo[3]

LISTEN GoMex Team:

Melissa S. Soldevilla[2], Kaitlin E. Frasier[1], Héloïse Frouin-Mouy[2], Adolfo Gracia Gasca [4], Lance P. Garrison[1], John A. Hildebrand[1], Lynne Hodge[2], Matthieu Le Henaff[5], Joel Ortega Ortiz[5], Itzel Pérez Carballo[3], Macey A. Rafter[1], Arturo Serrano Solis[3], Carrie Wall-Bell[6]

[1]Scripps Institution of Oceanography, University of California San Diego

[2]NOAA NMFS Southeast Fisheries Science Center

[3]Universidad Veracruzana

[4]Instituto de Ciencias del Mar y Limnología, UNAM

[5]Cooperative Institute for Marine and Atmospheric Studies, University of Miami

[6]University of Colorado Boulder and NOAA National Centers for Environmental Information

December 22, 2022

Suggested Citation

Rafter, M.R., Frasier K.E., Soldevilla, M.S., Hodge, L., Frouin-Mouy H., Pérez Carballo, I. (2022) LISTEN GoMex: 2010-2021 - Long-term Investigations into Soundscapes, Trends, Ecosystems, and Noise in the Gulf of Mexico. Marine Physical Laboratory, Scripps Institution of Oceanography, University of California San Diego, La Jolla, CA. MPL Technical Memorandum #662.

Table of Contents

1 Executive Summary

In 2010, the *Deepwater Horizon* (DWH) oil spill had unprecedented impacts on the Gulf of Mexico ecosystem, including the twenty cetacean species inhabiting the oceanic waters of this semi-enclosed large marine ecosystem. Due to the impacts from DWH oil, restoration projects focused on oceanic cetaceans are being enacted in the Gulf, which require basic information on species' spatiotemporal density patterns, Gulf-wide movement patterns, Gulf-wide population sizes, long-term abundance trends, and species' responses to oceanographic and anthropogenic processes, along with information on Gulf-wide ambient noise levels and the contributions from anthropogenic noise sources. To address these needs, NOAA's Southeast Fisheries Science Center (SEFSC), UCSD's Scripps Institution of Oceanography (SIO), and partners initiated a comprehensive, long-term, multi-scale passive acoustic monitoring program throughout US and Mexican Gulf waters over the 2020 – 2025 period to collect data needed to develop predictive habitat models to assess the processes driving seasonal, interannual, and decadal trends in spatial distribution, density, and abundance of oceanic cetaceans and to assess contributions of ambient noise sources to the Gulf soundscape. This collaborative study annually deploys moored HARPs instruments, continuously recording over the 10-100 kHz band, over the 5-year period at a total of A) 8 five-year long-term sites to identify temporal trends and variability at reference sites over the study period, B) 20 one-year short-term sites over a broad area of the Gulf to capture spatial trends and variability in cetacean density and environmental processes, C) 3 six-month sites with targeted sampling using tracking arrays to obtain acoustic behavior data for density estimation, and D) 2 or more 1-year sites focused on areas of importance to the DWH Restoration noise reduction project. Additionally, the study leverages 10 years of historic HARP recordings at 5 long-term sites, collected by SIO as part of the DWH damage assessment to enhance the assessment of trends in cetacean density and noise.

This report compiles the preliminary results from ten years of HARP recordings at 5 historic sites, over the 2010-2020 period, and from the first year of HARP recordings at 13 sites collected under the LISTEN Gulf of Mexico (GoMex) project over the 2020-2021 period. The historic recordings come from HARPs deployed at five offshore long-term sites named for nearby oceanographic features: Main Pass (site MP) at seafloor 80 m depth, De Soto Canyon (site DC) at 250 m depth, Dry Tortugas (site DT) at 1200 m depth, Green Canyon (site GC) at 1100 m depth, and Mississippi Canyon (site MC) at 1200 m depth. Recordings from the first year of the LISTEN GoMex study include four of the historic long-term sites (DC, DT, GC, and MC), four new long-term sites (Alaminos Canyon (site AC) at 1100 m depth, Loop Current (site LC) at 3200 m depth, Mexican Ridges (site MR) at 1100 m depth, and Campeche Escarpment(site CE) at 2100 m depth), three short-term sites (site Y1B at 3330 m depth, site Y1C at 2900 m depth, and site Y1D at 550 m depth), and two short-term noise sites (Galveston (site GA) at site 215 m depth and Southern Louisiana (site SL) at 220 m depth).

Data analysis primarily consisted of automated detection and classification of marine mammal echolocation signals and anthropogenic noise. Data analyses for specific sound sources were conducted in at least one of three frequency bands: low-frequency (10 - 1,000 Hz), mid-frequency (10 - 5,000 Hz), and high-frequency (1 - 100 kHz). Ambient soundscape and seismic airgun analyses were conducted in the low-frequency band. Marine mammal and ship noise sound analyses were conducted in the mid-frequency and high-frequency bands. Analyses for low frequency marine mammal vocalizations, such as those expected from mysticete whales, are on-going and are not included in this report.

Echolocation clicks from six acoustically-identifiable odontocete species / groups were detected: Cuvier's beaked whale, Gervais' beaked whale, Blainville's beaked whale, sperm whales, *Kogia* spp., and Risso's dolphins. Three click categories that are not yet assigned to a species, but are presumed to be associated with various delphinids, were also detected. Detections of Cuvier's beaked whales occurred at all deep sites but were highest at site CE. Gervais' beaked whale densities were highest at historic sites GC and MC, as well as Loop Current-dominated sites LC and Y1B. Blainville's beaked whales were not historically common at northern sites, but a new potential hotspot was identified in the southern GoMex at the 1-year Y1C site. Sperm whales were consistently detected at all sites, but densities were highest at the historic MC and GC sites, and at a new potential hotspot identified within the Mexican Ridges region (site MR). *Kogia* spp. densities were highest at site Y1D. Risso's dolphin occurrence was strongly seasonal, but seasonal peaks differed between sites, and densities were higher at eastern sites. Most delphinid detections were primarily nocturnal; however, distinctive frequency-banded unidentified delphinid type (UD 3P) exhibited a crepuscular pattern at the West Florida Shelf sites (DC and Y1D), and daytime detections were common at the shallow sites MP and DC. Further, snapping shrimp signals, identified during odontocete click classification analyses, exhibited episodic periods of high activity at the shallow historic Main Pass and De Soto Canyon sites (MP and DC).

The low-frequency ambient soundscape, between 10-1000 Hz, was dominated by sounds from anthropogenic activities: seismic exploration at deep sites, and shipping at shallow sites. Seismic survey signals dominated the ambient soundscape below 100 Hz throughout the historic time series and at the new 2020-2021 sites, with the same surveys detected simultaneously at distant sites throughout the Gulf. Ambient sound levels were lowest at site DC, within the Rice's whale core habitat. Unsurprisingly, ship noise dominated the ambient soundscapes at the two shipping lane sites (GA and SL), where the highest number of ship detections and longest time with ship noise present occurred. At sites outside of the shipping lanes, vessel transit detections and time present were high at Alaminos Canyon (near ports of Corpus Christi and Houston), Mexican Ridges (near the Port of Tampico), and site Y1B.

2 Introduction

2.1 Project Background

In 2010, the *Deepwater Horizon* (DWH) oil spill had unprecedented impacts on the Gulf of Mexico ecosystem, including the twenty cetacean species inhabiting the oceanic waters of this semi-enclosed large marine ecosystem. Due to the impacts from DWH oil, science and restoration projects focused on oceanic cetaceans are being enacted in the Gulf to enhance their conservation and recovery, including one focused on reducing impacts of noise on marine mammals. These science and restoration projects require basic information on species' spatio-temporal density patterns, Gulf-wide movement patterns, Gulf-wide population sizes, long-term abundance trends, and species' responses to oceanographic and anthropogenic processes, along with information on Gulf-wide ambient noise levels and the contributions from anthropogenic noise sources.

To address these needs, NOAA's Southeast Fisheries Science Center (SEFSC), UCSD's Scripps Institution of Oceanography (SIO), and partners initiated the LISTEN GoMex project, a comprehensive, long-term, multi-scale passive acoustic monitoring program throughout US and Mexican Gulf waters. The LISTEN GoMex project combines several collaborative projects including:

- *"Assessing Long-term Trends and Processes Driving Variability in Cetacean Density throughout the Gulf of Mexico using Passive Acoustic Monitoring and Habitat Modeling"*, funded by the RESTORE Science Program to improve our understanding of where and when cetaceans occur throughout the Gulf and how and why that is changing over time.
- *"Reduce Impacts of Anthropogenic Noise on Cetaceans"*, a restoration project funded by the *Deepwater Horizon* Restoration Open Ocean Marine Mammal Trustee Implementation Group to improve understanding of how noise-producing human activities affect the Gulf soundscape and cetaceans, and to work with industry partners to reduce human-produced noise impacts on cetaceans.
- *"Environmental Characterization using Ambient Seismic Sources"*, funded by the US Navy Task Force Ocean to improve understanding of how we can use opportunistic sound sources to characterize the inner structure of the ocean, for example, deep Loop Current features.

To meet these objectives, the Gulf-wide passive acoustic monitoring program is being implemented over the 2020 – 2025 period to collect data needed to develop predictive habitat models to assess the processes driving seasonal, interannual, and decadal trends in spatial distribution, density, and abundance of oceanic cetaceans and to assess contributions of ambient noise sources to the Gulf soundscape. The collaborative, multi-scale study annually deploys moored High-frequency Acoustic Recording Package (HARP) instruments over the 5-year period at a total of A) 8 five-year long-term sites to identify temporal trends and variability at reference sites over the study period, B) 20 one-year short-term sites over a broad area of the Gulf to capture spatial trends and variability in cetacean density and environmental processes, C) 3 six-month sites with targeted sampling using tracking arrays to obtain acoustic behavior data for density estimation, and D) 2 or more 1-year sites focused on areas of importance to the DWH Restoration noise reduction project. Additionally, the study leverages 10 years of historic HARP recordings at 5 long-term sites, collected by SIO as part of the DWH damage assessment to enhance the assessment of trends in cetacean density and noise.

This report compiles the preliminary results from ten years of HARP recordings at 5 historic sites, over the 2010-2020 period, and from the first year of HARP recordings at 13 sites collected under the LISTEN GoMex project over the 2020-2021 period. The historic recordings come from HARPs deployed at five offshore long-term sites named for nearby oceanographic features: Main Pass (site MP) at 80 m seafloor depth, De Soto Canyon (site DC) located within the Rice's whale core habitat at 260 m depth, Dry Tortugas (site DT) at 1200 m depth, Green Canyon (site GC) at 1100 m depth, and Mississippi Canyon (site MC) at 1200 m depth (Figure 1, Table 2). Recordings from the first year of the LISTEN GoMex study include four of the historic long-term sites (DC, DT, GC, and MC), four new long-term sites (Alaminos Canyon (site AC) at 1100 m depth, Loop Current (site LC) at 3200 m depth, Mexican Ridges (site MR) at 1100 m depth, and Campeche Escarpment (site CE) at 2100 m depth), three short-term sites (site Y1B at 3330 m depth, site Y1C at 2900 m depth, and site Y1D at 550 m depth), and two short-term noise sites Galveston (site GA) at site 215 m depth and Southern Louisiana (site SL) at 220 m depth) (Figure 1). These sites are all located in oceanic Gulf waters beyond the continental shelf (>200 m depths with the exception of MP) in the US and Mexico.

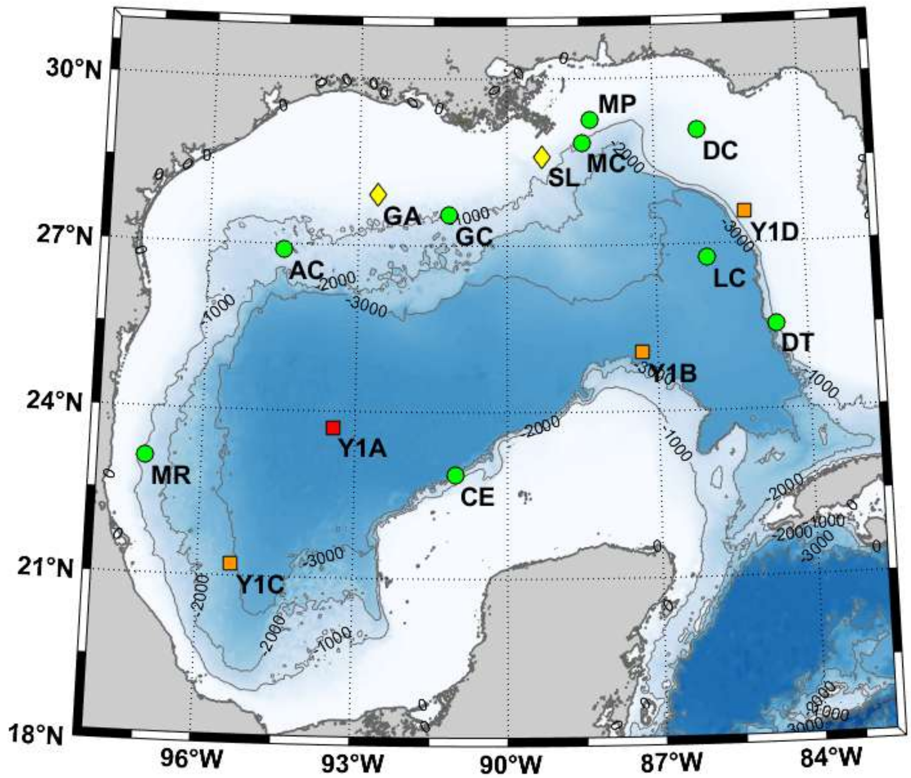

Figure 1: Location of the High-Frequency Acoustic Recording Packages (HARPs) and Mid-Acoustic Frequency Recording Packages (MARPs). Green circles represent multi-year HARP sites, orange squares represent single-year HARP sites, yellow diamonds represent MARP sites and the red square represents sites where there was no effort due to data quality issues.

2.2 High Level Data Description

High-frequency Acoustic Recording Packages (HARPs) are autonomous underwater acoustic recording devices that, dependent on configuration, can record sounds over a bandwidth from 10 Hz up to 160 kHz and are capable of approximately one year of continuous recording. 20 to September 2021 period (Table 2, Figures 1, 2). Of the 16 HARPs deployed over this period, 12 were deployed to record signals from all marine mammal species, anthropogenic sound sources, and ambient soundscapes, 2 were deployed to focus on ambient soundscapes and anthropogenic sound sources, and 2 were deployed as part of an array for marine mammal tracking. During all historic recordings and at 12 of the new sites, the HARPs were set to record continuously at a sampling rate of 200 kHz, sufficient to record sounds from all sources of interest. At the two soundscape sites (GA and SL), the HARPs were set to record continuously at a sample rate of 20 kHz, sufficient to record anthropogenic noise sources of interest, and are referred to as Mid-frequency Acoustic Recording Packages (MARPs). At one of the 12 sites (MC), two additional 4-ch HARPs deployed as part of a 3-unit tracking array, were set to record continuously at 100 kHz, sufficient to record most sounds from odontocetes and all lower frequency sounds.

The HARPs at sites with seafloor depths less than 1200 m were deployed in small mooring configurations with the hydrophones suspended approximately 20 m above the seafloor. At sites with seafloor depths greater than 1200 m, deep mooring configurations were used, with the hydrophones buoyed to approximately 1000 m depth. Each HARP hydrophone was calibrated in the laboratory to allow for quantitative analysis of the received sound field. Representative data loggers and hydrophones have also been calibrated at the Navy's TRANSDEC facility to verify the laboratory calibrations (Wiggins and Hildebrand 2007).

Of the 16 HARPs deployed over the August 2020-2021 period, 13 HARPs were successfully recovered with high-quality data recordings (Table 2). Two HARPs did not record data successfully: 1) the HARP at Y1A exhibited internal corrosion issues that prevented recovery of recordings, and 2) the second 4-Ch HARP at MC did not wake up to start recording the following deployment due to an unexpected restart. Finally, one of the HARPS, the standard 200 kHz HARP at MC, is presumed to have become entangled upon release and is awaiting recovery.

Site	Deployment	Start Date	End Date	Recording Duration (Days)
AC	01	8/29/2020	9/5/2021	372
CE	01	9/2/2021	9/1/2022	365
DC	02	10/21/2010	2/6/2011	108
DC	03	3/21/2011	7/6/2011	106
DC	04	10/26/2011	3/2/2012	128

DC	05	3/3/2012	12/9/2012	277
DC	06	12/9/2012	9/25/2013	144
DC	07	12/18/2013	7/27/2014	217
DC	08	10/3/2014	5/25/2015	235
DC	09	8/3/2015	5/19/2016	144
DC	10	8/25/2016	7/18/2017	326
DC	11	7/17/2017	6/9/2018	327
DC	12	11/11/2018	11/25/2018	11
DC	13	8/15/2020	8/23/2021	108
DT	01	8/9/2010	10/26/2010	79
DT	02	3/4/2011	6/24/2011	111
DT	03	7/13/2011	11/14/2011	124
DT	04	12/14/2011	1/9/2012	26
DT	05	5/27/2012	12/7/2012	195
DT	06	12/7/2012	8/18/2013	253
DT	07	11/1/2013	8/17/2014	289
DT	08	9/28/2014	7/15/2015	289
DT	09	8/2/2015	3/15/2016	226
DT	10	6/22/2016	7/18/2017	391
DT	11	7/17/2017	6/27/2018	345
DT	12	10/19/2018	1/26/2020	465
DT	13	8/17/2020	8/27/2021	374
GA	01	8/30/2020	9/6/2021	373
GC	01	7/15/2010	10/11/2010	84
GC	02	11/8/2010	2/2/2011	86
GC	03	3/23/2011	8/8/2011	138
GC	04	9/23/2011	2/17/2012	118
GC	05	2/28/2012	12/12/2012	288
GC	06	12/13/2012	9/10/2013	267
GC	07	1/13/2014	9/29/2014	252
GC	08	10/19/2014	6/10/2015	198
GC	09	8/7/2015	5/23/2016	289
GC	10	7/20/2016	5/17/2017	301
GC	11	5/16/2017	5/1/2018	349
GC	12	9/30/2018	12/26/2019	448

GC	13	8/12/2020	8/20/2021	373
LC	01	8/16/2020	8/24/2021	372
MC	01	5/16/2010	8/28/2010	104
MC	02	9/7/2010	12/19/2010	103
MC	03	12/20/2010	3/21/2011	91
MC	04	3/22/2011	8/15/2011	146
MC	05	9/22/2011	2/21/2012	152
MC	06	2/28/2012	12/11/2012	288
MC	07	12/11/2012	8/3/2013	235
MC	08	1/9/2014	1/21/2014	12
MC	09	4/23/2014	9/28/2014	159
MC	10	9/29/2014	7/15/2015	289
MC	11	8/7/2015	3/11/2016	217
MC	12	7/20/2016	5/16/2017	299
MC	13	5/17/2017	3/14/2018	301
MC	14	11/11/2018	3/15/2020	489
MC	15*	8/13/2020	–	–
MC	15_01_C4	8/13/2020	2/28/2021	199
MC	15_02_C4*	8/13/2020	–	–
MP	01	7/4/2010	9/25/2010	83
MP	02	11/7/2010	2/19/2011	100
MP	03	3/23/2011	9/6/2011	167
MP	04	9/22/2011	3/1/2012	161
MP	05	2/29/2012	11/24/2012	270
MP	06	12/10/2012	9/25/2013	289
MP	08	10/2/2014	5/7/2015	217
MP	09	8/9/2015	5/4/2016	269
MP	10*	7/19/2016	5/17/2017	301
MP	11	5/17/2017	5/29/2018	377
MP	12	11/11/2018	4/2/2020	507
MR	01	9/7/2020	9/4/2021	362
SL	01	8/13/2020	8/21/2021	374
Y1	Y1A_01*	–	–	–
Y1	Y1B_01	8/21/2020	8/26/2021	370

Y1	Y1C_01	9/5/2020	9/3/2021	363
Y1	Y1D_01	8/15/2020	8/23/2021	373
			Total Days	17,264
			Total Years	47.30

Table 2: Dates and durations of HARP deployments spanning from 2010-2021. Deployments with a (*) denote deployments with hardware issues or are still deployed resulting in incomplete data (see text for more information).

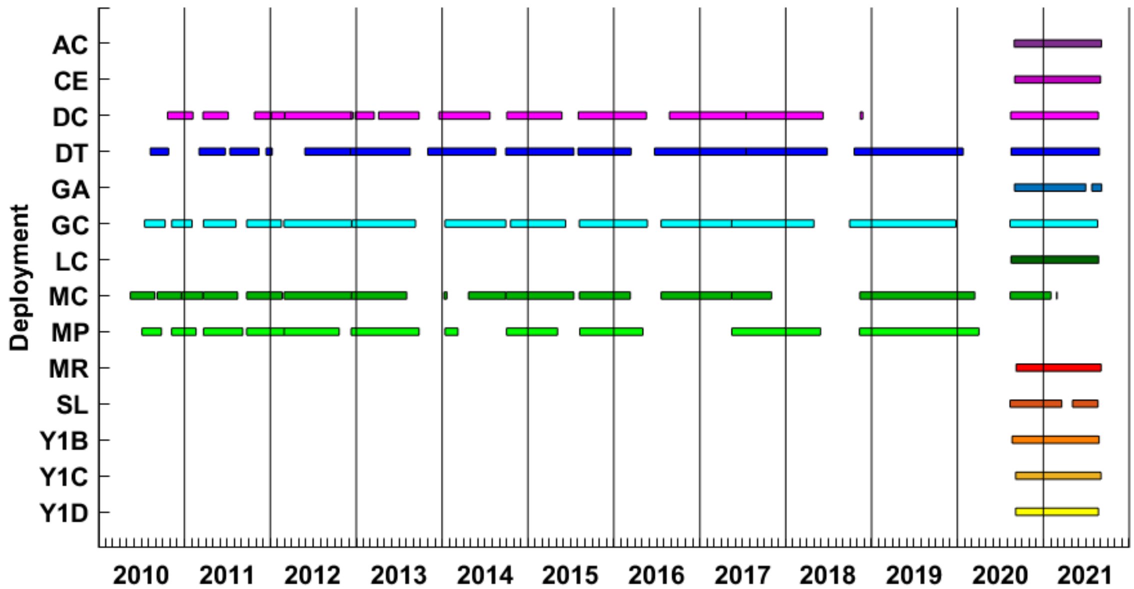

Figure 2: Recording effort for Gulf of Mexico sites from 2010-2021. Data collection is ongoing.

3 Data Analysis

The data analysis process is described below in terms of the major classes of odontocete vocalizations, anthropogenic sounds, and low-frequency ambient soundscape in the Gulf of Mexico region, and the procedures used to detect and characterize them. Analysis of the low-frequency band for baleen whale calls is ongoing and is not included in this report.

We summarize and characterize sounds detected at all the sites across the Gulf of Mexico. Weekly estimated density was calculated for each species or species group where appropriate. Weekly occurrence is reported for non-biological signals. Diel, seasonal and interannual patterns for the occurrence of various signals are reported for each monitoring site and compared across sites. Vessel noise analyses detail vessel categories and sound levels. Low frequency ambient noise dominated by anthropogenic sound sources is compared across sites.

3.1 Odontocete Analyses

3.1.1 Click Classification

Odontocete sounds can be categorized as echolocation clicks, burst pulses, or whistles. Echolocation clicks are broadband impulses with peak energy between 1 and 150 kHz, dependent upon the species. Buzz or burst pulses are rapidly repeated clicks that have a creak or buzz-like sound quality; they are generally lower in frequency than echolocation clicks. Dolphin whistles are tonal calls predominantly between 1 and 20 kHz that vary in frequency content, their degree of frequency modulation, as well as duration. These signals are easily detectable in an LTSA as well as the spectrogram. Analyses in this report focus only on echolocation clicks as a proxy for odontocete presence because they are currently the most promising call type for species classification in the region. Future analysis might identify distinguishing whistle or burst pulse characteristics.

Odontocete echolocation clicks were detected automatically using an energy detector with a minimum received level threshold of 120 dBpp re: 1 μPa (Roch et al. 2011; Frasier et al. 2016). To classify detected clicks to putative taxonomic groups, dominant click types and false positive categories at these sites were identified using automated unsupervised clustering methods (Frasier 2021). Detections were clustered within successive five-minute windows and dominant click types were identified in each window using spectral features, inter-click interval, and waveform envelope. Regular clicks were the focus of this analysis, therefore clicks with an ICI less than 0.001 sec were excluded from this analysis to limit the inclusion of buzz clicks. An automated clustering algorithm was then used to identify recurrent types based on spectral features and inter-click interval (ICI) distributions at each site (Frasier et al. 2017). Common click types were manually aggregated across all of the sites in the Gulf of Mexico to form classifier training and testing sets for 13 signal types including 9 odontocete signals and 4 sources of false positives. Click types were attributed to a specific species if acoustically identifiable (e.g. beaked whales and Risso's dolphin) or assigned an unidentified category if the species was unknown. A deep neural network was trained to classify these signal types with 98 percent classification accuracy on a balanced test set. This trained network was used to classify all five-minute windows across all sites. Classifications were retained if classification probability exceeded 85 percent and the classified bin contained at least 5 clicks. Classifier confusion was evaluated manually using a subset of the recordings from the historic data set (sites MC, GC, DT & DC) from 2010-2019 (Table 3). An analyst manually annotated 3% of all hours for estimation of species-specific error rates (ER), based on the occurrence of false positive (FP), false negative (FN), true positives (TP) and true negative (TN) detections of each species, computed as:

$$ER = (FP + FN)/(FN + FP + TP + TN) \tag{1}$$

Odontocete detectors were not run on the 2020-2021 MC_15 4-channel or GA & SL MARP datasets since the recording bandwidth was not sufficient.

3.1.2 Click Classification: Main Pass

The historic site at Main Pass, which was discontinued under the LISTEN GoMex program, is the only site situated on the continental shelf and is the shallowest of all of the sites (90 m bottom depth). Detection methodologies were the same as above, however, the species present on the continental shelf differ from those in Gulf oceanic waters. Classifier training was conducted separately and included fewer signal types. Common click types were manually aggregated across all ten years of data to form classification training and testing sets for 4 dominant signal types (unidentified delphinids, snapping shrimp, boats, and noise). Further, labels from this site were fully manually reviewed and corrected where appropriate by an expert analyst, therefore classification error rates are assumed to be negligible at the level of 5-minute windows. The acoustic encounters were manually reviewed using comparative panels in the custom MATLAB-based program called *DetEdit* (Solsona-Berga et al. 2020). *DetEdit* presents panels of long-term spectral averages, received level, and ICI of individual clicks over time, as well as spectral and waveform plots of selected individual signals along with comparative overlays of average waveforms, spectra, and ICIs for the dominant signal types. Within each encounter, false detections were manually removed when the spectral amplitude, ICI, or waveform of the detections were inappropriate for the identified sonar, snapping shrimp or delphinid signal category.

3.1.3 Density Estimation

Point-transect-based density estimation methods were used to convert presence in 5-minute windows into weekly estimates of marine mammal densities at each site for each putative marine mammal taxonomic class. For each class and site combination, the probability of detecting a group of animals in a five-minute time window was estimated using a Monte Carlo simulation, taking into account minimum detection thresholds, echolocation click frequency content and signal attenuation, taxon-specific dive depths and vocalization rates, and local oceanographic conditions. Weekly animal densities were computed following Marques et al. (2009) for group counting, using previously-published parameter estimates for beaked whales (Hildebrand et al. 2015), sperm whales (Solsona Berga 2019), delphinids (Frasier 2015), and *Kogia* spp. (Hildebrand et al. 2019). This study used a different minimum received level threshold than that used in previously published studies. All models were therefore re-evaluated for this project with a consistent minimum received level (125 dB peak-to-peak) for all species (Table 4). Climatological mean sound speed profiles for the month of January were extracted from the Generalized Digital Environment Model (GDEM v 3.0) and used for frequency-dependent propagation loss estimation at each site. Summer sound speed profiles estimates were tested but not significantly different for these species in deeper (>100 m) waters. The goal of our analysis is estimation of animal densities from the passive acoustic monitoring data. Our basic assumption is that the acoustic detections for each species at each site give a measure of the relative density over time. The analysis was conducted for each HARP site, and to provide sufficient data for each density estimate, the data were averaged over weekly time intervals.

	Site			
Species	**MC**	**GC**	**DT**	**DC**
Sperm whale	5.31%	2.73%	1.77%	0.02%
Cuvier’s beaked whale	0.08%	0.07%	0.81%	N/A
Gervais’ beaked whale	0.01%	0.01%	0.01%	N/A
Blainville’s beaked whale	0.08%	0.09%	0.36%	N/A
Risso’s dolphins	0.76%	0.39%	1.74%	0.34%
Other delphinids (All)	3.04%	3.42%	4.66%	4.62%
Kogia spp.	0.09%	0.18%	0.08%	0.18%

Table 3: Error rates for each species for each site based on manual review of 3% of hours of data sampled across the historic dataset (2010-2019). Error rates for other delphinids represent all three groups of unidentified delphinids. Individual confusion statistics and error rates for the various delphinid categories will be computed once final categories have been defined in future reports.

Site	Sperm whale	Cuvier's BW	Gervais' BW	Blainville's BW	Risso's dolphin	Unid. delphinid	*Kogia* spp.
AC	59.2 (3.8)	29.8 (2.5)	22.7 (1.9)	23.8 (2.2)	19.6 (4.4)	8.1 (2.4)	20.8 (2.1)
CE	52.2 (3.7)	28.4 (2.5)	21.3 (2.1)	21.7 (2.2)	20.0 (4.2)	8.7 (2.8)	22.2 (2.1)
DC	–	–	–	–	19.6 (2.4)	12.5 (2.4)	–
DT	38.7 (3.3)	29.3 (2.3)	22.4 (2.0)	23.5 (2.3)	20.8 (4.5)	8.4 (2.5)	19.4 (2.3)
GC	43.6 (2.7)	29.4 (2.4)	22.5 (2.0)	23.5 (2.2)	20.9 (4.4)	8.4 (2.5)	19.5 (2.0)
LC	58.4 (5.2)	29.4 (2.3)	22.4 (2.1)	23.4 (2.2)	19.0 (4.1)	7.7 (2.4)	19.5 (2.2)
MC	37.7 (2.1)	29.7 (2.3)	22.6 (2.0)	23.7 (2.2)	20.9 (4.4)	9.2 (2.6)	23.3 (1.9)
MR	47.1 (2.7)	30.2 (2.4)	23.1 (2.0)	24.3 (2.2)	20.3 (4.4)	8.0 (2.4)	20.6 (2.1)
Y1B	56.7 (4.9)	29.4 (2.5)	22.1 (2.0)	22.4 (2.2)	19.2 (4.1)	7.1 (2.2)	19.5 (2.1)
Y1C	56.9 (5.3)	29.4 (2.3)	22.3 (2.0)	23.1 (2.2)	19.0 (4.5)	7.7 (2.3)	19.5 (2.4)
Y1D	56.7 (4.9)	29.4 (2.5)	22.5 (2.0)	23.4 (2.2)	20.7 (3.7)	10.7 (2.5)	23.3 (1.9)

Table 4: Detection probability by species computed based on species-specific Monte Carlo simulations within a defined maximum detection radius (Pm: 20 km, Beaked whales: 3 km, Dolphins: 5 km, *Kogia*: 1 km).

3.2 Odontocete Species Call Descriptions

A description of the identifying features of each species' call types and identified noise sources follows. For all species and noise source descriptions, the following figures are presented, from top to bottom, and left to right, representing 1) a long-term average spectrogram of an acoustic encounter over 1 hour, 2) a standard spectrogram of acoustic signals over 5 minutes, 3) the average spectrum of an acoustic signal type with associated variance, 4) a histogram of average ICIs for an acoustic signal type, and 5) the envelope of the signal waveform.

List of species found in the Gulf of Mexico:

- Rice's whale (*Balaenoptera ricei*) (ESA-Listed)
- Sperm whale (*Physeter macrocephalus*) (ESA-Listed)
- Dwarf sperm whale (*Kogia sima*)
- Pygmy sperm whale (*Kogia breviceps*)
- Cuvier's beaked whale (*Ziphius cavirostris*)
- Blainville's beaked whale (*Mesoplodon densirostris*)
- Gervais' beaked whale (*Mesoplodon europaeus*)
- Short-finned pilot whale (*Globicephala macrorhynchus*)
- Killer whale (*Orcinus orca*)
- False killer whale (*Pseudorca crassidens*)
- Pygmy killer whale (*Feresa attenuata*)
- Melon-headed whale (*Peponocephala electra*)
- Common bottlenose dolphin (*Tursiops truncatus*)
- Risso's dolphin (*Grampus griseus*)
- Rough-toothed dolphin (*Steno bredanensis*)
- Fraser's dolphin (*Lagenodelphis hosei*)
- Pantropical spotted dolphin (*Stenella attenuata*)
- Striped dolphin (*Stenella coeruleoalba*)
- Clymene dolphin (*Stenella clymene*)
- Spinner dolphin (*Stenella longirostris*)

3.2.1 Cuvier's Beaked Whale

Beaked whales can be identified acoustically by their echolocation signals (Baumann-Pickering et al. 2014). These signals are frequency-modulated (FM) upsweep pulses, which appear to be species specific and distinguishable by their spectral and temporal features. Identifiable signals are described for all beaked whales known to occur in the region, namely Blainville's, Cuvier's, and Gervais' beaked whales.

Cuvier's echolocation signals are polycyclic, with a characteristic FM pulse upsweep, peak frequency around 40 kHz (Figures 3 & 4), and uniform inter-click interval (ICI) of about 0.5 s (Johnson et al. 2004; Zimmer et al. 2005). An additional feature that helps with the identification of Cuvier's FM pulses is that they have two characteristic spectral peaks around 17 and 23 kHz.

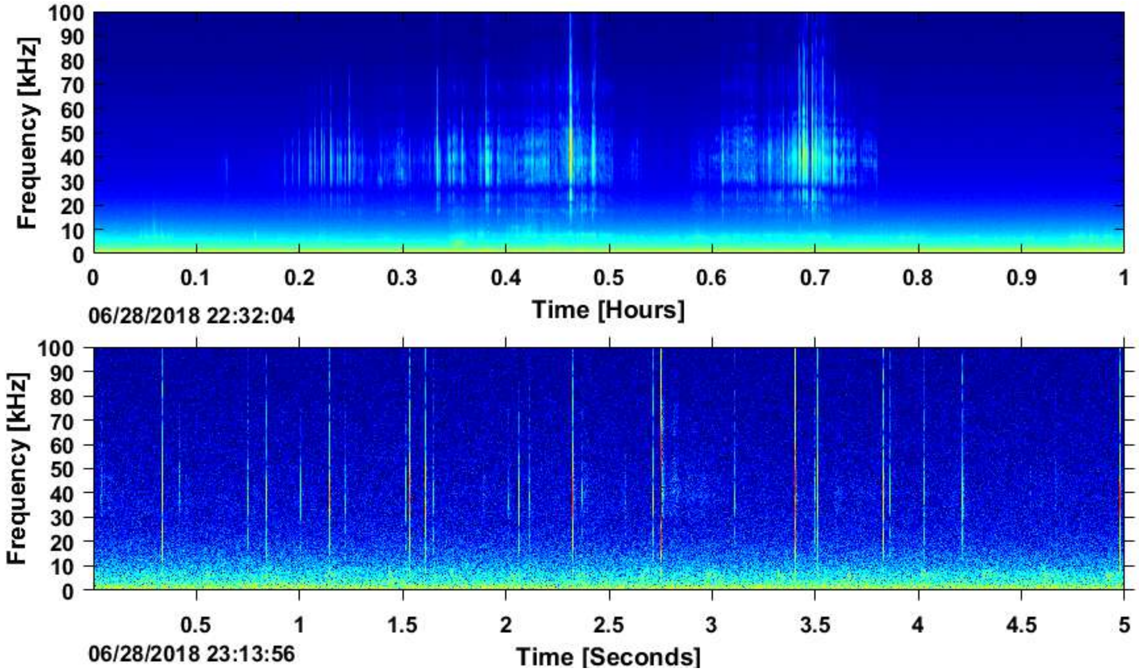

Figure 3: Cuvier's beaked whale signal in LTSA (top) and spectrogram (bottom).

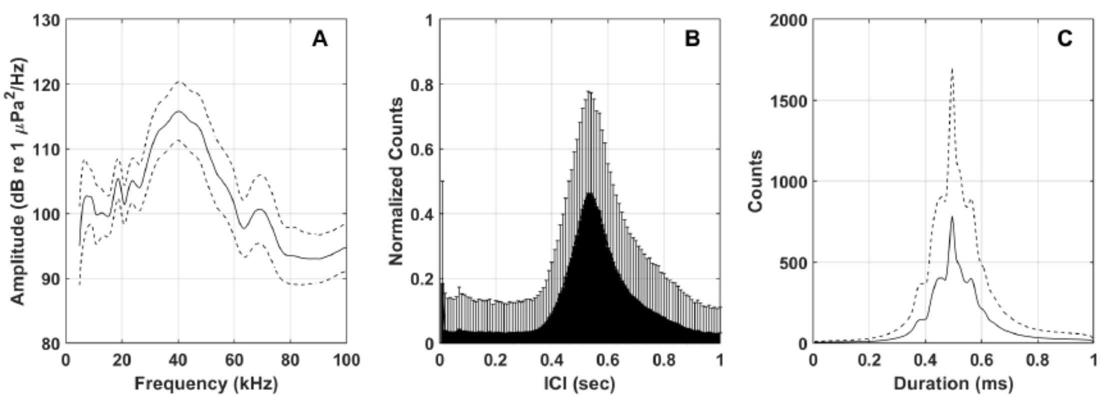

Figure 4: Left: Mean frequency spectrum of Cuvier's beaked whale echolocation clicks (solid line) and 25th and 75th percentiles (dashed lines); Center: Inter-click interval distribution with peak near 0.5 s; Right: Mean waveform envelope (solid line) and standard deviation (dashed line) of representative clicks.

3.2.2 Gervais' Beaked Whale

Gervais' beaked whale echolocation signals have energy concentrated in the 30-50 kHz band (Gillespie et al. 2009), with a peak at 44 kHz (Baumann-Pickering et al. 2013) (Figures 5 & 6). While Gervais' beaked whale signals are similar to those of Cuvier's and Blainville's beaked whales, the Gervais' beaked whale FM pulses are at a slightly higher frequency than those of the other two species. Similar to all beaked whales, Gervais' beaked whale FM pulses sweep up in frequency. The ICI for Gervais' beaked whale signals is typically around 0.28 s (Baumann-Pickering et al. 2013).

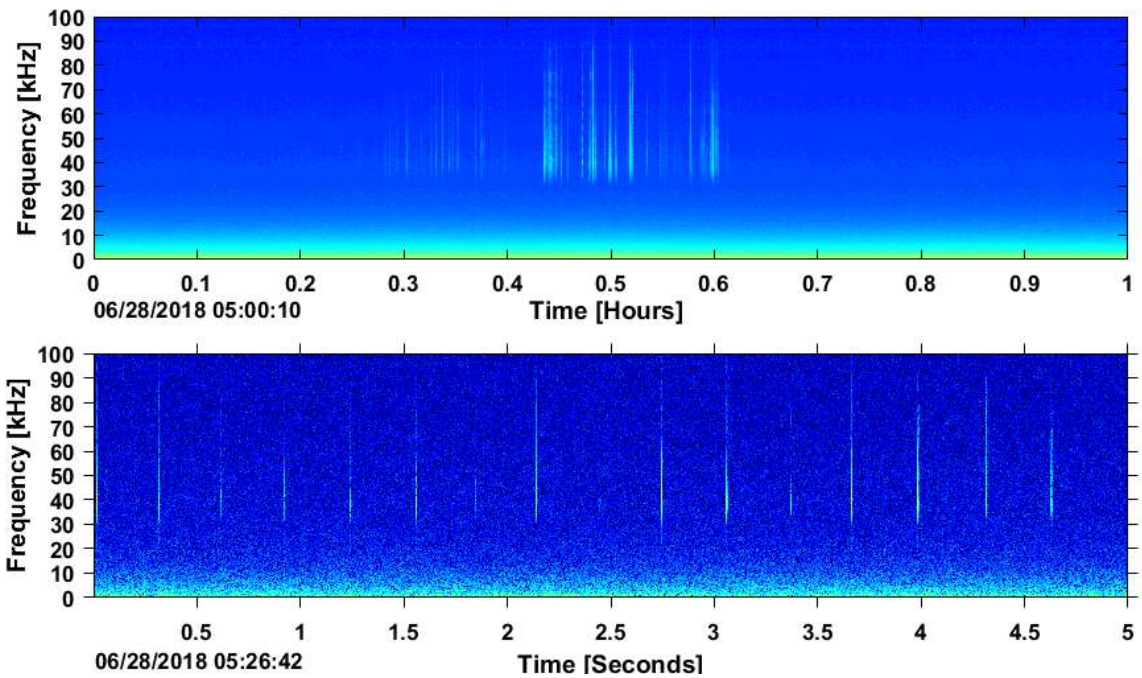

Figure 5: Gervais' beaked whale signal in LTSA (top) and spectrogram (bottom).

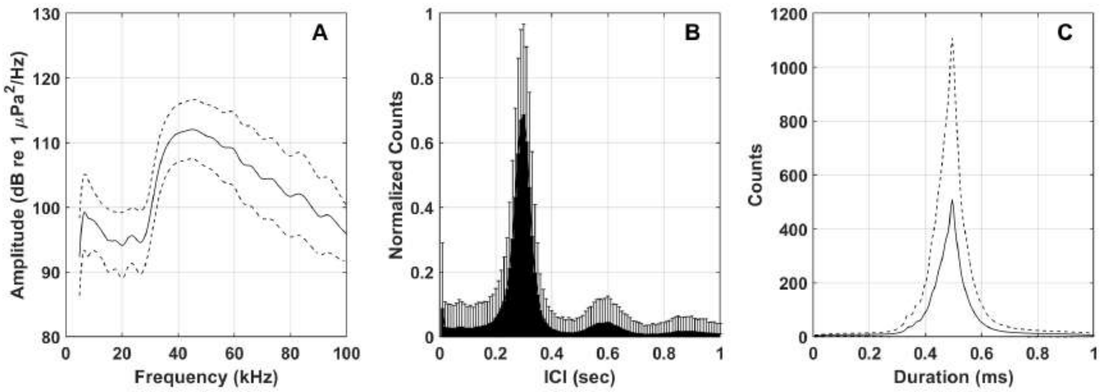

Figure 6: Left: Mean frequency spectrum of Gervais' beaked whale echolocation clicks (solid line) and 25th and 75th percentiles (dashed lines); Center: Inter-click interval distribution with peak near 0.3 s. Smaller peaks can occur at multiples of the main peak, and represent cases where a subset of clicks in a click train have been missed by the detector or classifier; Right: Mean waveform envelope of representative clicks.

3.2.3 Blainville's Beaked Whale

Blainville's beaked whale echolocation signals are, like most beaked whales' signals, poly-cyclic with a characteristic frequency-modulated upsweep, and are identifiable by a peak frequency around 34 kHz and uniform ICI of about 0.28 s (Johnson et al. 2004, Baumann-Pickering et al. 2013). Blainville's FM pulses are also distinguishable in the spectral domain by their sharp energy onset around 25 kHz with only a small energy peak at around 22 kHz (Figures 7 & 8).

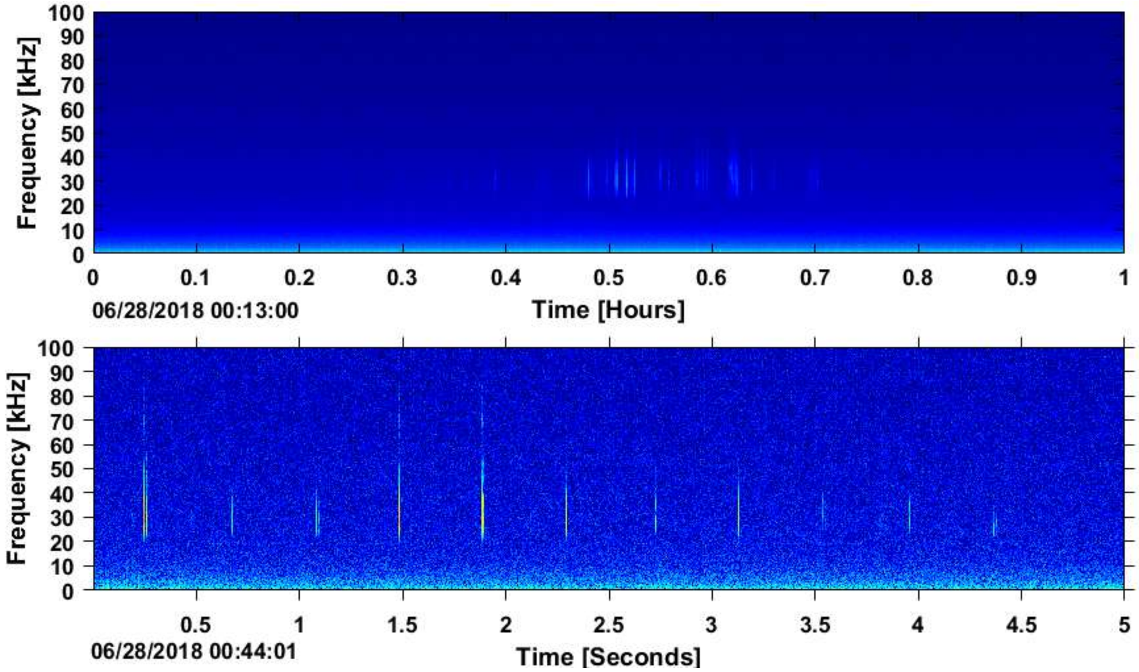

Figure 7: Blainville's beaked whale signal in LTSA (top) and spectrogram (bottom).

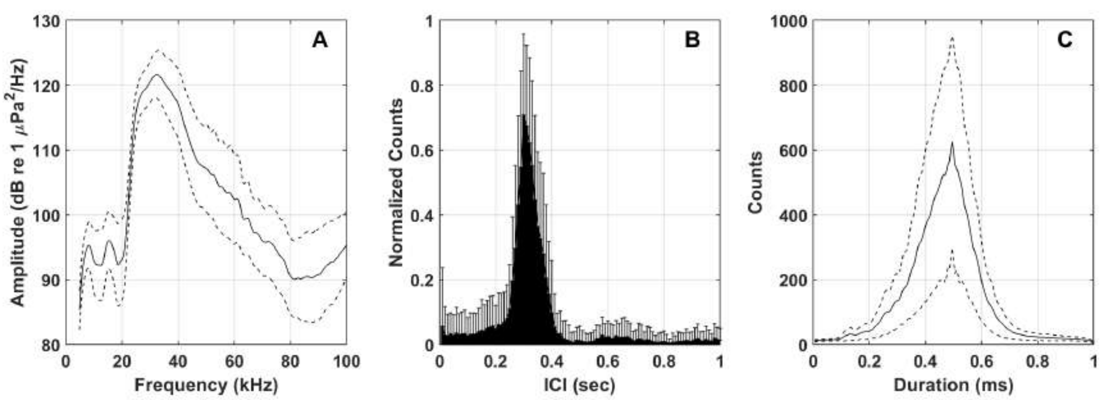

Figure 8: Left: Mean frequency spectrum of Blainville's beaked whale echolocation clicks (solid line) and 25th and 75th percentiles (dashed lines); Center: Inter-click interval distribution with peak near 0.3 s; Right: Mean waveform envelope of representative clicks.

3.2.4 Sperm Whales

Sperm whale clicks contain energy from 1-20 kHz, with the majority of energy between 10-15 kHz (Møhl et al. 2003) (Figures 9 & 10). With predominantly lower frequency energy, their echolocation clicks are highly distinguishable from those of other odontocetes. Regular clicks, observed during foraging dives, demonstrate an ICI from 0.25-2 s (Goold and Jones 1995, Madsen et al. 2002). Short bursts of closely spaced clicks called creaks are observed during foraging dives and are believed to indicate a predation attempt (Watwood et al. 2006). Effort was not expended to denote whether sperm whale detections were codas, creaks, regular or slow clicks, or to associate clicks with demographic groups (e.g. males vs. females, Solsona-Berga et al. 2022). Most sperm whale clicks in this dataset are likely produced by females and juveniles, as indicated by the relatively short modal ICI near 0.5 s.

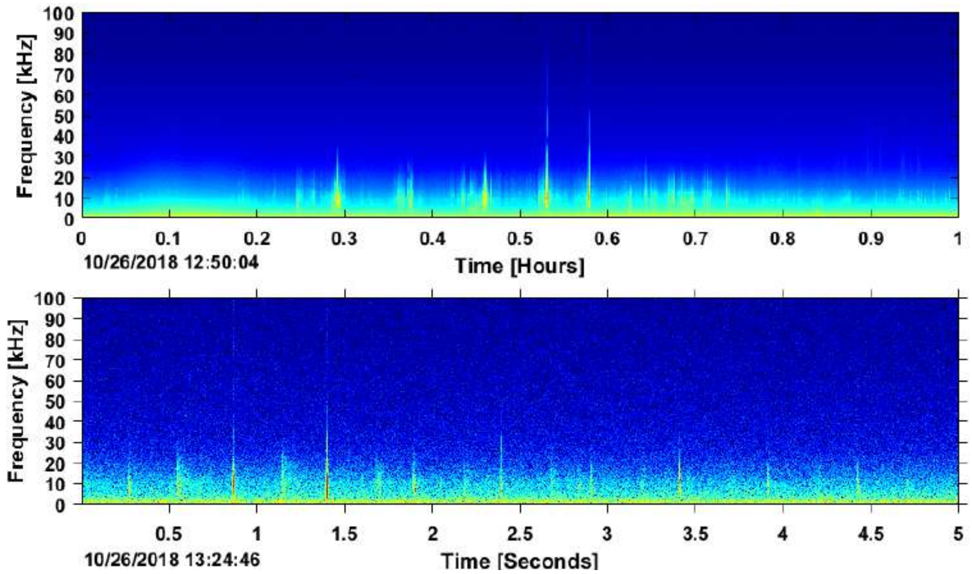

Figure 9: Sperm whale signals in LTSA (top) and spectrogram (bottom).

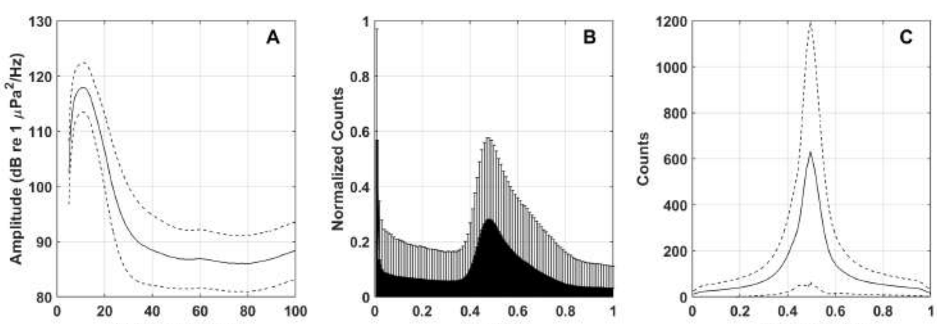

Figure 10: Left: Mean frequency spectrum of sperm whale echolocation clicks (solid line) and 25th and 75th percentiles (dashed lines); Center: Inter-click interval distribution with peak near 0.5 s; Right: Mean waveform envelope of representative clicks.

3.2.5 *Kogia* spp.

Dwarf and pygmy sperm whales emit echolocation signals which have peak energy at frequencies near 130 kHz (Au 1993). Their clicks can readily be distinguished from other species in the Gulf, but not from each other. While the peak frequency of these clicks is above the upper frequency band recorded by the HARP during these deployments, energy from *Kogia* clicks can be recorded within the 100 kHz HARP bandwidth (Figure 11). The observed signal may result both from the low-frequency tail of the *Kogia* echolocation click spectra, and from aliasing of energy from above the Nyquist frequency of 100 kHz (Figures 11 & 12). Typical modal ICIs for *Kogia* spp. are near 0.1 s.

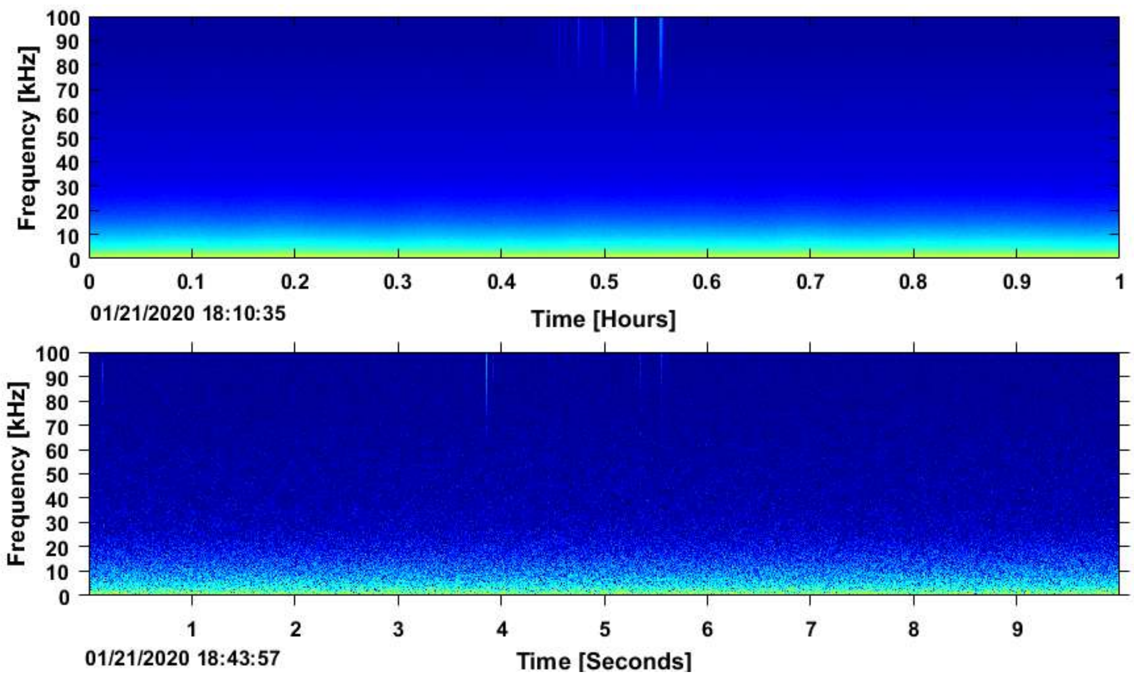

Figure 11: *Kogia* spp. signals in LTSA (top) and spectrogram (bottom).

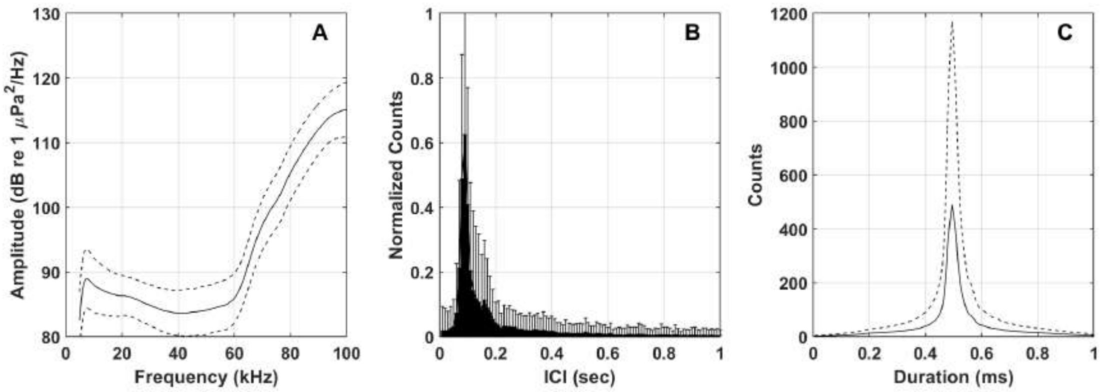

Figure 12: Left: Mean frequency spectrum of *Kogia* spp. echolocation clicks (solid line) and 25th and 75th percentiles (dashed lines); Center: Inter-click interval distribution with peak near 0.1 s; Right: Mean waveform envelope of representative clicks.

3.2.6 Risso's Dolphins

Risso's dolphin clicks (Figures 13 & 14) have frequency peaks at approximately 22, 26, and 33 kHz. These clicks have a modal ICI of approximately 0.15 seconds. Past studies have shown that spectral properties of Risso's dolphin clicks have slight variations with geographic region (Soldevilla et al. 2017), although the multiple sharp frequency peaks and average ICI found in the Gulf of Mexico are similar to what has been found elsewhere.

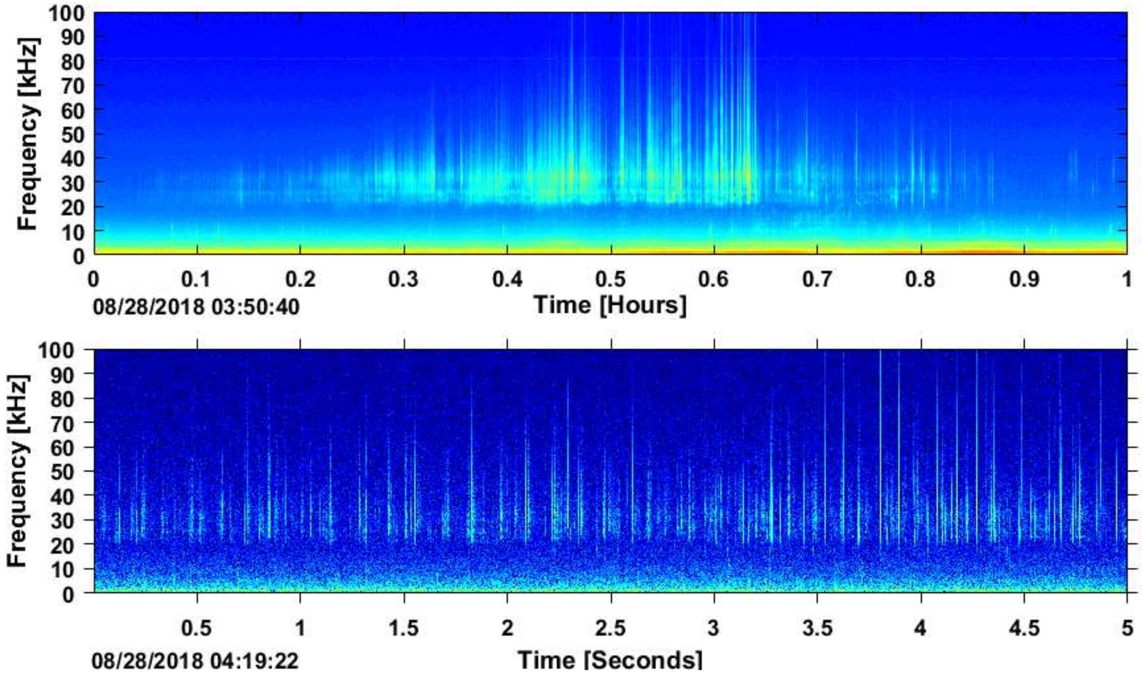

Figure 13: Risso's dolphins signals in LTSA (top) and spectrogram (bottom).

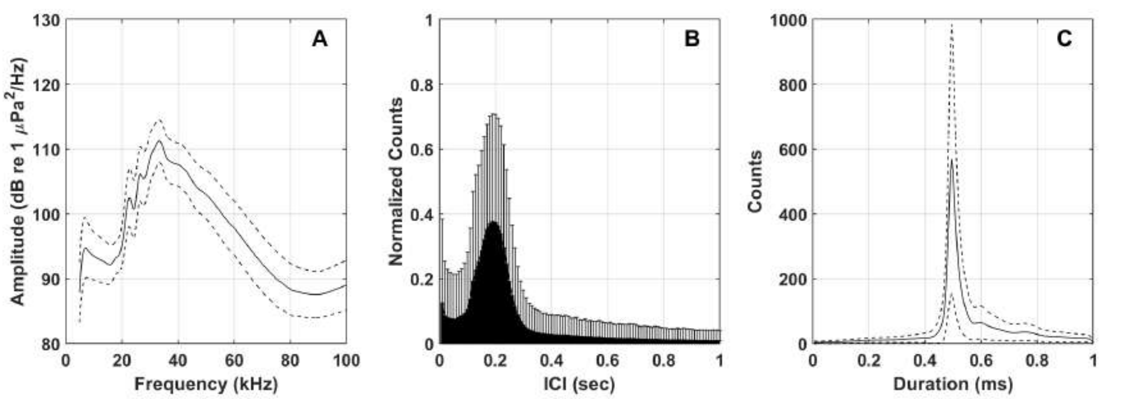

Figure 14: Left: Mean frequency spectrum of Risso's dolphins echolocation clicks (solid line) and 25th and 75th percentiles (dashed lines); Center: Inter-click interval distribution with peak near 0.2 s; Right: Mean waveform envelope of representative clicks.

3.2.7 Unidentified Dolphins: High-Frequency

High-frequency unidentified dolphins clicks (UD HF) were one of the dominant click types identified by the unsupervised cluster classification algorithm, which are distinctive, but that have not previously been associated with a specific species. The majority of events in this grouping likely represents delphinids in the genus *Stenella*, primarily pantropical spotted dolphins (*Stenella attenuata*). Spinner dolphins (*Stenella longirostris*), Clymene dolphins (*Stenella clymene*), and striped dolphins (*Stenella coeruleoalba*) are also likely included, and their clicks may or may not be acoustically distinguishable from the dominant pantropical spotted dolphin (Frasier et al. 2017). Offshore common bottlenose and offshore Atlantic spotted dolphins (*Tursiops trucatus* and *Stenella frontalis*, respectively) are also likely included in this category. These two will likely be acoustically distinguishable from the other Stenella species based on observed differences between click spectral features and ICI at shallow sites (DC and MP), where closely-related bottlenose and Atlantic spotted dolphins are presumed to be the dominant species, and deep sites, where oceanic Stenella species dominate. This distinction effort is in progress. It remains to be determined whether further distinctions are possible within this group. The majority of the UD HF clicks have peak frequencies between 30 and 45 kHz (Figures 15 & 16). Two peaks are visible in the ICI distribution. The dominant peak at 65 ms is likely associated with the Stenella category (primarily *S. attenuata*). The secondary peak at approximately 0.1 s is likely associated with offshore bottlenose dolphins. In the future, further analyses will be undertaken to refine this type into two or more click types and to reduce classification confusion between similar types.

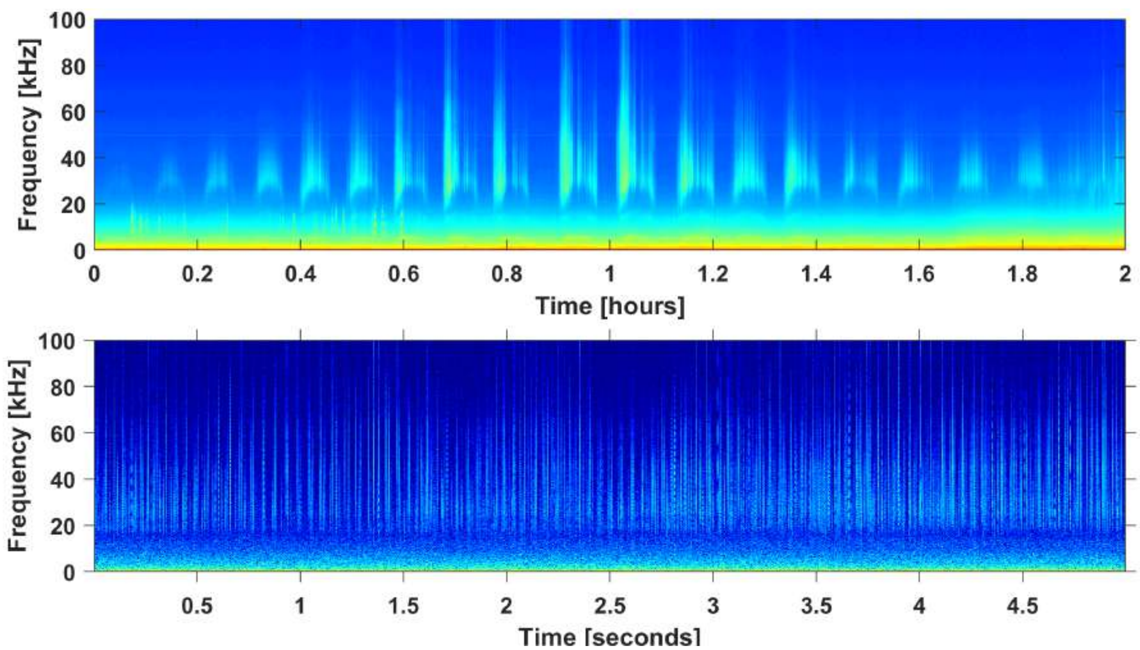

Figure 15: Unidentified dolphin high-frequency (UD HF) echolocation signals in LTSA (top) and spectrogram (bottom).

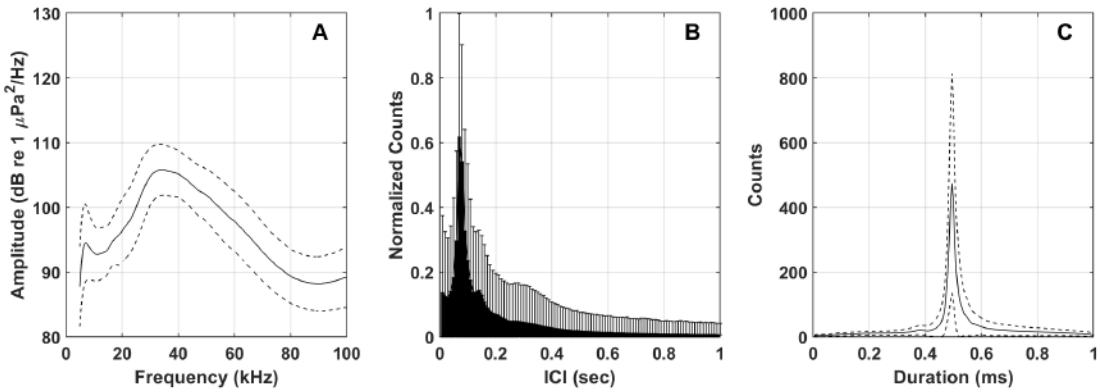

Figure 16: Left: Mean frequency spectrum of unidentified dolphin high-frequency (UD HF) echolocation clicks (solid line) and 25th and 75th percentiles (dashed lines); Center: Inter-click interval distribution with peak near 0.06 s; Right: Mean waveform envelope of representative clicks.

3.2.8 Unidentified Dolphins: Three-Peak

An unidentified dolphin click type with three distinct spectral peaks (UD 3P) was one of the dominant click types identified by the unsupervised cluster classification algorithm. The type is distinctive, but has not previously been associated with a specific species. UD 3P type clicks (Figures 17 & 18) have small spectral peaks at 13 and 19 kHz, with a large, broad energy peak between 30 and 50 kHz. These clicks have a modal ICI of approximately 0.1 s. In the future, further analysis will be required to refine unidentified click types and reduce classification confusion between similar types.

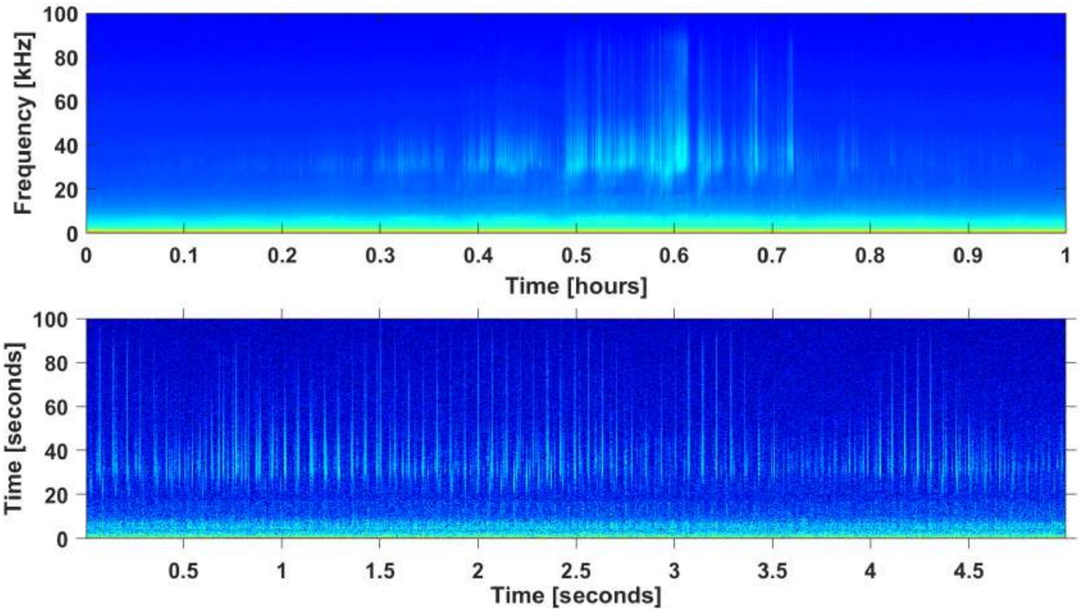

Figure 17: Unidentified dolphin three-peak (UD 3P) echolocation signals in LTSA (top) and spectrogram (bottom).

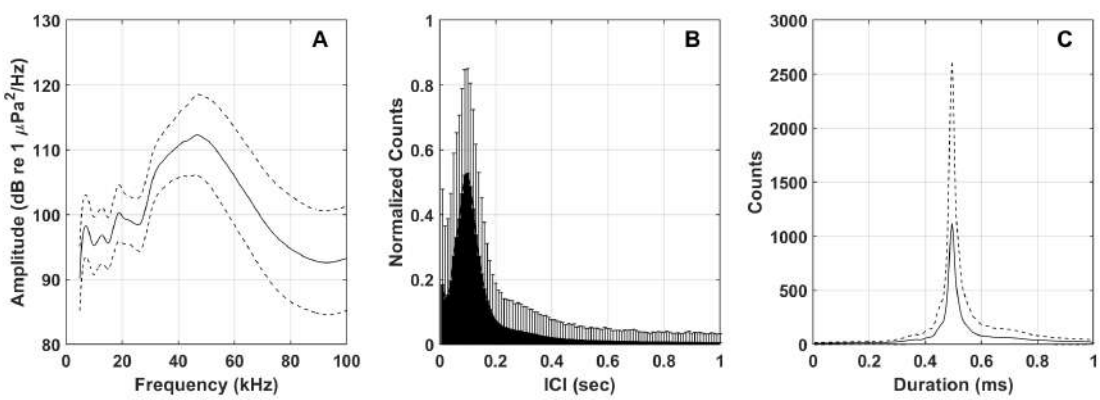

Figure 18: Left: Mean frequency spectrum of unidentified dolphin three-peak (UD 3P) echolocation clicks (solid line) and 25th and 75th percentiles (dashed lines); Center: Inter-click interval distribution with peak near 0.1 s; Right: Mean waveform envelope of representative clicks.

3.2.9 Unidentified Dolphins: Low-Frequency

A low frequency delphinid echolocation click category (UD LF) was another dominant click category identified by the unsupervised clustering algorithm. This category likely represents some of the large delphinid species including short finned pilot whale (*Globicephala macrorhynchus*; Cohen et al. 2022), melon-headed whale (*Peponocephala electra*), false killer whale (*Pseudorca crassidens*), pygmy killer whale (*Feresa attenuata*), and killer whale (*Orcinus orca*; Leu et al. 2022). UD LF type clicks (Figures 19 & 20) are characterized by a peak frequency below 30 kHz and a variable modal ICI near 0.2 s. This is a diverse category, and further analyses currently in progress are likely to result in the identification of multiple subtypes which may be attributable to individual species.

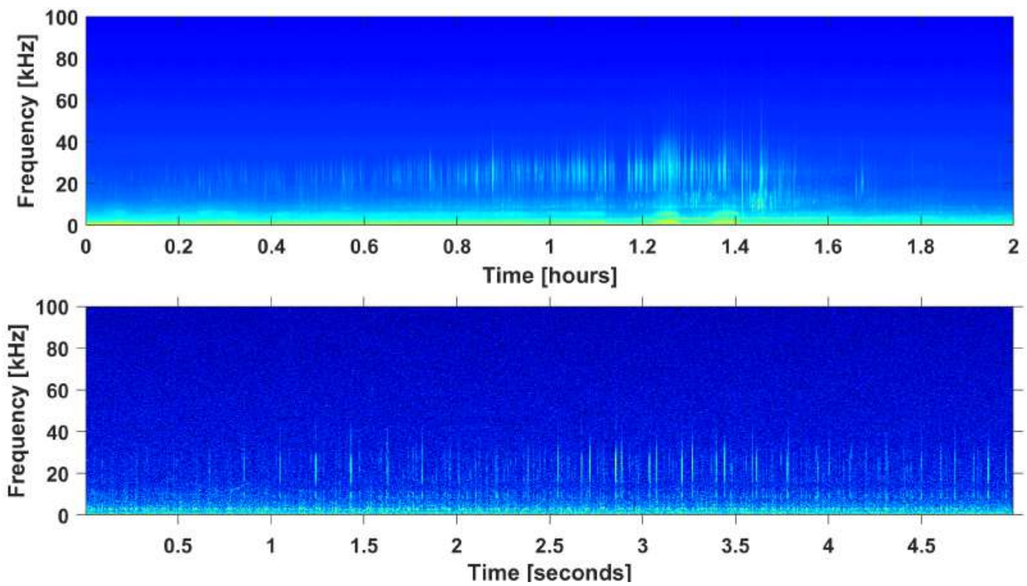

Figure 19: Unidentified dolphin low-frequency (UD LF) echolocation signals in LTSA (top) and spectrogram (bottom).

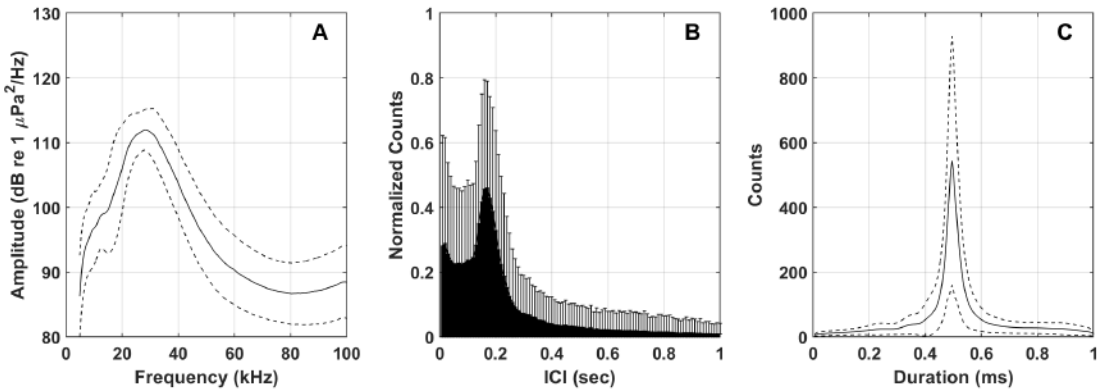

Figure 20: Left: Mean frequency spectrum unidentified dolphin low-frequency (UD LF) echolocation clicks (solid line) and 25th and 75th percentiles (dashed lines); Center: Inter-click interval distribution with peak near 0.18 s; Right: Mean waveform envelope of representative clicks.

3.3 Other Noise Source Descriptions

In addition to odontocete echolocation clicks, other noise sources are commonly detected by the automated click detection algorithm. A description of the signal features of these common noise sources follows. The automated neural network classifiers were trained on these categories to avoid misclassification as marine mammal signals.

3.3.1 Ship Noise

Broadband ship sound occurs when a ship passes within a few kilometers of the hydrophone. Ship sound can occur for many hours at a time, but broadband ship sound typically lasts from 10 minutes up to 3 hours. Noise can extend above 10 kHz, although sound levels typically decrease rapidly above a few kHz (Figures 21 & 22).

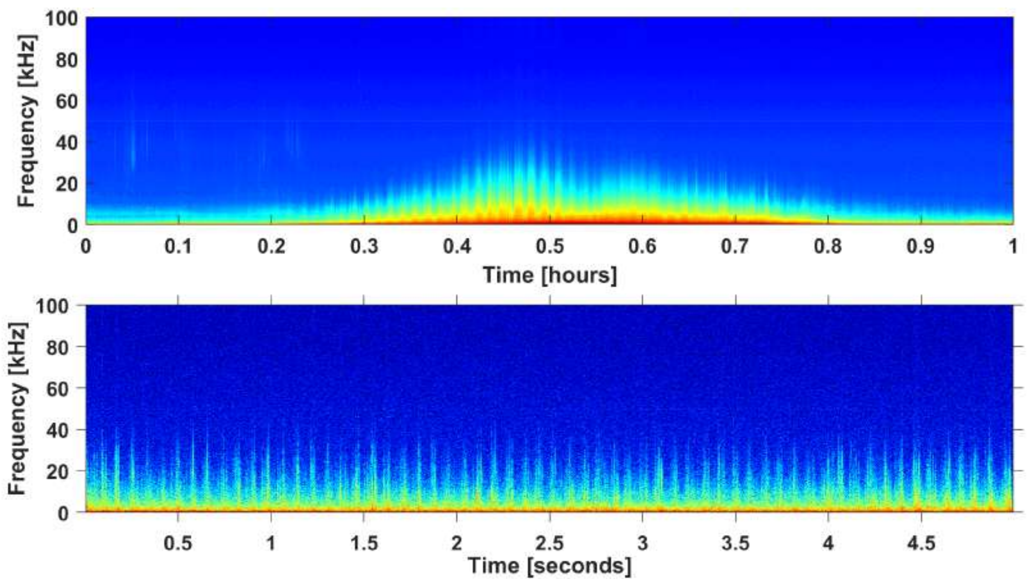

Figure 21: Broadband ship signals in LTSA (top) and spectrogram (bottom).

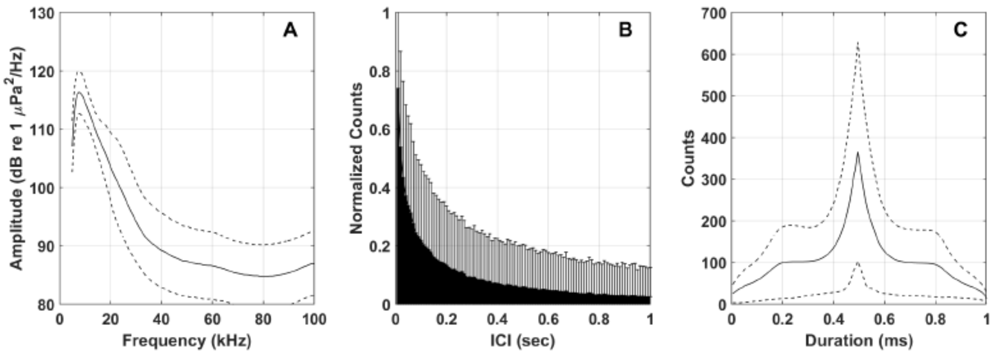

Figure 22: Left: Mean frequency spectrum of broadband ship noise (solid line) and 25th and 75th percentiles (dashed lines); Center: Inter-detection interval distribution; Right: Mean waveform envelope of representative signals. Note that this representation of ship noise is used in the context of the echolocation click classification process. Therefore, it is band passed to exclude frequencies below 5 kHz.

3.3.2 Noise - High and Low Frequency

Noise is a general category used to recognize and classify occasional and unusual signals, often within a particular dataset. Sources may include mooring noise generated during high current events, recording system noise, and other short, broadband signals that might be mistaken for echolocation.

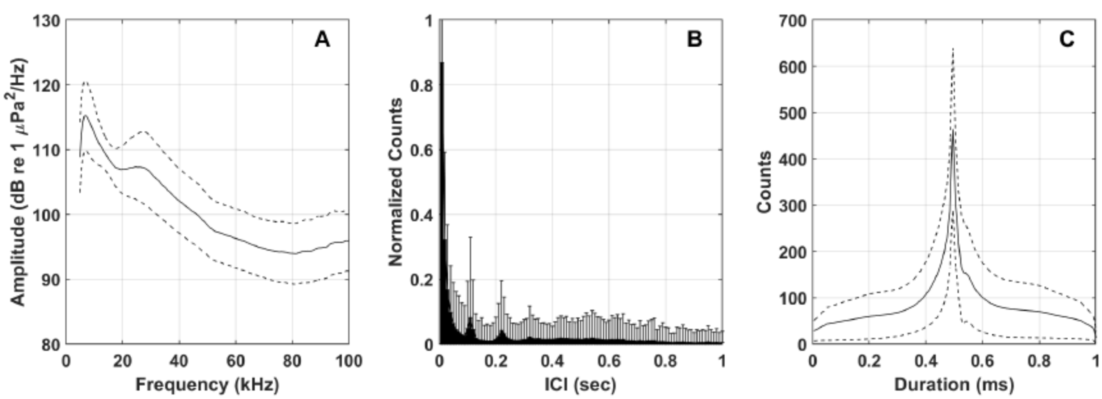

Figure 23: Left: Mean frequency spectrum of noise (solid line) and 25th and 75th percentiles (dashed lines); Center: Inter-detection interval distribution; Right: Mean waveform envelope of representative signals.

3.3.3 Sonar

The sonar category consists of three types of sonar: mid-frequency, high-frequency, and echosounders. Sounds from mid-frequency active (MFA) sonar vary in frequency (1–10 kHz) and are composed of pulses of both frequency modulated (FM) sweeps and continuous wave (CW) tones. High-frequency active (HFA) sonar is used for specialty military and commercial applications including high-resolution seafloor mapping, short-range communications, such as with Autonomous Underwater Vehicles (AUVs), multi-beam fathometers, and submarine navigation (Cox 2004). Echosounders are used by many varieties of commercial and private vessels and vary in frequency from 5-75 kHz. This category was included when classifying signals at all sites.

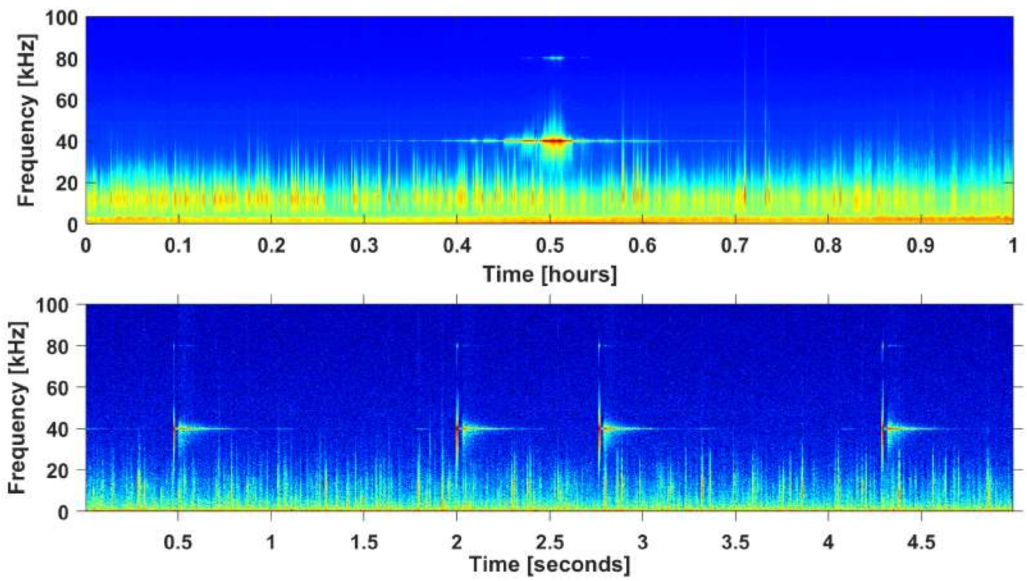

Figure 24: Echosounder signals (40 kHz) in LTSA (top) and spectrogram (bottom). This example image also includes sperm whale echolocation clicks.

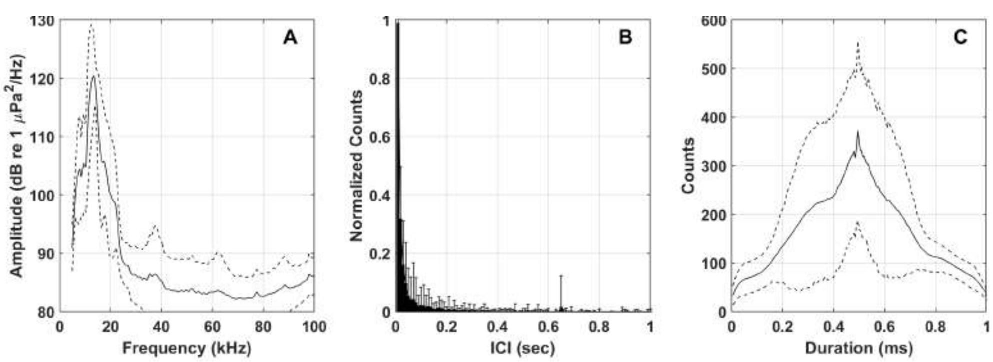

Figure 25: Left: Mean frequency spectrum of sonar (solid line) and 25th and 75th percentiles (dashed lines); Center: Inter-detection interval distribution; Right: Mean waveform envelope of representative signals.

3.3.4 Snapping Shrimp

Snapping shrimp signals were only found at Main Pass (MP) and De Soto Canyon (DC) sites during manual reviews of the recordings. Snapping shrimp produce broadband snapping sounds with their claws (Everest et al. 1948). In shallow environments, this signal can dominate soundscapes. These snaps are acoustically similar to dolphin echolocation clicks, however, the timing is irregular (Figures 26 & 27). To reduce classifier confusion, the snapping shrimp class was only included when classifying signals at the shallow MP and DC sites. This signal may be a useful indicator of shrimp occurrence.

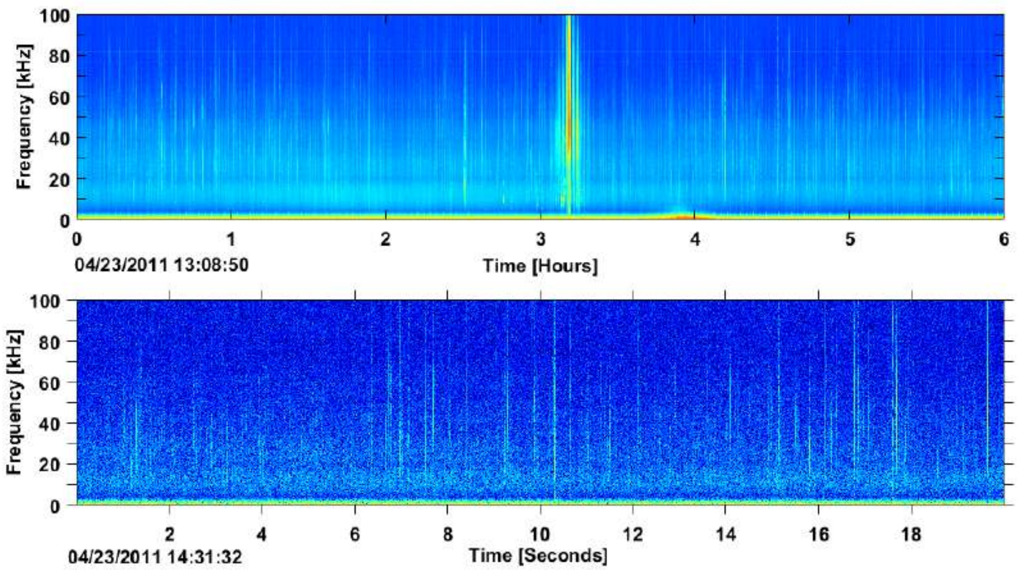

Figure 26: Snapping shrimp signals in LTSA (top) and spectrogram (bottom).

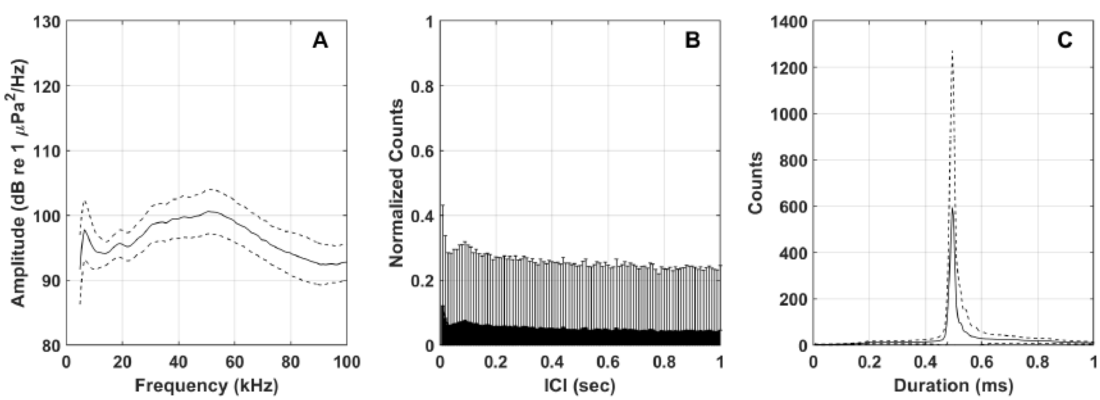

Figure 27: Left: Mean frequency spectrum of sonar (solid line) and 25th and 75th percentiles (dashed lines); Center: Inter-detection interval distribution; Right: Mean waveform envelope of representative snaps.

3.4 Ambient and Anthropogenic Noise Analyses

Analyses of ambient noise levels provide information on the natural and anthropogenic contributions of noise sources and how they vary over time and space. Hourly long-term spectrograms were produced at each site to document ambient noise levels over time. The statistical distributions of ambient noise curves and third-octave and octave band sound levels were computed for the low-frequency band.

Several anthropogenic sound sources that are prolific in the Gulf of Mexico may be of interest for the noise reduction restoration project. The previously described noise classes were included in the odontocete signal analyses only to reduce misclassification errors for marine mammal detections. Additional automated detectors, described below, were developed specifically to document the occurrence of anthropogenic noise sources of interest, including: broadband ship noise, explosions, airguns, and echosounders. The start and end of each individual sound or the overall acoustic event was logged and their durations were added to estimate cumulative hours present per week.

At the two noise-restoration project noise monitoring sites (GA and SL), additional analyses were conducted to estimate the source levels of commercial vessels transiting directly over the HARPs (those with a Closest Point of Approach (CPA) <= 200 m). Radiated noise levels and monopole source levels for identified cargo ships, tug-tows, tankers, cruise ships and a number of other vessels were developed during these analyses.

3.4.1 Ambient Noise Levels

Long-term spectrograms and ambient noise curves were estimated from the following methods from Wiggins et al. 2016 at three different resolutions:

- Low frequency, factor of 100 decimated data, 10 Hz-1 kHz in 1 Hz bins.
- Mid frequency, factor of 20 decimated data, 10 Hz-5 kHz in 10 Hz bins.
- Full frequency, 10 Hz-100 kHz in 100 Hz bins.

In each case, consecutive, five-s waveforms were transformed into sequential sound pressure spectral density estimates with 1 Hz bin resolution using the Welch method (Welch 1967). During recording, HARPs write sequential 75 s acoustic records to standard laptop-style computer hard disk drives such that there were 15 five-s spectra for each 75 s acoustic record. However, system self-noise can be present when the HARP is writing to disk (12 s out of each 75 s record), so the first three five-s spectra were not used for the following soundscape analyses. Statistical distributions of the noise spectra were computed per hour and per day after discarding partial days and days with deployment/recovery ships sounds or with known instrument self-noise problems. These distributions were calculated with custom MATLAB-based software to provide hourly and daily average and percentile sound pressure spectrum levels for all sites over the deployment periods in addition to long-term spectrograms. For conciseness, this report focuses on the low frequency output, which is most indicative of anthropogenic noise sources.

3.4.2 Broadband Ships

Broadband ship noise, from sources including the engine, propeller, and cavitation, occurs in the 30 Hz to 10 kHz or higher frequency range when a ship passes within a few kilometers of the hydrophone. At lower frequencies, particularly in the 30-150 Hz band, noise from global shipping can occur near-continuously. While elevated low-frequency noise levels from distant ships can occur for many hours at a time, broadband ship noise during closer approaches typically lasts from 10 minutes up to 3 hours. Ship noise has a characteristic frequency-range-dependent pattern of constructive and destructive interference (bright and dark bands) in the LTSA due to the combination of direct and surface reflected sound paths (Figure 28; McKenna et al. 2012). Noise can extend above 10 kHz when vessels are very close to the recorders, while sound levels typically decrease rapidly above a few kHz.

To determine the contribution of shipping noise to the soundscape at the Gulf of Mexico HARP sites between 2010-2021, and to determine the ship types that transit near each recording location, a combination of (1) automated ship detections in the HARP acoustic recordings and (2) Automatic Identification System (AIS) data were used. The AIS data, obtained from Marine Cadastre, included ship information such as MMSI, vessel name, vessel type, vessel size, time as well as position at the time of each detection, and other vessel specifics. These data were used to examine ship types commonly found within 15 km of the deployed HARPs and the distances at which the ships passed each site (up to 15 km).

To analyze the HARP acoustic data for ship noise, a modified version of the custom ship detector in Matlab-based software Triton (github.com/MarineBioAcousticsRC/Triton/wiki/Ship-Detector) was used. The detector identifies shipping events within Long-Term Spectral Averages (LTSAs) by examining power spectral density estimates in three user-defined frequency bands. Events meeting three conditions based on amplitude above a threshold and duration are logged as a ship passage. The original ship detector was designed to run on full bandwidth LTSAs to prevent misclassification of ship noise at sperm whale frequencies (1-10 kHz) as sperm whale clicks during odontocete detection and classification analyses. This detector was modified to meet the current objective of detecting all close approaches of ships (within 15 km) over the full bandwidth of shipping noise (30 Hz to 10 kHz). To meet these objectives, the original ship detector was modified to: 1) use the higher-resolution mid-frequency band LTSAs, 2) extend the three user-defined frequency bands to frequencies below 5 kHz, and 3) expand the 1-step detector to a 2-step detector to enhance detection of both ships with only low-frequency energy content and those with broader band energy. The frequencies for the three user-defined frequency bands were chosen to maximize the detection of shipping noise while minimizing the detection of airgun surveys. In general, for the first-step parameters, the low-frequency band ranged from 100-250 Hz or 300-850 Hz, the mid-frequency band from 250-500 Hz or 850-3000 Hz, and the high-frequency band from 500-1000 Hz or 3000-5000 Hz. For the second-step parameters, the low-frequency band ranged from either 300-850 Hz (site DC only) or 100-500 Hz, the mid-frequency band from 850-3000 Hz (site DC only) or 500-1000 Hz, and the high-frequency band from 3000-5000 Hz. At each site, optimal settings were selected by comparing detector results with manual ship detections in a subset of data. False positive rates for these settings are currently in development. Preliminary reviews of the results indicate the ship detector is effective at detecting ships with broadband shipping noise present, but ineffective at detecting ships with primarily tonal noise bands present. Additional investigation is needed to identify the types of vessels that have primarily tonal characteristics.

To better understand received ship levels with respect to ship type, distance, speed, and other characteristics, and to understand the frequency of occurrence of shipping noise from vessels not equipped with AIS, automated ship detections were linked to associated ship tracks in the AIS data. Shipping data results are presented at each site as the number of acoustic detections of passing ships, the daily duration of vessel noise presence, the daily number of AIS-equipped ships passing nearby, and the annual percentage of ships per ship type passing nearby. Multiple ship passings close in time are typically detected as a single detection; therefore, ship detection results represent a minimum number.

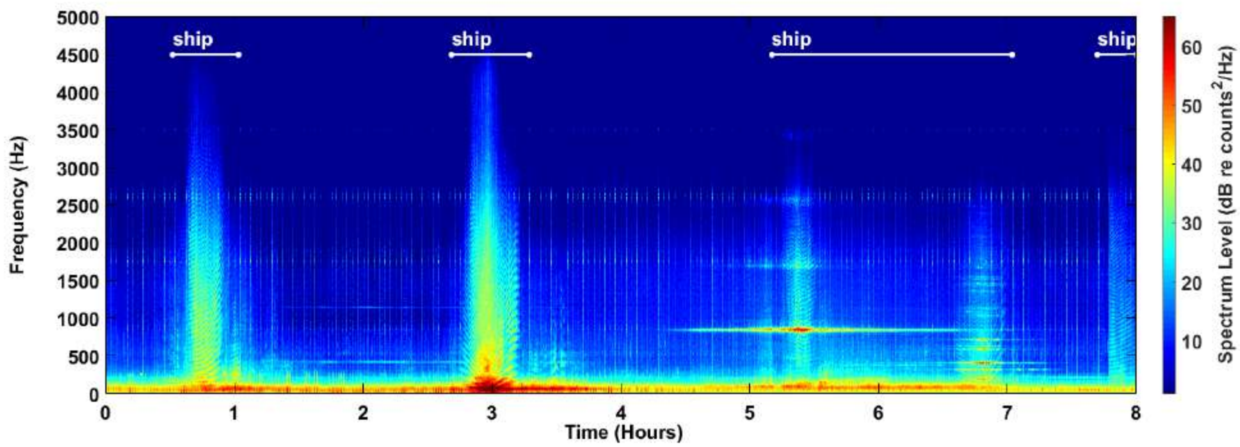

Figure 28: Example of ship detections made over an 8-hr period with the customized ship sound detector. Note the presence of tonal sound associated with the 3rd and 4th ships, as well as the merging of those two ship transits into one detection.

3.4.3 Ship Received Levels and Source Levels

Radiated Noise Levels (RNL) were calculated based on ASA/ANSI (2009) and ISO (2019) specifications. Monopole Source Levels (MSL), correcting for the effect of Lloyd's mirror, were estimated using the approach of Gassmann et al 2017. Both sound levels, RNL and MSL, were estimated for one-third-octave bands from 10 Hz to 4 kHz. Each vessel transit recording was divided into non-overlapping segments with a duration of 1 s. A 10,000-point (NFFT) Fast Fourier Transform (FFT) was applied to each 1 second segment to provide a frequency bin resolution of 1 Hz. The magnitude of the FFT squared was multiplied by $2/NFFT^2$ to correct for the processing gain of the FFT. Over the duration of the transit, the mean sound pressure level (SPL) was computed over each 5-s segment every 3 s to smooth the time-frequency distribution. The resulting SPLs were reported in decibels (dB) summed from 5 to 1000 Hz with a reference pressure of 1 μPa^2, and at 1 Hz and third-octave band resolution with a reference pressure of 1 μPa^2/Hz. To estimate RNL, a spherical spreading propagation loss model (N$_{SS}$) was calculated with the following equation:

$$N_{SS} = 20log_{10}(R/r_0) \tag{2}$$

where R is the distance from the dipole source to the receiver and r$_0$ is the reference distance (1 m). The N$_{SS}$ used to compute RNL does not require a source depth (d$_S$), therefore the d$_S$ is assumed to be the dipole source for all transits. The N$_{SS}$ was applied to the SPL to achieve RNL (3).

$$RNL = SPL + N_{SS} \tag{3}$$

A propagation loss model that corrects for the Lloyd's mirror effect (NPL) was applied to estimate MSL to account for reflected image interference at the sea surface and for compliance with ISO (2019, Equation 4). The N$_{PL}$ model ignores sound refraction in the water column and reflections with the seafloor and solely accounts for reflections from the sea surface (Gassmann et al. 2017; Audoly and Meyer 2017). The propagation loss of a sound source near the surface in deep water considering the Lloyd's mirror effect is given by:

$$N_{PL} = -20log_{10}\left(r_0\left|\frac{e^{ijkr_1}}{r_1} - \frac{e^{ijkr_2}}{r_2}\right|\right) \tag{4}$$

$$MSL = SPL + N_{PL} \tag{5}$$

where r$_1$ is the distance from the source to the receiver, r$_2$ is the distance from the reflected image source to the receiver, and k is the wave number (k = 2πf/c) in rad/m. Source depth was taken to be equal to 50% of the actual vessel draft. Harmonic mean sound speeds were calculated from depth, temperature, and salinity data obtained from the Global Ocean Forecasting System (GOFS) 3.1: 41-layer HYCOM + NCODA Global 1/12^o analysis.

A modification of the Lloyd's mirror model was established in Gassmann et al. (2017) to remove mismatched interference lobes identified with ship noise measurements in compliance with ANSI/ASA (2009) and ISO (2016). The modification includes using the Lloyd's mirror model from 5 Hz up to the lowest frequency at which the Lloyd's mirror model and the spherical spreading model intersect. At the higher frequencies, the spherical spreading model was used (Gassmann et al. 2017). The intersection frequency was unique for each passage.

3.4.4 Airguns

Airguns are regularly used in seismic surveys for oil and gas exploration to investigate the ocean floor and what lies beneath it. An airgun is a container of high-pressure air that periodically vents into the surrounding water, producing an air-filled cavity which expands and contracts several times (Barger and Hamblen, 1980) producing an intense low-frequency broadband explosive impulse. Airgun pulses have energy as low as 5 Hz and can extend up to 250 Hz or higher (Blackman et al. 2004), lasting up to a few seconds including the reverberations depending on propagation conditions and the distance between the source and receiver. While most of the energy produced by an airgun array falls below 250 Hz, airguns can produce significant energy at frequencies up to at least 1 kHz (Blackman et al. 2004). Source levels generally are over 200 dB re 1 μPa $\cdot$ m peak-to-peak (Amundsen and Landro, 2010), and have been measured up to 260 dB rms re 1 μPa $\cdot$ m (Hildebrand 2009). These pulses typically have an inter-pulse interval of approximately 10 s and bouts can last from several hours to weeks (Figure 29).

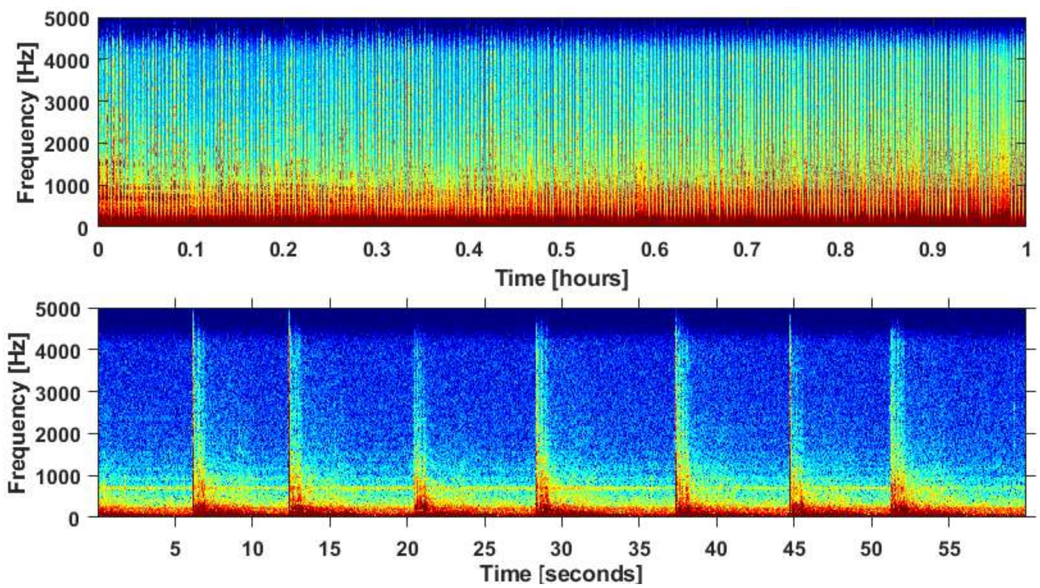

Figure 29: Airgun signals in LTSA (top) and spectrogram (bottom).

Airguns were detected automatically using a matched filter detector on the low-frequency band data. The acoustic recording timeseries were filtered with a 10th order Butterworth bandpass filter between 25 and 200 Hz. Cross correlation was computed between 75 s of the envelope of the filtered timeseries and the envelope of a filtered example explosion (0.7 s, Hann windowed) as the matched filter signal. The cross correlation was squared to 'sharpen' peaks of airgun pulse detections. A floating threshold was calculated by taking the median cross-correlation value over the current 75 s of data to account for detecting airguns within noise, such as shipping. A cross-correlation threshold of 2*10^{-6} above the median was set. When the correlation coefficient exceeded this threshold, the detection was sent to a phase 2 detection and classification step. Thresholds were determined based on a manual review of a subset of data.

Consecutive airgun pulse detections were required to have a minimum start time difference of 2 s. A 0.03 s running average energy across the detection was computed. The start and end times of the detection were marked when the energy rose by more than 0.5 dB above the median energy across the detection. The peak-to-peak (pp) and root-mean-square (rms) received levels (RLs) were computed over the potential pulse as well as before and after the explosion. The potential airgun pulse was classified as a false detection and removed if 1) the signal dB difference of pp and rms RLs between the during and AFTER detection periods was < 0.5 dB; 2) the dB difference of pp and rms RLs between the signal and the time BEFORE the signal was < 0.5 dB; and 3) the detection duration was shorter than 0.5 s. Further, detections with a peak-to-peak amplitude of < 120 dB were removed for this analysis.

4 Results

4.1 Odontocetes

Densities were computed for each odontocete category at each site (Table 5). The density estimation methods require estimates of subsurface behavior and odontocete group sizes. Where behavior is not well quantified (e.g., deep divers in shallow waters at sites DC and MP) or group sizes are not appropriate (e.g., snapping shrimp at site MP), density is not estimated, and other more suitable metrics such as duration of occurrence are reported. Density estimates are reviewed in detail in each species' section below.

Site	Sperm Whale	Cuvier's BW	Gervais' BW	Blainville's BW	Risso's Dolphin	UD HF	UD 3P	UD LF	Kogia spp.
DC (Hist)	–	–	–	–	1.3	358.0	219.9	2.8	–
DT (Hist)	1.6	136.1	53.3	0.4	17.8	377.0	7.8	43.0	1.4
GC (Hist)	2.9	6.6	18.9	4.6	1.2	298.6	2.0	56.1	6.6
MC (Hist)	8.0	8.1	11.7	1.2	2.7	396.4	14.3	33.3	8.6
MP (Hist)	–	–	–	–	–	603.7	–	–	–
AC	2.6	15.0	5.4	8.1	1.6	203.0	24.7	56.5	17.6
CE	1.6	240.4	0.5	16.1	0.3	164.3	60.0	46.4	7.8
DC	–	–	–	–	0.3	374.5	180.2	6.53	–
DT	3.3	65.1	10.9	0.1	12.8	301.1	3.0	32.7	0.8
GC	2.7	5.5	7.2	2.3	0.2	255.8	1.3	41.9	3.6
LC	0.4	22.9	18.0	1.3	2.3	530.1	159.3	34.5	16.1
MR	4.3	16.5	10.6	5.8	0.4	123.4	29.3	103.9	17.1
Y1B	1.7	23.0	19.6	1.1	1.6	335.5	153.2	42.5	16.9
Y1C	2.3	25.5	7.4	64.4	1.9	147.5	61.2	91.4	25.9
Y1D	0.3	0.4	0.2	0.6	17.9	344.8	136.8	55.5	8.0

Table 5: Mean density by species as number of animals per 1000 km^2 over the entire recording period. For historic data (Hist), this includes the June 2010 to September 2021 period. For all other data, this includes the August 2020 to September 2021 period.

4.1.1 Cuvier’s Beaked Whale

Among the three beaked whale species, Cuvier’s beaked whales generally had the highest densities at HARP sites throughout the study period (Table 5). Analyses of the 10 years of weekly density timeseries at historic sites indicate Cuvier’s beaked whale densities were highest at Dry Tortugas (DT) with 136.1 animals per 1,000 km^2 followed by Mississippi Canyon (MC) with 8.1 animals per 1,000 km^2 and Green Canyon (GC) with 6.6 animals per 1,000 km^2 (Figure 30, Table 5). Densities at site DT appear to have declined over the 10 year monitoring period. Episodic peaks in density occurred at the GC and MC sites during some years, typically in late fall and early winter, suggesting potential seasonal movements to this site, and a similar winter increase may be occurring at the DT site. Cuvier’s beaked whales were not detected at either of the shallower historic sites (MP, DC).Analyses of the 2020-2021 deployments indicate Cuvier’s beaked whale mean weekly density was highest at Campeche Escarpment (CE; 240.4 animals per 1,000 km^2), higher than previously observed at the historically elevated site DT (Table 5, Figure 31). Cuvier’s beaked whale clicks were consistently seen throughout the year at nearly every site but were lowest at the moderately shallow (500 m bottom depth) short-term site Y1D (0.44 animals per 1,000 km^2), and they are not typically observed at the shallow long term site DC. Distinct seasonal patterns are not apparent in the 2020-2021 density timeseries, but some indication of potential seasonality is evident at the DT and Y1C sites (Figures 31 & 35). No apparent diel pattern exists among historical data or one-year sites (Figures 32, 33 & 34). While density of Cuvier’s beaked whales was more variable among sites during the 2020-2021 deployment (Figures 31 & 35), there was less variability in numbers of days present at sites throughout the year, with presence on more than 210 days per year at many sites (Figure 36).

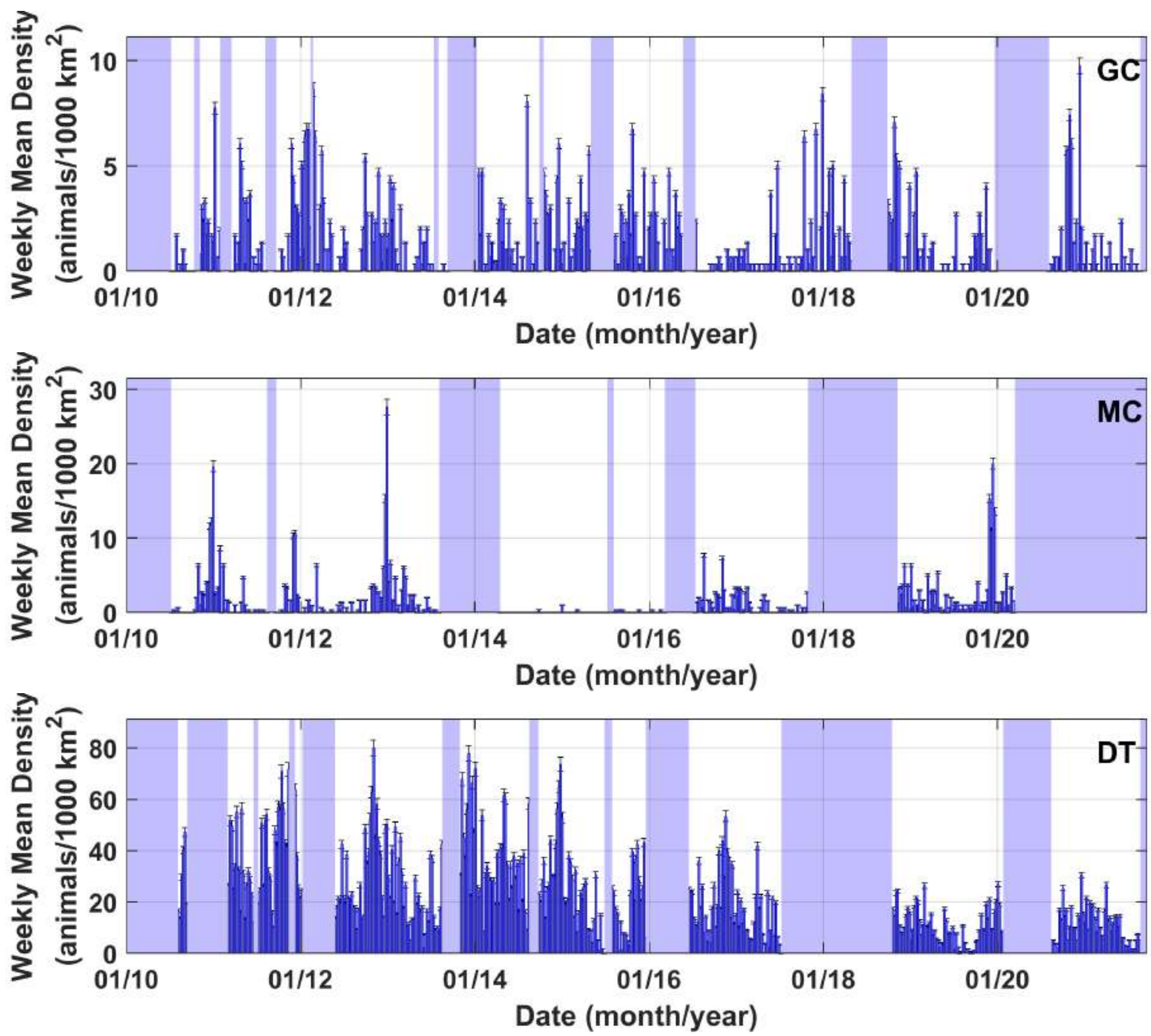

Figure 30: Historical weekly mean daily density (blue bars) of Cuvier's beaked whale echolocation clicks between 2010-2021 at sites GC, MC, and DT. Error bars represent ± 1 standard deviation. Shaded blue sections represent periods with no recording effort. Note: y-axis values vary for each site based on detection levels.

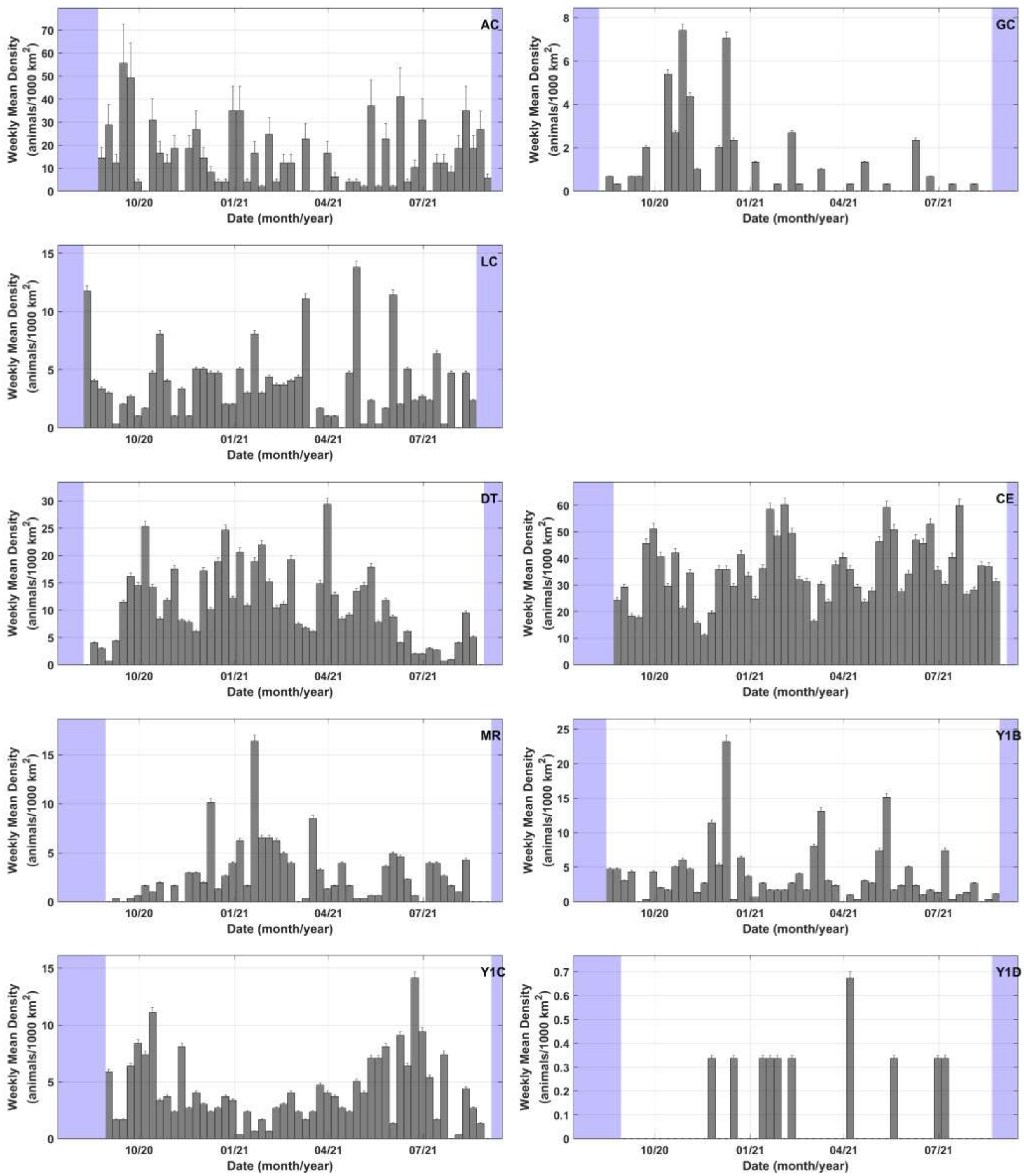

Figure 31: Weekly mean daily density (gray bars) of Cuvier's beaked whale echolocation clicks between 2020-2021 at sites AC, GC, LC, DT, CE, MR, Y1B, Y1C, Y1D. Error bars represent ± 1 standard deviation. Shaded blue sections represent periods with no recording effort. Note: y-axis values vary for each site based on detection levels.

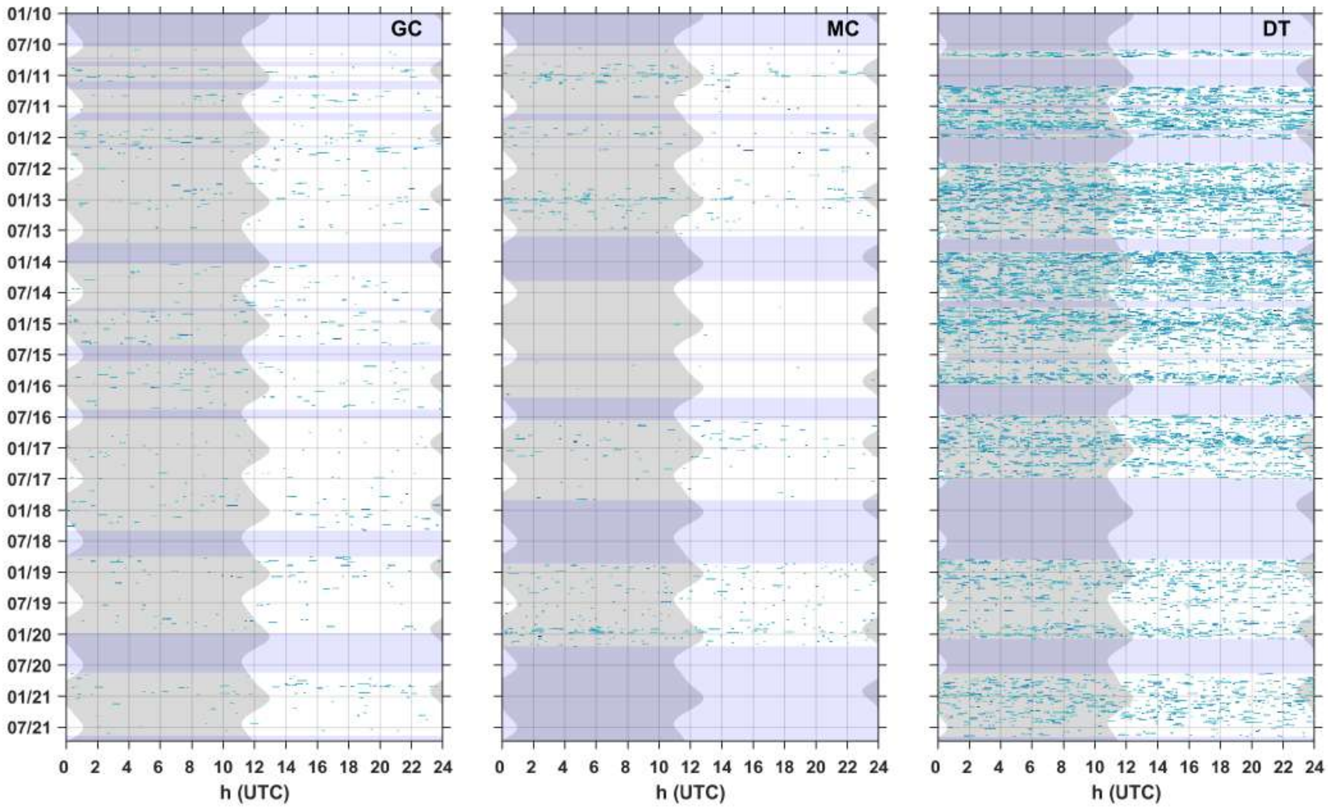

Figure 32: Cuvier's beaked whale echolocation clicks in five-minute bins at historic sites GC, MC, and DT from 2010-2021. Gray vertical shading denotes nighttime and light blue horizontal shading denotes absence of acoustic data. Color denotes number of detections per 5 minutes (light blue: <100; mid blue: 100-1000; dark blue: >1000).

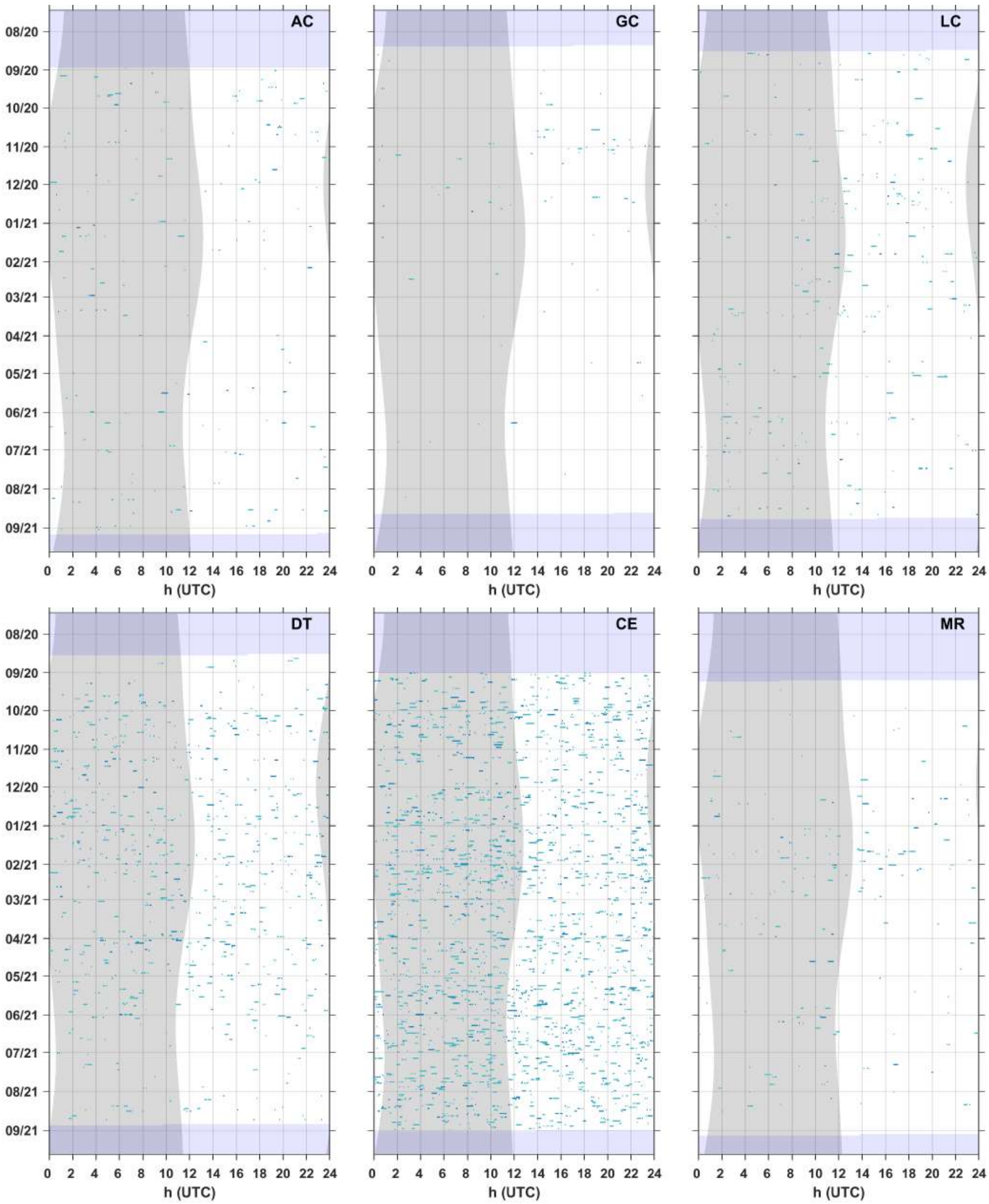

Figure 33: Cuvier's beaked whale echolocation clicks in five-minute bins at sites AC, GC, LC, DT, CE, and MR from 2020-2021. Gray vertical shading denotes nighttime and light blue horizontal shading denotes absence of acoustic data. Color denotes number of detections per 5 minutes (light blue: <100; mid blue: 100-1000; dark blue: >1000).

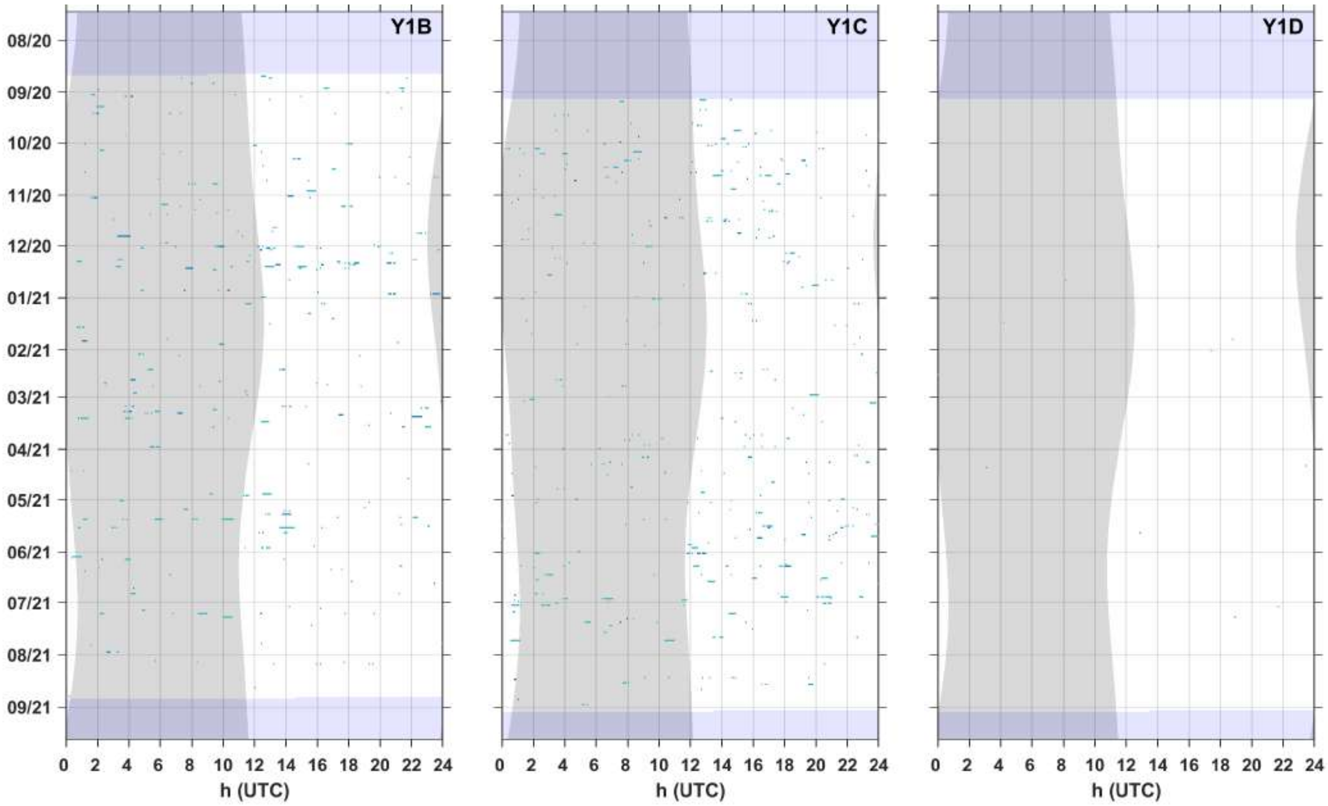

Figure 34: Cuvier's beaked whale echolocation clicks in five-minute bins at one-year sites Y1B, Y1C, and Y1D from 2020-2021. Gray vertical shading denotes nighttime and light blue horizontal shading denotes absence of acoustic data. Color denotes number of detections per 5 minutes (light blue: <100; mid blue: 100-1000; dark blue: >1000).

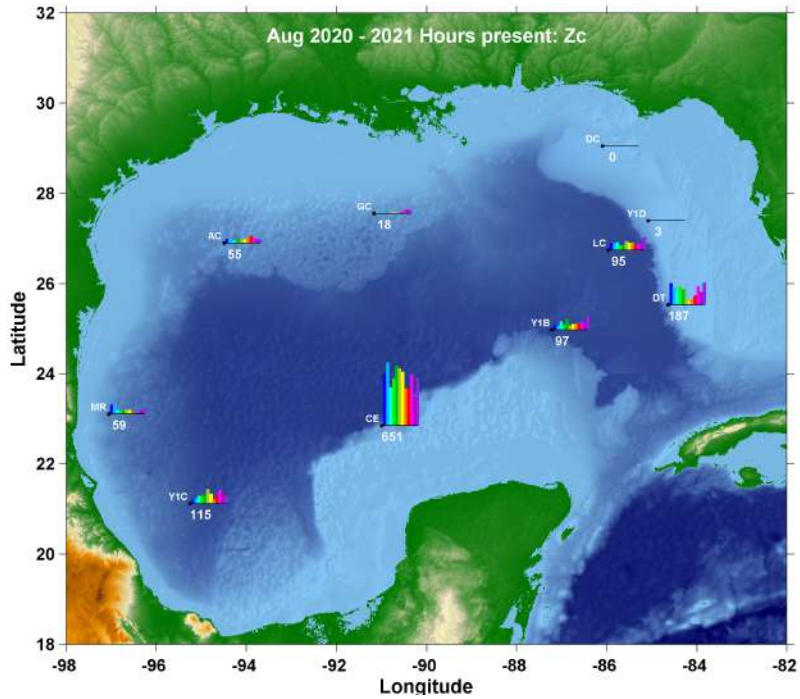

Figure 35: Hourly presence per month of Cuvier's beaked whale echolocation clicks from 2020-2021. Values below bar plots represent total hours per year present.

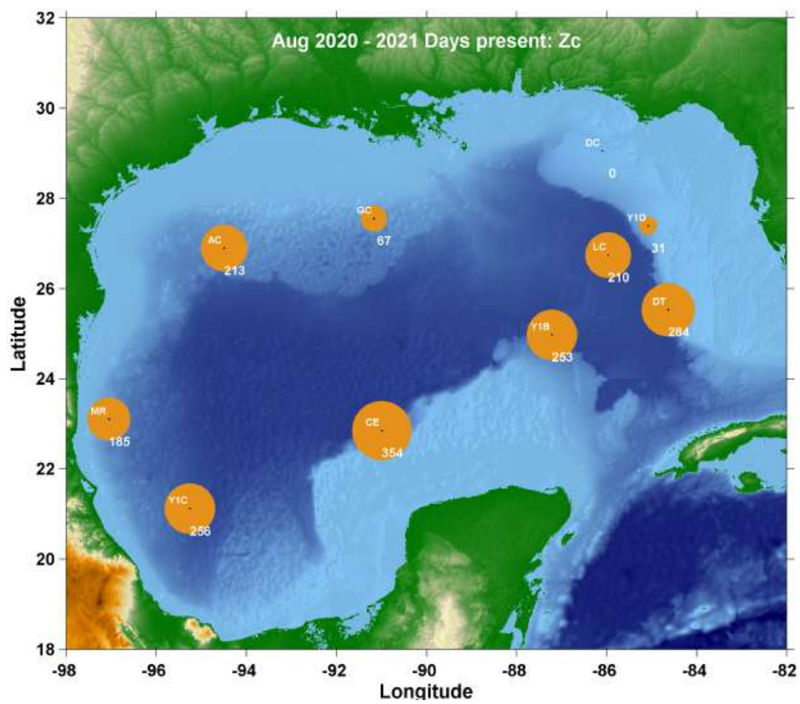

Figure 36: Days present per year for Cuvier's beaked whale echolocation clicks from 2020-2021.

4.1.2 Gervais' Beaked Whale

Analyses of the 10 years of weekly density timeseries at historic sites indicate Gervais' beaked whale densities were highest at Dry Tortugas (DT) with 53.27 animals per 1,000 km^2 followed by Green Canyon (GC) with 18.9 animals per 1,000 km^2 and Mississippi Canyon (MC) with 6.6 animals per 1,000 km^2 (Figure 37, Table 5). Gervais' beaked whales were not detected at either of the shallower historic sites (MP, DC). Densities of Gervais' beaked whales appear to have declined at all three historic sites with Gervais' beaked whales present over the historic monitoring period. Analyses of the 2020-2021 deployments indicate Gervais' beaked whale mean weekly density was highest at short term site Y1B (19.6 animals per 1,000 km^2) and at the new long-term Loop Current site (LC) (18.0 animals per 1,000 km^2) (Table 5, Figure 38). Both are lower than historic densities previously observed at DT. The elevated densities at these locations echo a previously-observed strong association with Gulf Stream waters in the western North Atlantic (Cohen et al. 2022). Gervais' beaked whale clicks are consistently seen at nearly every site but are lowest at Campeche Escarpment (CE) (0.5 animals per 1,000 km^2) where Cuvier's beaked whale density is high, and at the moderately shallow short-term site Y1D (0.2 animals per 1,000 km^2). Gervais' beaked whales were not detected at the shallow DC site. There is no clear evidence of seasonal patterns in Gervais' beaked whale densities or hourly presence in the historic data or in the 2020-2021 data for Gervais' beaked whale clicks (Figures 37, 38, & 42). No diel pattern is apparent in the historical data or one-year sites (Figures 39, 40 & 41). Similar to the relative consistency in Gervais' beaked whale density and hourly presence among sites during the 2020-2021 deployment (Figures 38 & 42), there was low variability in numbers of days present at sites throughout the year, with presence ranging between 67 to 193 days per year at all sites with Gervais' beaked whales detected (Figure 43).

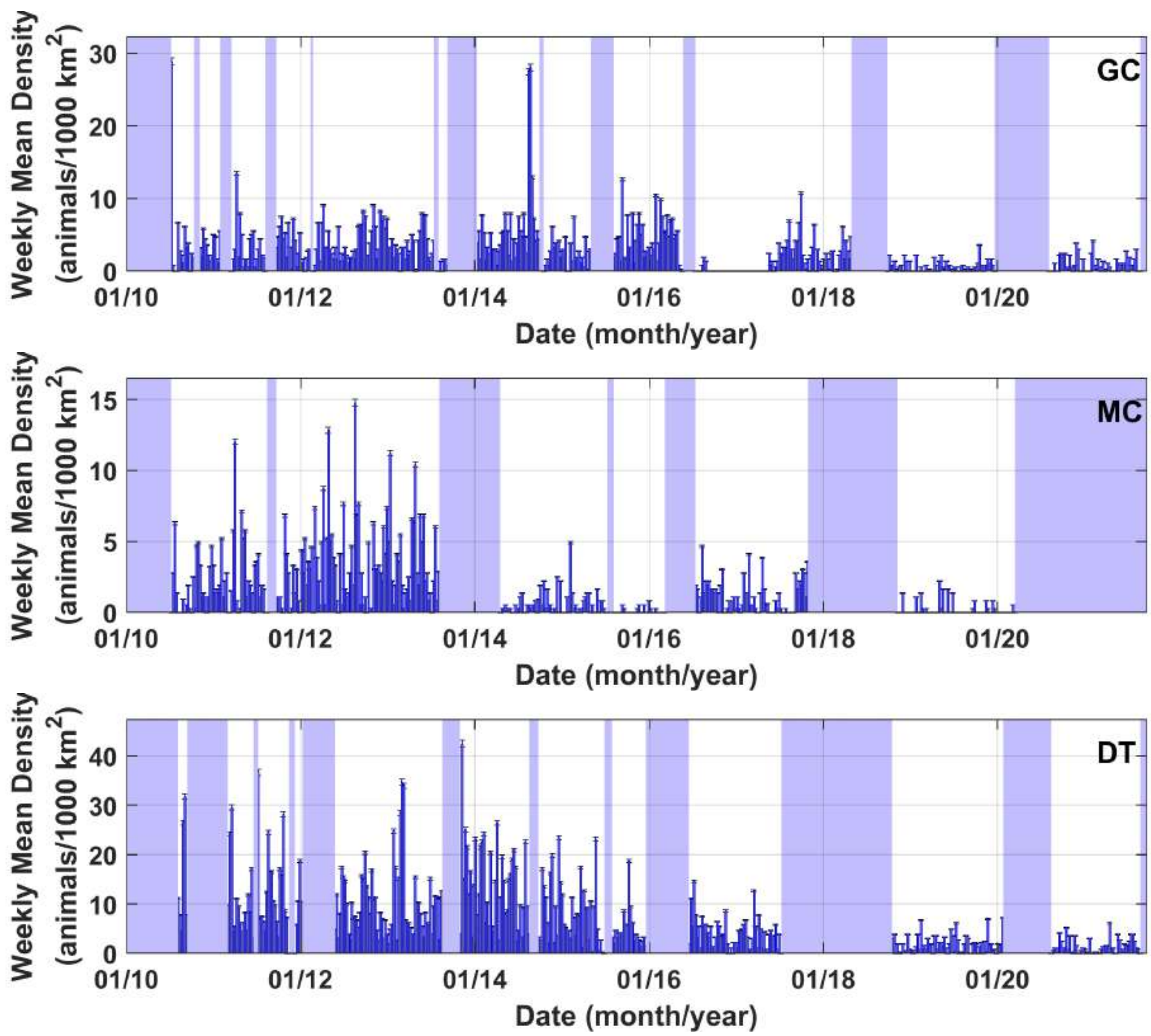

Figure 37: Historical weekly mean daily density (blue bars) of Gervais' beaked whale echolocation clicks between 2010-2021 at sites GC, MC, and DT. Error bars represent ± 1 standard deviation. Shaded blue sections represent periods with no recording effort. Note: y-axis values vary for each site based on detection levels.

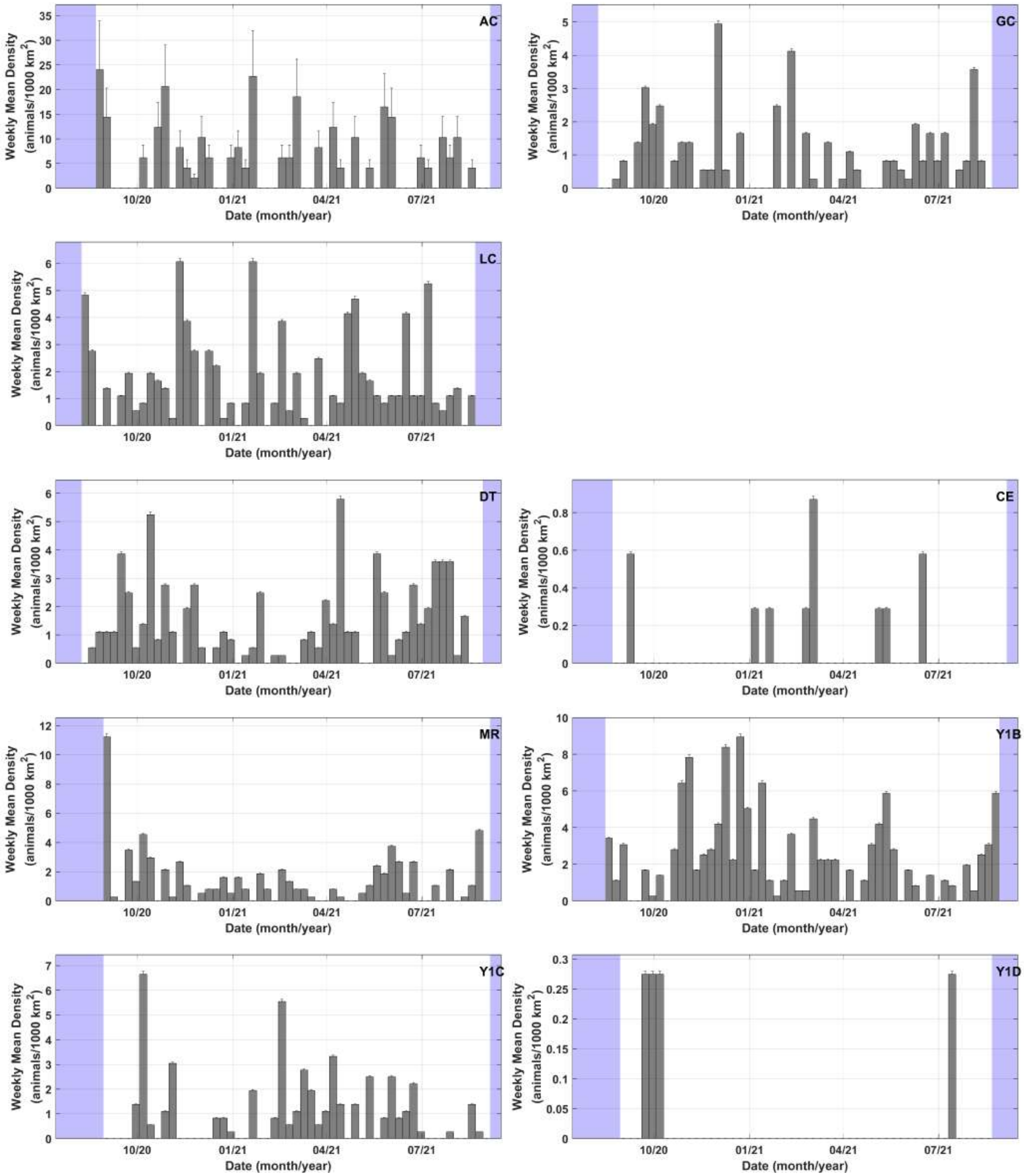

Figure 38: Weekly mean daily density (gray bars) of Gervais' beaked whale echolocation clicks between 2020-2021 at sites AC, GC, LC, DT, CE, MR, Y1B, Y1C, Y1D. Error bars represent ± 1 standard deviation. Shaded blue sections represent periods with no recording effort. Note: y-axis values vary for each site based on detection levels.

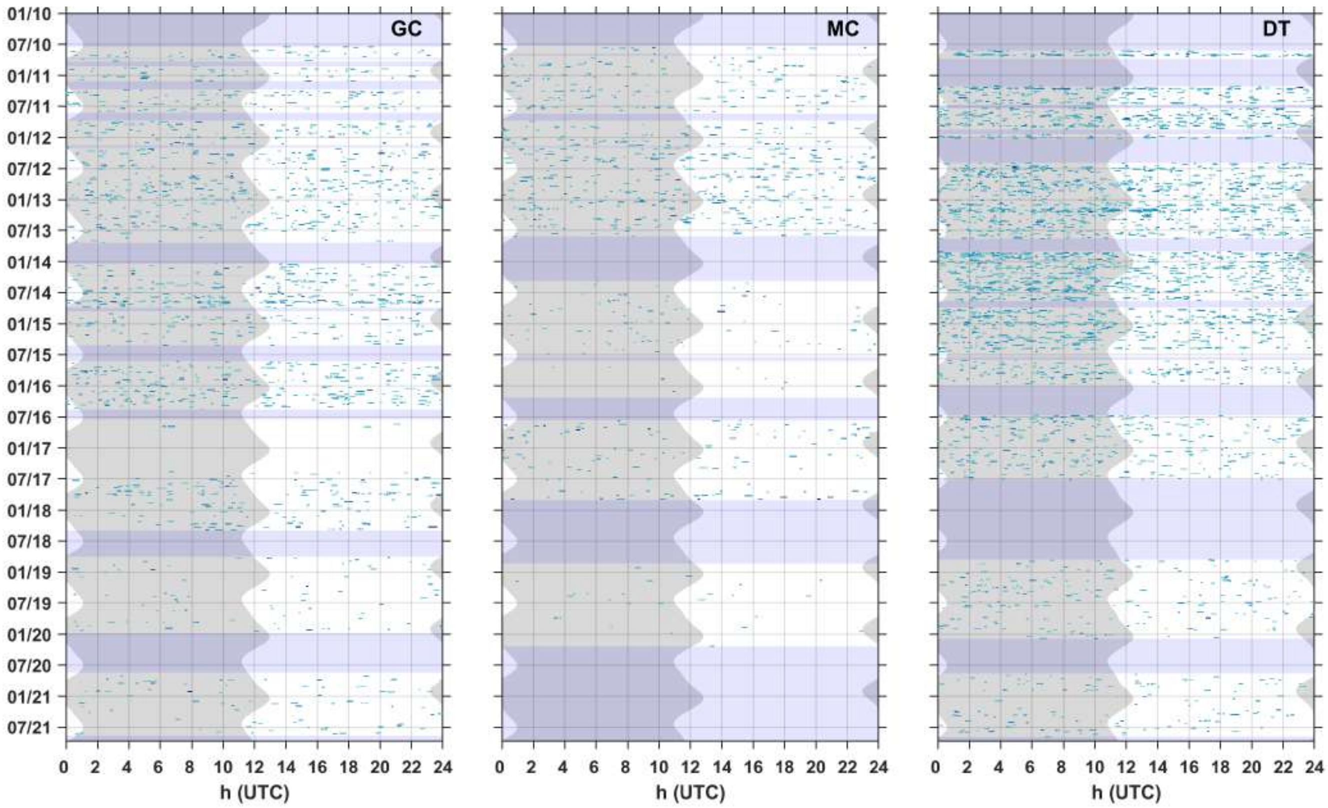

Figure 39: Gervais' beaked whale echolocation clicks in five-minute bins at historic sites GC, MC, and DT from 2010-2021. Gray vertical shading denotes nighttime and light blue horizontal shading denotes absence of acoustic data. Color denotes number of detections per 5 minutes (light blue: <100; mid blue: 100-1000; dark blue: >1000).

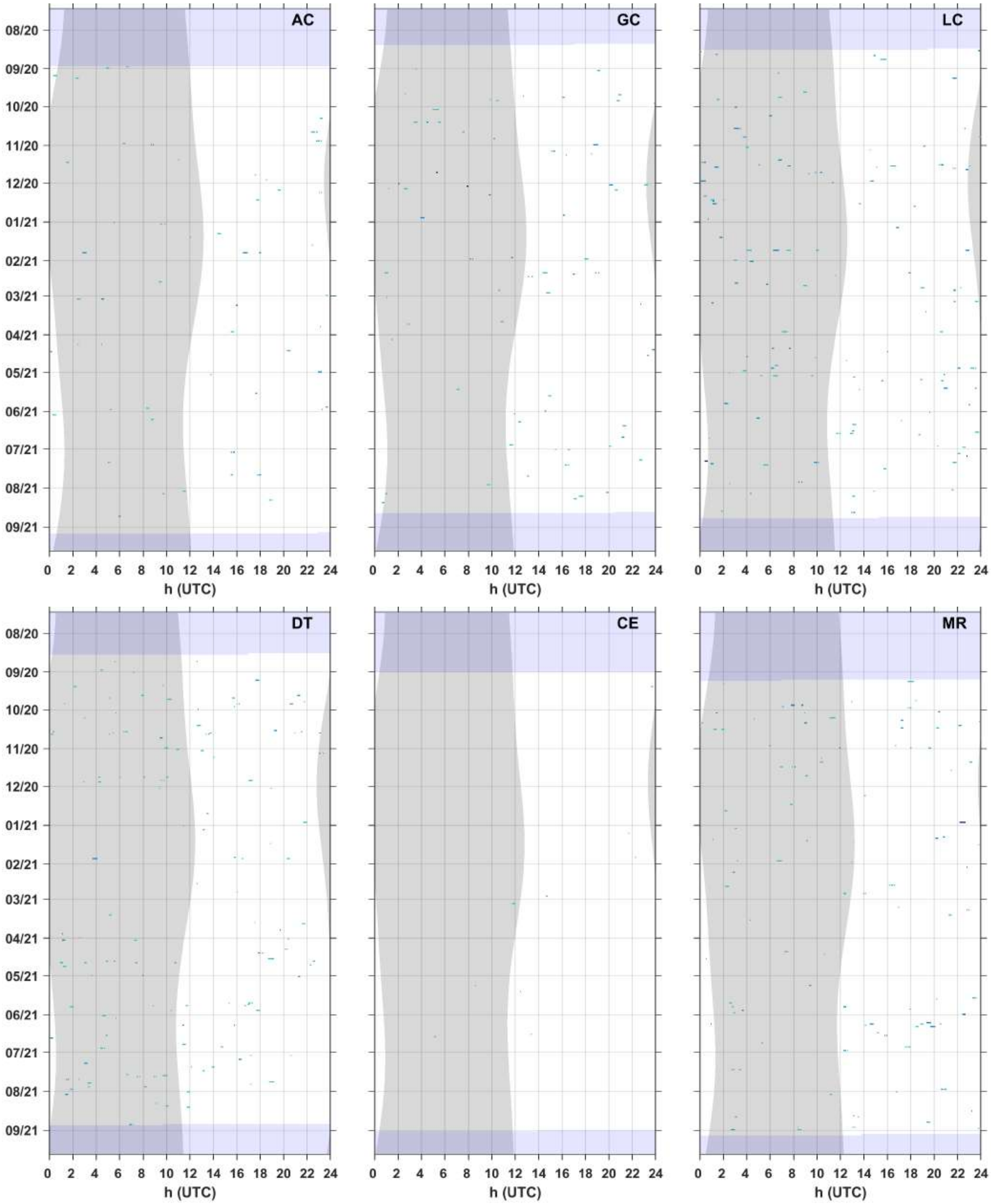

Figure 40: Gervais' beaked whale echolocation clicks in five-minute bins at sites AC, GC, LC, DT, CE, and MR from 2020-2021. Gray vertical shading denotes nighttime and light blue horizontal shading denotes absence of acoustic data. Color denotes number of detections per 5 minutes (light blue: <100; mid blue: 100-1000; dark blue: >1000).

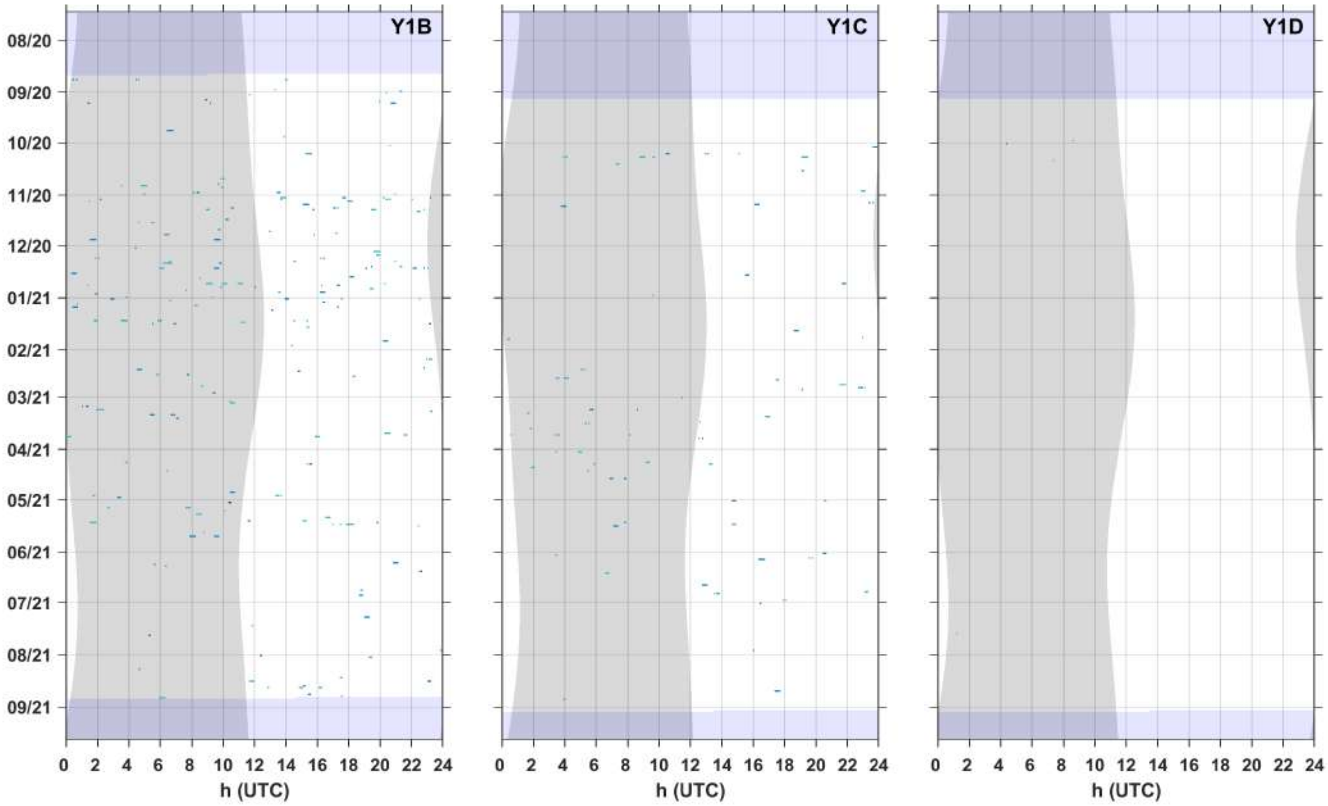

Figure 41: Gervais' beaked whale echolocation clicks in five-minute bins at one-year sites Y1B, Y1C, and Y1D from 2020-2021. Gray vertical shading denotes nighttime and light blue horizontal shading denotes absence of acoustic data. Color denotes number of detections per 5 minutes (light blue: <100; mid blue: 100-1000; dark blue: >1000).

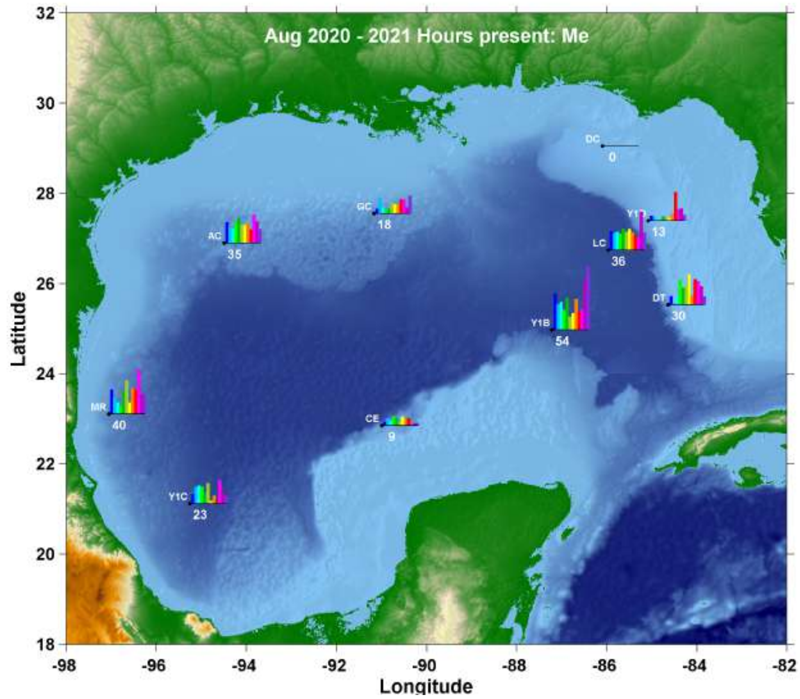

Figure 42: Hourly presence per month for Gervais' beaked whale echolocation clicks from 2020-2021. Values below bar plots represent total hours per year present.

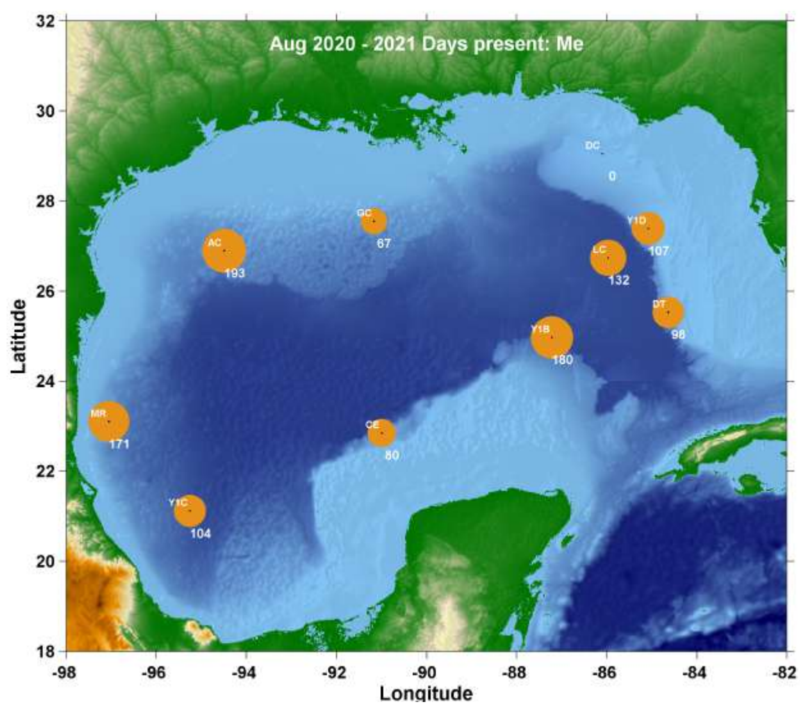

Figure 43: Days present per year for Gervais' beaked whale echolocation clicks from 2020-2021.

4.1.3 Blainville's Beaked Whale

Densities for Blainville's beaked whale are typically the lowest of the three beaked whale species (Table 5). Densities were very low over the 10 years of weekly density timeseries at the historic sites (Figure 44, Table 5). However, in the 2020-2021 data, high densities of Blainville's were observed in the southern GoMex at the short-term site Y1C (64.4 animals per 1,000 km^2), and at the new long-term site CE (16.1 animals per 1,000 km^2), where Cuvier's beaked whale densities were also high (Figure 45, Table 5). Blainville's beaked whale clicks are intermittently observed at other sites (Figure 45). No apparent diel pattern exists among historical data or one-year sites (Figures 46, 47 & 48). There is no clear evidence of seasonal patterns in Blainville's beaked whale densities or hourly presence in the historic data or in the 2020-2021 data (Figures 44, 46, & 49). Similar to the high variability in Gervais' beaked whale density and hourly presence among sites during the 2020-2021 deployment (Figures 38 & 42), there was high variability in numbers of days present throughout the year among sites, ranging between 14 to 214 days per year at all sites with Gervais' beaked whales detected (Figure 50).

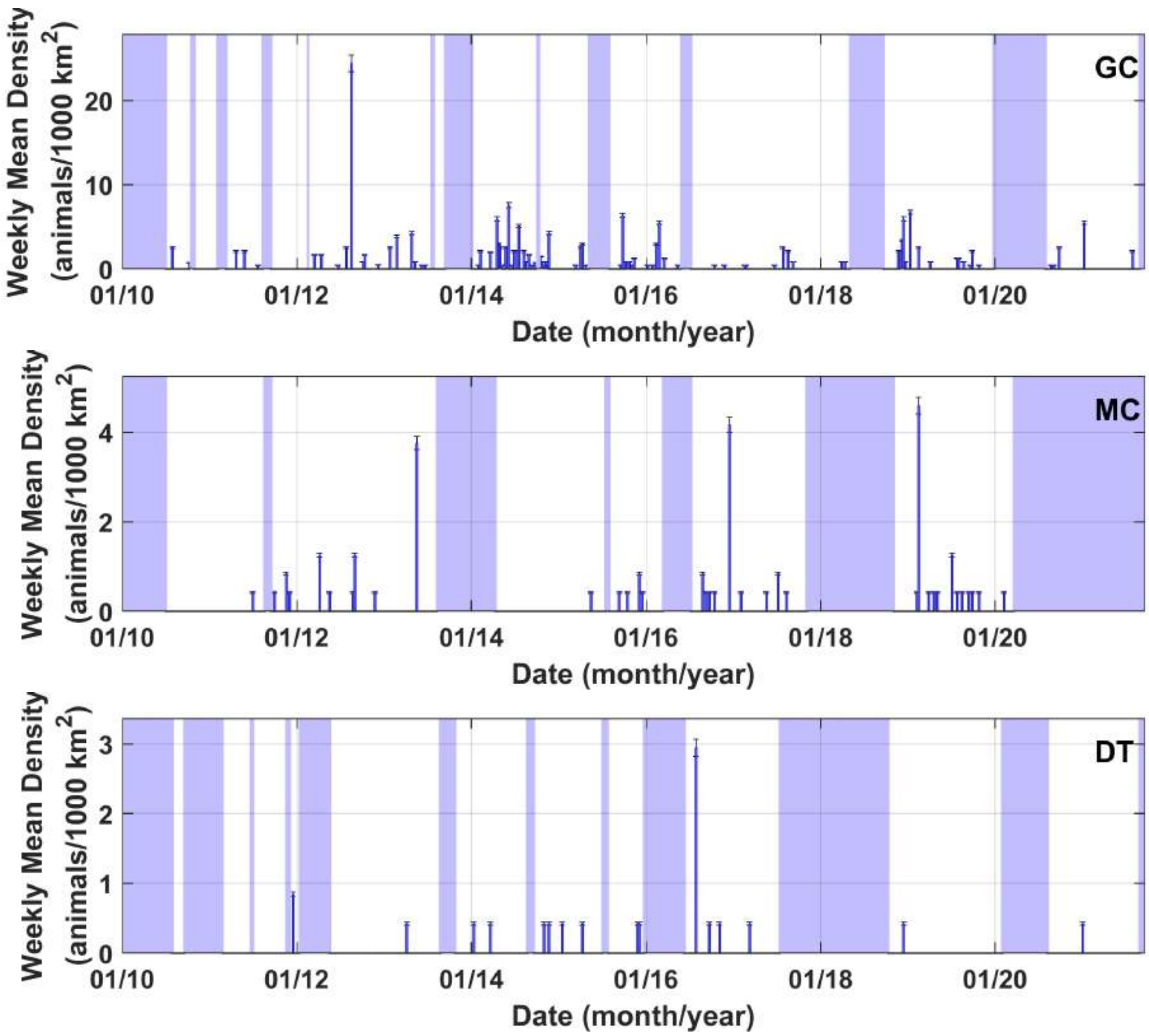

Figure 44: Historical weekly mean daily density (blue bars) of Blainville's beaked whale echolocation clicks between 2010-2021 at sites GC, MC, and DT. Error bars represent ± 1 standard deviation. Shaded blue sections represent periods with no recording effort. Note: y-axis values vary for each site based on detection levels.

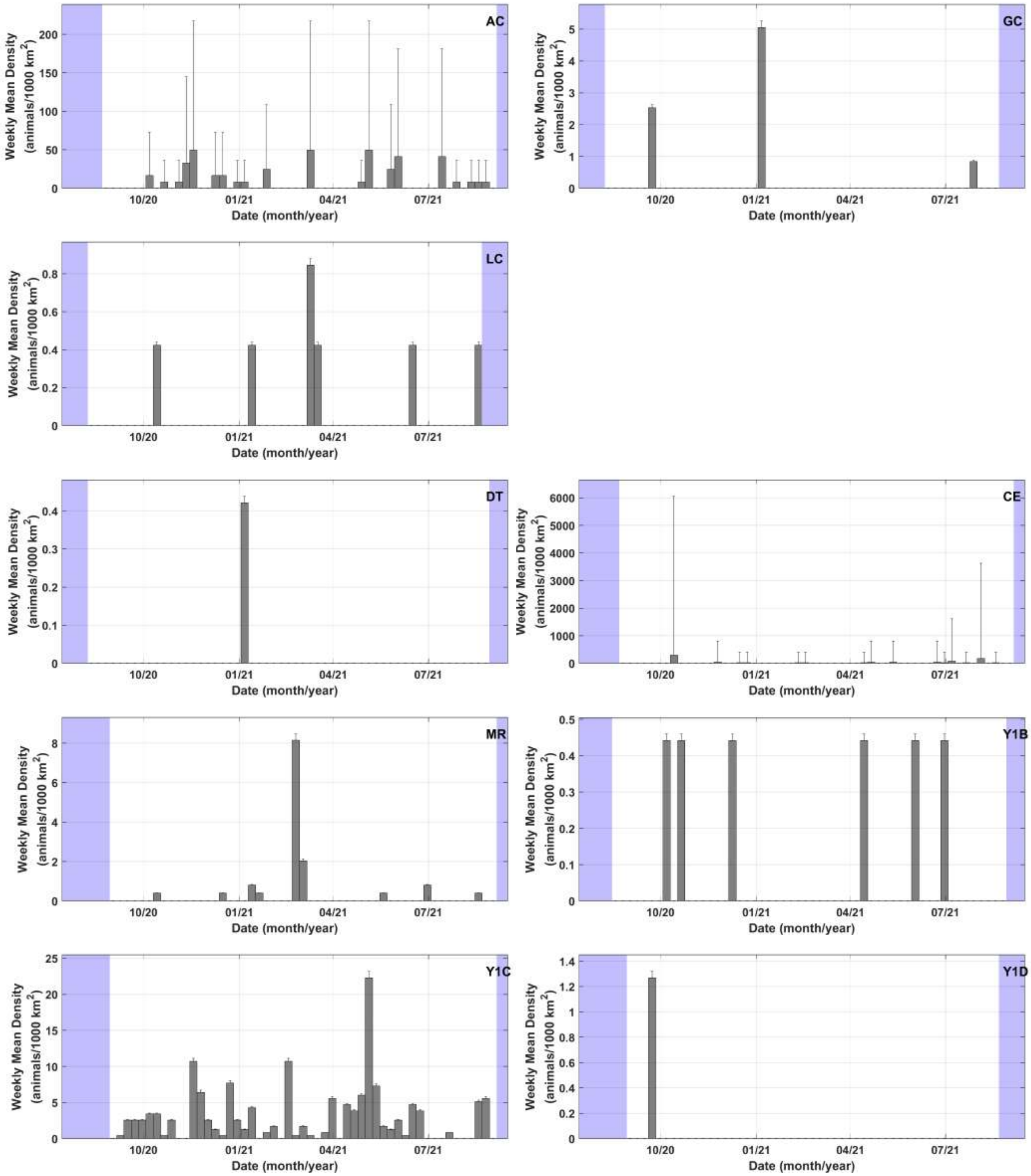

Figure 45: Weekly mean daily density (blue bars) of Blainville's beaked whale echolocation clicks between 2020-2021 at sites AC, GC, LC, DT, CE, MR, Y1B, Y1C, Y1D. Error bars represent ± 1 standard deviation. Shaded blue sections represent periods with no recording effort. Note: y-axis values vary for each site based on detection levels.

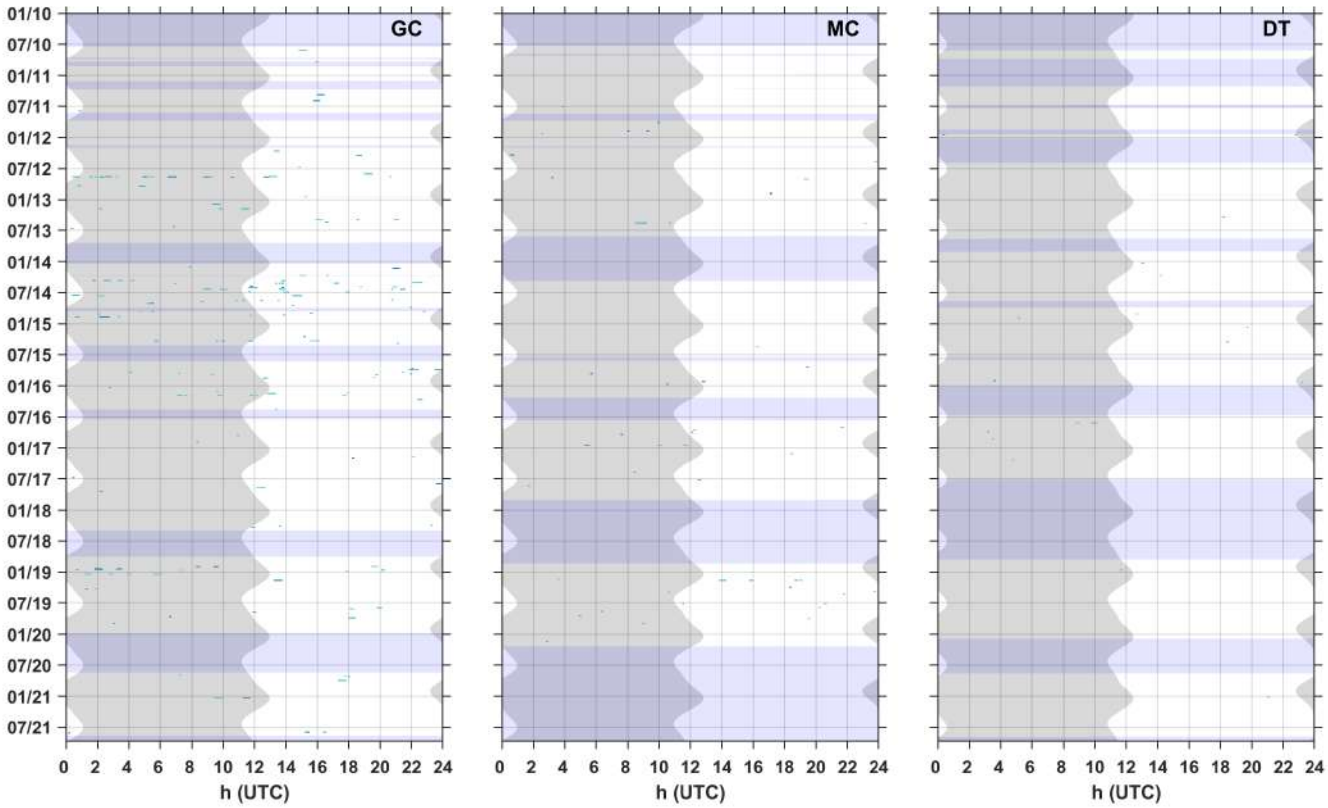

Figure 46: Blainville's beaked whale echolocation clicks in five-minute bins at historic sites GC, MC, and DT from 2010-2021. Gray vertical shading denotes nighttime and light blue horizontal shading denotes absence of acoustic data. Color denotes number of detections per 5 minutes (light blue: <100; mid blue: 100-1000; dark blue: >1000).

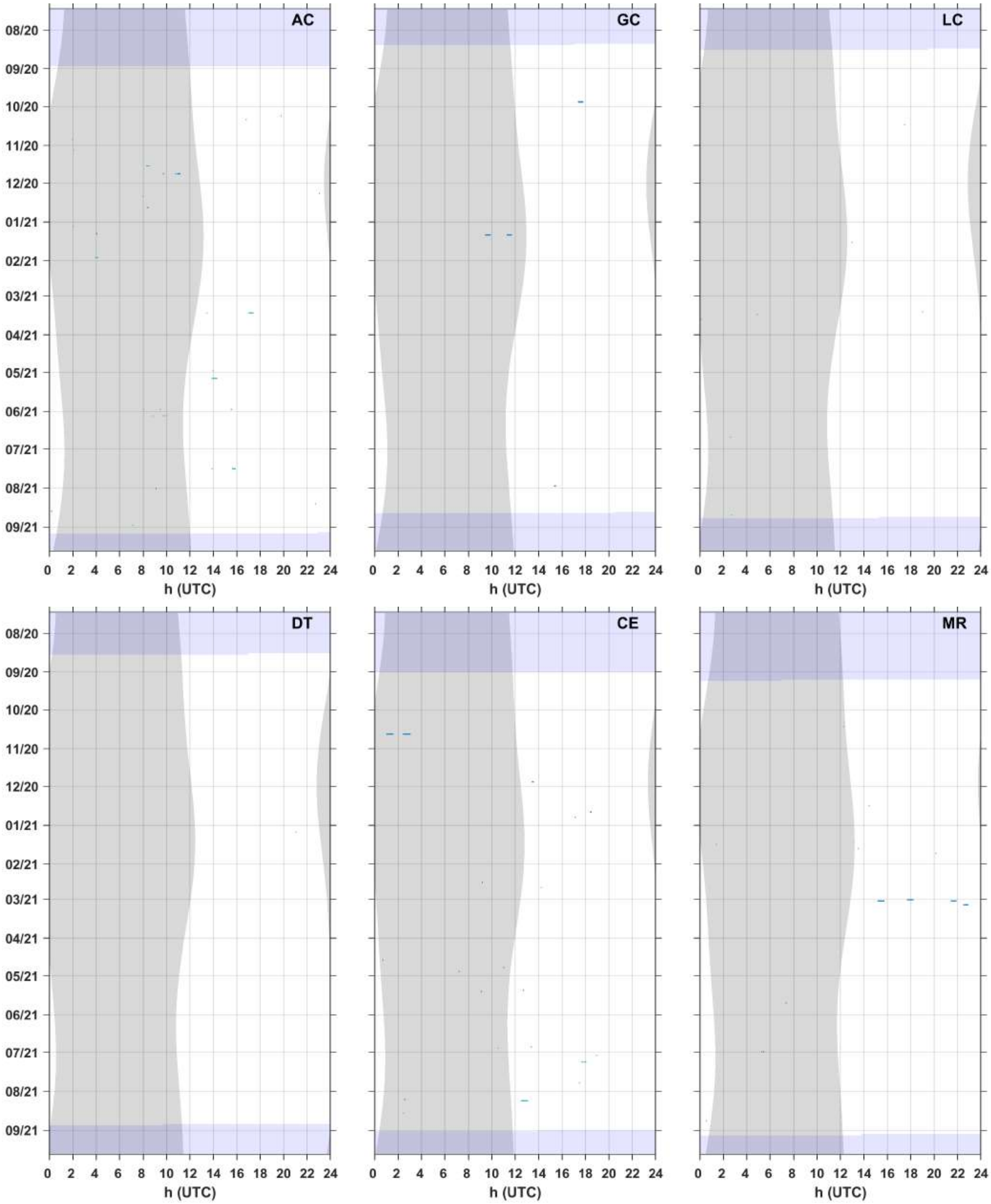

Figure 47: Blainville's beaked whale echolocation clicks in five-minute bins at sites AC, GC, LC, DT, CE, and MR from 2020-2021. Gray vertical shading denotes nighttime and light blue horizontal shading denotes absence of acoustic data. Color denotes number of detections per 5 minutes (light blue: <100; mid blue: 100-1000; dark blue: >1000).

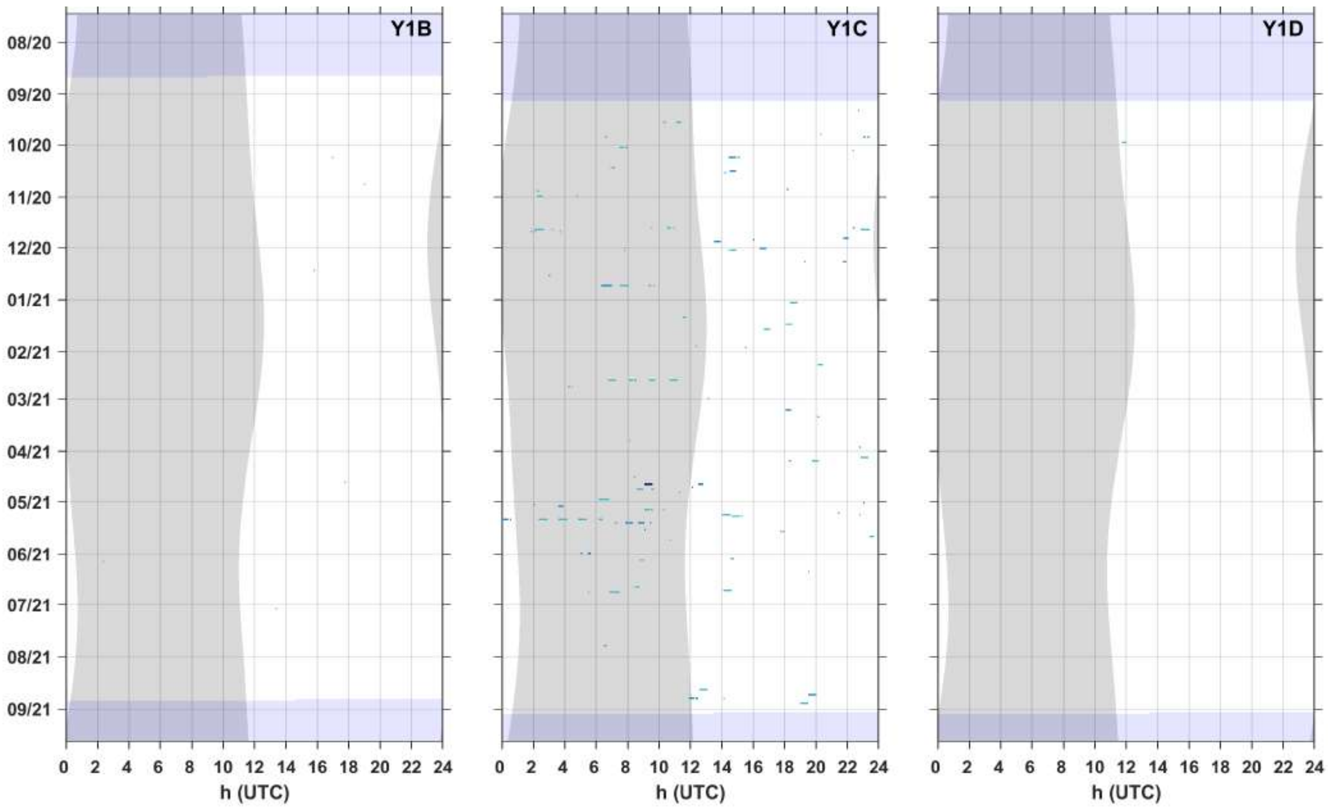

Figure 48: Blainville's beaked whale echolocation clicks in five-minute bins at one-year sites Y1B, Y1C, and Y1D from 2020-2021. Gray vertical shading denotes nighttime and light blue horizontal shading denotes absence of acoustic data. Color denotes number of detections per 5 minutes (light blue: <100; mid blue: 100-1000; dark blue: >1000).

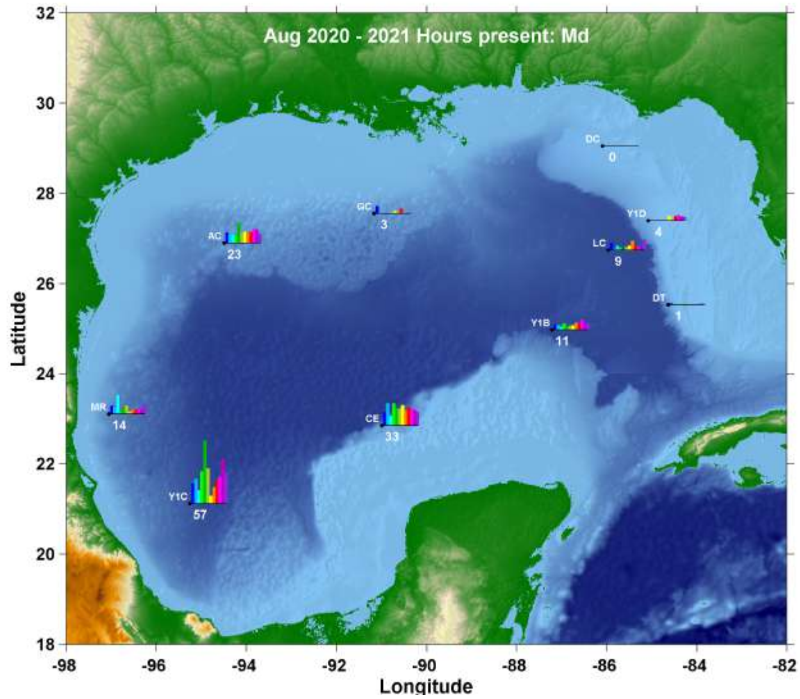

Figure 49: Hourly presence per month for Blainville's beaked whale echolocation clicks from 2020-2021. Values below bar plots represent total hours per year present.

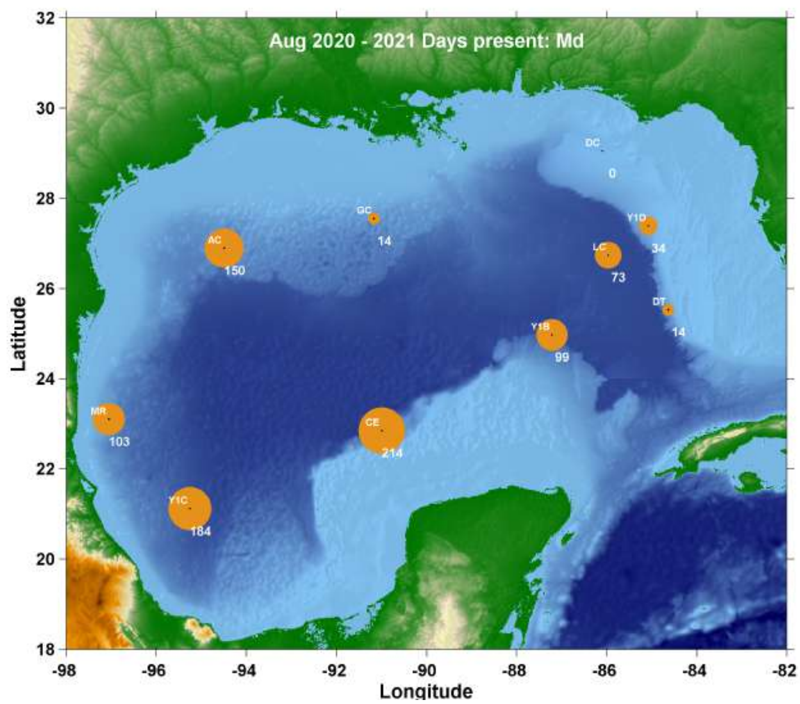

Figure 50: Days present per year for Blainville's beaked whale echolocation clicks from 2020-2021.

4.1.4 Sperm Whales

Analyses of the 10 years of weekly density timeseries at historic sites indicate sperm whale densities were highest at Mississippi Canyon (MC) with 8.0 animals per 1,000 km^2 followed by Green Canyon (GC) with 2.9 animals per 1,000 km^2 and Dry Tortugas (DT) with 1.6 animals per 1,000 km^2 (Figure 51, Table 5). Sperm whales were not detected at the shallower DC and MP sites. Densities at site DT appear to have increased over the 10-year monitoring period. Analyses of the 2020-2021 deployments indicate sperm whale mean weekly density was highest at Mexican Ridges (MR) (4.3 animals per 1,000 km^2) (Table 5). Sperm whale clicks are consistently detected at nearly every site but densities are lowest at short-term site Y1D (0.3 animals per 1,000 km^2), and LC (0.4 animals per 1,000 km^2) and they are not typically observed at the shallow site DC (Figure 53, Table 5). No strong seasonal patterns in density or hourly presence are in the historic data or 2020-2021 data (Figures 51, 52 & 56), due to the high variability, but there appear to be elevated densities in fall at site MR, and in late summer at DT (Figures 51 & 52) and increased hourly presence in summer at GC, fall to early winter at MR, and spring and fall at sites Y1C and CE (Figure 53). No diel pattern is apparent in the historical data or the 2020-2021 data (Figures 53, 54 & 55). Sperm whale hourly and daily presence is high across most sites, in part due to the long detection distances associated with their high source level, low to mid-frequency echolocation clicks (Figures 56 & 57). Sperm whale clicks are present most days of the year at most sites, ranging from 240 to 344 days per year at sites with moderate to high densities (Figure 57, Table 5).

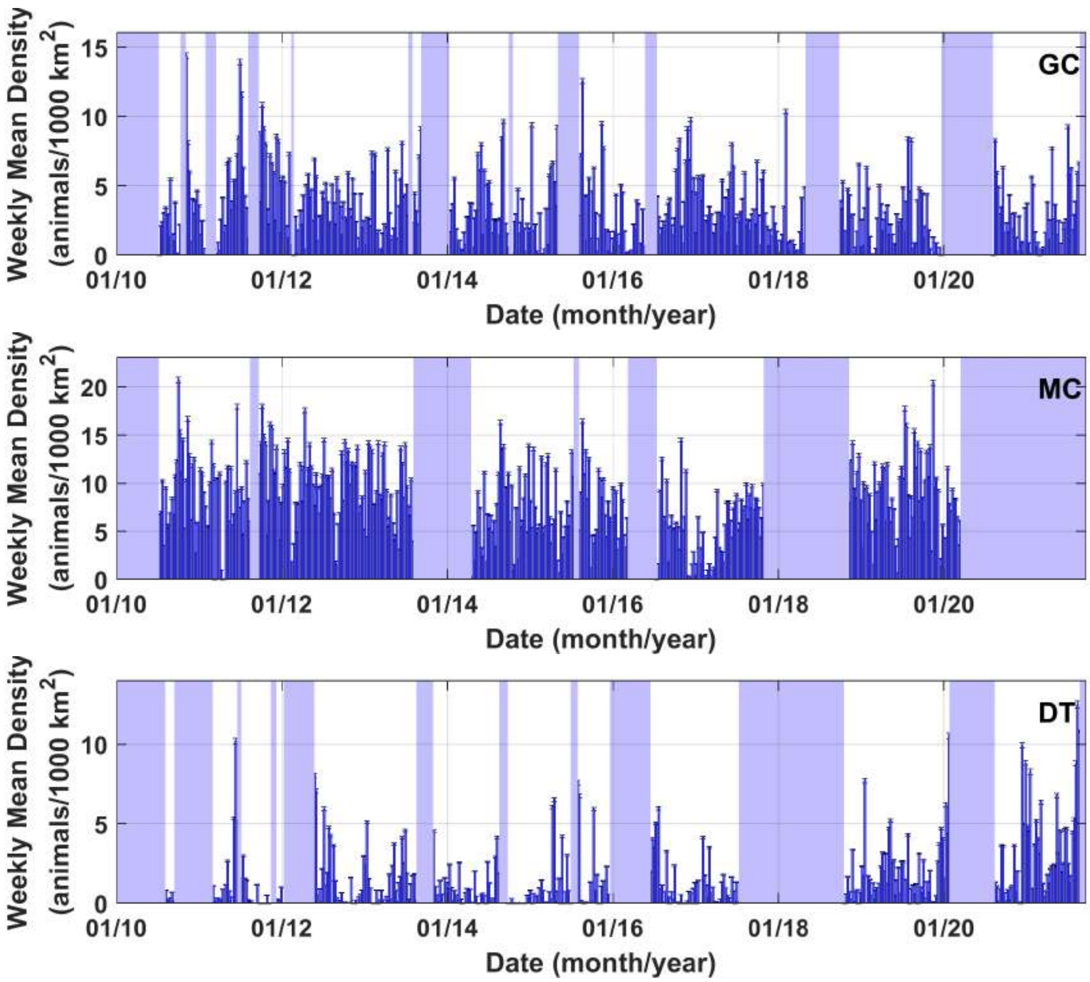

Figure 51: Historical weekly mean daily density (blue bars) of sperm whale echolocation clicks between 2010-2021 at sites GC, MC, and DT. Error bars represent ± 1 standard deviation. Shaded blue sections represent periods with no recording effort. Note: y-axis values vary for each site based on detection levels.

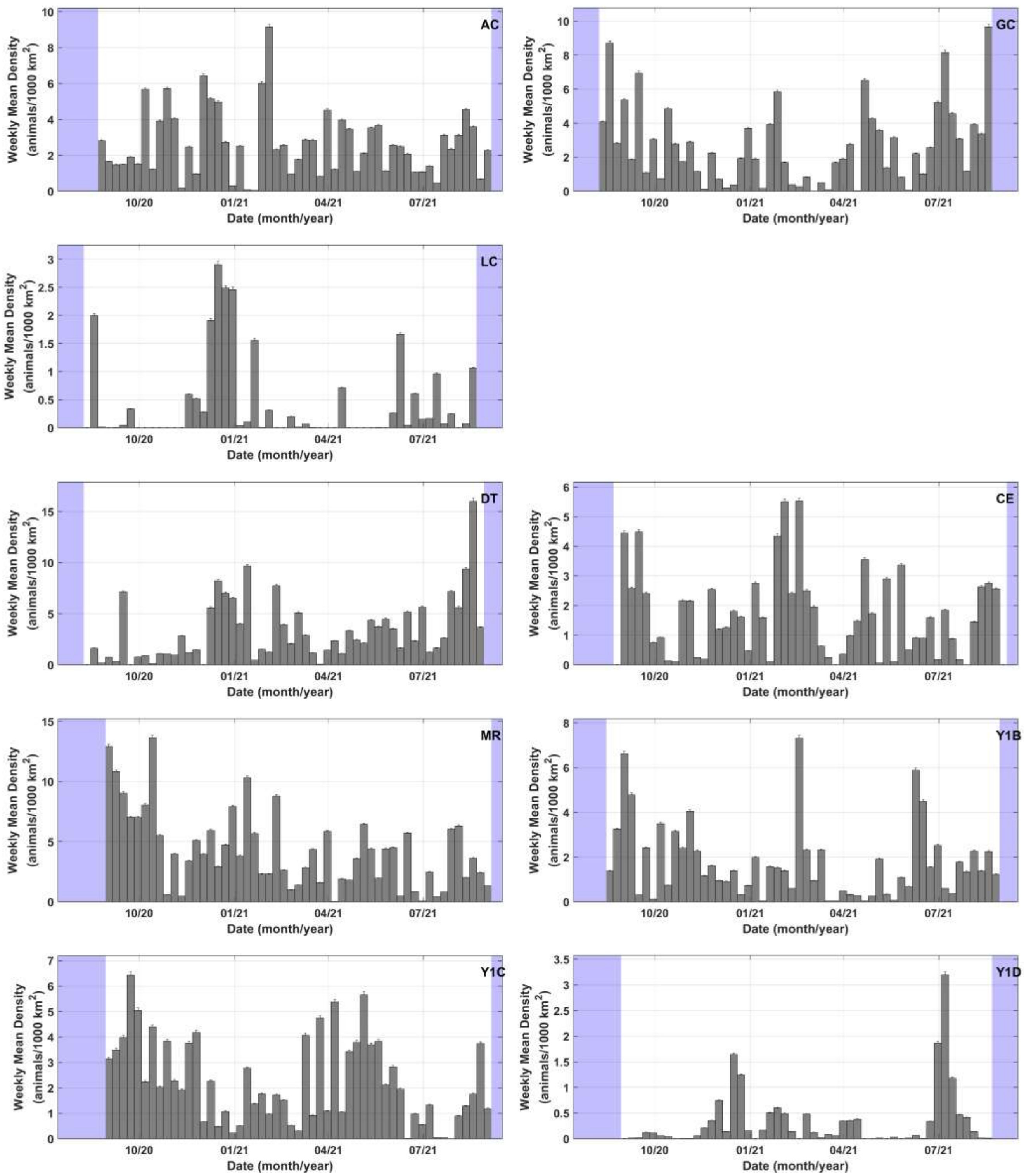

Figure 52: Weekly mean daily density (blue bars) of sperm whale echolocation clicks between 2020-2021 at sites AC, GC, LC, DT, CE, MR, Y1B, Y1C, Y1D. Error bars represent ± 1 standard deviation. Shaded blue sections represent periods with no recording effort. Note: y-axis values vary for each site based on detection levels.

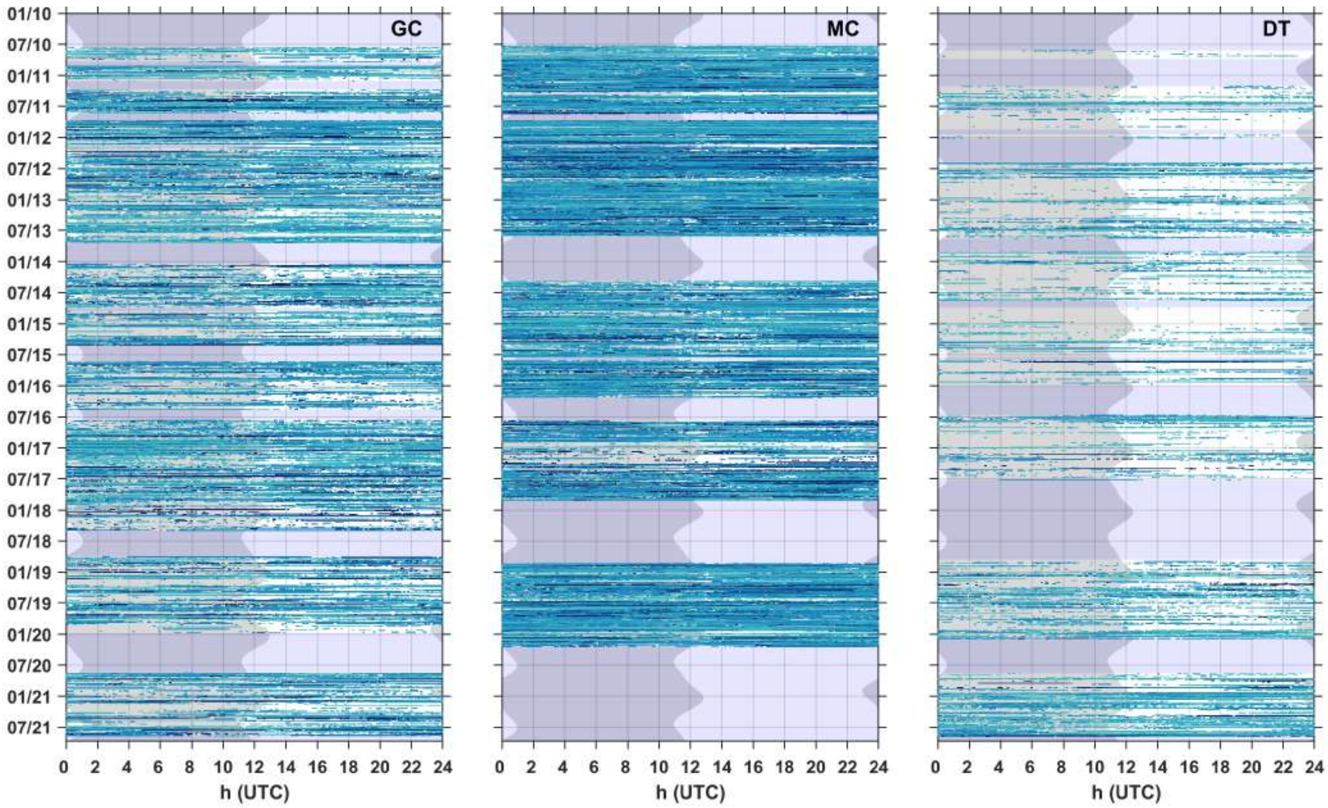

Figure 53: Sperm whale echolocation clicks in five-minute bins at historic sites GC, MC, and DT from 2010-2021. Gray vertical shading denotes nighttime and light blue horizontal shading denotes absence of acoustic data. Color denotes number of detections per 5 minutes (light blue: <100; mid blue: 100-1000; dark blue: >1000).

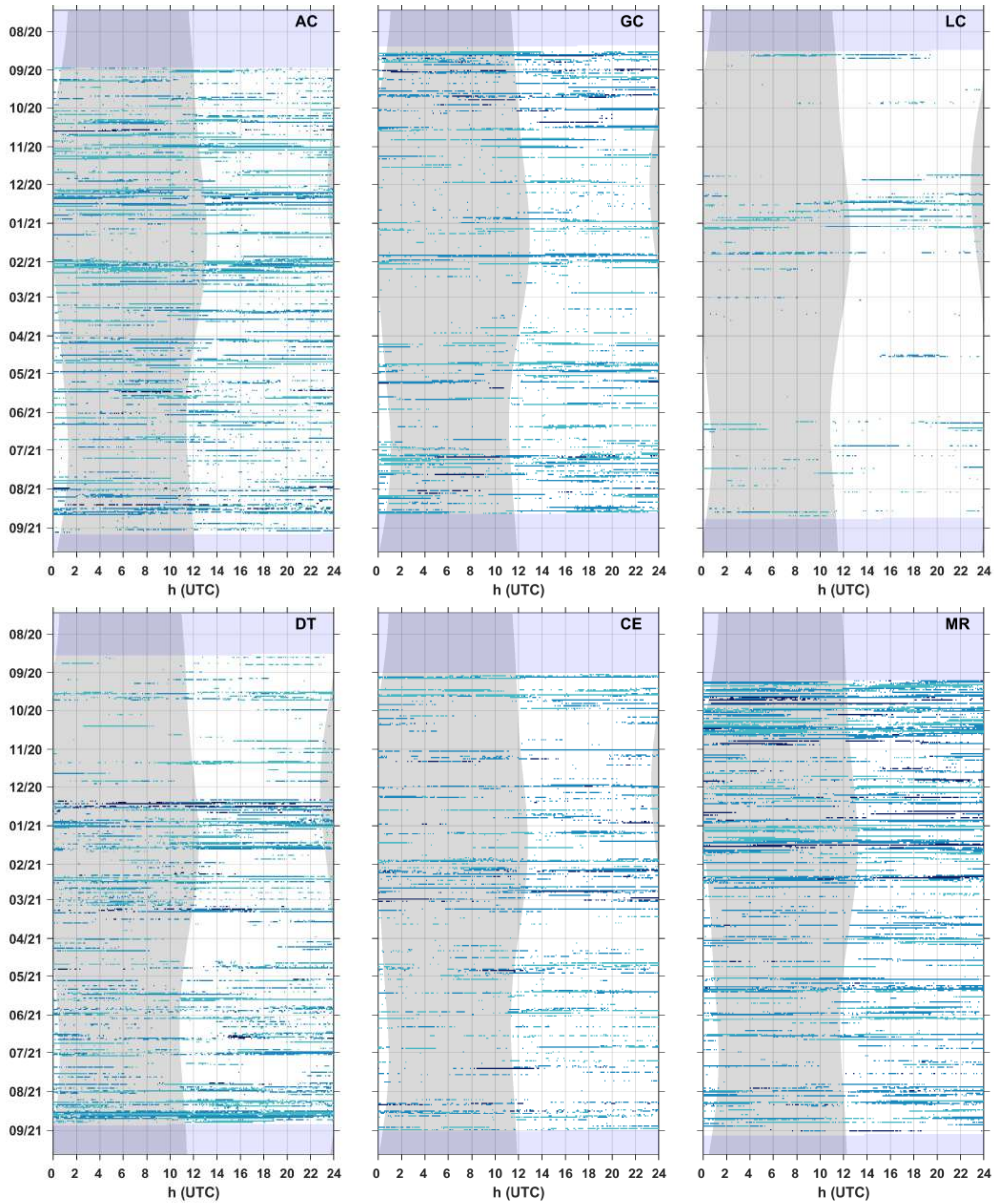

Figure 54: Sperm whale echolocation clicks in five-minute bins at sites AC, GC, LC, DT, CE, and MR from 2020-2021. Gray vertical shading denotes nighttime and light blue horizontal shading denotes absence of acoustic data. Color denotes number of detections per 5 minutes (light blue: <100; mid blue: 100-1000; dark blue: >1000).

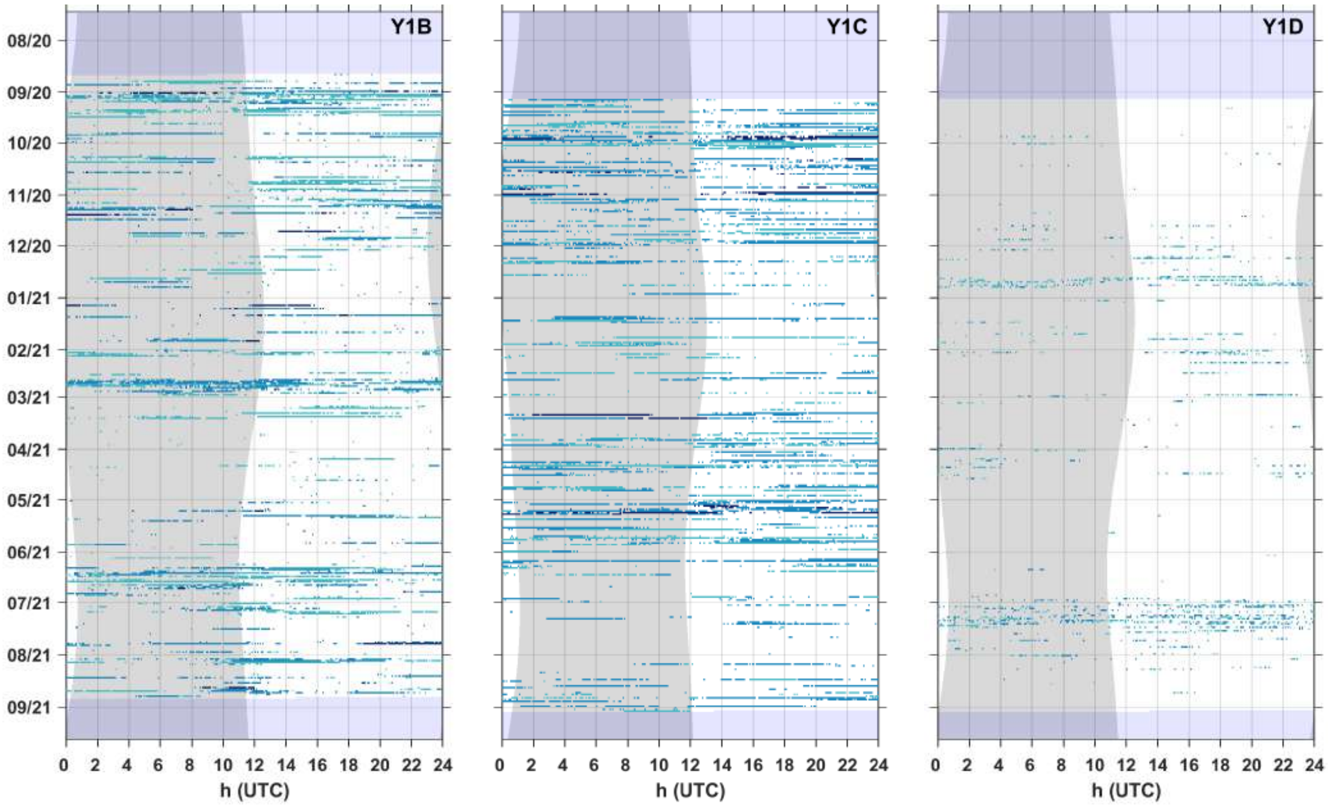

Figure 55: Sperm whale echolocation clicks in five-minute bins at one-year sites Y1B, Y1C, and Y1D from 2020-2021. Gray vertical shading denotes nighttime and light blue horizontal shading denotes absence of acoustic data. Color denotes number of detections per 5 minutes (light blue: <100; mid blue: 100-1000; dark blue: >1000).

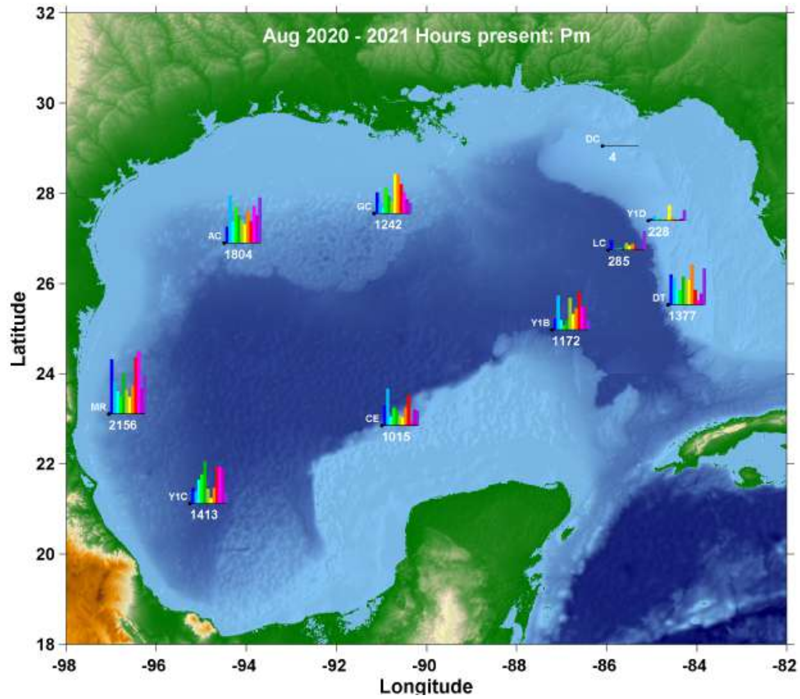

Figure 56: Hourly presence per month of sperm whale echolocation clicks from 2020-2021. Values below bar plots represent total hours per year present.

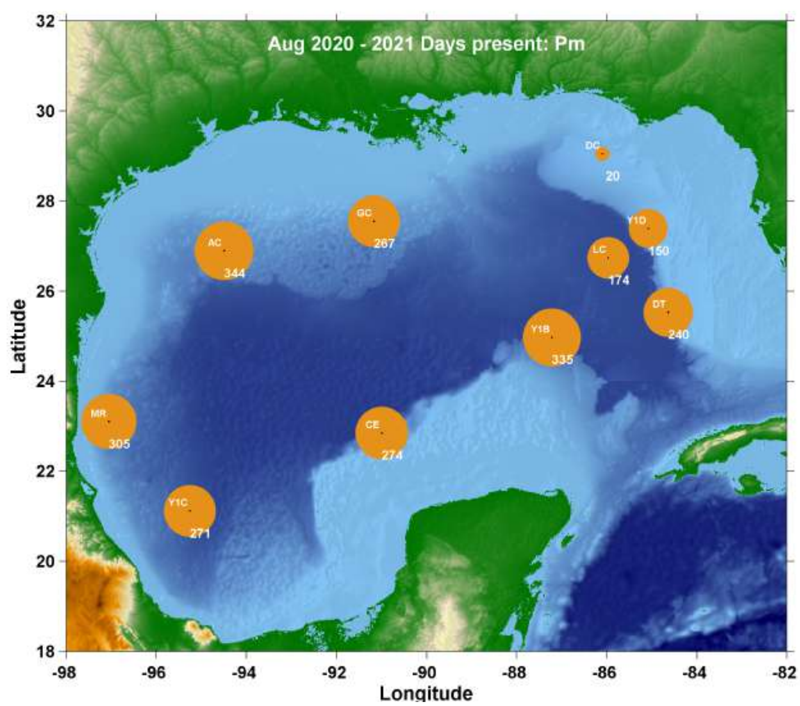

Figure 57: Days present per year for sperm whale echolocation clicks from 2020-2021.

4.1.5 *Kogia* spp.

Analyses of the 10 years of weekly density timeseries at historic sites indicate densities for *Kogia* spp. were highest at Mississippi Canyon (MC) with 8.6 animals per 1,000 km^2 followed by Green Canyon (GC) with 6.6 animals per 1,000 km^2 and Dry Tortugas (DT) with 1.4 animals per 1,000 km^2 (Figure 58, Table 5). While no consistent density trends were evident over the 10 year time-period, there appears to be interannual variation at sites GC and MC with increased densities in some years compared to others, and years with high densities at GC tend to have low densities at MC (Figure 58). Analyses of the 2020-2021 deployments indicate *Kogia* spp. mean weekly in the new sites density was highest at Y1C (25.9 animals per 1,000 km^2) (Table 5). High densities relative to the historic sites were also observed at Y1B, MR, LC and AC (Figure 59, Table 5). *Kogia* clicks are consistently detected at nearly every site but densities were lowest at site DT (0.8 animals per 1,000 km^2), and they are not typically observed at the shallow site DC. No strong seasonal patterns in density are apparent in the historic data or the 2020-2021 data, but hourly presence was increased in late summer to fall at site Y1D (Figures 58, 59, & 63). No apparent diel pattern exists among the historical or 2020-2021 data (Figures 60, 61 & 62). At most sites, other than DC, DT, and GC, *Kogia* spp. were present most days of the year, typically ranging from 171 to 293 days per year (Figure 64).

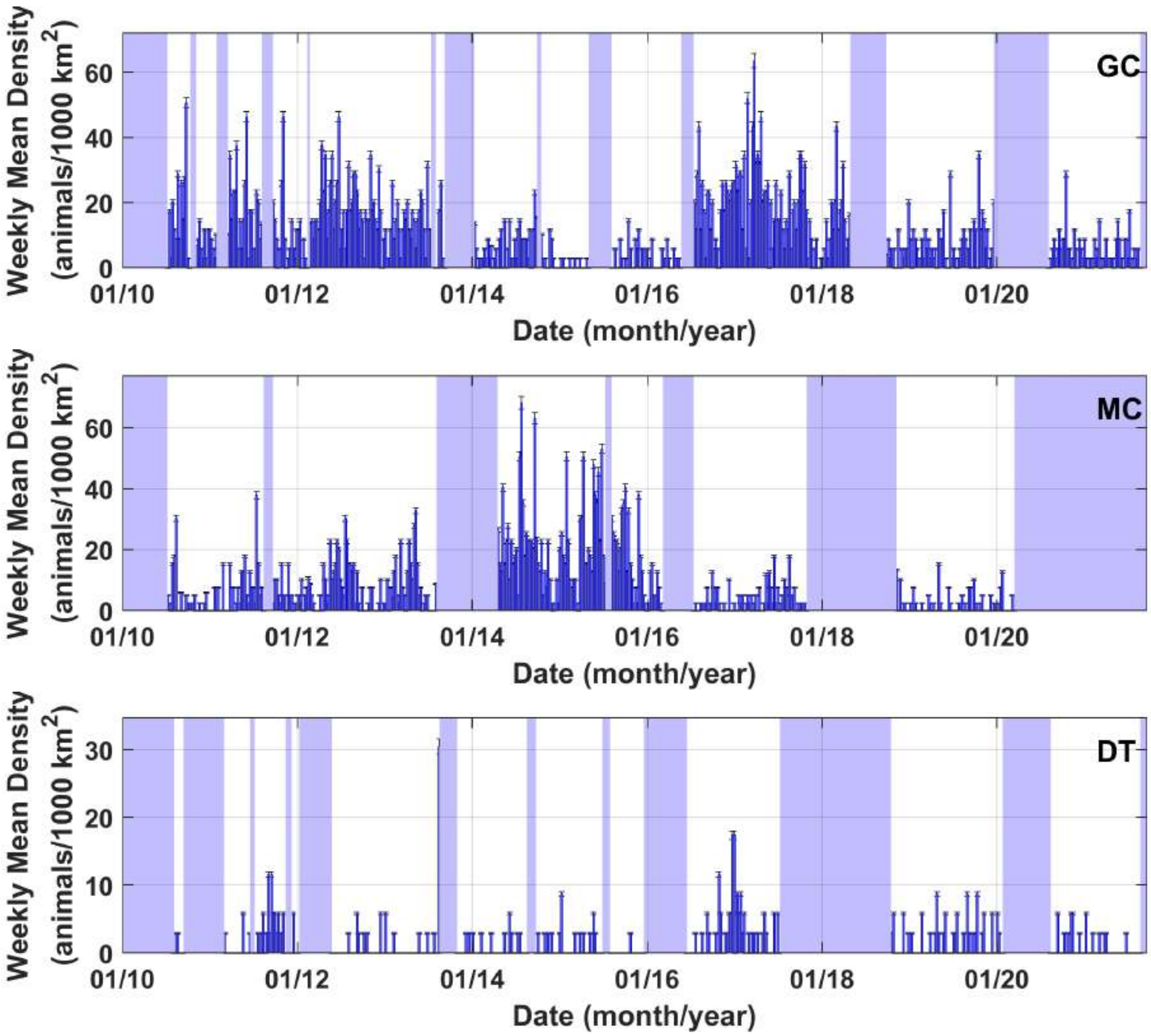

Figure 58: Historical weekly mean daily density (blue bars) of *Kogia* spp. echolocation clicks between 2010-2021 at sites GC, MC, and DT. Error bars represent ± 1 standard deviation. Shaded blue sections represent periods with no recording effort. Note: y-axis values vary for each site based on detection levels.

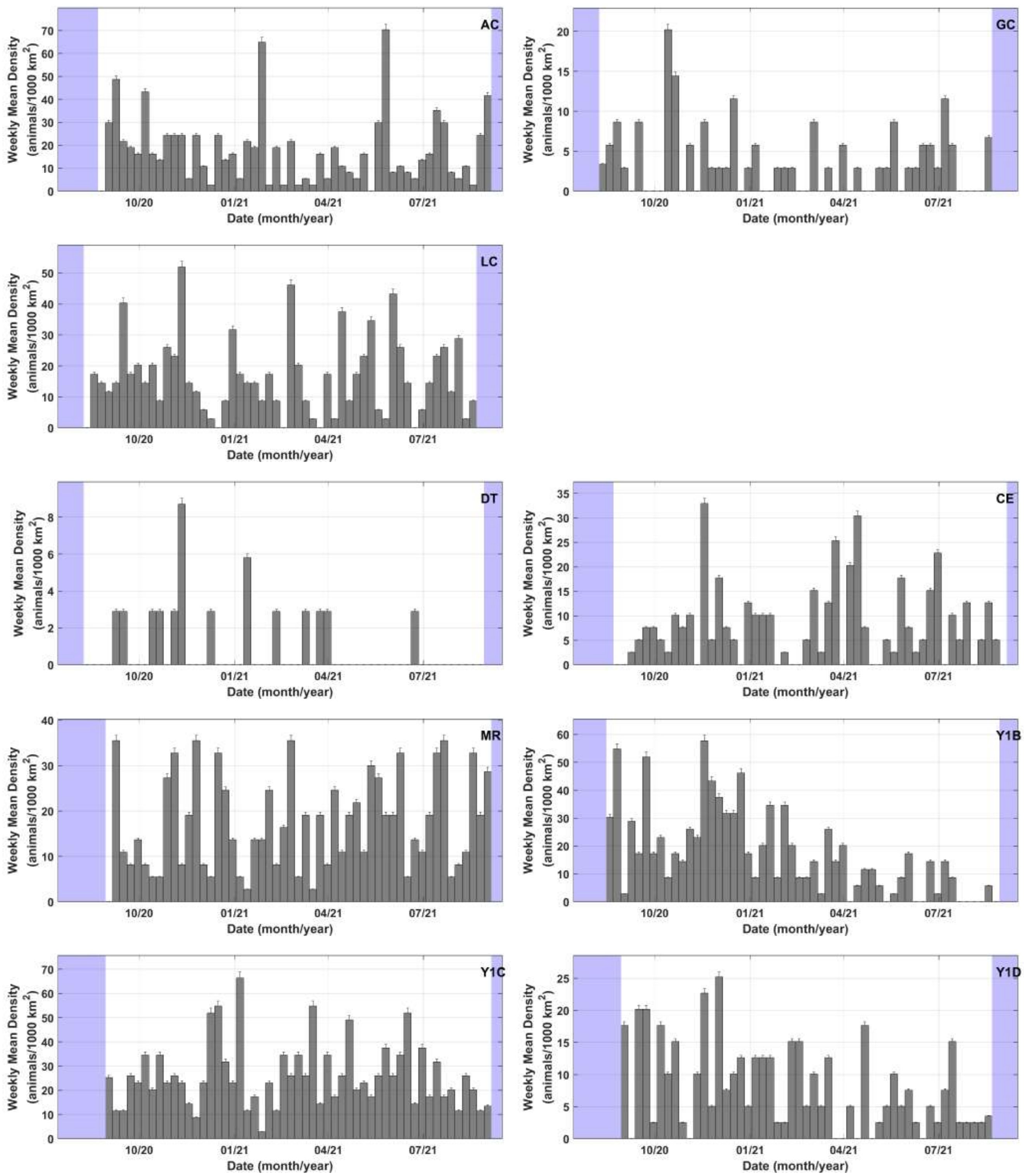

Figure 59: Weekly mean daily density (blue bars) of *Kogia* spp. echolocation clicks between 2020-2021 at sites AC, GC, LC, DT, CE, MR, Y1B, Y1C, Y1D. Error bars represent ± 1 standard deviation. Shaded blue sections represent periods with no recording effort. Note: y-axis values vary for each site based on detection levels.

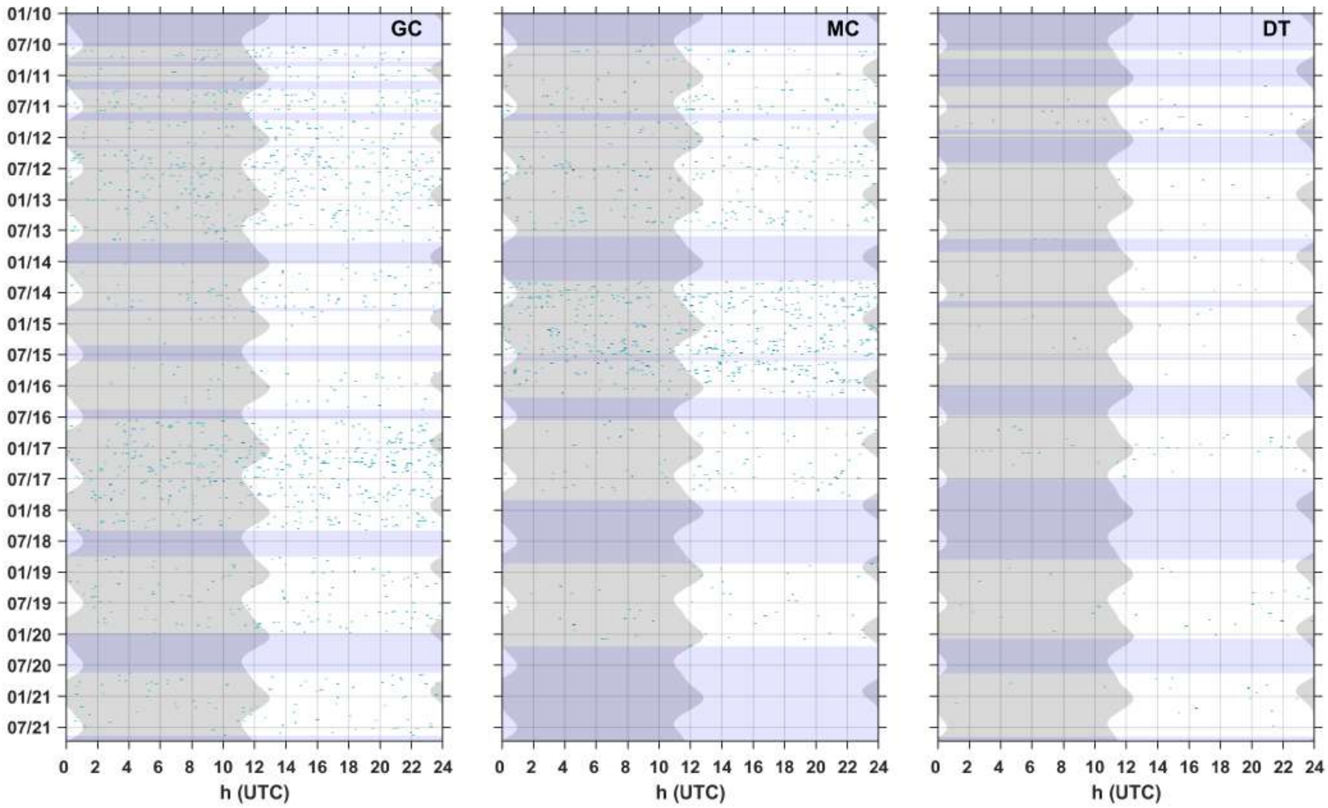

Figure 60: *Kogia* spp. echolocation clicks in five-minute bins at historic sites GC, MC, and DT from 2010-2021. Gray vertical shading denotes nighttime and light blue horizontal shading denotes absence of acoustic data. Color denotes number of detections per 5 minutes (light blue: <100; mid blue: 100-1000; dark blue: >1000).

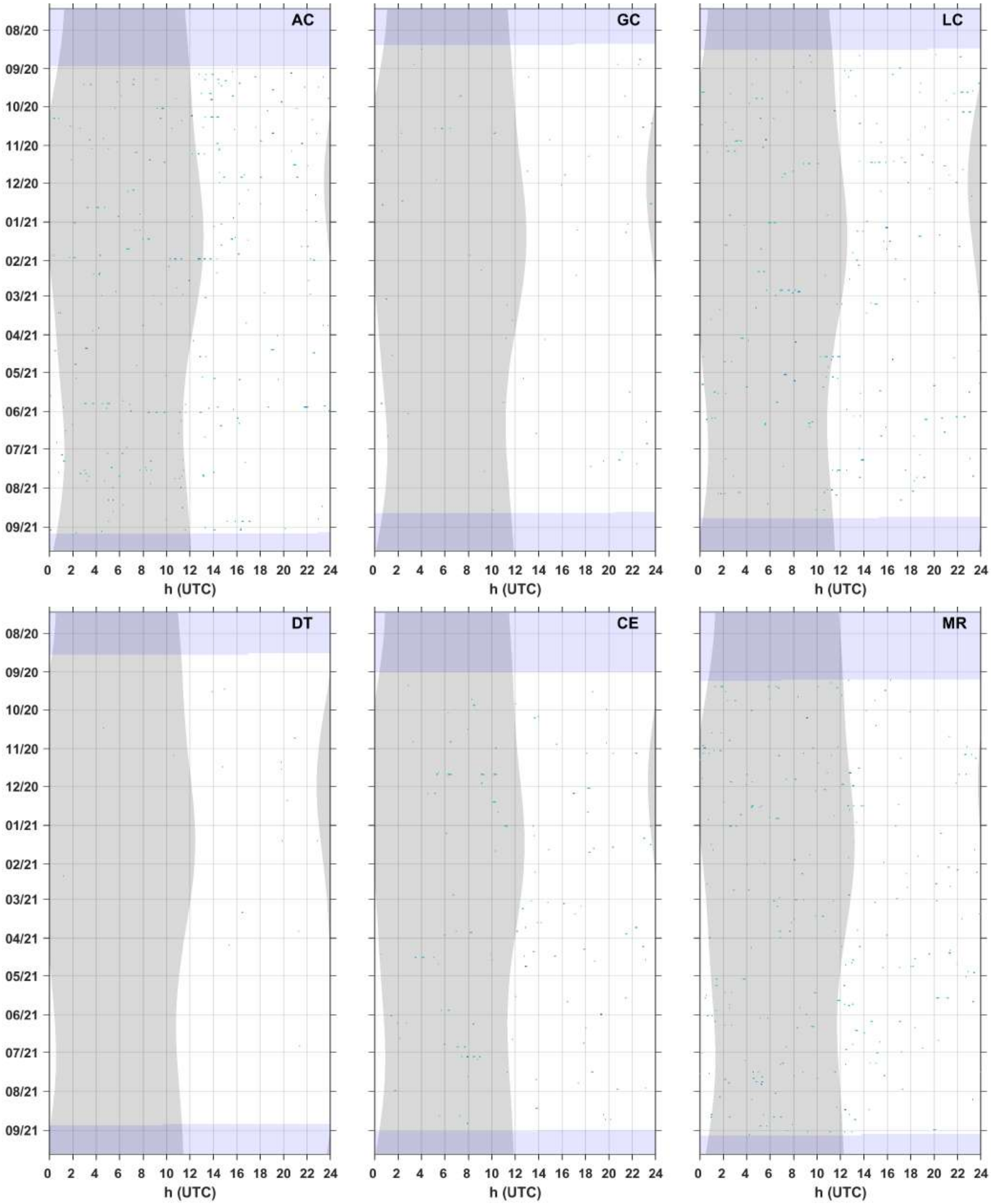

Figure 61: *Kogia* spp. echolocation clicks in five-minute bins at sites AC, GC, LC, DT, CE, and MR from 2020-2021. Gray vertical shading denotes nighttime and light blue horizontal shading denotes absence of acoustic data. Color denotes number of detections per 5 minutes (light blue: <100; mid blue: 100-1000; dark blue: >1000).

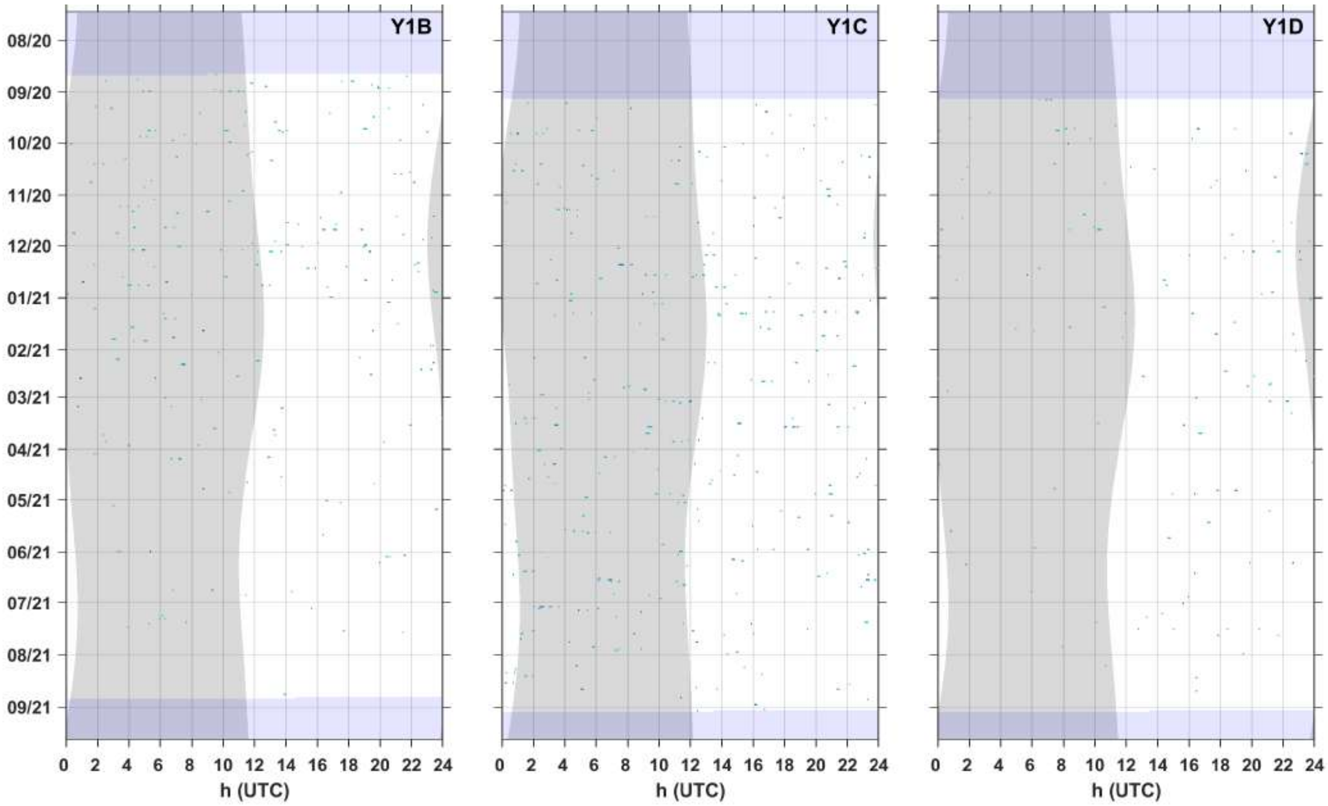

Figure 62: *Kogia* spp. echolocation clicks in five-minute bins at one-year sites Y1B, Y1C, and Y1D from 2020-2021. Gray vertical shading denotes nighttime and light blue horizontal shading denotes absence of acoustic data. Color denotes number of detections per 5 minutes (light blue: <100; mid blue: 100-1000; dark blue: >1000).

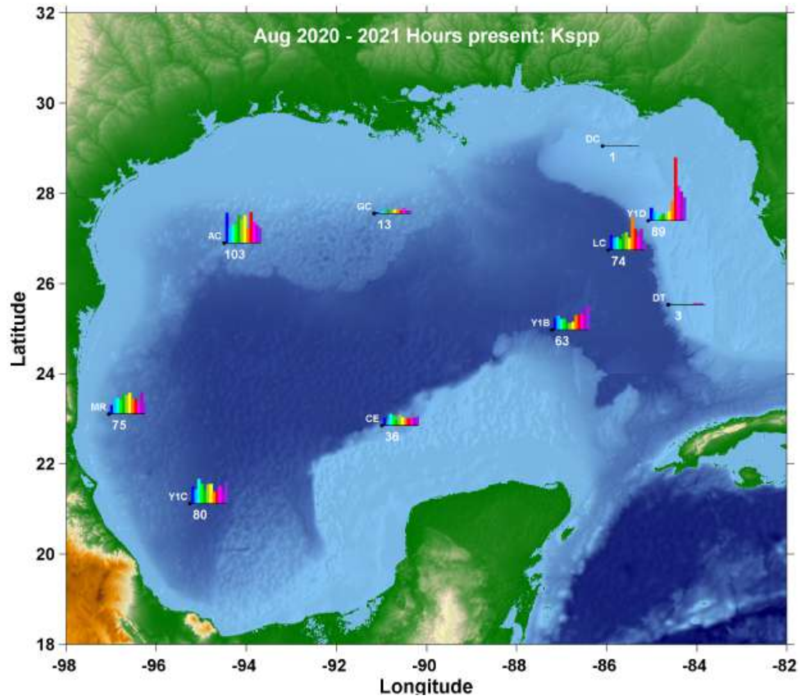

Figure 63: Hourly presence per month of *Kogia* spp. echolocation clicks from 2020-2021. Values below bar plots represent total hours per year present.

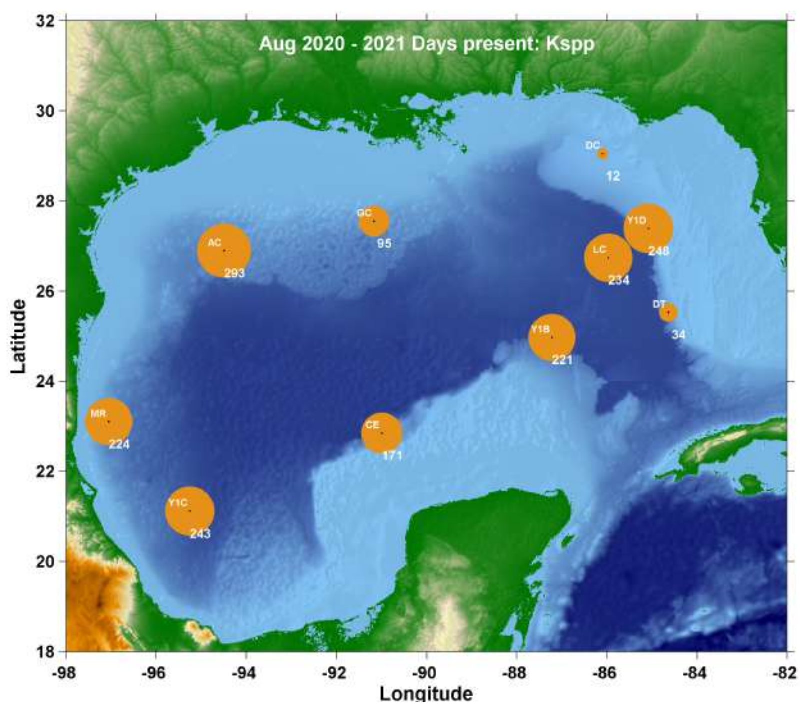

Figure 64: Days present per year for *Kogia* spp. echolocation clicks from 2020-2021.

4.1.6 Risso's Dolphins

Analyses of the 10 years of weekly density timeseries at historic sites indicate densities of Risso's dolphins were highest at the historic Dry Tortugas (DT) site with 17.8 animals per 1,000 km^2 with relatively low densities elsewhere (1.2 - 2.7 animals per 1,000 km^2) (Figure 65, Table 5). Densities at the historic sites appear to have decreased over the 10 year monitoring period (Figure 65). Analyses of the 2020-2021 deployments indicate Risso's dolphin mean weekly density was highest at Y1D (17.9 animals per 1,000 km^2) where they were comparable with historic and 2020-2021 densities at DT. All other sites featured considerably lower densities (Figure 66, Table 5). Strong seasonal patterns in density and hourly presence are apparent at most sites in the historic and 2020-2021 data (Figures 65, 66 & Figure 70), however the timing of peak occurrence differs between sites. A strong tendency toward nocturnal detections is visible in historical and 2020-2021 data (Figures 67, 68 & 69). Variability in days present was evident across sites, with Risso's dolphins occurring on few days in the western Gulf (ranging from 18 - 96) compared to at eastern Gulf sites in closer proximity to the Loop Current (Y1B, LC, Y1D, and DT) where days present ranged from 134 - 236 (Figure 70).

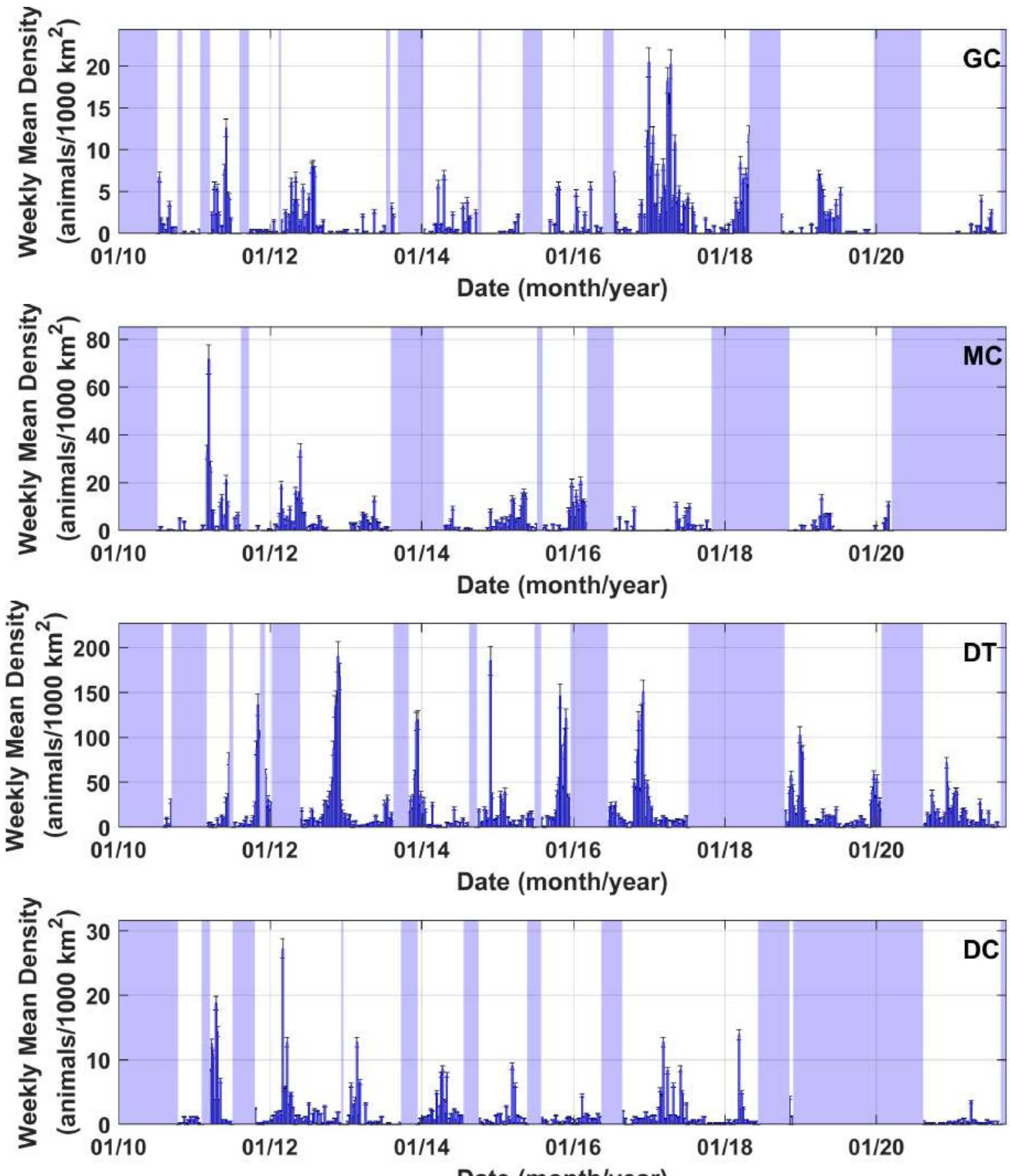

Figure 65: Historical weekly mean daily density (blue bars) of Risso's dolphin echolocation clicks between 2010-2021 at sites GC, MC, and DT. Error bars represent ± 1 standard deviation. Shaded blue sections represent periods with no recording effort. Note: y-axis values vary for each site based on detection levels.

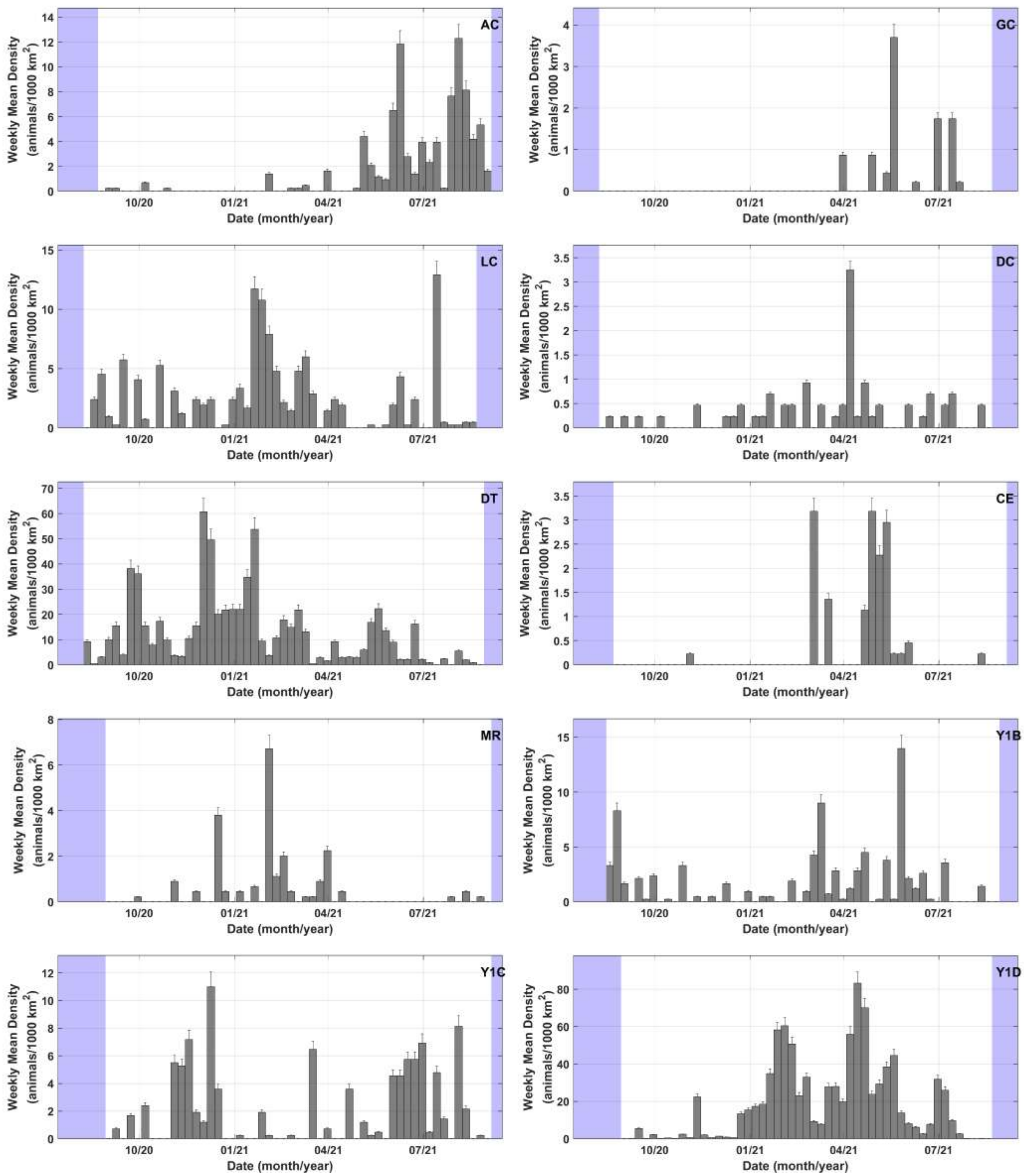

Figure 66: Weekly mean daily density (blue bars) of Risso's dolphin echolocation clicks between 2020-2021 at sites AC, GC, LC, DC, DT, CE, MR, Y1B, Y1C, Y1D. Error bars represent ± 1 standard deviation. Shaded blue sections represent periods with no recording effort. Note: y-axis values vary for each site based on detection levels.

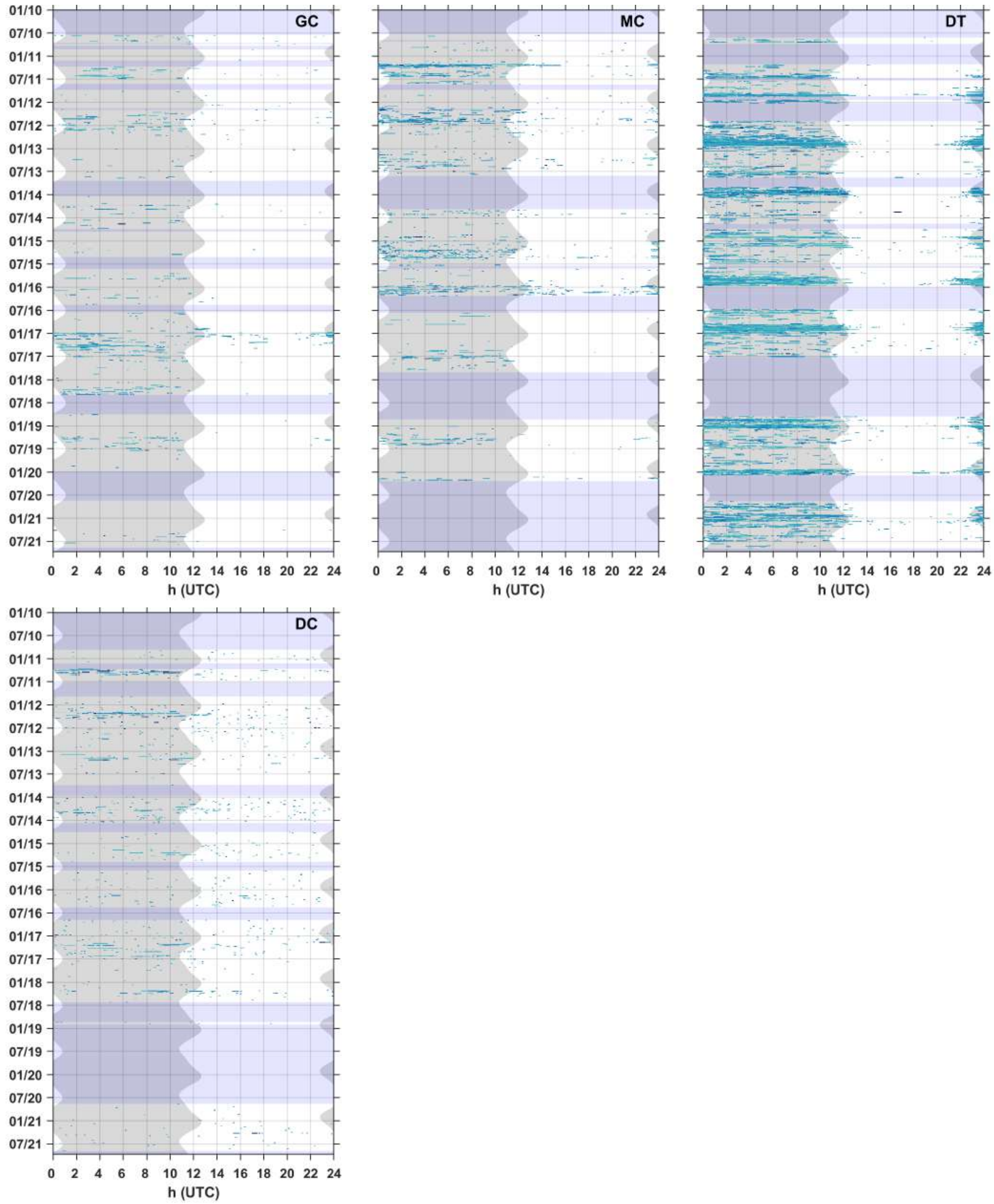

Figure 67: Risso's dolphin echolocation clicks in five-minute bins at historic sites GC, MC, DT, and DC from 2010-2021. Gray vertical shading denotes nighttime and light blue horizontal shading denotes absence of acoustic data. Color denotes number of detections per 5 minutes (light blue: <100; mid blue: 100-1000; dark blue: >1000).

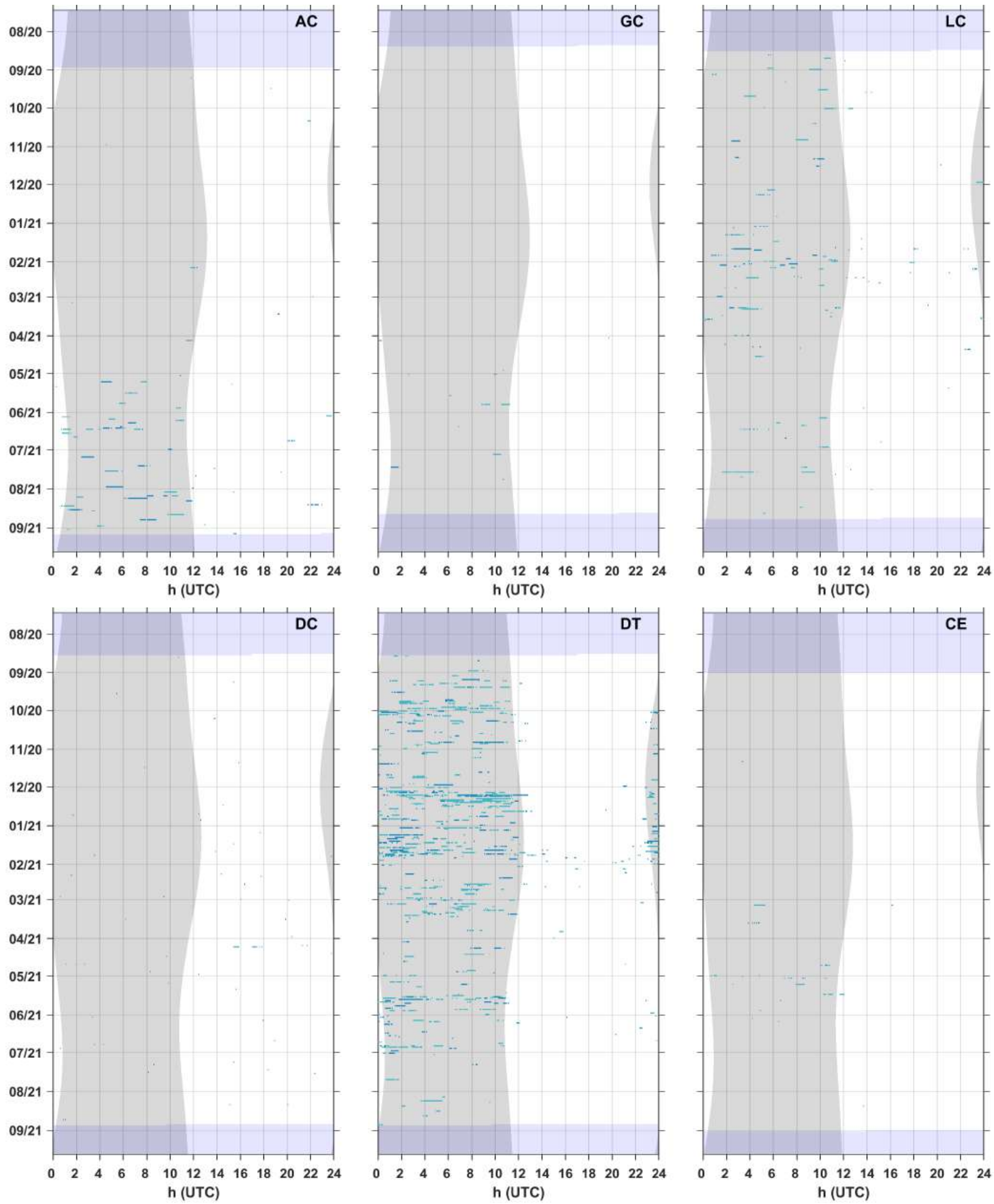

Figure 68: Risso's dolphin echolocation clicks in five-minute bins at sites AC, GC, LC, DC, DT, and CE from 2020-2021. Gray vertical shading denotes nighttime and light blue horizontal shading denotes absence of acoustic data. Color denotes number of detections per 5 minutes (light blue: <100; mid blue: 100-1000; dark blue: >1000).

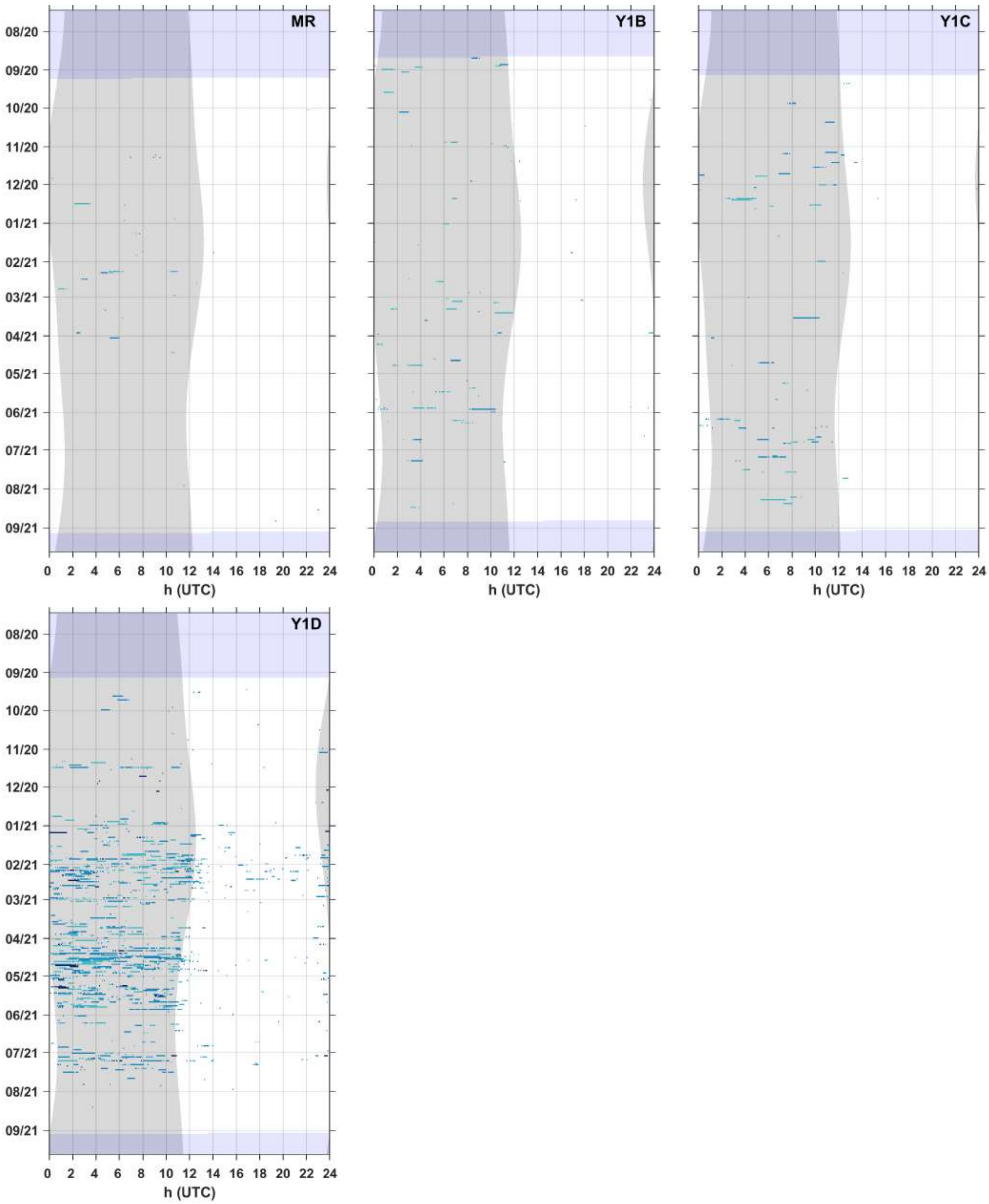

Figure 69: Risso's dolphin echolocation clicks in five-minute bins at one-year sites MR, Y1B, Y1C, and Y1D from 2020-2021. Gray vertical shading denotes nighttime and light blue horizontal shading denotes absence of acoustic data. Color denotes number of detections per 5 minutes (light blue: <100; mid blue: 100-1000; dark blue: >1000).

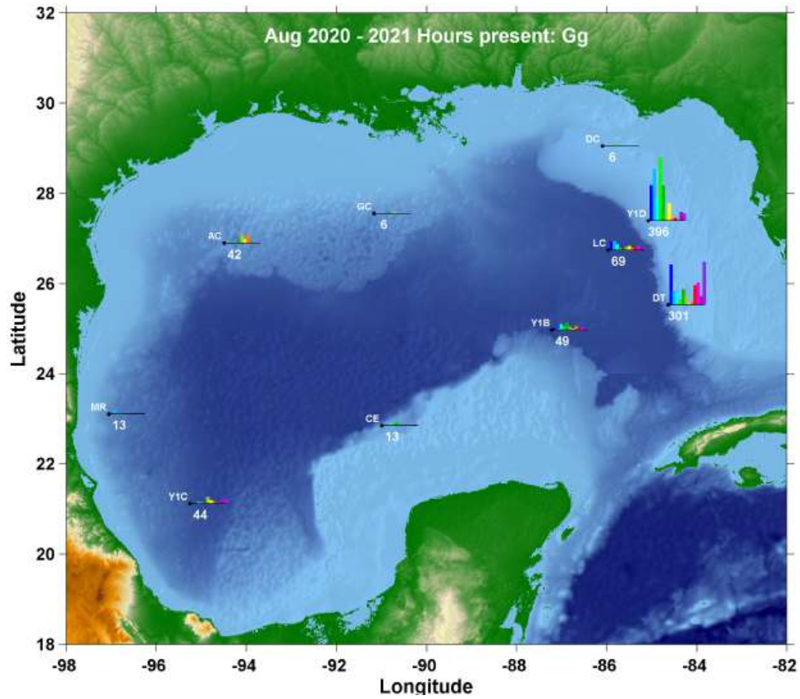

Figure 70: Hourly presence per month of Risso's dolphins echolocation clicks from 2020-2021. Values below bar plots represent total hours per year present.

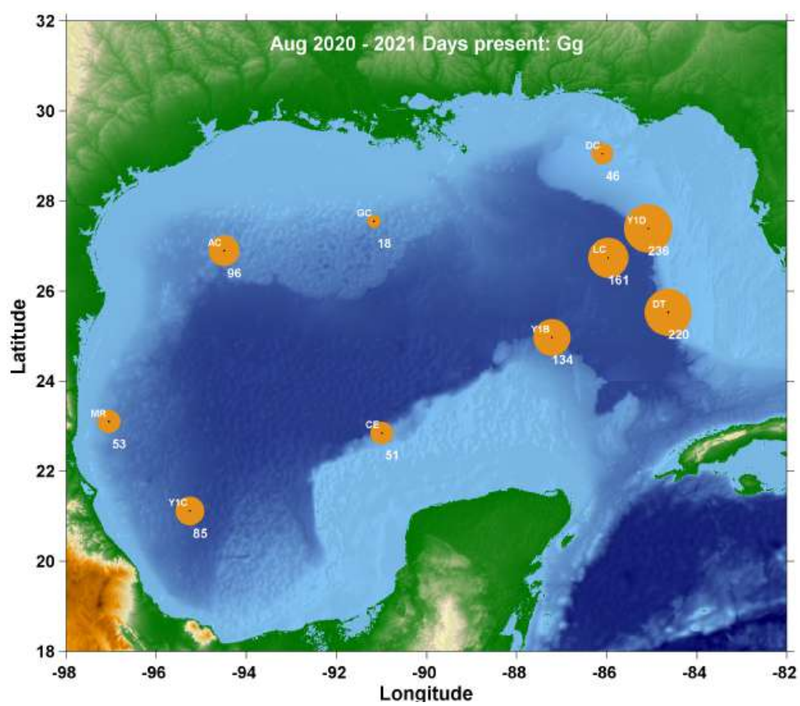

Figure 71: Days present per year for Risso's dolphin echolocation clicks from 2020-2021.

4.1.7 Unidentified Dolphins: High-Frequency

Analyses of the 10 years of weekly density timeseries at historic sites indicate densities for unidentified high-frequency dolphins (presumed primarily *Stenella* spp. and offshore *Tursiops truncatus*) were generally high, with highest densities at the historic MC site with 396 animals per 1,000 km^2 and, followed by sites DT and DC (377 and 358 animals per 1,000 km^2 respectively) (Figure 72, Table 5) with lowest densities at GC (299 animals per 1,000 km^2). Densities at the historic MC and GC sites appear to have decreased over the 10 year monitoring period, while densities at the shallow DC location appear to have increased (Figure 72). At the shallow site MP, an initial period of lower densities from 2010-2012 is followed by an increase in late 2012 and stable levels thereafter. Analyses of the 2020-2021 deployments indicate UD HF mean weekly densities were generally high at most sites, but were highest at LC (530 animals per 1,000 km^2, Table 5). Densities were lower at the southern sites CE, MR, and Y1C (ranging from 123 - 164 animals per 1,000 km^2) relative to northern sites (ranging from 203 - 530 animals per 1,000 km^2; Table 5, Figure 74). Strong seasonal patterns in density are apparent in the historic data at sites GC and MC, with high densities typically observed in summer, and low densities in winter months (Figures 72 & 74), however this pattern is less visible at the shallow locations and at the southern site DT. Seasonal trends in density and hourly presence were not clearly discernible in the 2020-2021 data, but may become more apparent with additional data collection (Figures 74 & 78). Potential trends at site AC and GC appear consistent with the previously observed summer increase at GC and MC. Density and hourly presence were higher at site Y1B from September through February, at site DT in spring, and at site LC in both winter and late summer. These differing seasonal patterns among sites may be related to specific species' movement patterns that may become easier to interpret if this species group can be differentiated at a finer taxanomic resolution.

A strong tendency toward nocturnal detections is visible in both historical data and 2020-2021 sites (Figure 75). However, this pattern is weaker at shallow sites (DC and MP), and seems to disappear entirely between 2015 and 2018 at MP (Figure 73). This may reflect differences in foraging preferences related to prey availability, and may also be related to differences in delphinid species composition relative to deeper sites. Diel patterns at the sites in the 2020-2021 data are comparable to previously observed patterns at historic sites (Figures 76 & 77). Spatial patterns in daily presence of UD HF detections are similar to those observed for densities, with lower presence at southern sites, and range from 163 - 339 days per year present (Figure 79).

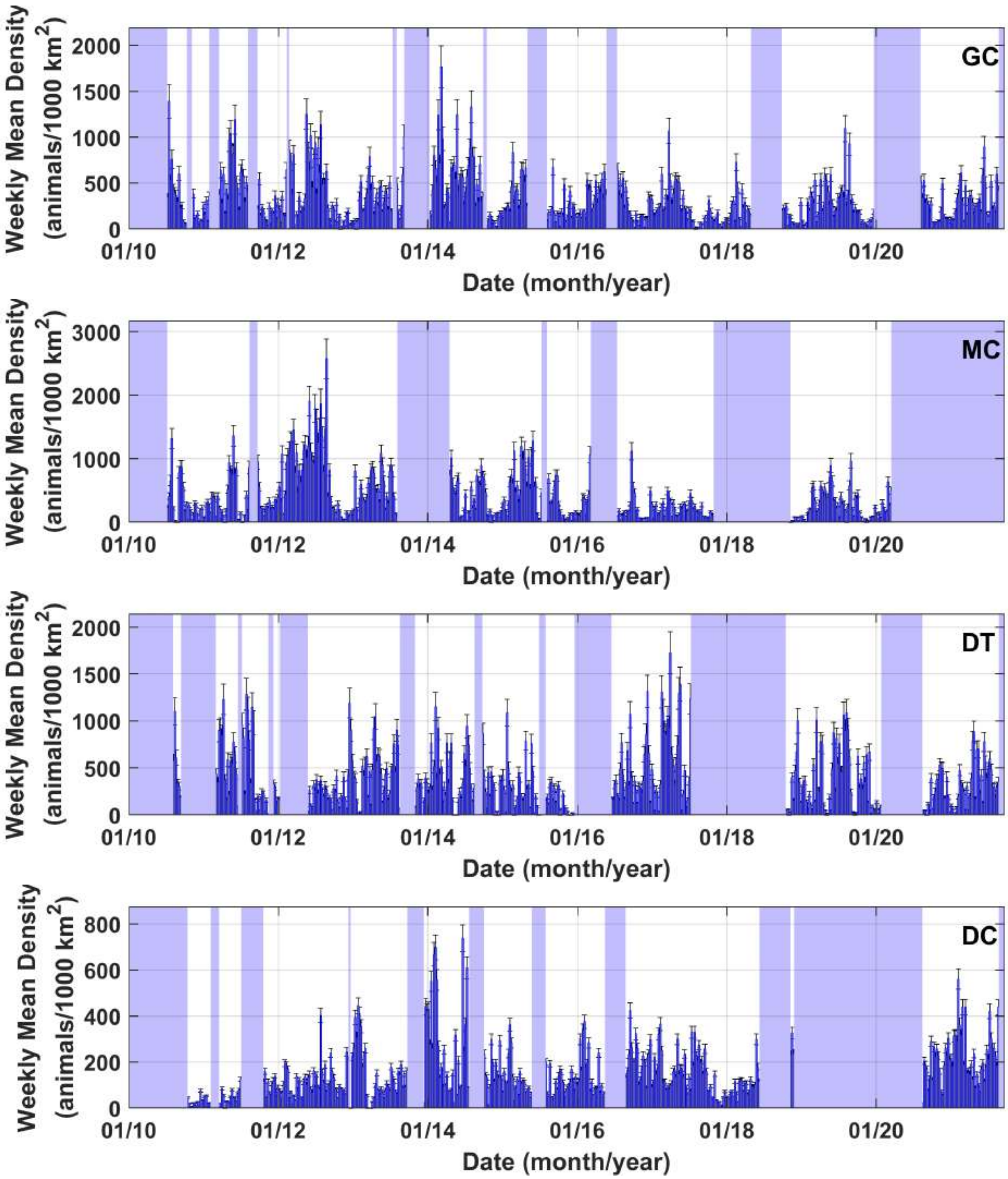

Figure 72: Historical weekly mean daily density (blue bars) of unidentified dolphin high-frequency (UD HF) echolocation clicks between 2010-2021 at sites GC, MC, and DT. Error bars represent ± 1 standard deviation. Shaded blue sections represent periods with no recording effort. Note: y-axis values vary for each site based on detection levels.

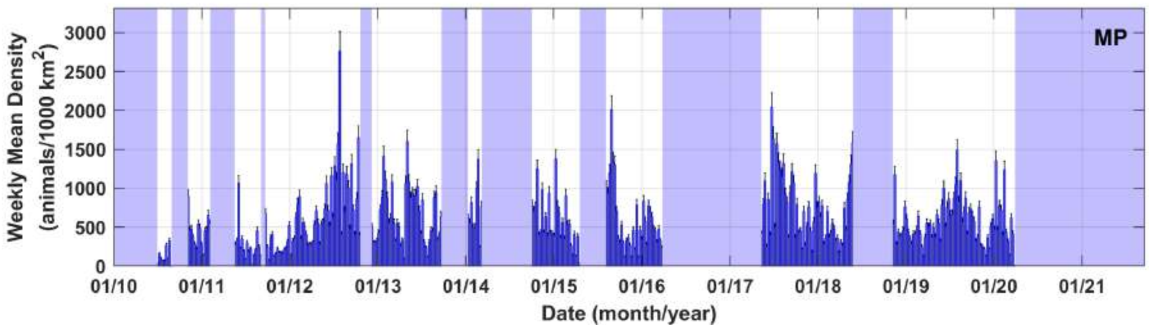

Figure 73: Historical weekly mean daily density (blue bars) of unidentified dolphin high-frequency (UD HF) echolocation clicks between 2010-2021 at shallow site MP. Error bars represent ± 1 standard deviation. Shaded blue sections represent periods with no recording effort.

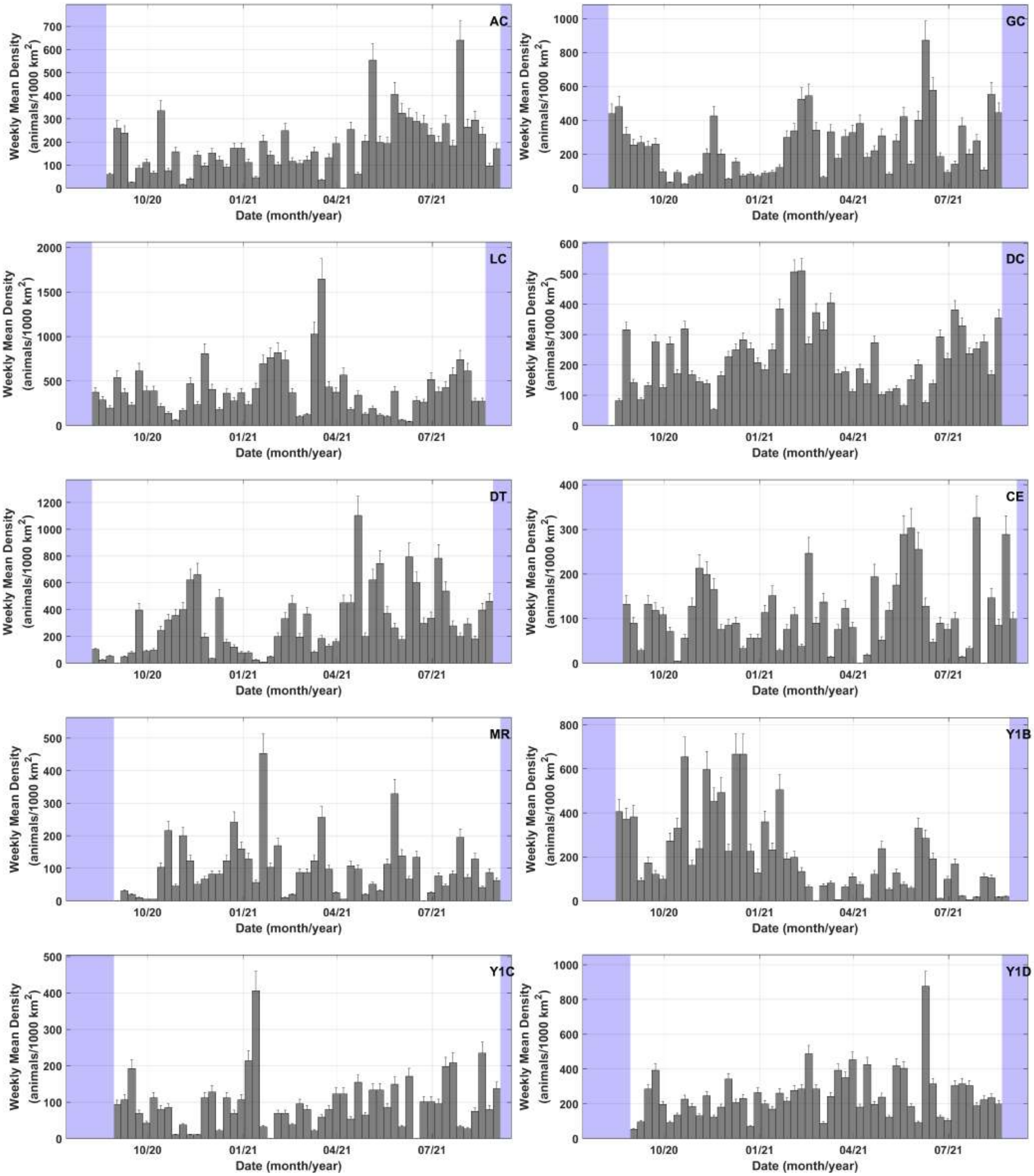

Figure 74: Weekly mean daily density (blue bars) of unidentified dolphin high-frequency (UD HF) echolocation clicks between 2020-2021 at sites AC, GC, LC, DC, DT, CE, MR, Y1B, Y1C, Y1D. Error bars represent ± 1 standard deviation. Shaded blue sections represent periods with no recording effort. Note: y-axis values vary for each site based on detection levels.

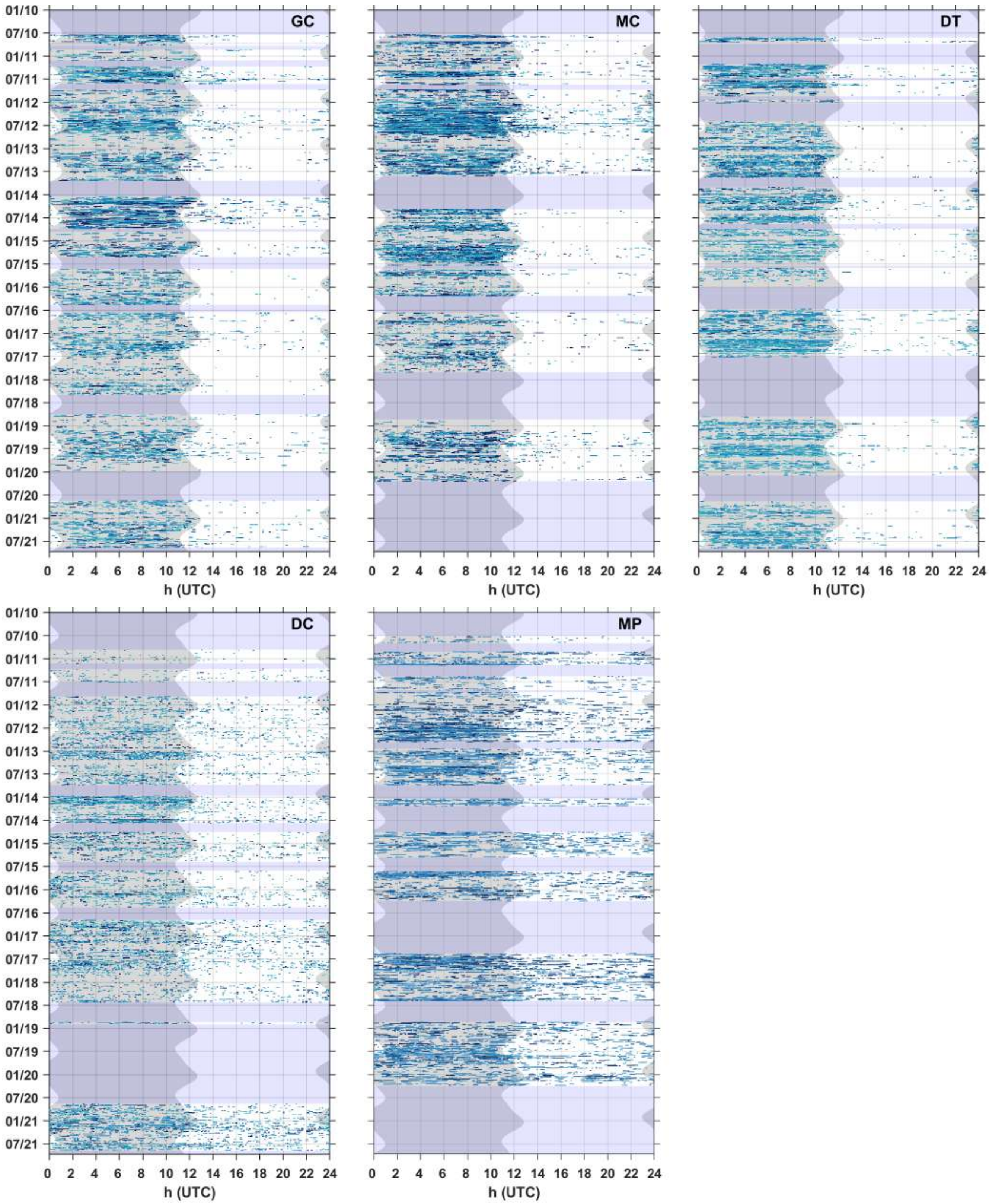

Figure 75: Unidentified dolphin high-frequency (UD HF) echolocation clicks in five-minute bins at historic sites GC, MC, DT, DC, and MP from 2010-2021. Gray vertical shading denotes nighttime and light blue horizontal shading denotes absence of acoustic data. Color denotes number of detections per 5 minutes (light blue: <100; mid blue: 100-1000; dark blue: >1000).

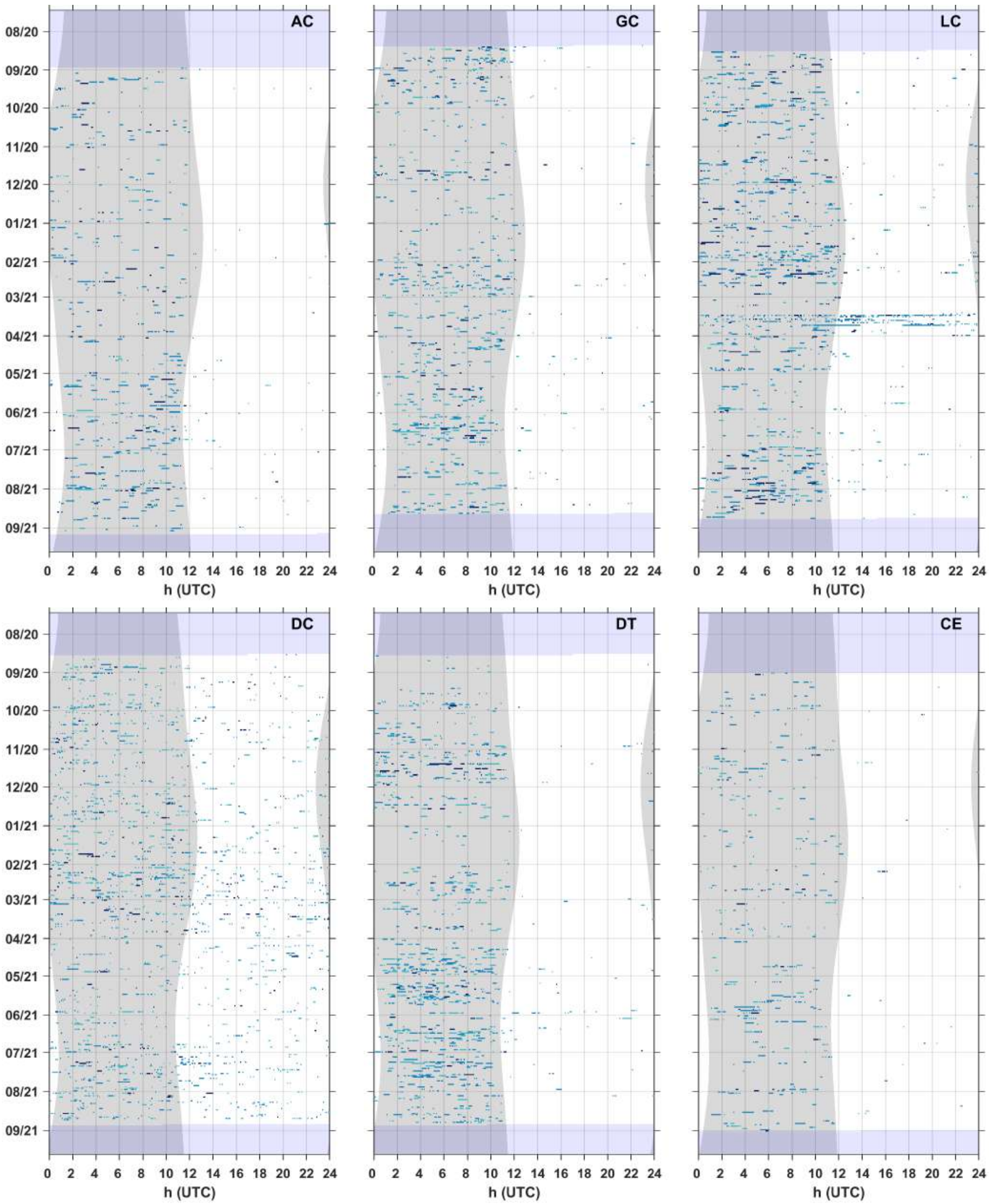

Figure 76: Unidentified dolphin high-frequency (UD HF) echolocation clicks in five-minute bins at sites AC, GC, LC, DC, DT, and CE from 2020-2021. Gray vertical shading denotes nighttime and light blue horizontal shading denotes absence of acoustic data. Color denotes number of detections per 5 minutes (light blue: <100; mid blue: 100-1000; dark blue: >1000).

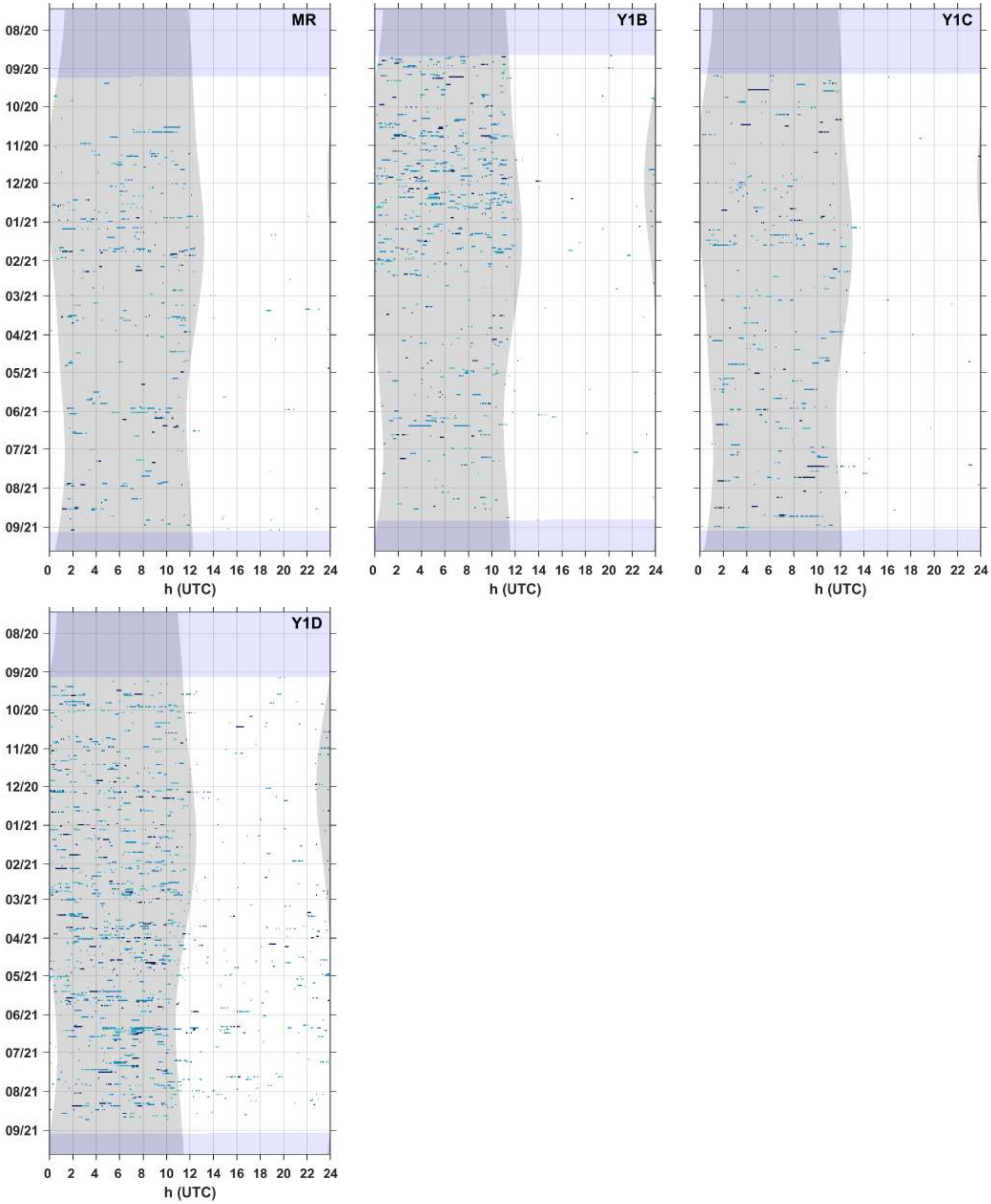

Figure 77: Unidentified dolphin high-frequency (UD HF) echolocation clicks in five-minute bins at one-year sites MR, Y1B, Y1C, and Y1D from 2020-2021. Gray vertical shading denotes nighttime and light blue horizontal shading denotes absence of acoustic data. Color denotes number of detections per 5 minutes (light blue: <100; mid blue: 100-1000; dark blue: >1000).

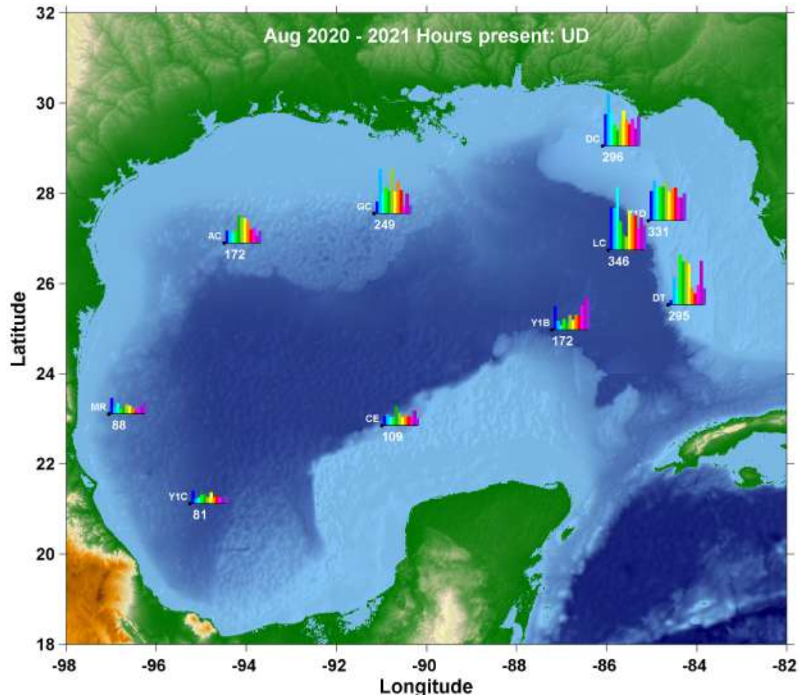

Figure 78: Hourly presence per month of unidentified dolphin high-frequency (UD HF) echolocation clicks from 2020-2021. Values below bar plots represent total hours per year present.

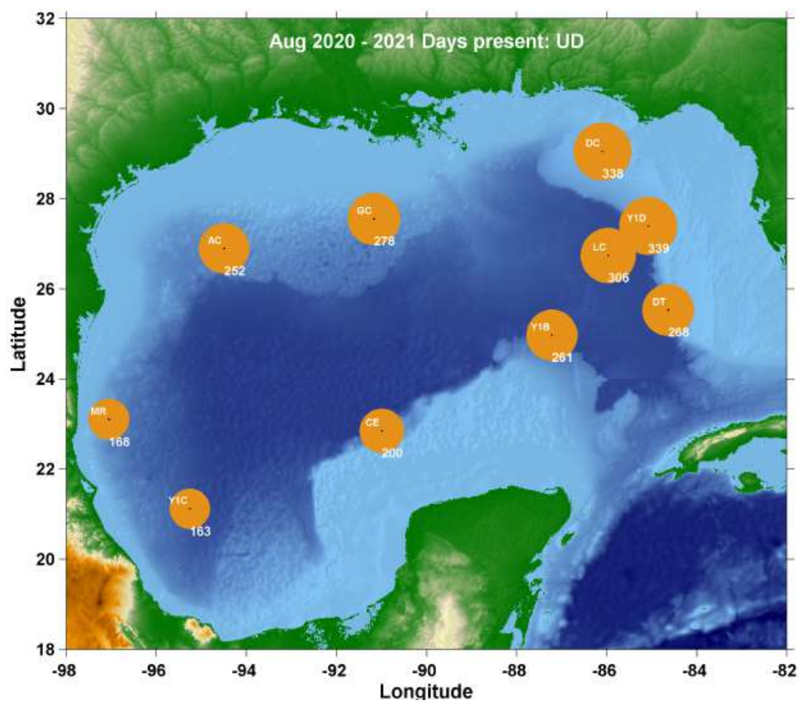

Figure 79: Days present per year for unidentified dolphin high-frequency (UD HF) echolocation clicks (primarily *Stenella* spp.) from 2020-2021.

4.1.8 Unidentified Dolphins: Three-Peak

Analyses of the 10 years of weekly density timeseries at historic sites indicate densities for unidentified dolphin three-peak (UD 3P) were highest at the historic DC site with an estimated 220 animals per 1,000 km^2) and lower at all other historic sites (2-14 animals per 1,000 km^2; Figure 80, Table 5). Densities at site DC appear to have increased over the 10 year monitoring period (Figure 80). Analyses of the 2020-2021 deployments indicate UD 3P mean weekly densities remained high at DC, and were elevated at LC, Y1B, and Y1D (137-180 animals per 1,000 km^2, Table 5). Densities at the new sites were all higher than those observed in the historic and 2020-2021 data (Table 5). Seasonal patterns in density were only apparent at site DT which had peaks in December in the historical data (Figure 80). In the 2020-2021 data, sharper peaks in density and hourly presence occurred in December and January at Y1B and DT, in January and February at LC, and in February and March at DC, while an increase in both the winter and late summer/early fall periods was evident at sites MR, Y1C, CE, and Y1D (Figures 80, 81, & 85).

Diel patterns at site DC, where this click type most commonly occurs, are complex and suggest a high degree of behavioral plasticity (Figure 82). A preference for crepuscular activity is visible, followed by day time activity, however nocturnal activity is occasionally high, as in late 2017-2018. Crepuscular activity is also seen at site Y1D (Figure 84), however at the remaining sites, occurrence is primarily nocturnal. In contrast with the spatial variability in UD 3P density (Table 5), the numbers of days with UD 3P detections present is relatively high across nearly all sites, ranging from 121 to 332 days present per year at sites other than GC and DT (Figure 86).

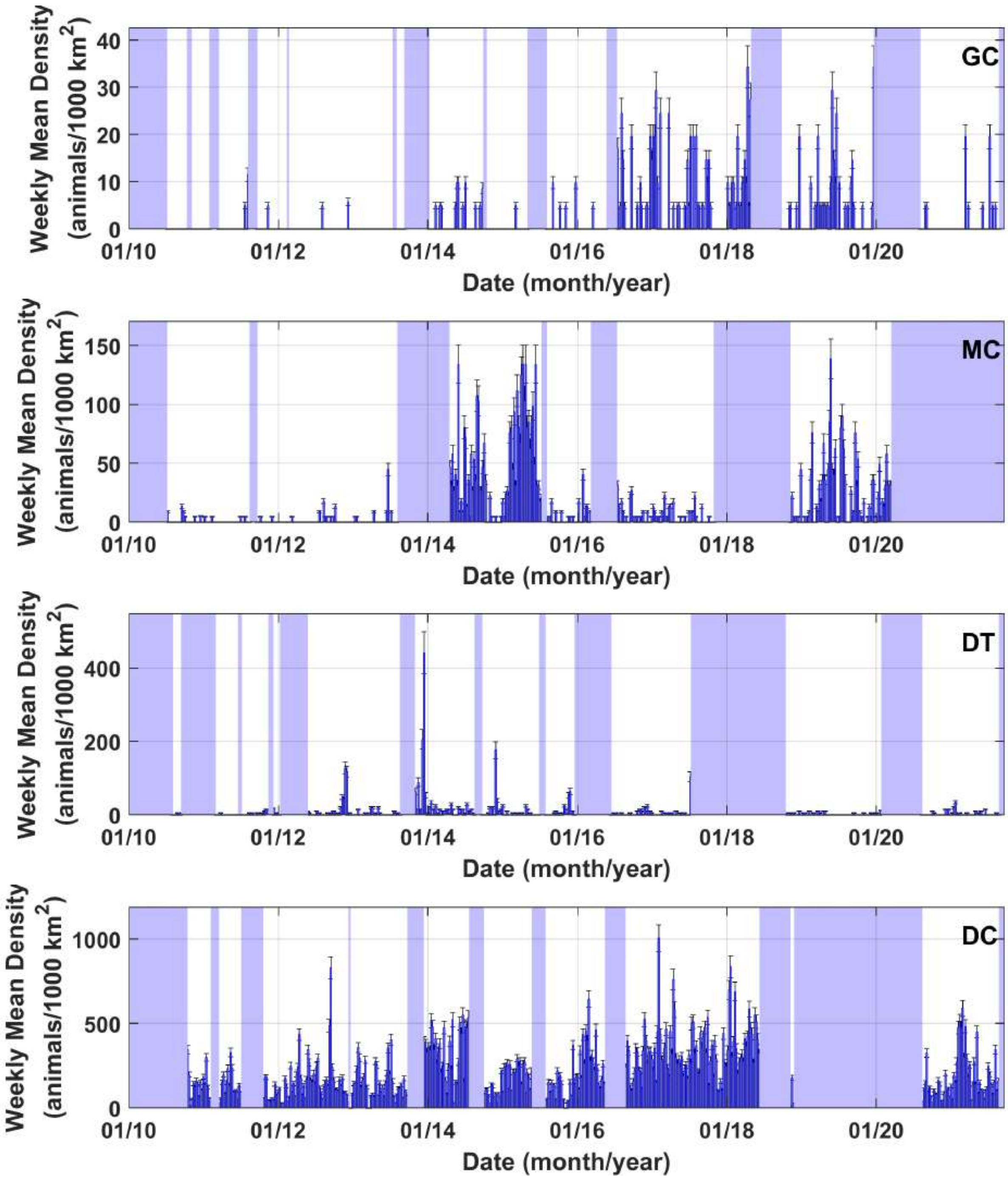

Figure 80: Historical weekly mean daily density (blue bars) of unidentified dolphin three-peak (UD 3P) echolocation clicks between 2010-2021 at sites GC, MC, and DT. Error bars represent ± 1 standard deviation. Shaded blue sections represent periods with no recording effort. Note: y-axis values vary for each site based on detection levels.

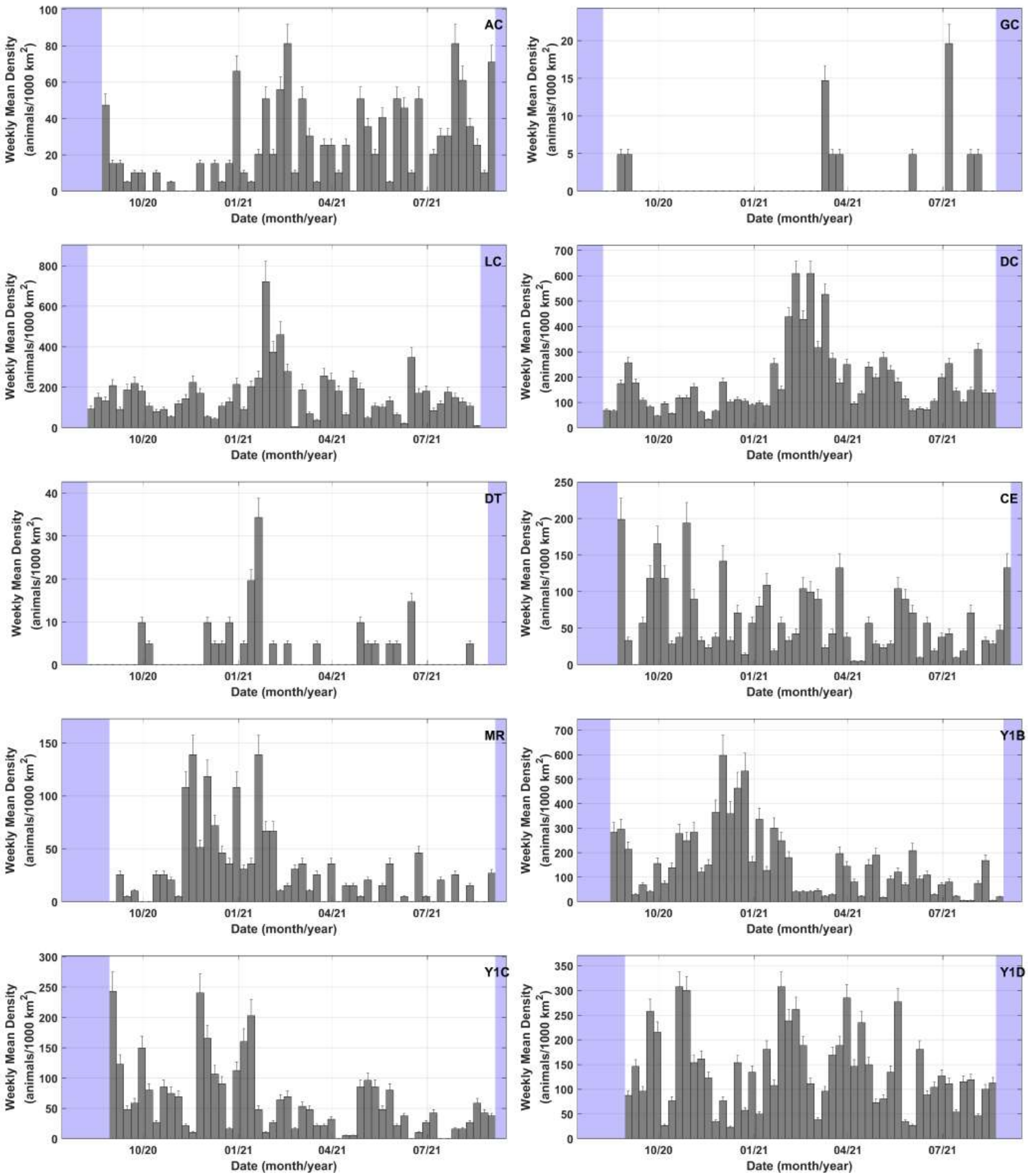

Figure 81: Weekly mean daily density (blue bars) of unidentified dolphin three-peak (UD 3P) echolocation clicks between 2020-2021 at sites AC, GC, LC, DC, DT, CE, MR, Y1B, Y1C, Y1D. Error bars represent ± 1 standard deviation. Shaded blue sections represent periods with no recording effort. Note: y-axis values vary for each site based on detection levels.

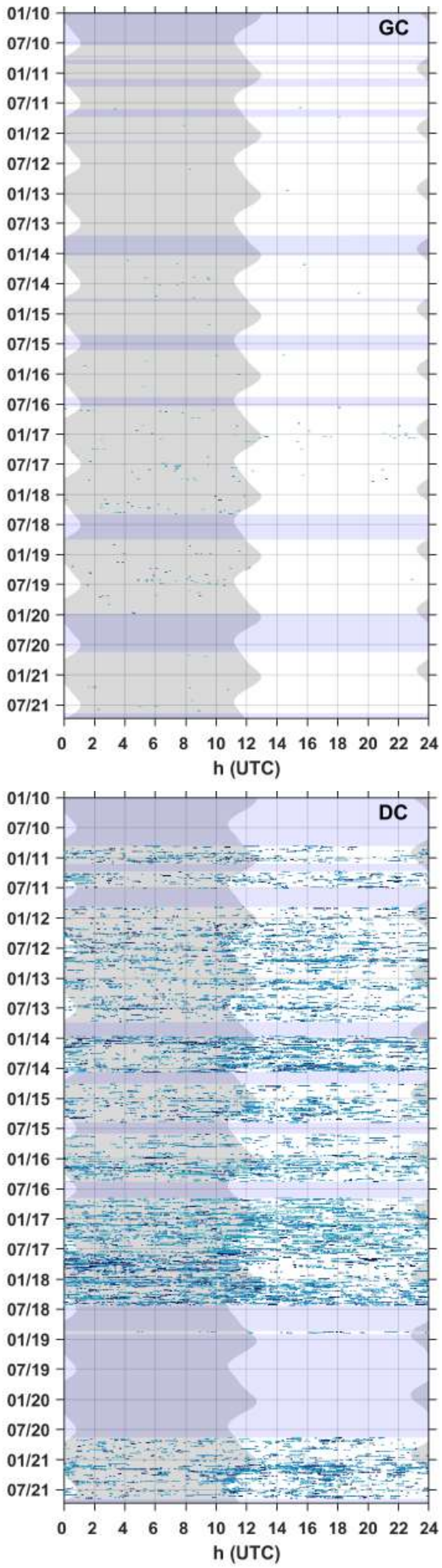

Figure 82: Unidentified dolphin three-peak (UD 3P) echolocation clicks in five-minute bins at historic sites GC, MC, DT, and DC from 2010-2021. Gray vertical shading denotes nighttime and light blue horizontal shading denotes absence of acoustic data. Color denotes number of detections per 5 minutes (light blue: <100; mid blue: 100-1000; dark blue: >1000).

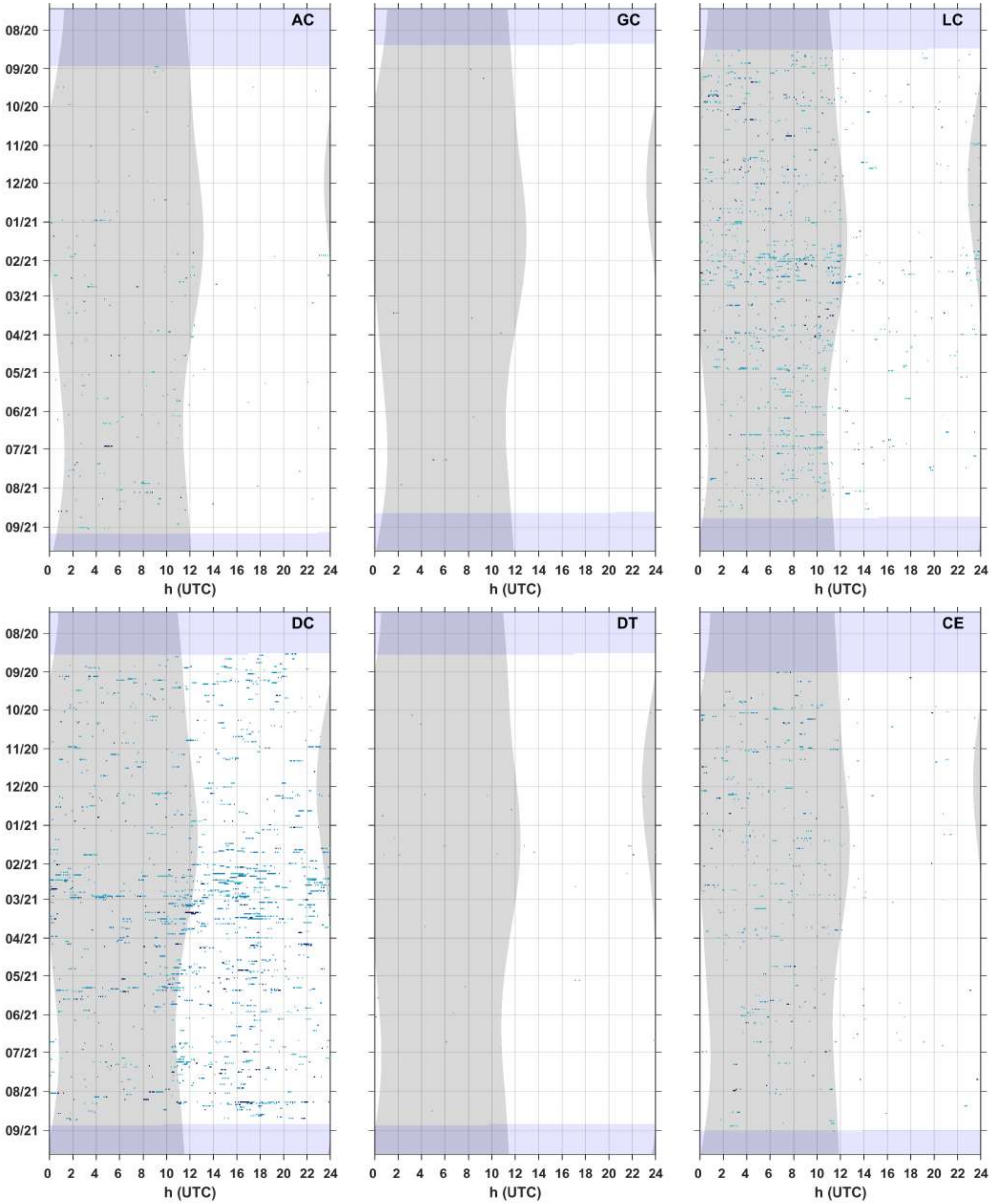

Figure 83: Unidentified dolphin three-peak (UD 3P) echolocation clicks in five-minute bins at sites AC, GC, LC, DC, DT, and CE from 2020-2021. Gray vertical shading denotes nighttime and light blue horizontal shading denotes absence of acoustic data. Color denotes number of detections per 5 minutes (light blue: <100; mid blue: 100-1000; dark blue: >1000).

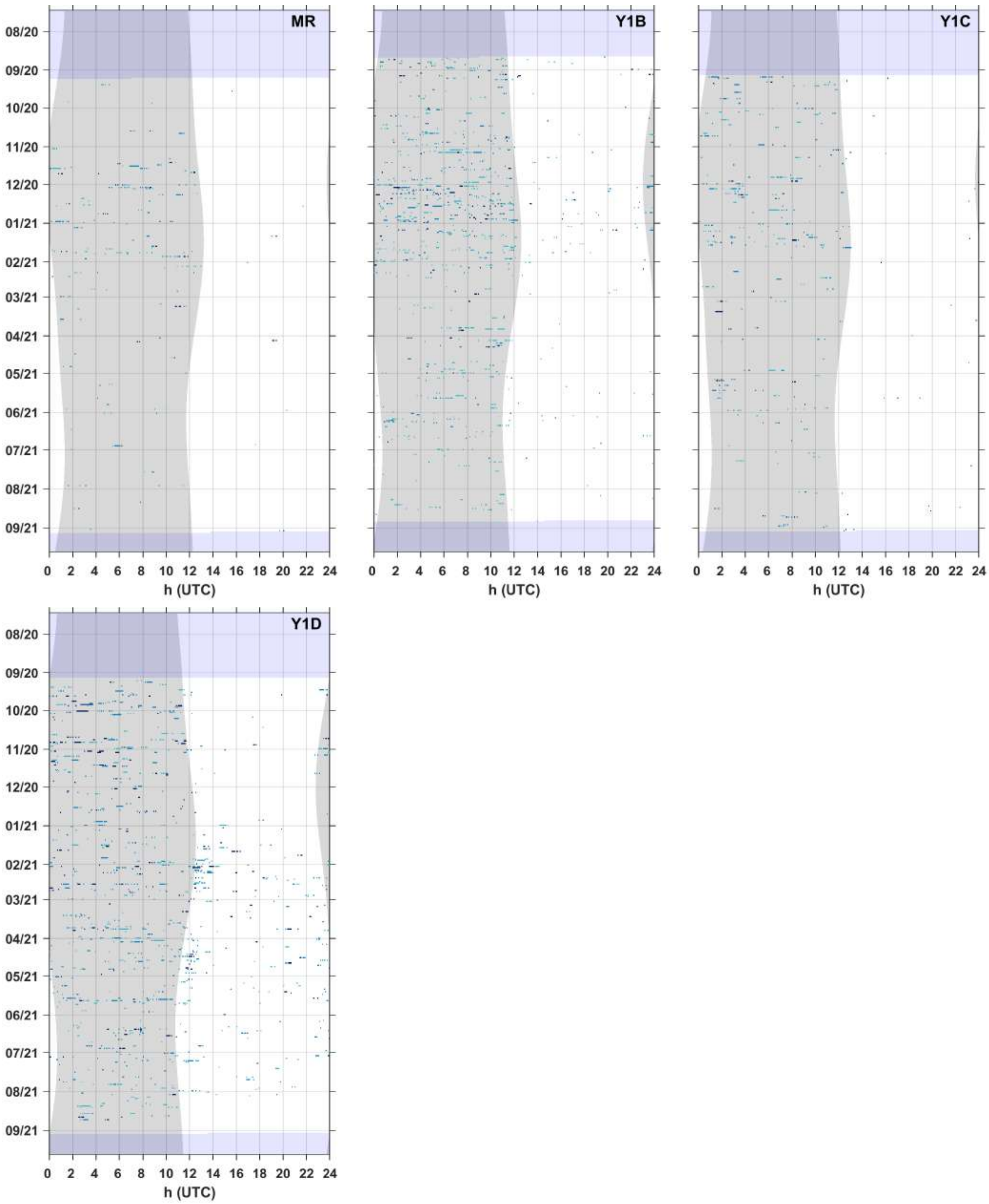

Figure 84: Unidentified dolphin three-peak (UD 3P) echolocation clicks in five-minute bins at one-year sites MR, Y1B, Y1C, and Y1D from 2020-2021. Gray vertical shading denotes nighttime and light blue horizontal shading denotes absence of acoustic data. Color denotes number of detections per 5 minutes (light blue: <100; mid blue: 100-1000; dark blue: >1000).

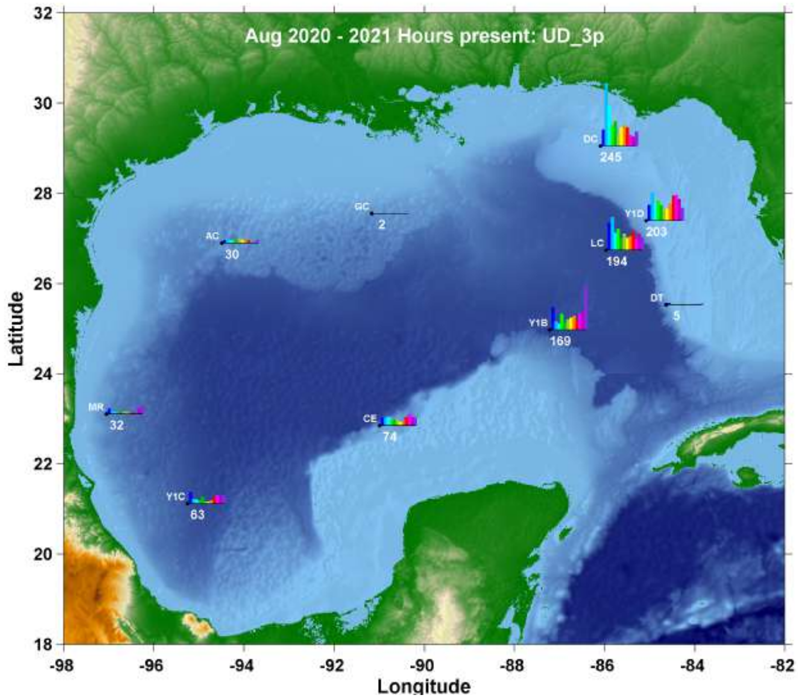

Figure 85: Hourly presence per month of unidentified dolphin three-peak (UD 3P) echolocation clicks from 2020-2021. Values below bar plots represent total hours per year present.

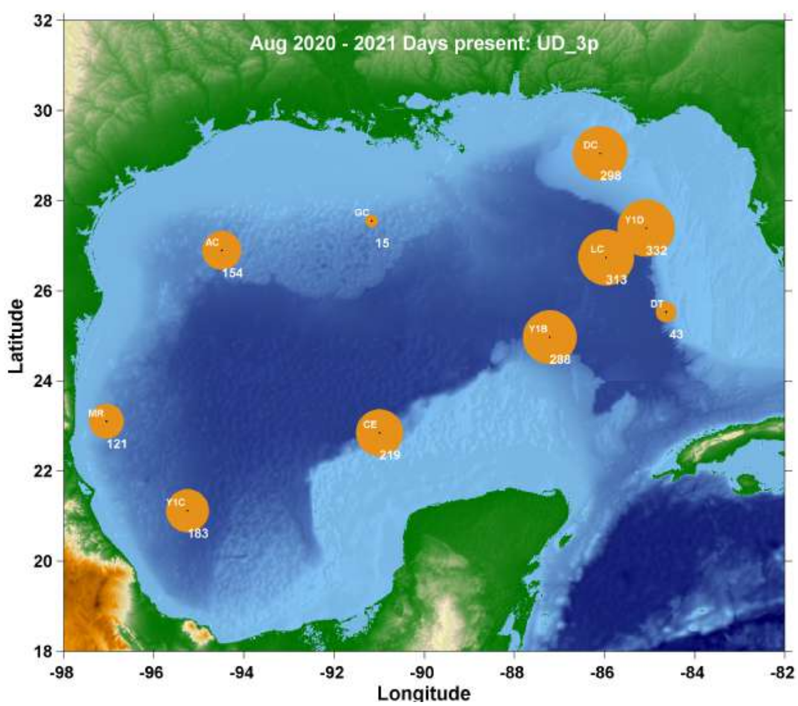

Figure 86: Days present per year for unidentified dolphin three-peak (UD 3P) echolocation clicks from 2020-2021.

4.1.9 Unidentified Dolphins: Low-Frequency

Analyses of the 10 years of weekly density timeseries at historic sites indicate densities for low-frequency dolphins (UD LF) (potentially representing multiple blackfish species) were highest at the historic GC site with an estimated 56 animals per 1,000 km^2, Table 5). Densities were similar at MC and DT, but much lower at the shallow historical site DC (Figure 87, Table 5). No long-term trends were readily apparent in the 10 years of UD LF density data at the historic sites, though variability was high. Analyses of the 2020-2021 deployments indicate UD LF mean weekly densities were higher at the new long-term MR (104 animals per 1,000 km^2) and short-term Y1C (91 animals per 1,000 km^2) sites than previously observed elsewhere, while densities at all other sites were similar to the historic deep sites, with site DC remaining low. Seasonal patterns in density are not readily apparent in the historical data, or 2020-2021 data (Figures 87 & 88).

A preference for nocturnal clicking activity is visible in the historic data (Figure 89). However, the year 1 data at new sites reveals few diel patterns (Figures 90 & 91), with the exception of MR and Y1D where detections of this type are primarily nocturnal. Daily presence is moderate, ranging from 51 to 131 days per year, and relatively consistent across all sites over the 2020-2021 period (Figure 93).

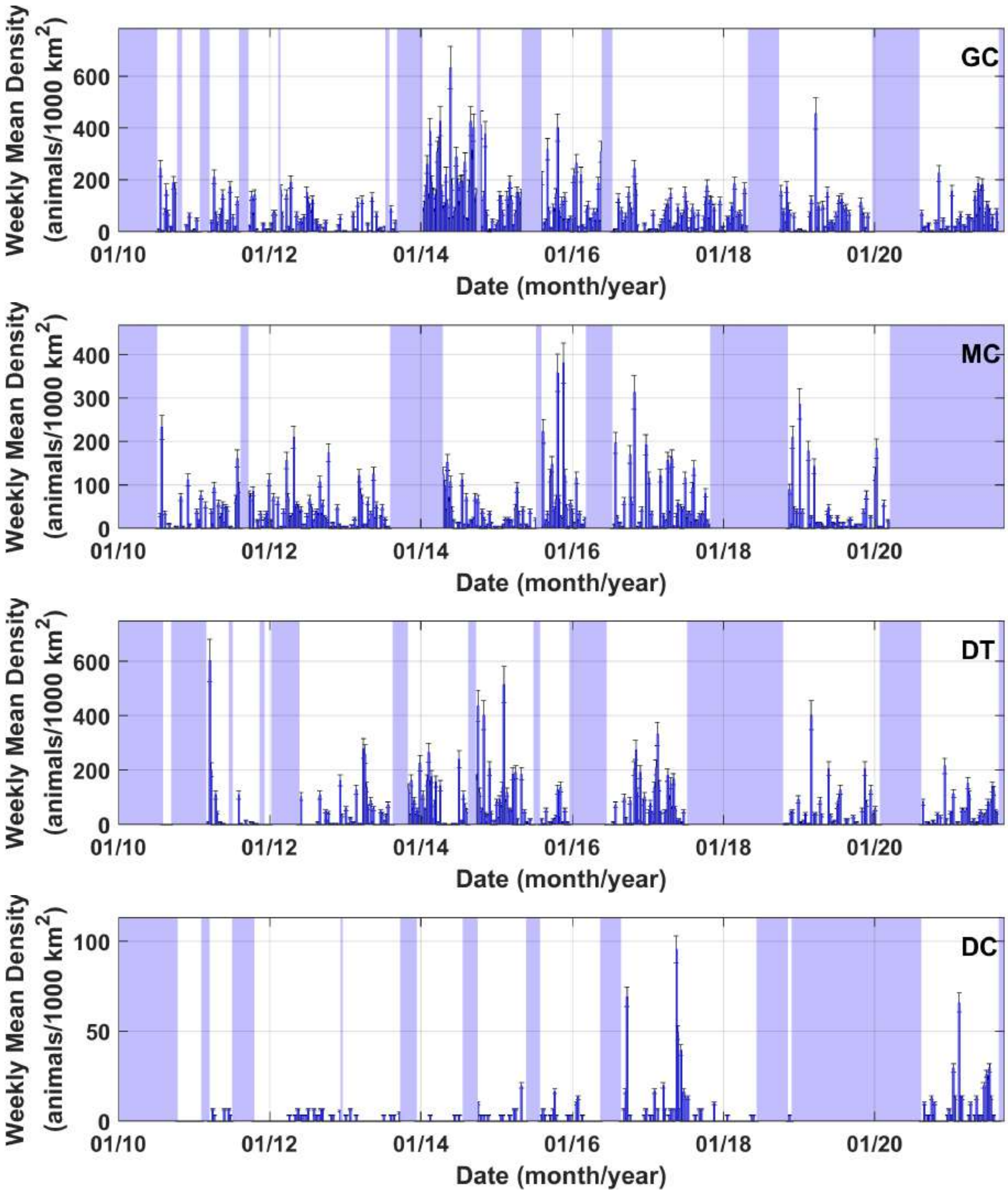

Figure 87: Historical weekly mean daily density (blue bars) of unidentified dolphin low-frequency (UD LF) echolocation clicks between 2010-2021 at sites GC, MC, and DT. Error bars represent ± 1 standard deviation. Shaded blue sections represent periods with no recording effort. Note: y-axis values vary for each site based on detection levels.

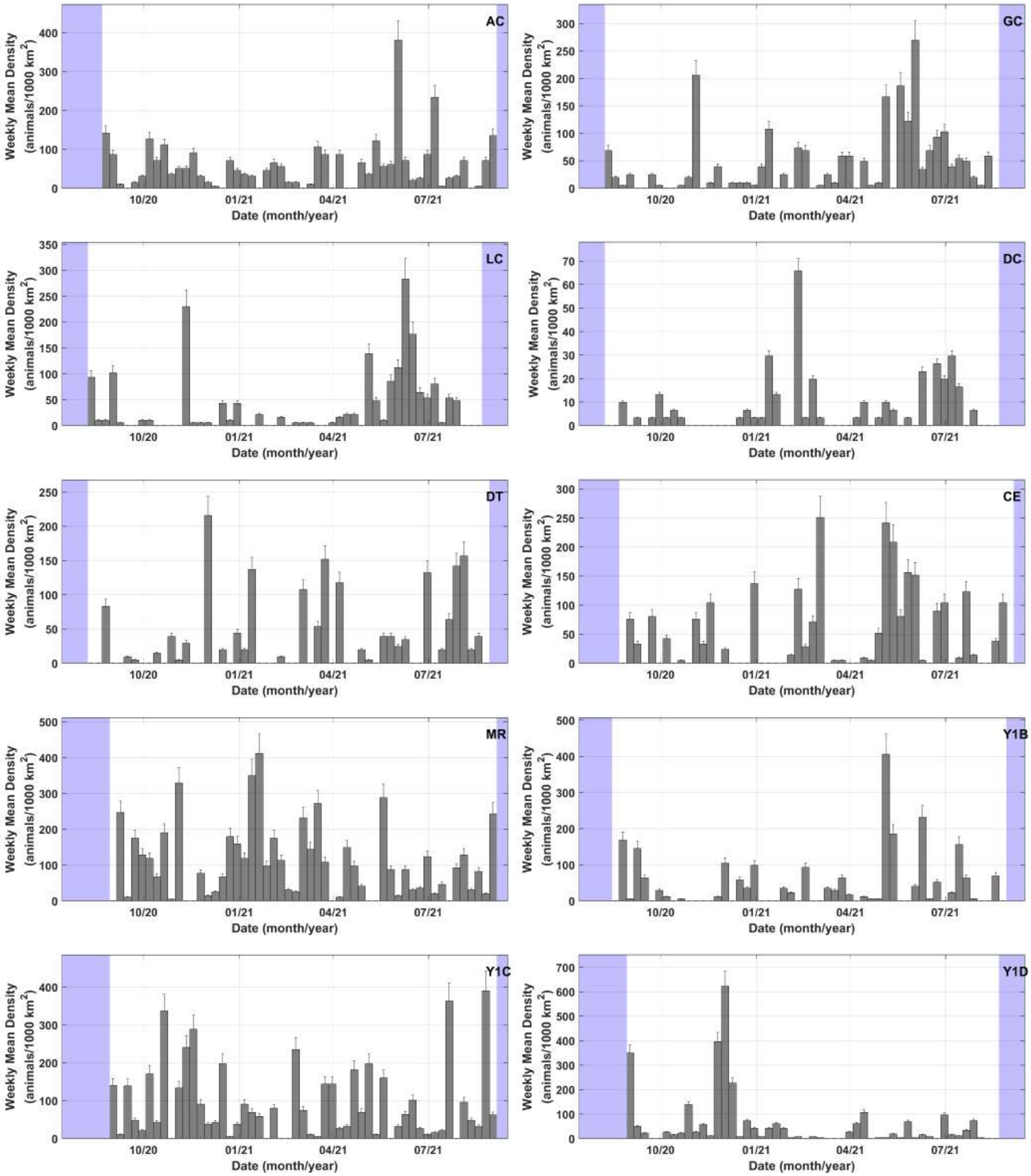

Figure 88: Weekly mean daily density (blue bars) of unidentified dolphin low-frequency (UD LF) echolocation clicks between 2020-2021 at sites AC, GC, LC, DC, DT, CE, MR, Y1B, Y1C, Y1D. Error bars represent ± 1 standard deviation. Shaded blue sections represent periods with no recording effort. Note: y-axis values vary for each site based on detection levels.

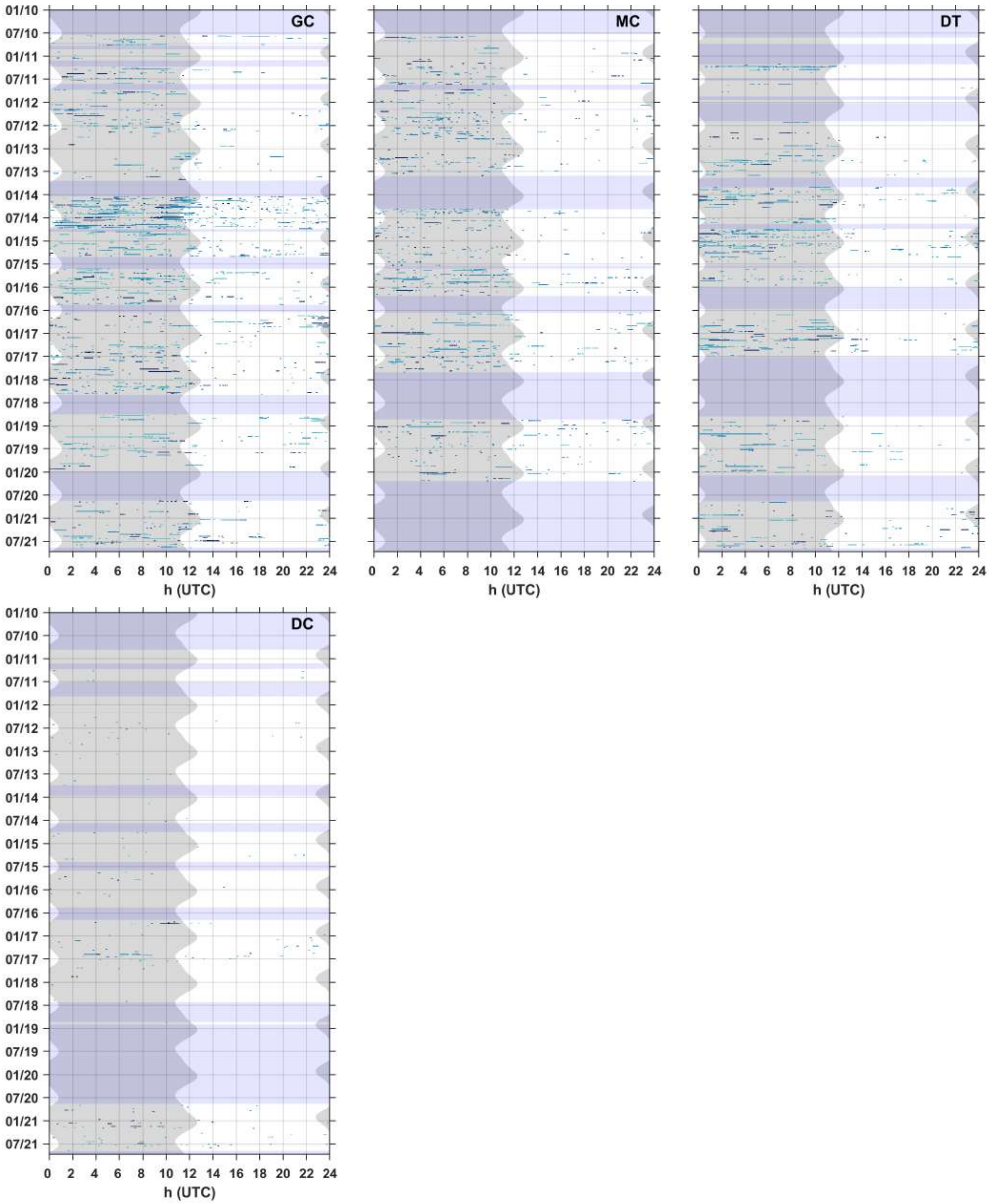

Figure 89: Unidentified dolphin low-frequency (UD LF) echolocation clicks in five-minute bins at historic sites GC, MC, DT, and DC from 2010-2021. Gray vertical shading denotes nighttime and light blue horizontal shading denotes absence of acoustic data. Color denotes number of detections per 5 minutes (light blue: <100; mid blue: 100-1000; dark blue: >1000).

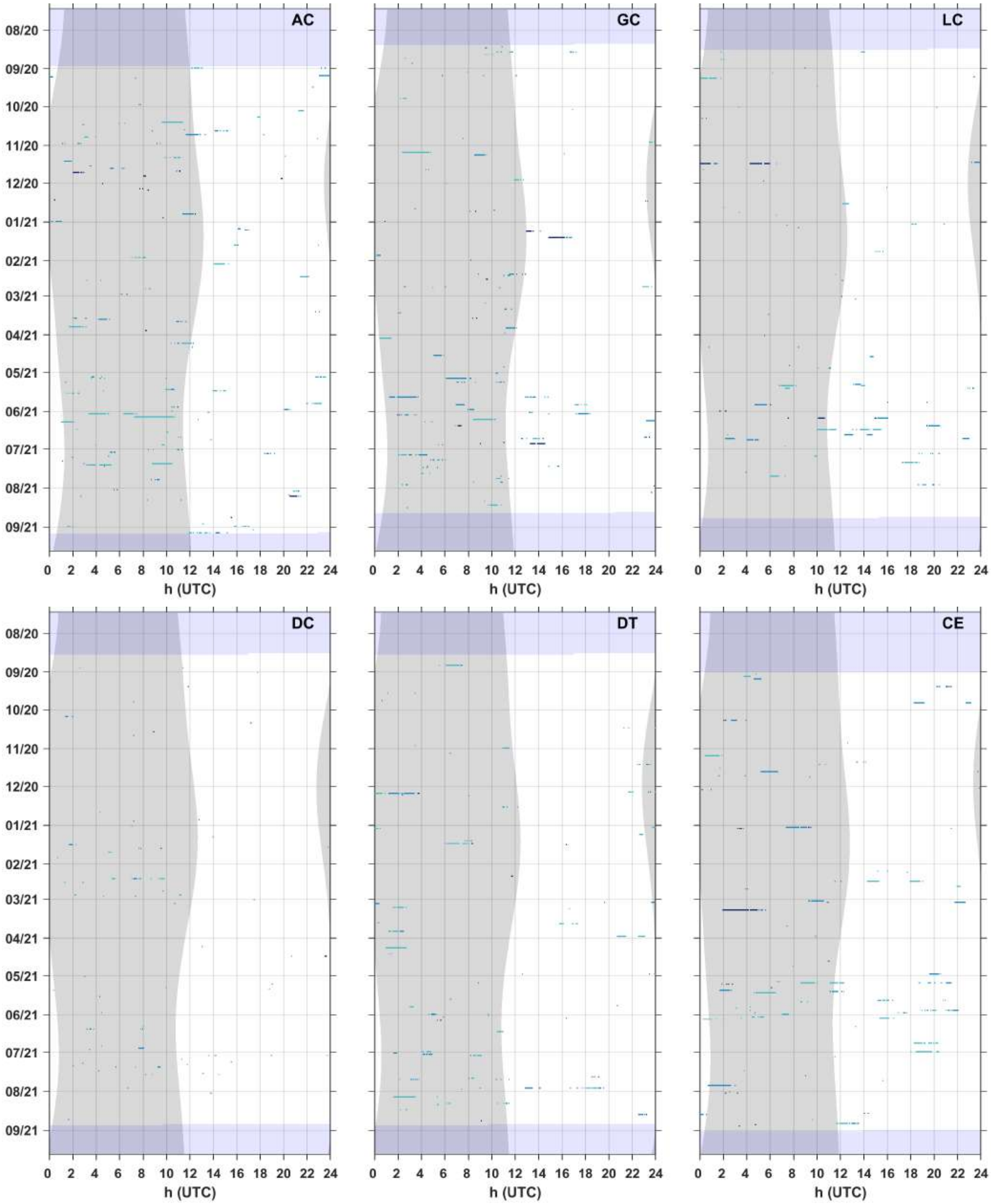

Figure 90: Unidentified dolphin low-frequency (UD LF) echolocation clicks in five-minute bins at sites AC, GC, LC, DC, DT, and CE from 2020-2021. Gray vertical shading denotes nighttime and light blue horizontal shading denotes absence of acoustic data. Color denotes number of detections per 5 minutes (light blue: <100; mid blue: 100-1000; dark blue: >1000).

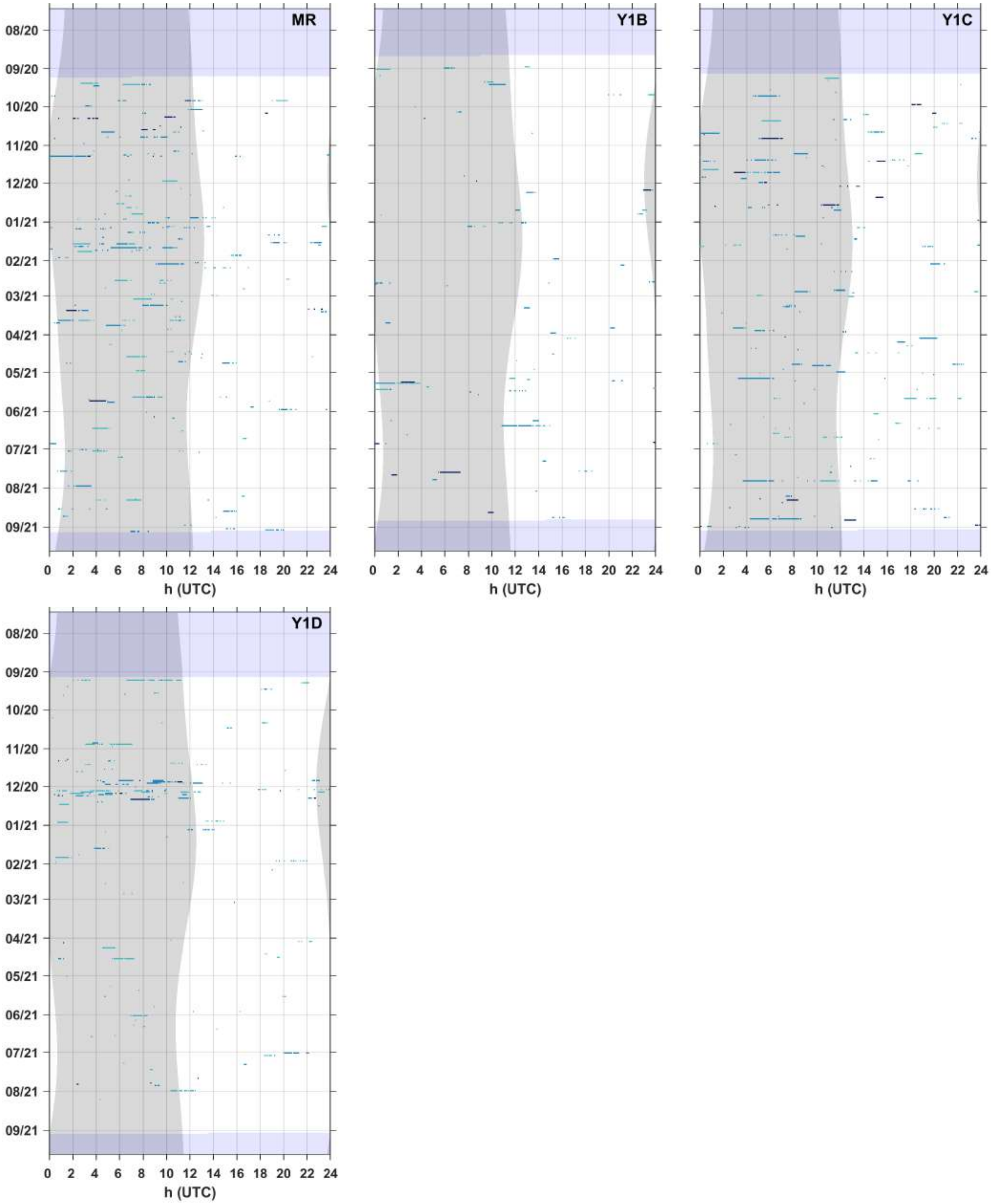

Figure 91: Unidentified dolphin low-frequency (UD LF) echolocation clicks in five-minute bins at one-year sites MR, Y1B, Y1C, and Y1D from 2020-2021. Gray vertical shading denotes nighttime and light blue horizontal shading denotes absence of acoustic data. Color denotes number of detections per 5 minutes (light blue: <100; mid blue: 100-1000; dark blue: >1000).

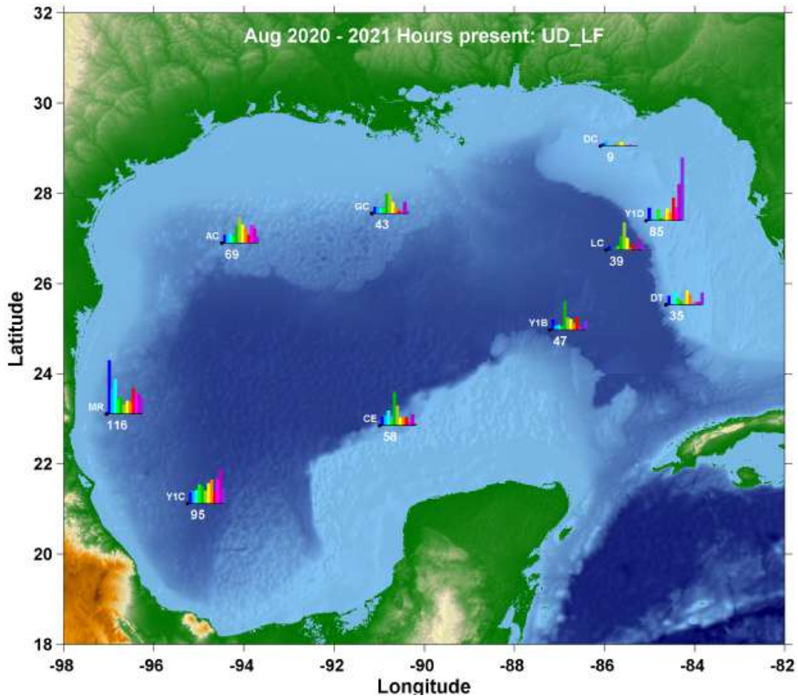

Figure 92: Hourly presence per month for unidentified low-frequency (UD LF) dolphin echolocation clicks from 2020-2021.

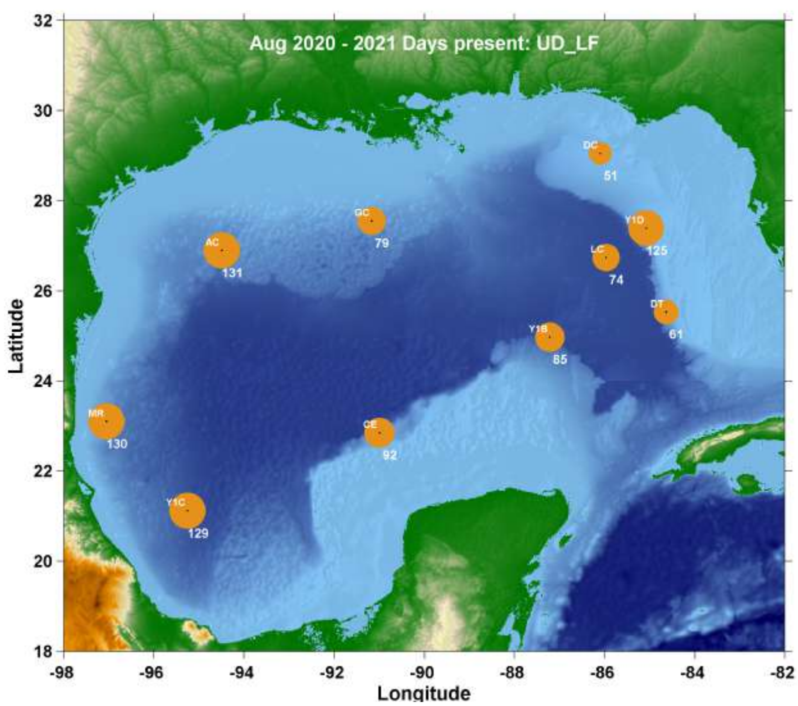

Figure 93: Days present per year for unidentified dolphin low-frequency (UD LF) echolocation clicks (incl. pilot whales) from 2020-2021.

4.2 Other

4.2.1 Snapping Shrimp

Snapping shrimp snaps were detected to eliminate false classifications of delphinid echolocation clicks, but may additionally provide information about the changing habitat at locations snapping shrimp are present at, and are presented here for a holistic view of the acoustic environment. Snapping shrimp snaps were detected in high quantities from 2010-2013 at site MP, dropping off in 2014 and increasing in number again starting in 2017 through to the end of recordings in 2020 (Figure 94). At site DC, snaps were recorded in high numbers in 2011 dropping off in 2012. Snaps picked up again in 2015 and 2016 with the highest recorded period of weekly mean minutes at DC occurring during 2011. Numbers at DC were extremely low in 2017 and 2018 compared to prior years but increased to moderate levels again during the 2020-2021 period. Weekly mean minutes varied differently between sites MP and DC, with opposite trends observed. A crepuscular peak is evident in snapping shrimp snaps at DC (Figure 95).

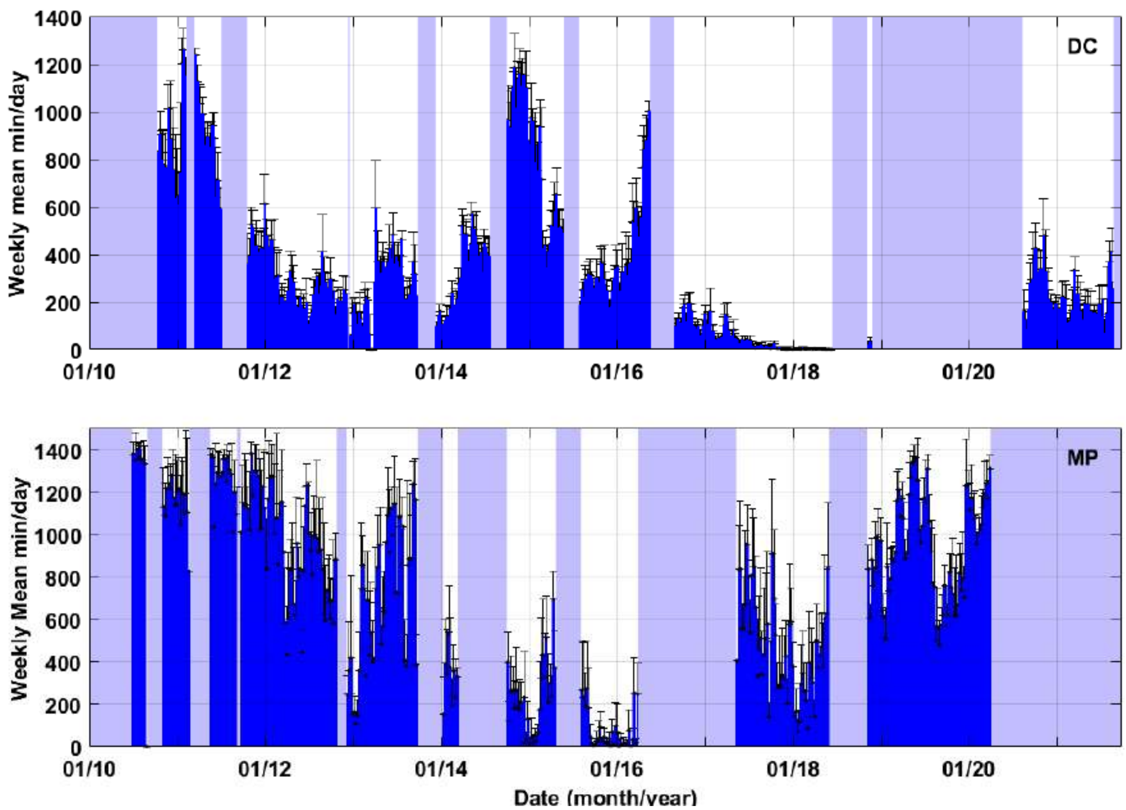

Figure 94: Weekly mean minutes (blue bars) of snapping shrimp between 2020-2021 at shallow sites DC and MP. Shaded blue sections represent periods with no recording effort.

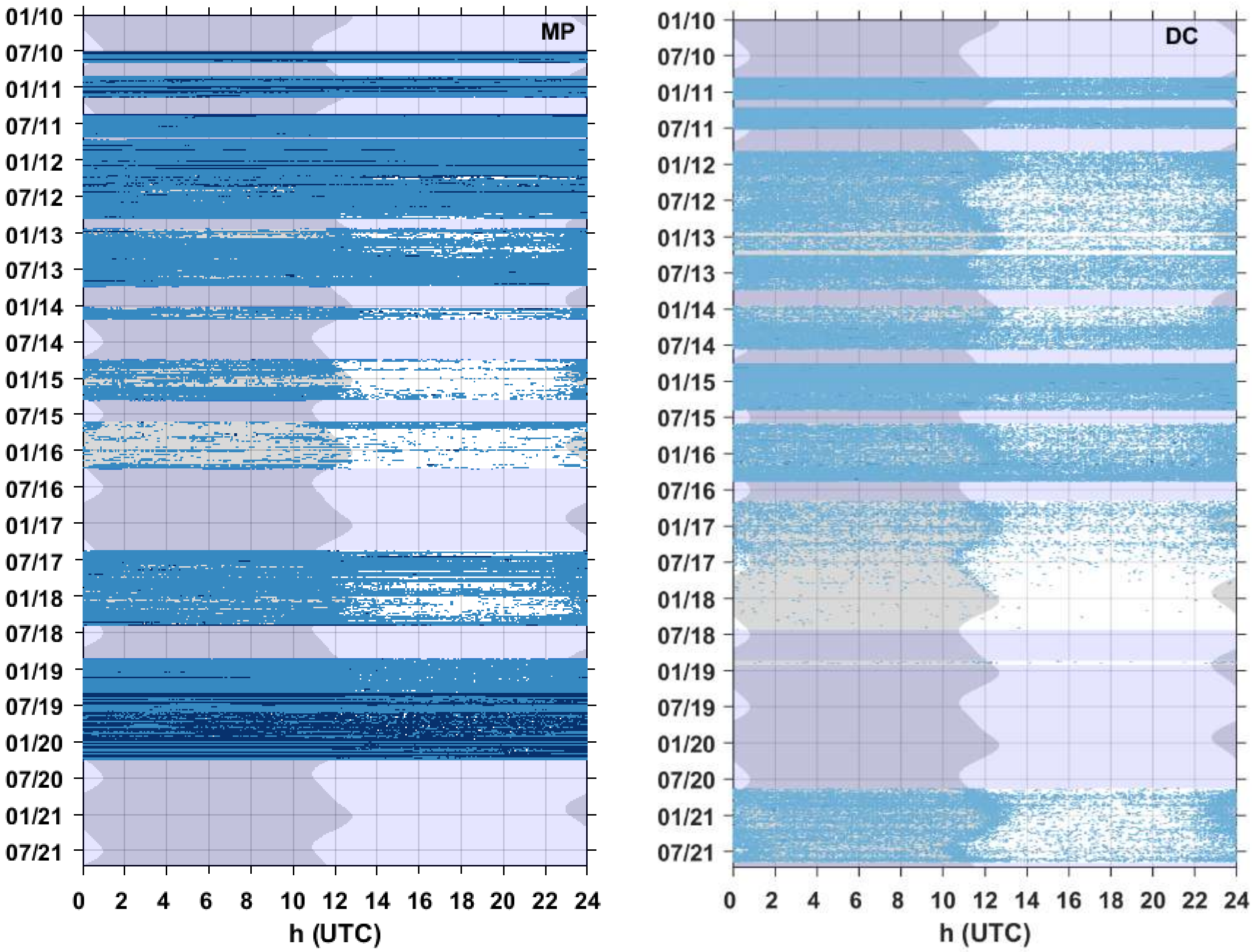

Figure 95: Snapping shrimp signals in five-minute bins at shallow sites MP and DC 2010-2021. Gray vertical shading denotes nighttime and light blue horizontal shading denotes absence of acoustic data. Color denotes number of detections per 5 minutes (light blue: <100; mid blue: 100-1000; dark blue: >1000).

4.3 Ambient and Anthropogenic Noise

4.3.1 Ambient Noise

In both the historic and 2020-2021 data, the ambient soundscape below 100 Hz is dominated at most locations by seismic survey signals (airguns) (Figures 96 & 97). Individual surveys up to months long in duration are visible in the long spectrograms, and in numerous cases, the same surveys appear simultaneously across multiple sensors illustrating the long range propagation of these intense low-frequency signals. Throughout the historic data, sound levels are elevated the most in the airgun frequency band (10 Hz to 100 Hz) at sites GC and MC, which are located within or near active lease blocks, and more moderately at site DT, where these deep water signals propagate effectively, but signals are not typically produced nearby. Transmission of these signals up slope from deep into shallow water environments is weak; therefore, levels in the seismic band are lower at sites DC and MP.

During quieter periods between seismic surveys, moderately elevated sound levels in the 30-90 Hz frequency band are often evident (e.g. at MC in summer 2017 and fall 2020, and at DT in fall 2019 and summer 2021), representing noise from vessel traffic (Figure 117). Across all sites, and particularly evident at the quieter DC site, vertical stripes across the 100-1000 Hz frequency band indicate periods of increased noise levels due to weather events (noise from wind, waves, and precipitation, Figure 117). Ambient noise conditions at the shallow MP site are noticeably different from those at the other sites, with lower levels at low frequencies, in part due to absorption of sound into the seafloor, and higher levels at higher frequencies (>100 Hz) due to the increased presence of smaller vessels as well as biological sounds from fish and invertebrates (Figure 96).

In the 2020-2021 data (Figure 97), similar soundscape patterns are evident across the sites due to the presence of similar sound sources over time. Specifically, a series of distinct seismic survey events are visible across all sites, with the exception of the shallow site SL, where levels are dominated by shipping. Levels at DC remain low during this time period compared to other deeper sites, though seismic signals are still evident. The energy peak between 30-90 Hz associated with commercial vessel transits is strongly evident at the shipping lane sites SL and GA, followed by AC and Y1B. It is also apparent at most sites in the quieter periods between seismic surveys. In the higher frequencies, above 100 Hz, the vertical stripes associated with weather are evident, with similar patterns across neighboring sites, and generally are increased during the winter period compared to the summer. Elevated sound levels in the first half of the SL timeseries may be partially related to a hydrophone malfunction. A period of high noise at LC in April of 2021 may be due to local currents (Figure 97).

Statistical distributions of the median hourly sound pressure levels during the 2020-2021 recording periods are presented for each site (Figure 98). A typical curve is observed across all sites, with sound levels highest at the lower frequencies (<100 Hz), followed by a steep drop off from 100 to 200-300 Hz, and then a continuing drop-off or leveling out between 200 to 1000 Hz. Variance tends to be highest below 100 Hz and above 200 Hz. At shipping lane sites GA and SL, a hump between 30-90 Hz is evident due to shipping noise. Sites AC, GC, CE, MR, and Y1C have particulalry high levels at lower frequencies, with harmonic peaks evident at 7, 14, and occasionally 21 Hz due to resonance features of airgun surveys. Sites GC, CE, and Y1B have an additional hum at 150 Hz (Figure 98) that appears to be associated in time with an airgun survey in the March - May 2021 period (Figure 97). Overall, sound levels are generally lowest at site DC, followed by sites MC, DT, and Y1D.

Octave Band (Hz)	Minimum RL (dB re μPa^2)	Maximum RL (dB re μPa^2)
16	83.0	110.2
31.5	84.9	114.4
63	82.4	115.3
125	77.0	105.4
250	74.7	99.7
500	77.8	93.8

Table 6: Minimum and maximum ambient band-levels received over the August 2020-2021 period in the octave bands centered on 31.5 Hz, 63 Hz, 125 Hz, and 500 Hz for Figure 99.

The spatial distribution of monthly median octave band-levels at each site over the 2020 - 2021 period highlights some of the noise sources described above (Figure 99, Table 6). The 31.5 Hz octave-band-level represents sound from airgun surveys well, the 63 and 125 Hz band-level represents noise from shipping traffic (e.g. Marine Strategy Framework Directive, Descriptor 11), and the 500 Hz band-level represents noise from weather. The 31.5 Hz octave band-levels are generally higher in the western Gulf than the eastern Gulf, which is expected given the distribution typical distribution of airgun energy in the northwestern Gulf of Mexico. The April, May, and December periods have particularly high levels across western sites, and in September, levels were especially high at the central Gulf sites (Figure 99). These correspond well with locations of seismic survey activity described below in section 4.3.4. Received levels in this band in the Rice's whale core habitat (site DC) were generally lowest, though levels were elevated in March and April. While the 63 Hz and 125 Hz octave band-levels are typically representative of shipping noise, maps of monthly median band-levels (Figure 99) follow similar patterns to those for the 31.5 Hz band-levels indicating seismic signals are still dominating these bands most of the time. In the Rice's whale core habitat, site DC has substantially lower noise levels in the 125 Hz octave band, which encompasses Rice's whale call frequencies, during spring and summer months compared to fall and winter (Figure 99C). This may be caused by the same seasonal weather variation seen at higher frequencies but is particularly apparent at this site due to the overall lower noise levels found here. Noise levels in the 500Hz band are relatively similar across sites, though seasonal differences are evident with lower noise levels in summer and high noise levels in fall and winter (Figure 99D). Site CE has higher levels in April and May than expected compared to other sites, during the period when a 200-300 Hz peak was associated with airgun activity.

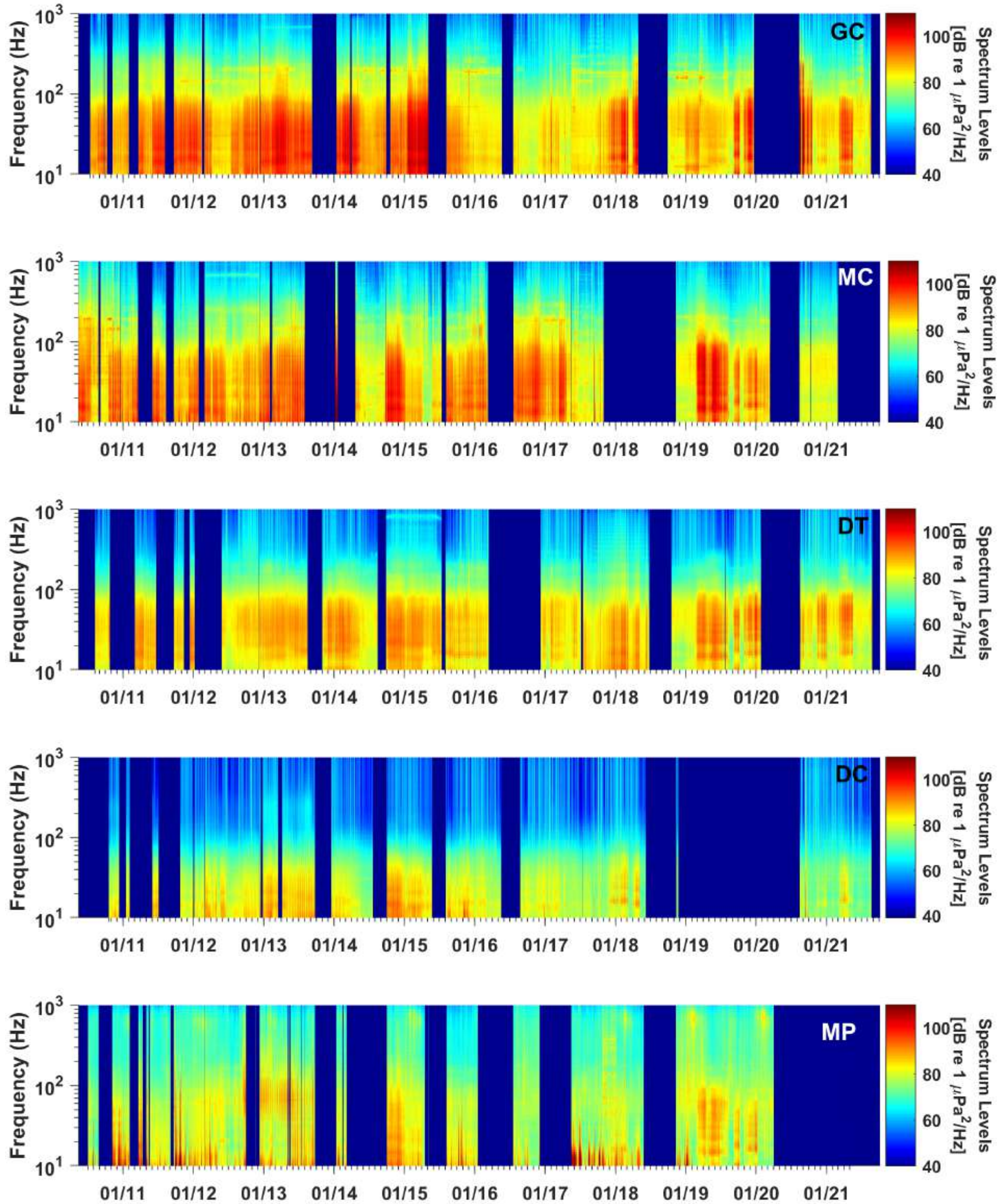

Figure 96: Long-term spectrograms using daily-averaged df100 (10-1000 Hz) spectra for 2010-2021 data recordings. Dark blue periods represent periods with no recordings.

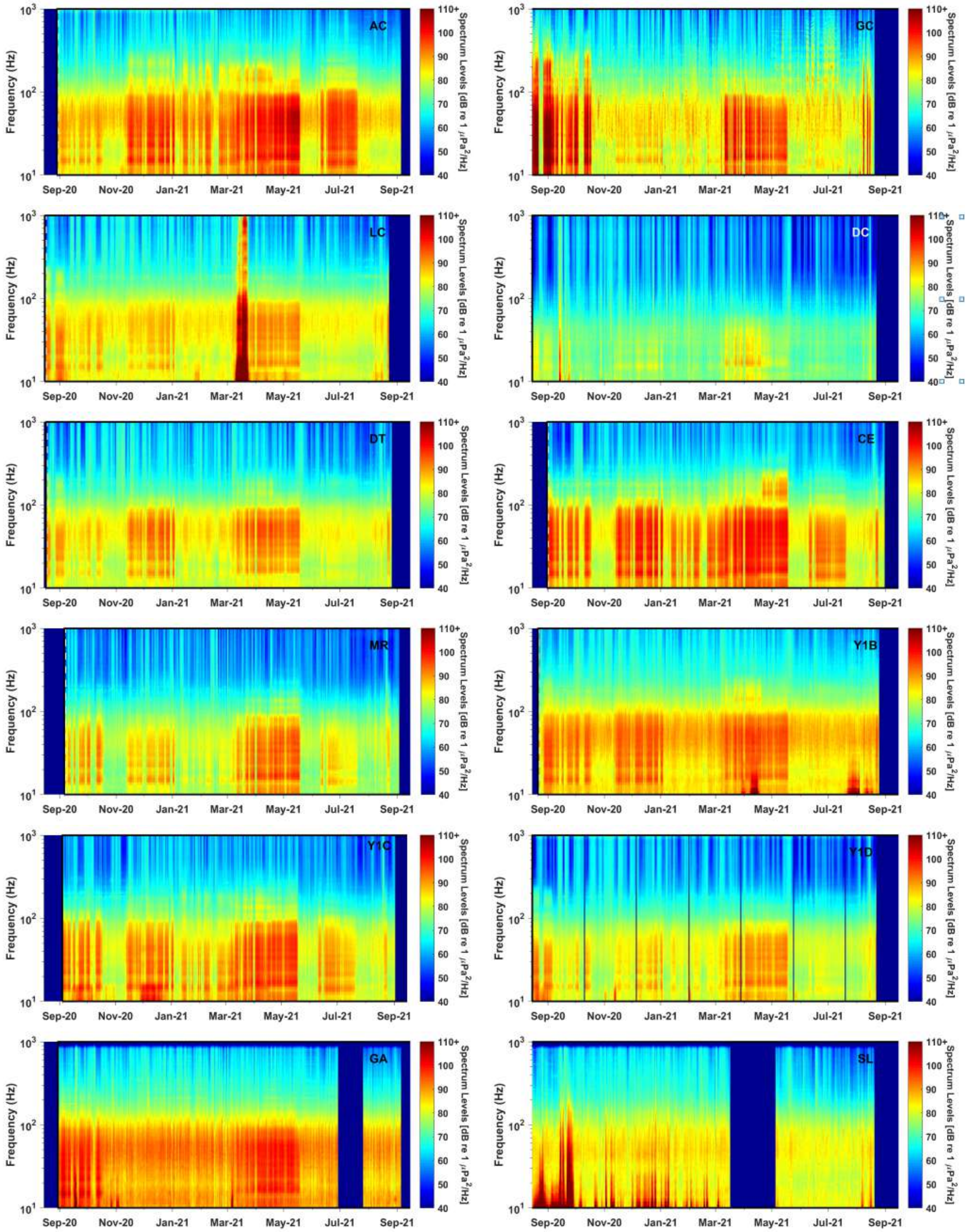

Figure 97: Long spectrograms using daily-averaged spectra for 2020-2021 data recordings. Dark blue blocks represent periods with no data recordings.

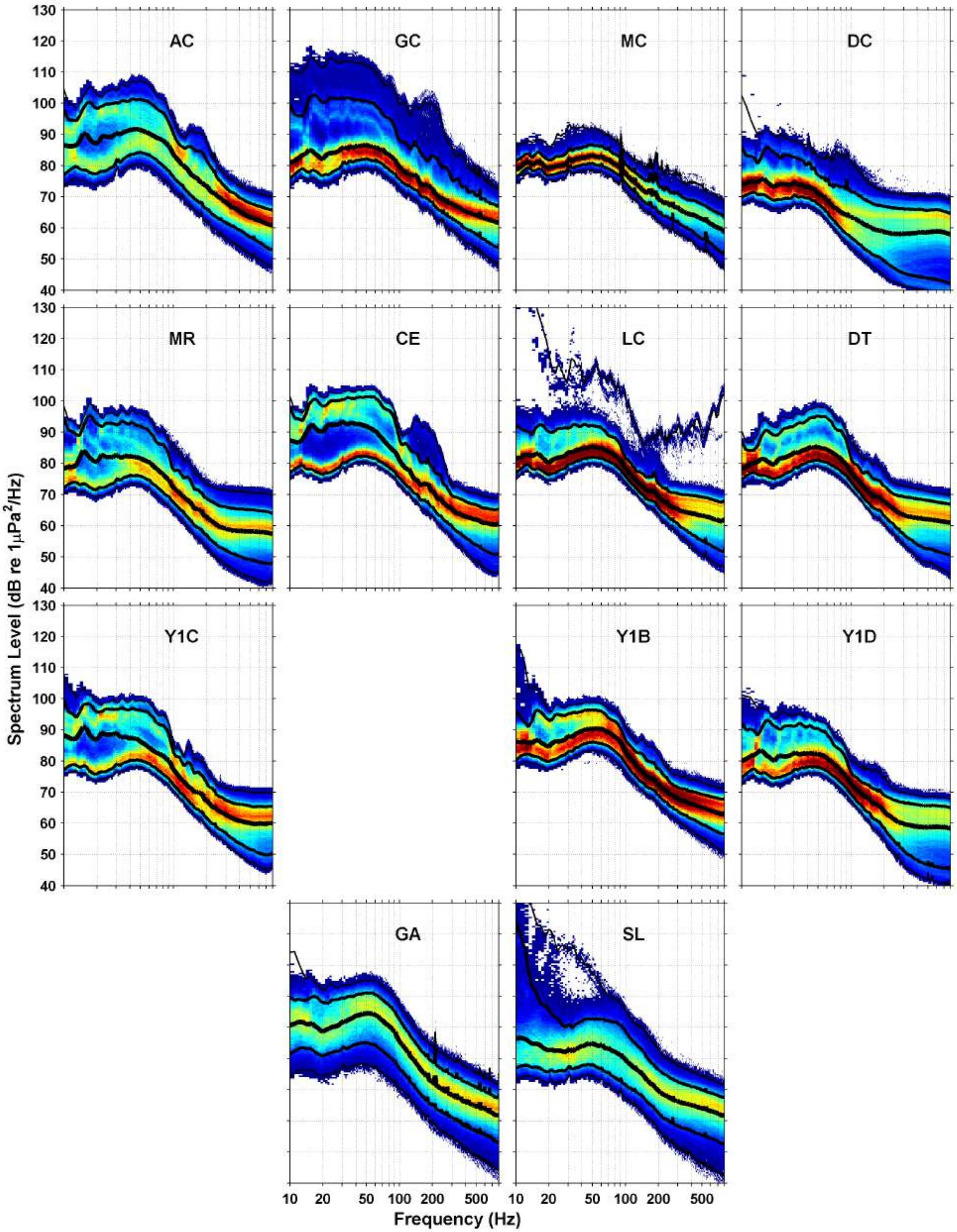

Figure 98: Heat map distribution of hourly mean ambient soundscape spectra for HARP and MARP sites from 2020-2021. The 50th (thickest), 25th and 75th (medium thickness), and 1st and 99th (thinnest) percentiles of hourly mean spectra are represented by solid lines.

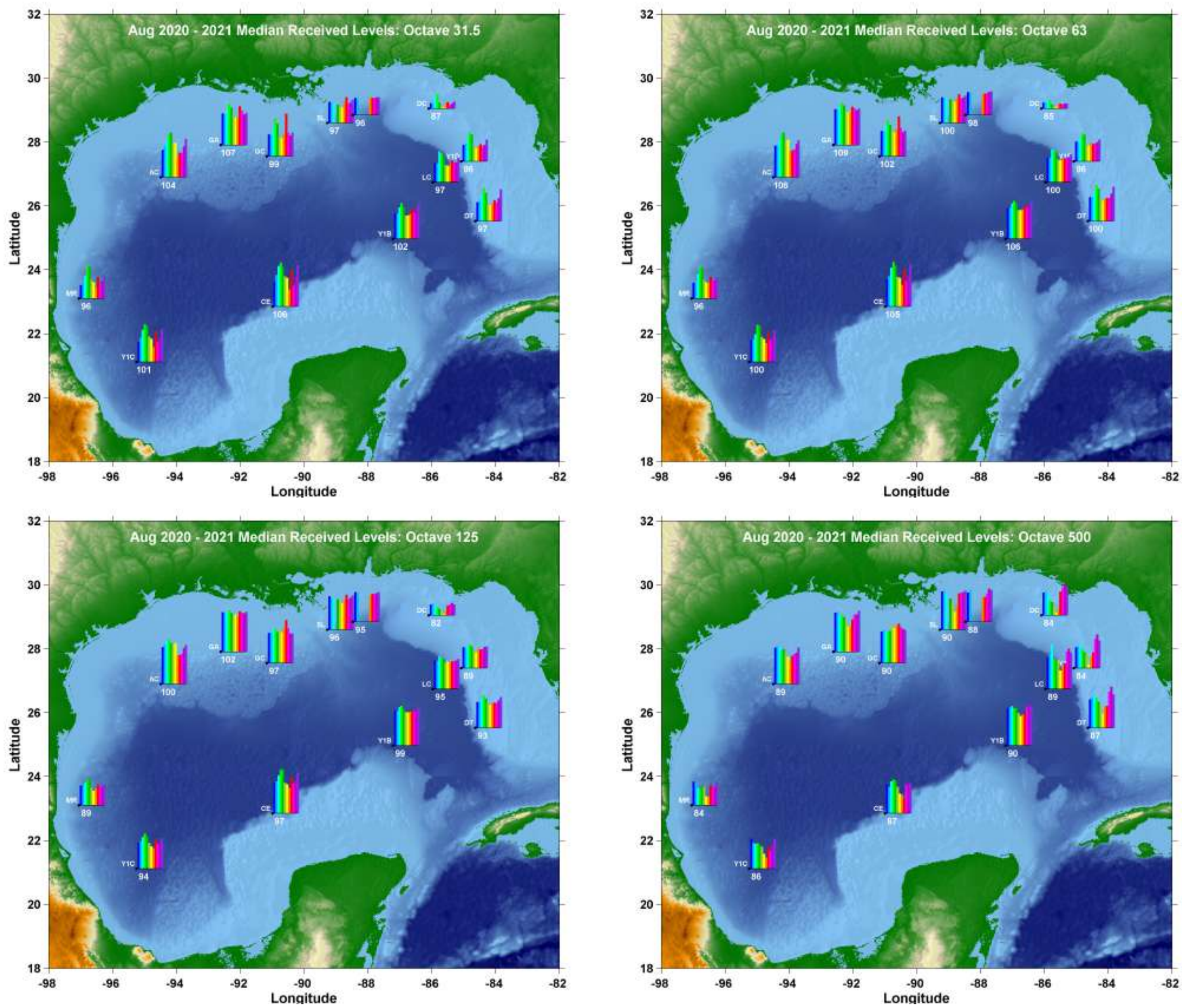

Figure 99: Monthly median ambient band-levels received at each site over the August 2020-2021 period in the octave bands centered on A) 31.5 Hz, B) 63 Hz, C) 125 Hz, and D) 500 Hz. Values below bars represent the annual median band-level at each site. Minimum and maximum values of bars are included in Table 6.

4.3.2 Broadband Ships

Analyses of shipping noise detections and AIS ship track data highlight the high levels of shipping activity in the Gulf of Mexico, and the variability in activity, noise levels, and vessel types among sites. More ships were detected at sites GC, MC, and MP (ranging from 21.0 to 25.6 mean ship detections per week), which are the sites located near major shipping lanes and oil rigs (Figure 100). Fewer ships were detected at sites DT and DC ranging from 12.4 to 9.8 mean ship detections per week (Figure 100). Similarly, shipping noise was present during more hours per week at sites GC and MP (27.9 to 24.4 mean hours per week; Figure 101).

Analyses of data from 2020-2021 indicate the highest number of detections and longest durations of ship noise presence occurred at sites GA (mean 127.1 detections; mean 55.7 hours present; Table 7) and SL (mean 78.1 detections; mean 35.8 hours present; Table 7), the two sites located within major shipping lanes (Figures 102 & 103). Sites AC, MR, and Y1B also had elevated numbers of nearby ship transits, likely due to their proximity to shipping lanes as well. Site AC also had long durations of ship noise present, with a mean of 37.2 hours per week. Sites CE, LC, Y1C, and Y1D had fewer ships detected as well as lower durations of ship noise presence.

The AIS data indicated variability in ship types, number of ships, and closest points of approach of ships at the different sites. Cargo ships were common at all sites except site GC (Figure 105). They were the dominant ship type at site DC, mostly passing at distances >13 km, as well as at sites CE (similar numbers between 0-14 km), LC (similar numbers at all distances), MR (with greater numbers >7 km away), and SL (especially within 2 km) (Figures 106 & 107). Sites MR and SL also had large numbers of tankers, passing at relatively similar distances at site MR and passing mostly within 2km at site SL. At site SL, the proportion of ships started to favor passenger ships after 3 km, the distance at which the number of ships passing significantly decreased. Sites AC, GA, and GC had mostly tankers, which mainly passed 8-9 km away at site AC, within 2km at site GA, and within 6 km at site GC. The number of ships passing by site GA significantly dropped after 3 km. Site GC also had elevated numbers of offshore supply vessels, and research vessels were also common at this site at distances >10 km. Site MC had high numbers of cargo ships, offshore supply vessels, passenger ships, and tug tows, with more ships passing >8 km away. Site MP had mostly passenger ships, which occurred at all distances from the HARP. A peak in cargo ships and offshore supply vessels occurred at 11 km. Site DT, which was near a shipping lane, had primarily cargo ships, tankers, and tug tows, with most ships >5 km away. Site Y1B had mostly cargo ships and tankers, with similar numbers at all distances. Site Y1D had a variety of ship types – including cargo ships, fishing vessels, pleasure vessels, tankers, and tug tows. Finally, it is important to note that AIS data were sparse for sites CE, LC, and Y1C. Note, the number of ships in Figures 105-108 is cumulative over the 2010-2021 period for all sites except GC, which spans 2015-2021, while the ship counts in Figures 106-108 are cumulative over the 2020-2021 period. Therefore, these results are not directly comparable.

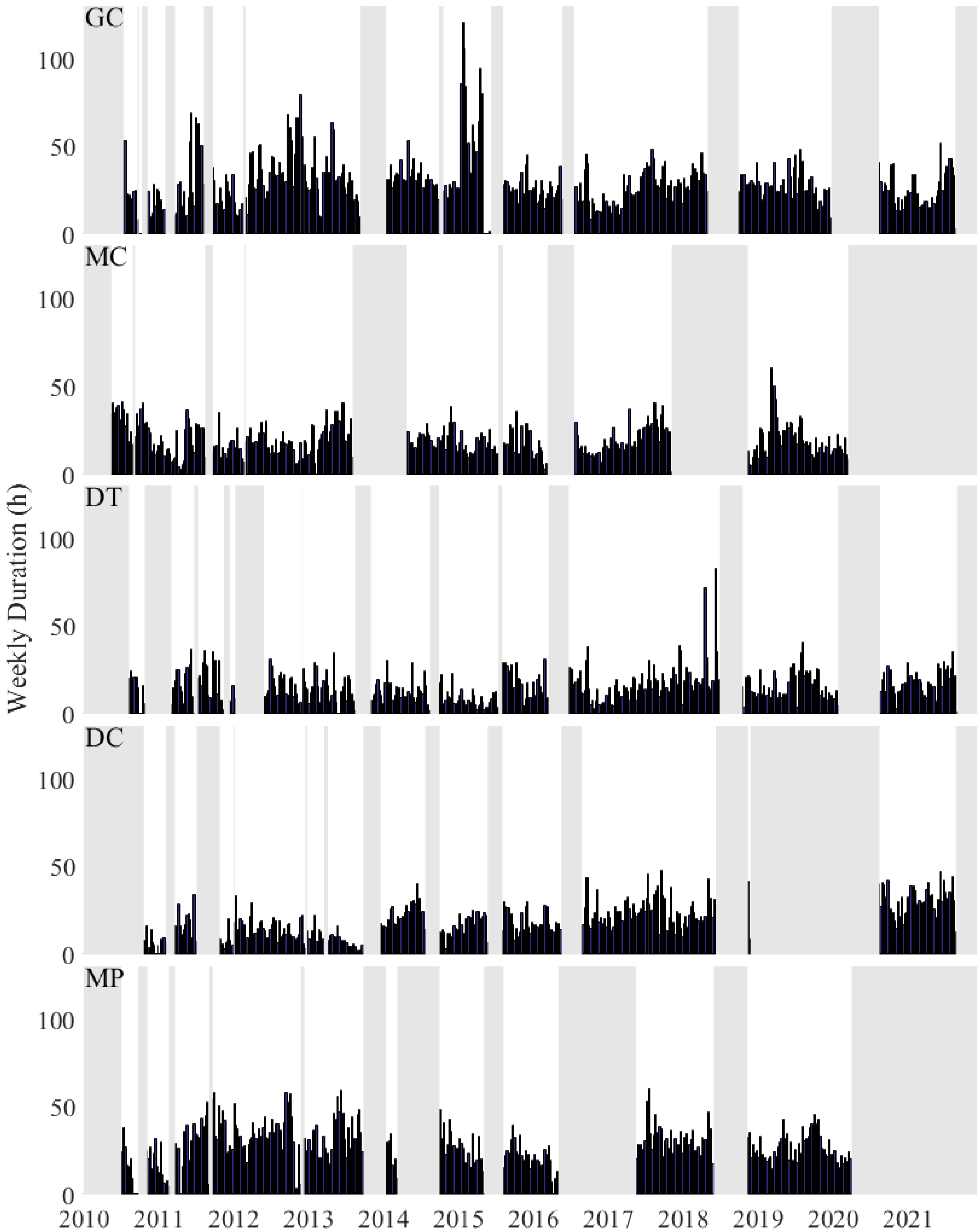

Figure 100: Weekly time present for ship transits detected at the historic sites from 2010-2021.

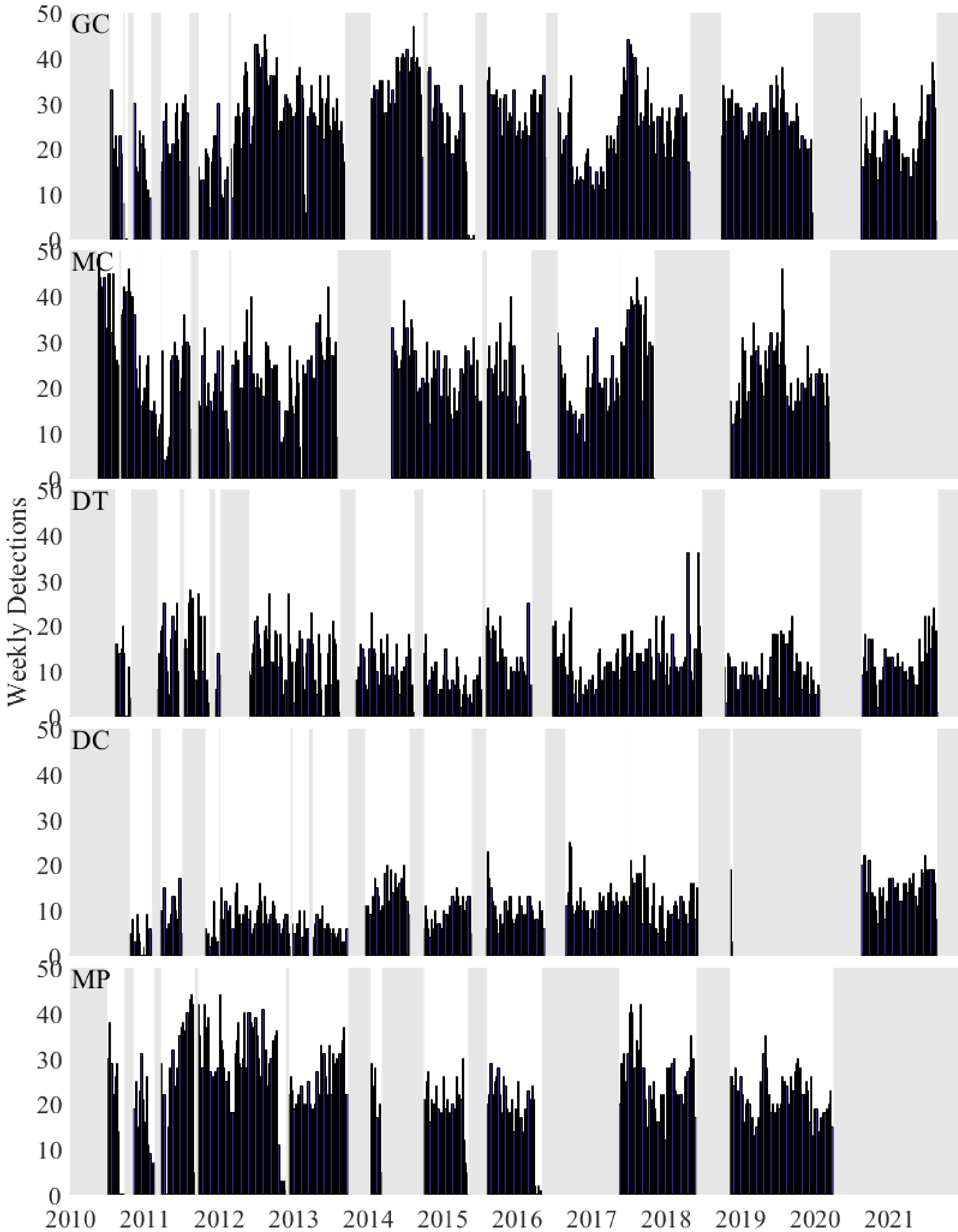

Figure 101: Cumulative weekly counts of ship transits detected at the historic sites from 2010-2021.

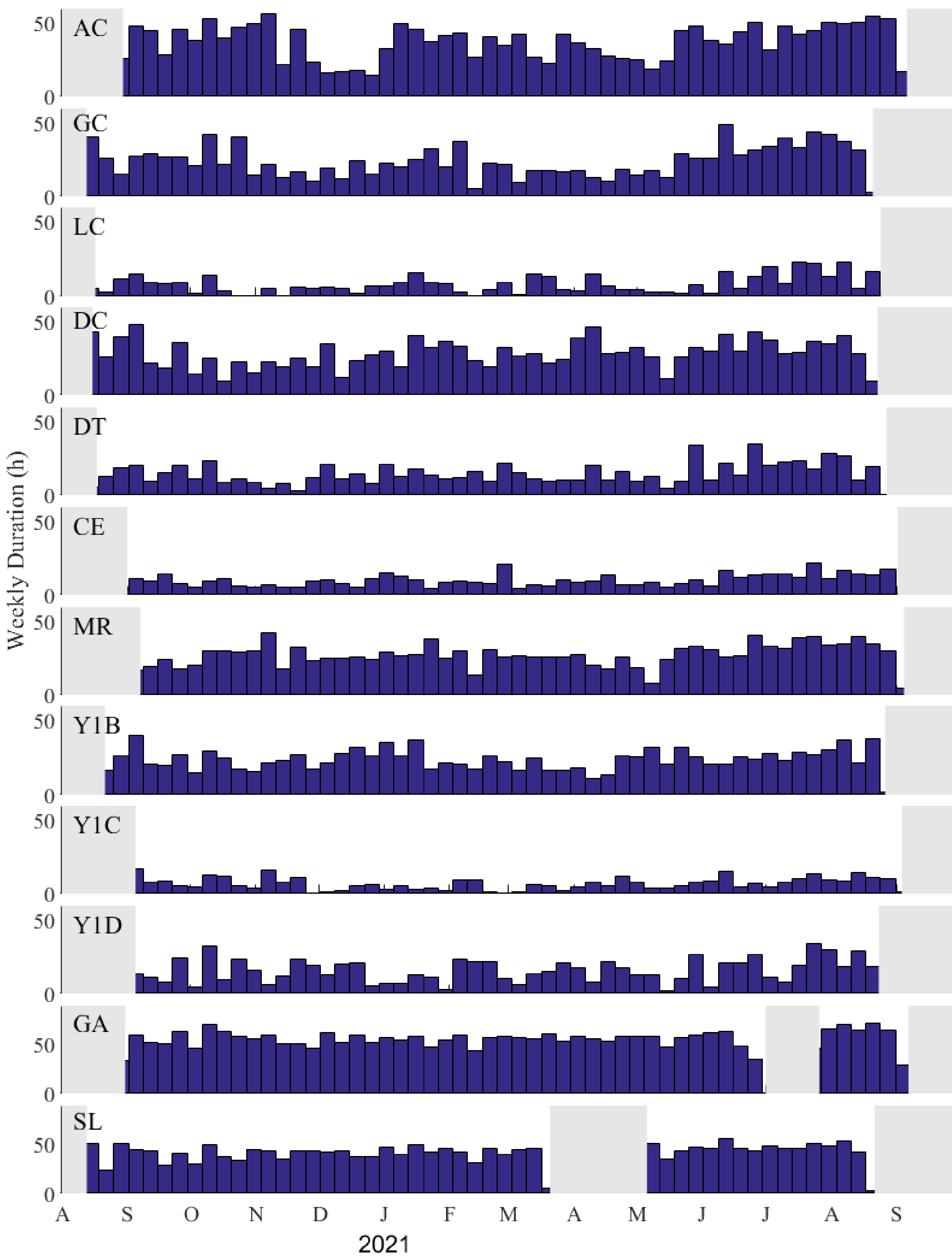

Figure 102: Weekly time present for ship transits detected at 2020-2021 sites. Note: Sites GA and SL have a different scale on the y-axis due to the higher number of ship transits in these shipping-lane sites.

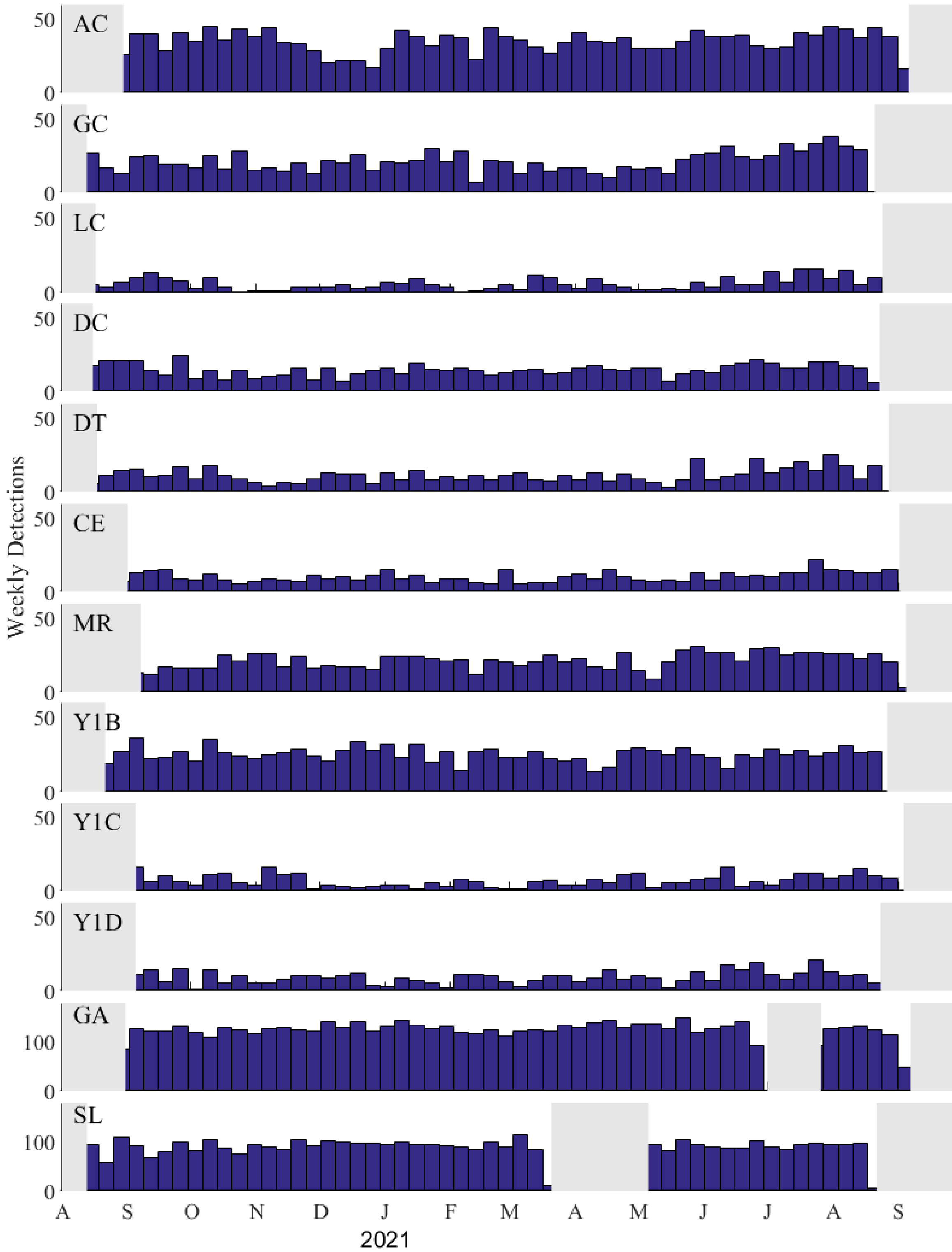

Figure 103: Cumulative weekly counts of ship transits detected at 2020-2021 sites.

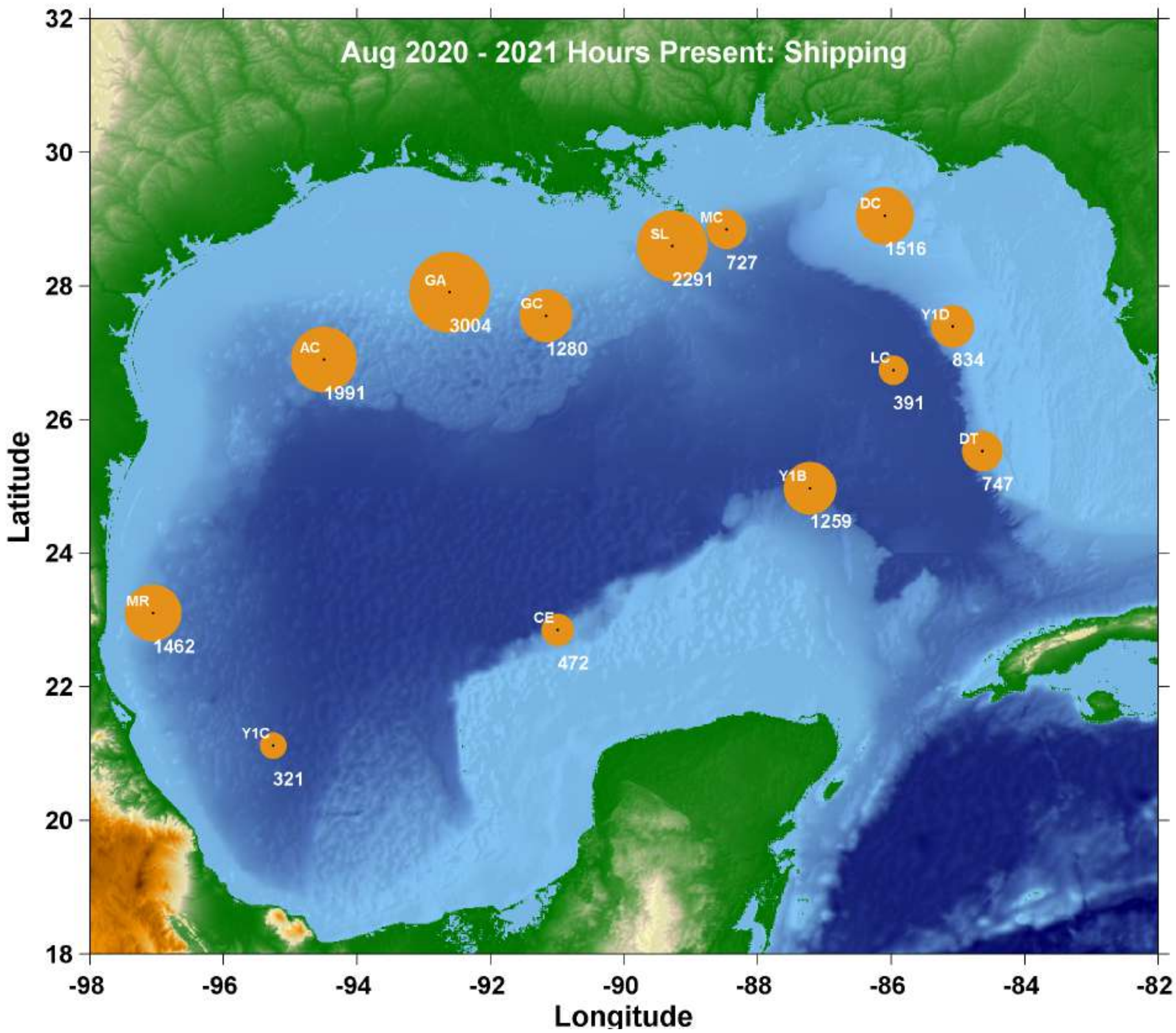

Figure 104: Hours per year with broadband shipping noise present at each HARP location from 2020-2021.

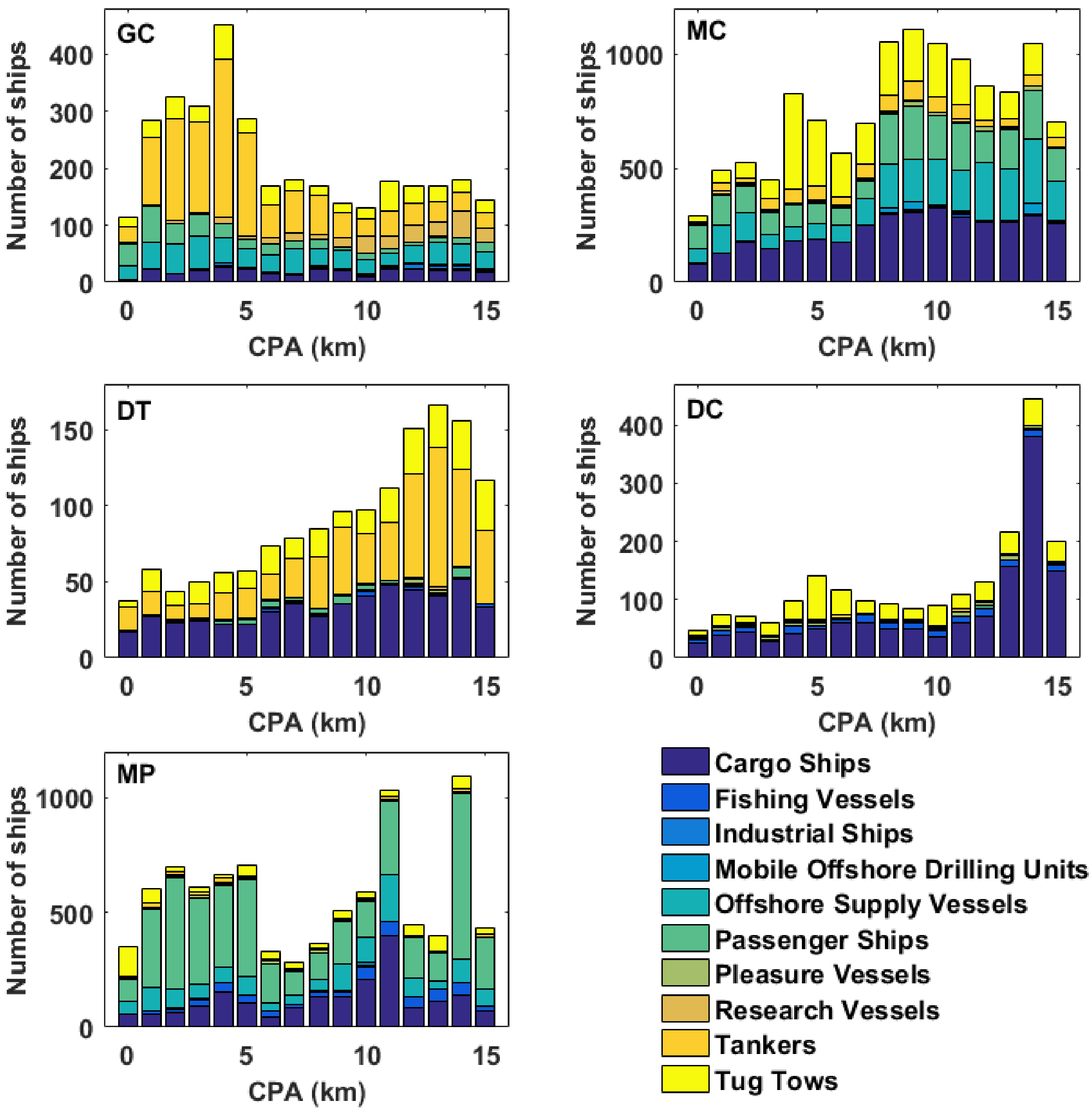

Figure 105: Ship closest point of approach (CPA) by vessel category for historic HARP sites. Note: GC counts do not include pre-2015 transits due to a lack of AIS data.

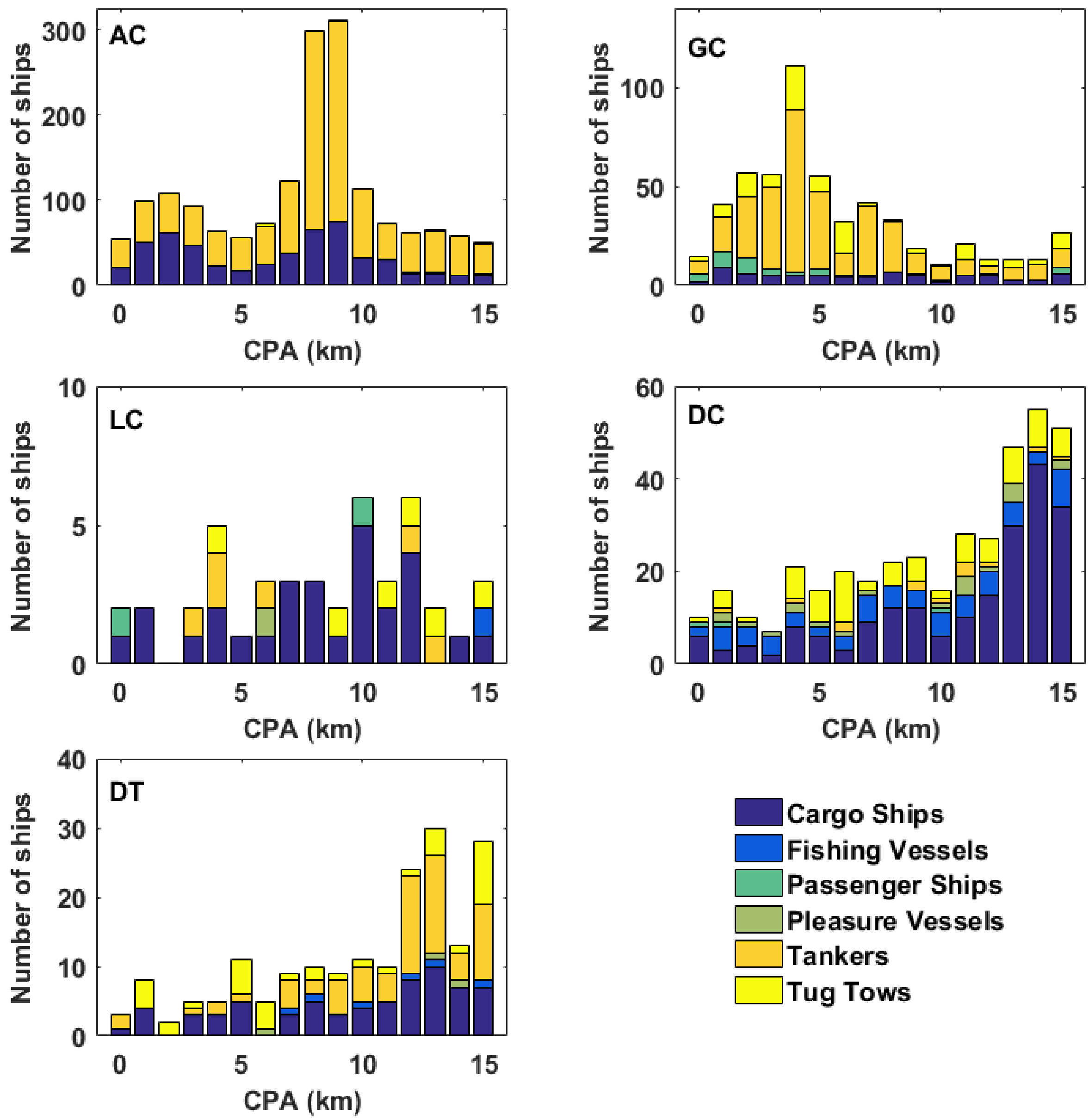

Figure 106: Ship closest point of approach (CPA) by vessel category for 2020-2021 for AC, GC, LC, DC, and DT sites.

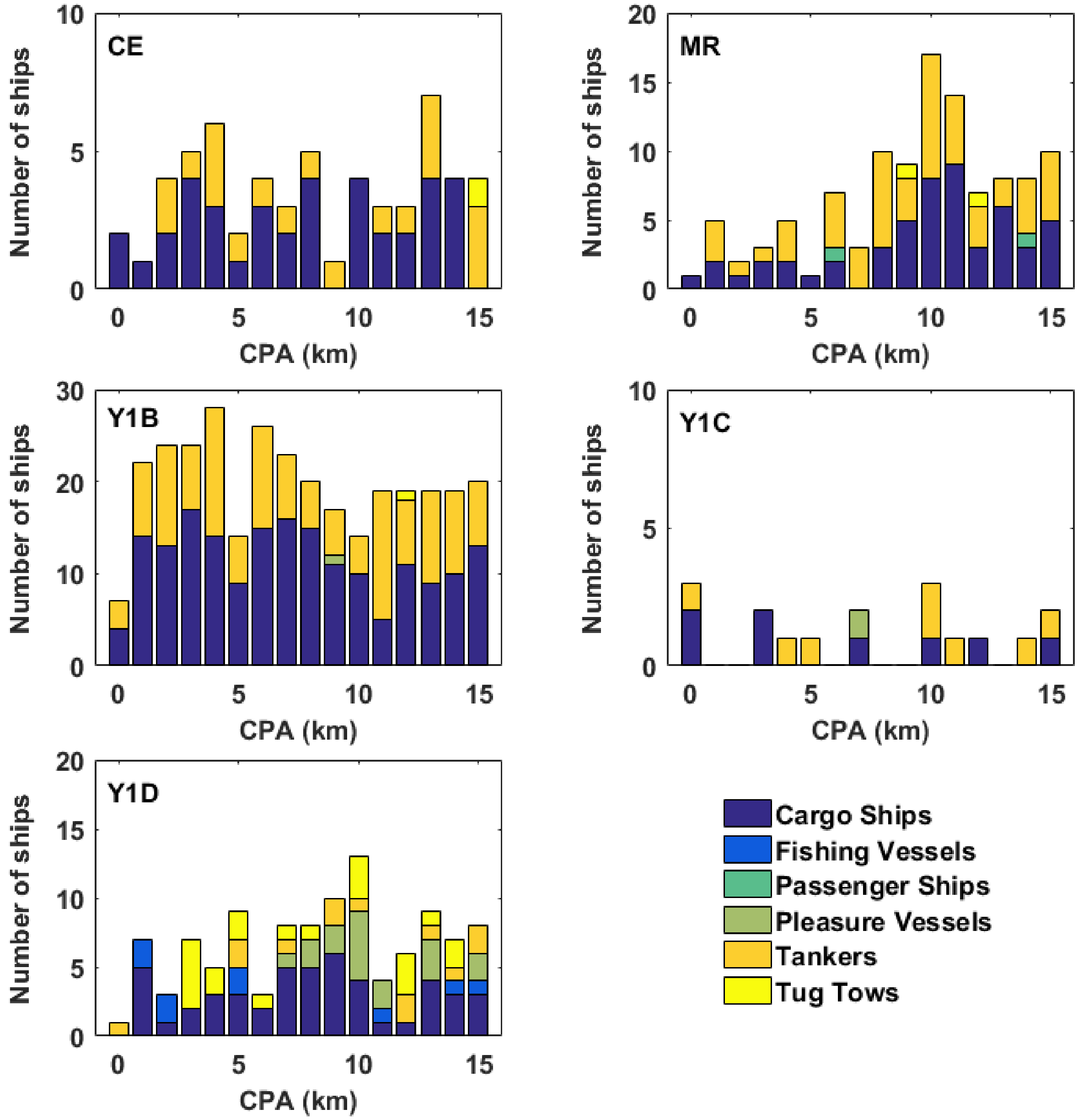

Figure 107: Ship closest point of approach (CPA) by vessel category for 2020-2021 for CE, MR, Y1B, Y1D, and Y1D.

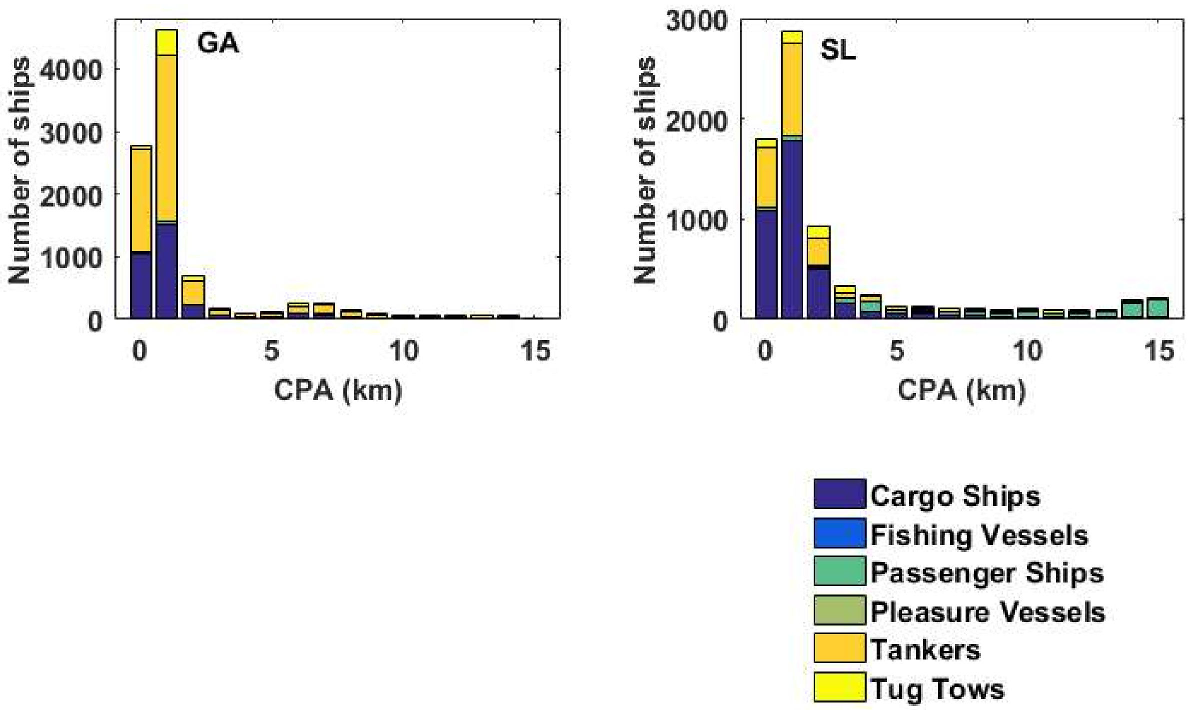

Figure 108: Ship closest point of approach (CPA) by vessel category for 2020-2021 for GA and SL.

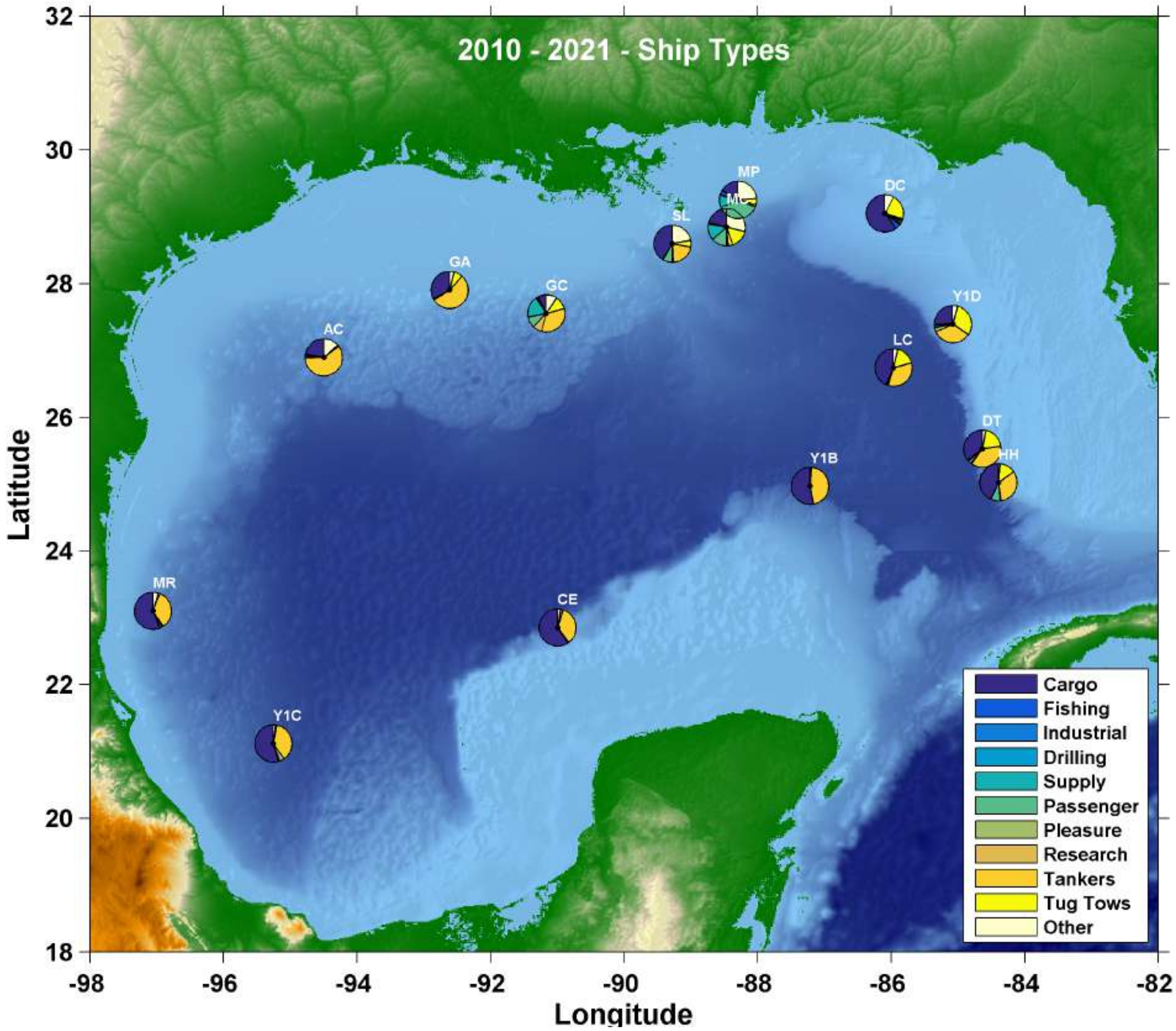

Figure 109: Proportion of ship types transiting within 15 km of each HARP location based on AIS data from 2010-2021.

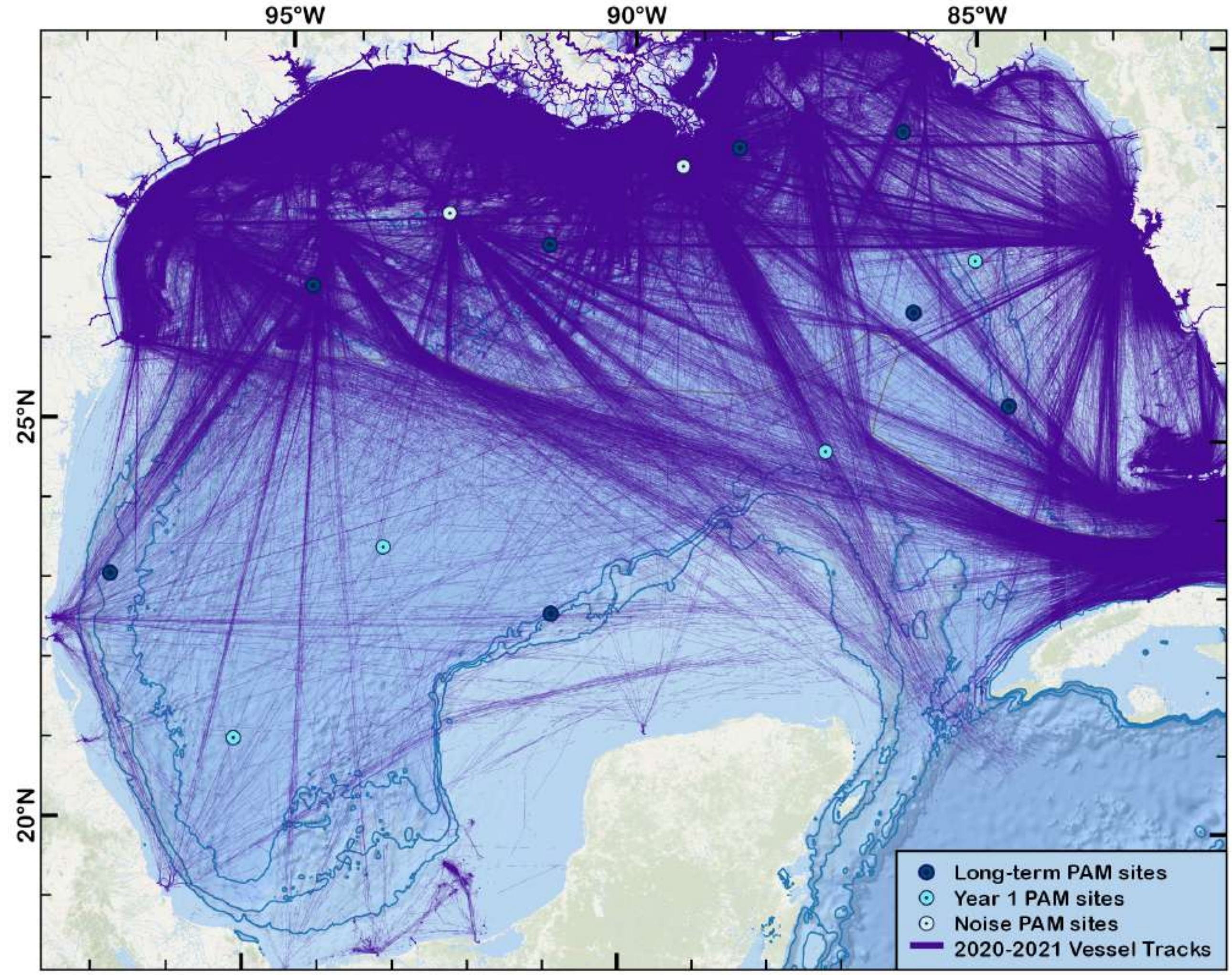

Figure 110: AIS-based vessel tracks (from MarineCadastre) in the Gulf of Mexico over the Aug. 12, 2020 to Aug. 31, 2021 period. Lighter levels of traffic in Mexican waters may be real, or may be an artifact of lower AIS-receiver coverage.

4.3.3 Vessel Source Levels

Vessels transiting over the MARP in the Galveston shipping lane site (GA) were primarily tankers (approximately 500 transits) and cargo ships (approximately 320 transits) (Figures 111 & 112). There were roughly twice as many close transits at the GA location compared with the Southern Louisiana (SL) site, where the majority of nearby vessels were primarily cargo ships (300 transits), with lower numbers of tankers (140 transits). Transit speeds were similar at the two sites, with a few higher speed transits (>15 knots) recorded at GA. The variability of harmonic mean sound speed estimates derived from HYCOM hindcasts was slightly higher at the SL location. The number of descriptive parameters for transiting vessels available from the Marine Cadastre AIS data used to inform this analysis was somewhat limited. Additional effort could be expended to refine categories within “Cargo” (likely includes a variety of bulk, container, and vehicle carriers), and to identify additional relevant characteristics.

Monopole source level (MSL) estimates for the major vessel categories were very similar across the two shipping lane sites (Figures 113 & 114), indicating that the modified Lloyd’s mirror model largely accounts for site specific differences for these close-approaching transits. A subset of transits at site SL recorded early in the monitoring period had elevated MSL estimates below 5 Hz, however these transits appear to co-occur with unidentified low frequency noise in the recordings, unrelated to the vessels. Median MSL was comparable for the two largest categories, cargo ships and tankers, at both sites, with an energy peak around 50 Hz. Tug/Tow vessel source levels were 5-10 dB lower at 50 Hz than the cargo ships and tankers. MSLs of the remaining vessel categories were highly variable, likely due to small sample sizes. Few strong correlations were observed between the predictor variables including speed over ground (SOG), vessel length, closest point of approach, or draft (Figures 115 & 116). SOG was positively correlated with broadband MSL for transits at site GA. The lack of a strong relationship between SOG and MSL at site SL may be due to low frequency strumming leading to overestimation of broadband MSL during some periods.

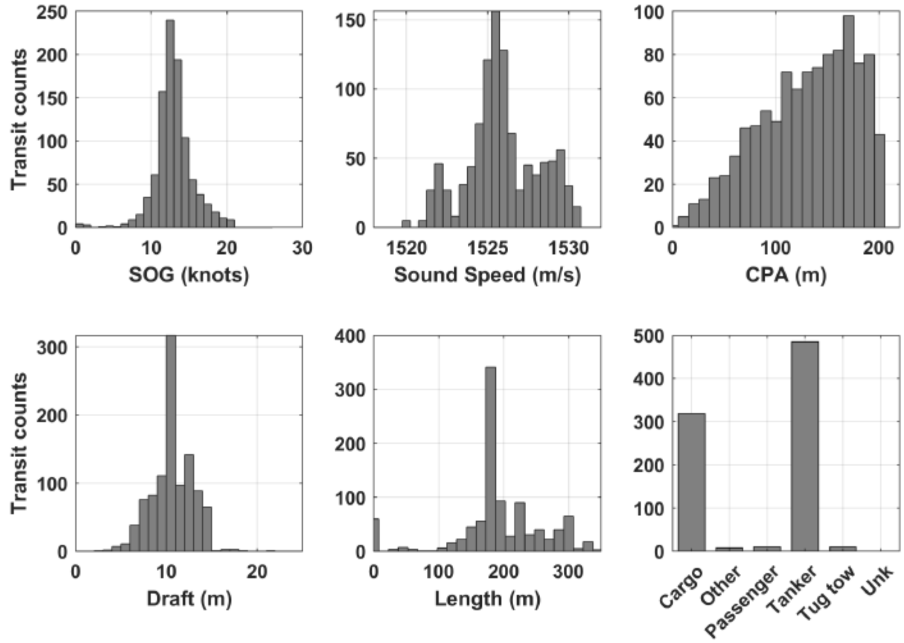

Figure 111: Distributions of AIS-derived vessel descriptors for vessel transits passing within 200 m of the GA HARP from mid 2020-2021.

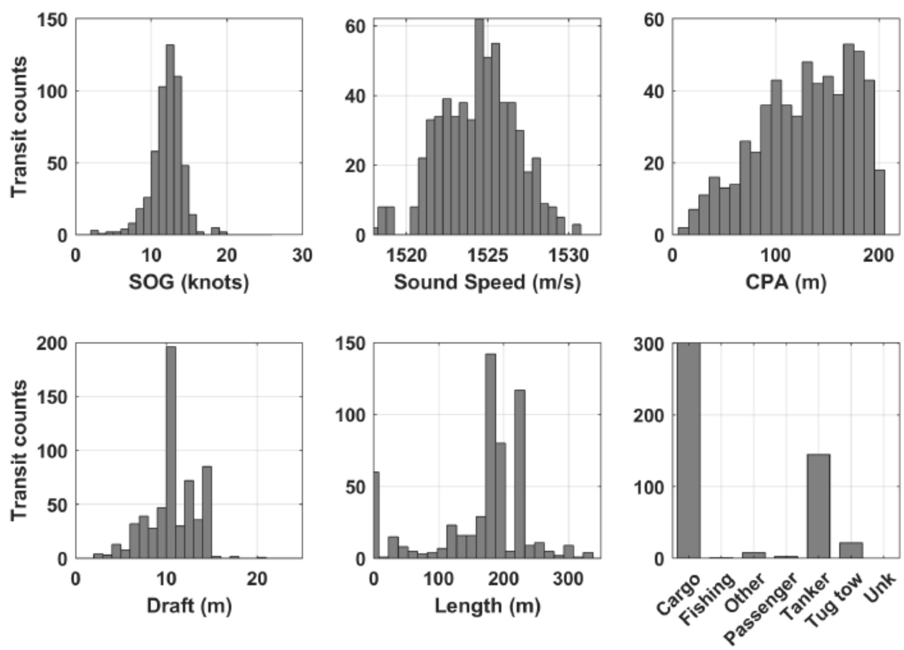

Figure 112: Distributions of AIS-derived vessel descriptors for vessel transits passing within 200m of the SL HARP from mid 2020-2021.

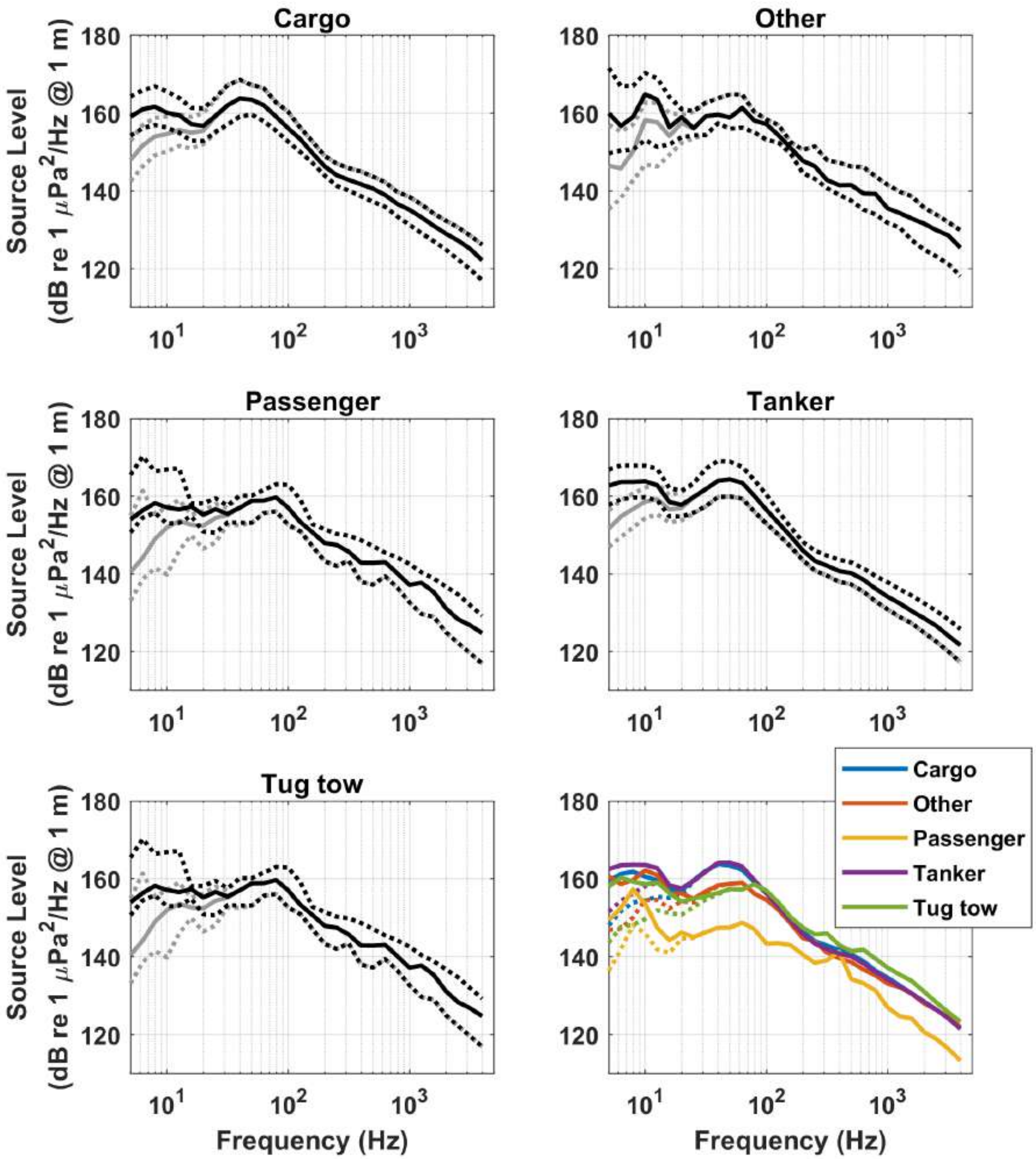

Figure 113: Mean (solid line) and 25th and 75th percentiles (dashed lines) of 3rd octave band MSL (black) and RNL (gray) estimates for different categories of vessels passing within 200vm of the GA HARP from mid 2020-2021. In the final subplot (color) MSL (solid lines) and RNL (dashed lines) estimates for all vessel types are plotted together.

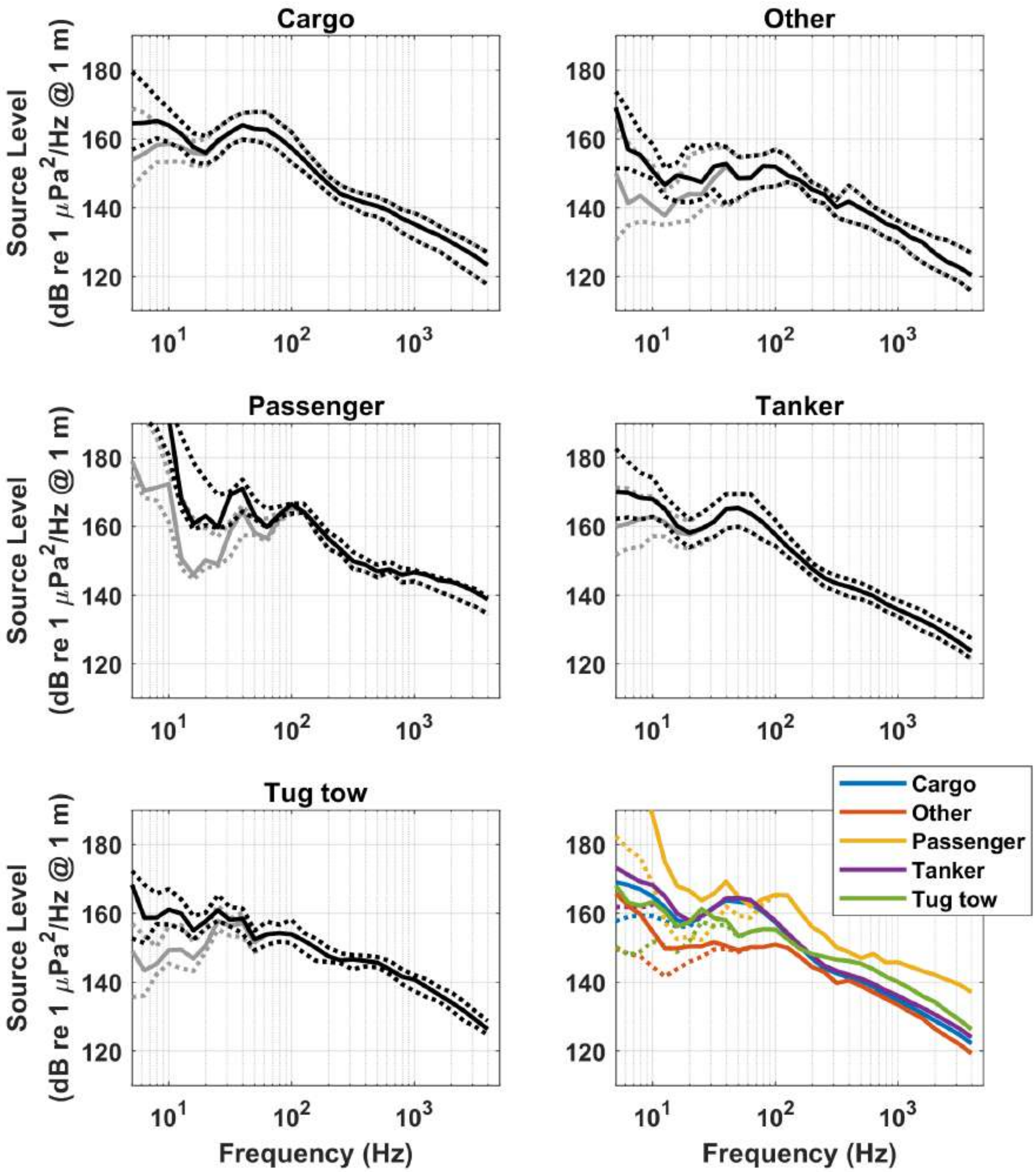

Figure 114: Mean (solid line) and 25th and 75th percentiles (dashed lines) of 3rd octave band MSL (black) and RNL (gray) estimates for different categories of vessels passing within 200 m of the SL HARP from mid 2020-2021. In the final subplot (color) MSL (solid lines) and RNL (dashed lines) estimates for all vessel types are plotted together.

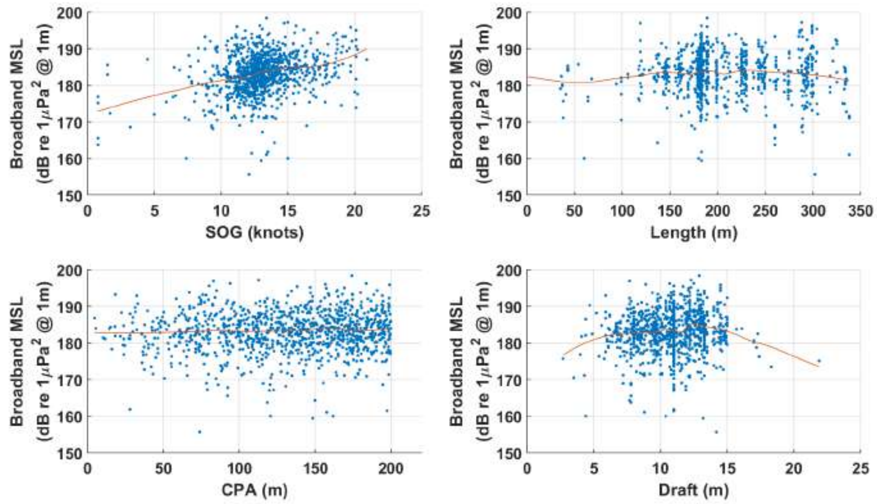

Figure 115: Correlations between AIS-derived vessel descriptors and broadband MSL estimates at site GA. Red lines represent smooths of the data, to elucidate potential trends.

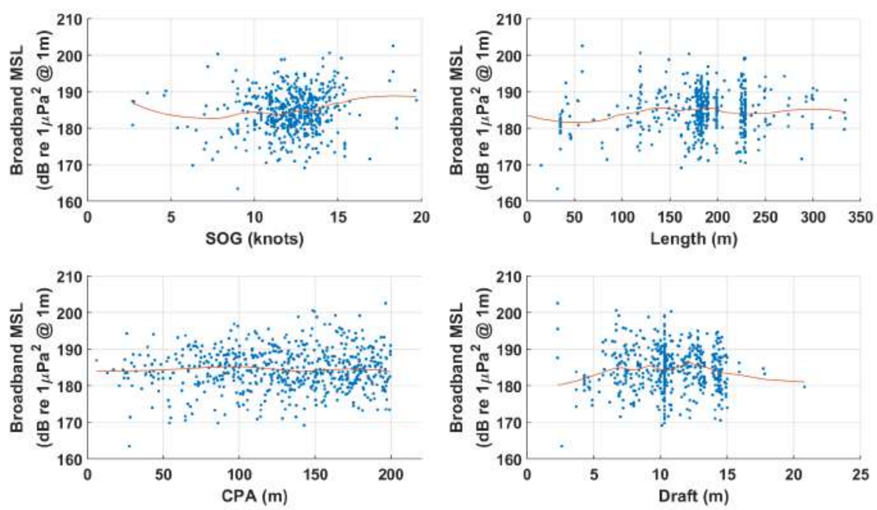

Figure 116: Correlations between AIS-derived vessel descriptors and broadband MSL estimates at site SL. Red lines represent smooths of the data, to elucidate potential trends.

4.3.4 Airguns

Analyses of the 10 years of airgun detections and presence (at 1 min granularity) at historic sites indicate that airgun survey signals with energy greater than 120 dB pp re $1\mu Pa^2$ were commonly present (and detected in high numbers) in recordings at all of the historic sites (GC, MC, DT, DC, MP) throughout this period (Figure 117). Airguns were most frequently present (and detected in greatest numbers) at site GC, followed by site MC, particularly prior to 2017 when airgun pulse detections typically were present more than 90% of the time. While site DC had airgun pulse detections present the least frequently of all the sites, their occurrence at both sites DC and DT was notably and consistently high despite these site's locations in the Eastern Planning Area, at considerable distances from the majority of presumed survey activity in the Central and Western Planning Areas. Sites GC, MC, and DC all had detections present less frequently after summer 2020, while site MC also had periods of low occurrence during the end of 2010 and the 2017-2018 period, and DC also had periods of lower occurrence during 2014 and 2017. Site MP on the shelf, had relatively high occurrence of airgun pulse detections as well, with notable periods of lower occurrence during 2010, 2014, and 2017. There were no apparent diel patterns for airgun pulses for all the historical sites, as surveys were conducted throughout the day and night (Figure 119).

Analyses of the 2020-2021 deployments show airgun pulses with energy greater than 120 dB pp re $1\mu Pa^2$ occurred most commonly at sites AC, CE, and Y1C (daily means of 2127-2401 pulse detections and 8.2-8.8 hours present) followed by sites Y1B and DT (Table 7), and were often present more than 50% of the time at these sites (Figure 118). Additionally, there were similar patterns of occurrence of airgun pulse detections across sites (Figure 118) indicating the same surveys were detected at sites spread broadly throughout the Gulf. Occurrence was higher at most sites in August through mid-October 2020 and mid-November through December 2020 with a period of low occurrence from mid-October to mid-November. At sites AC, CE, DT, and Y1C, occurrence remained relatively high from January through early June 2021. Airgun pulse detections also occurred more frequently during July 2021 at sites AC, CE, and Y1C, and during August 2021 at sites GC, LC, and Y1B. During the 2020-2021 period, airgun pulses were detected least frequently at sites MC, DC, and SL (daily means of 57 to 171 detections and 0.1 and 1.3 hours present, respectively), with notable increases at DC during August to September 2020 and August 2021 (Table 7, Figure 118). Sites GA, MR, and Y1D also generally had airgun pulses present less commonly than other sites. Similar to the findings from the historic analyses, there were no apparent diel patterns for airgun pulses from 2020-2021, as surveys were conducted throughout the day and night (Figures 120 & 121).

A spatial comparison of monthly occurrence patterns and monthly mean received levels of detected airgun pulses with locations of presumed seismic survey vessels from AIS tracks (from MarineCadastre) each month begins to give insight into the large-scale propagation of seismic survey airgun pulses throughout the Gulf of Mexico (Figures 122, 123, & 124).

- During August, September, and October, seismic survey activity was primarily occurring over and around site GC (Figure 122), and airgun pulse detections and presence during this period followed similar patterns across nearly all sites, with the exception of limited detection at sites SL, MC, and DC to the northeast of the surveys (Figure 118). Monthly median received levels of airgun pulses reached the highest levels of any site for the year (148-158 dB pp re $1\mu Pa^2$) at GC during these months (Figure 123). Additional seismic survey activity occurred around the De Soto Canyon during these three months (Figure 123) with highest monthly median received levels occurring at MC (146 dB pp re $1\mu Pa^2$) in August (Figure 122).

- During November, December, and early January, seismic survey activity was primarily occurring just south of the US/Mexico EEZ in the western Gulf, between sites AC and MR (Figure 123), and airgun pulse detections and presence with similar patterns occurred at primarily southern sites across the Gulf during this period, with limited detections at sites GA, GC, SL, MC, and DC in the north (Figure 118). Surprisingly, during this period, the number and occurrence of detections was highest at site DT, in the eastern Gulf, compared to other sites during this period, followed by Y1B and CE (Figure 122). It is unknown whether an additional survey was occurring in the southeastern Gulf during this time that has not been identified, or whether sound propagation conditions through the deep ocean led to higher detectability in these waters than waters closer to the survey.
- During January through April, the primary seismic survey activity was occurring in the western Gulf, just southwest of site AC (Figure 124). During Jan – Apr, pulse detections following similar patterns occurred at sites AC, Y1C, CE, Y1B, LC, Y1D, and DT, while not being detected at the five northernmost sites or, surprisingly, at nearby MR (Figure 118). Monthly median received levels during these months were highest at sites AC and CE (139-142 dB pp re $1\mu Pa^2$) followed by sites Y1C and Y1B (135-138 dB pp re $1\mu Pa^2$). Overlapping this period, another seismic survey south of site GA occurred during March to April (Figure 124). This may have primarily been detected at sites GA and GC (Figure 118), where monthly median received levels reached 134-138 dB pp re $1\mu Pa^2$. Further, during April to May there was additional seismic survey activity slightly northwest of the previously described survey, at similar distances from sites AC and GA, and some additional activity may have been occurring around MC during April in multiple small patches. Airgun pulse detections remained high from March through May at sites AC, Y1C, CE, and DT and could have included detections from any of these surveys during that time (Figure 118 & 122). An increase in detections at sites MR and LC during April to May may correspond to the survey between AC and GA (Figure 118 & 122).
- During June to July, the primary seismic survey activity occurred in the western Gulf just southwest of site AC again, with possible additional activity in small patches on the shelf north of MC during these months (Figure 124). Detections during this period occurred in greatest numbers at sites AC, CE, and Y1C, with detections also common at DT, GA, and MR (Figure 118 & 122). High monthly median received levels occurred at site AC during June and July (144-145 dB pp re $1\mu Pa^2$). There are no recordings at MC during this time.

	Airguns		Shipping	
Site	**Detections**	**Presence (h)**	**Detections**	**Presence (h)**
AC	2401	8.8	5	5.2
CE	2121	8.2	1	1.2
DC	157	0.6	2	4.0
DT	1732	6.8	2	2.0
GA	774	3.2	16	7.3
GC	1137	4.0	3	3.4
LC	1035	4.6	1	1.0
MC	27	0.1	1	1.0
MR	872	3.7	3	3.7
SL	171	1.3	11	5.2
Y1B	1579	7.4	3	3.3
Y1C	2201	8.8	1	0.8
Y1B	566	3.6	1	2.2

Table 7: Mean daily detections and mean daily presence of airgun pulses and shipping noise over the 2020-2021 period by site.

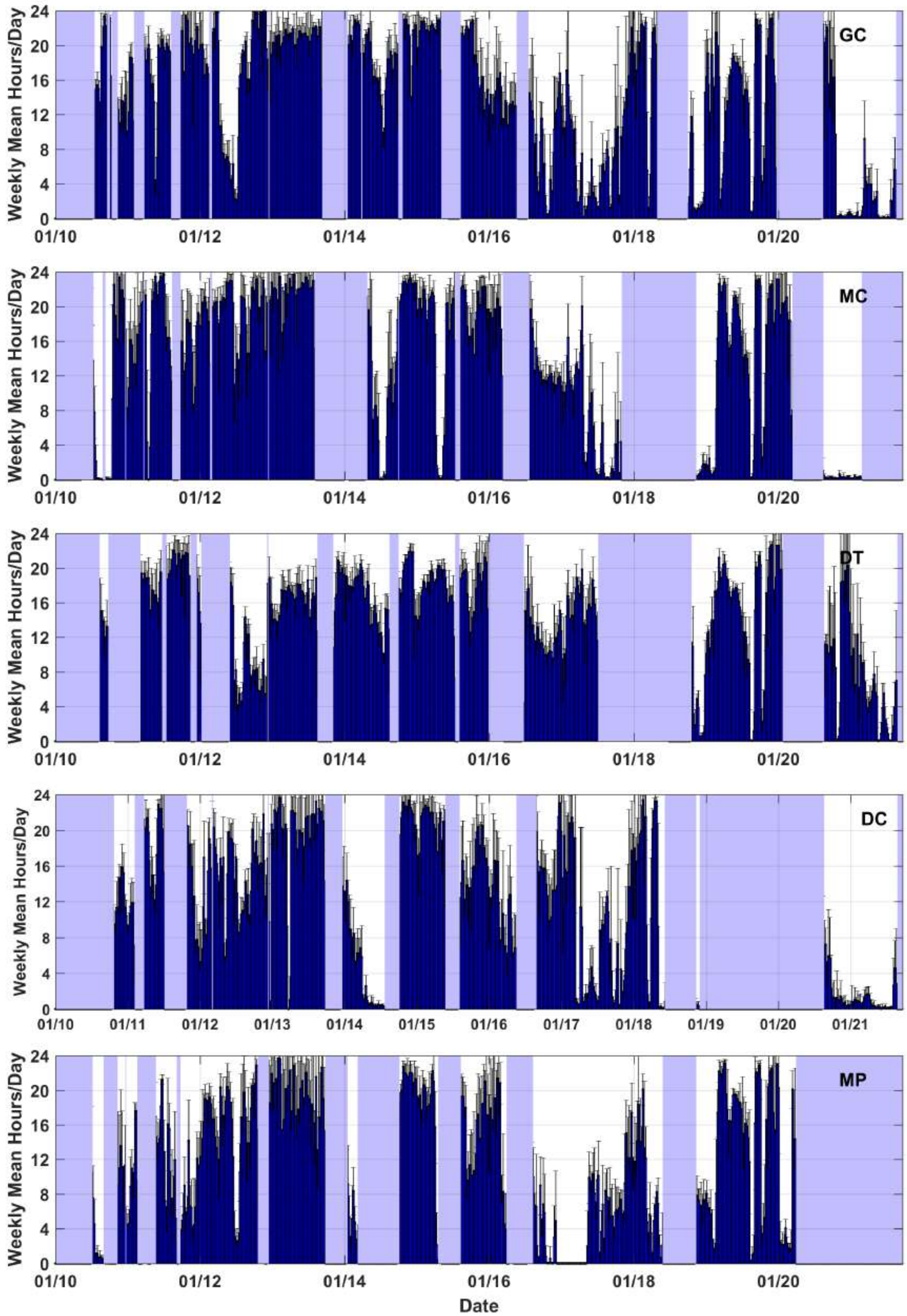

Figure 117: Weekly mean daily presence (blue bars) of airguns between 2010-2021 at historical sites GC, MC, DT, DC, and MP. Shaded blue sections represent periods with no recording effort.

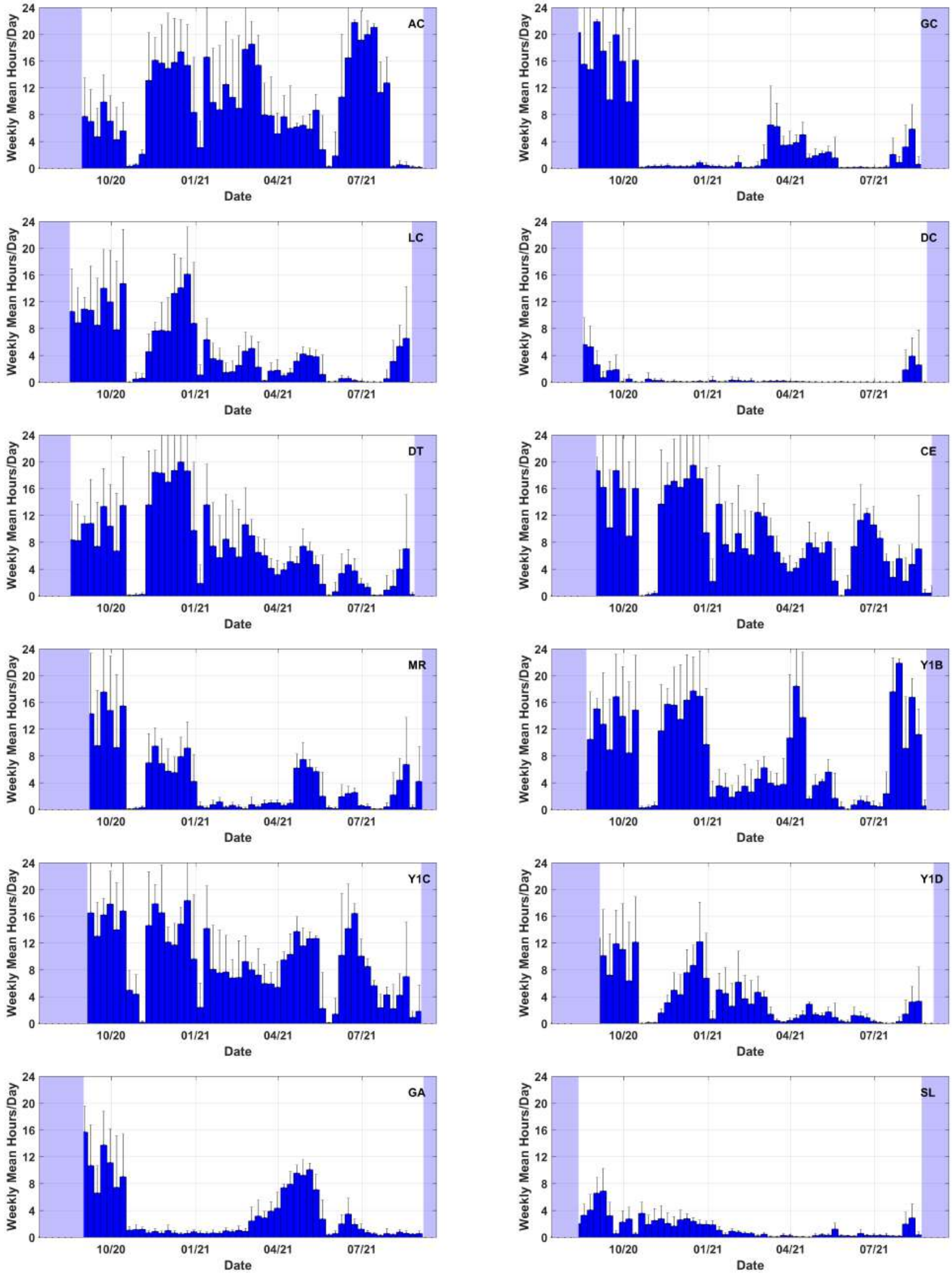

Figure 118: Weekly mean daily presence (blue bars) of airguns between 2020-2021 by site. Shaded blue sections represent periods with no recording effort.

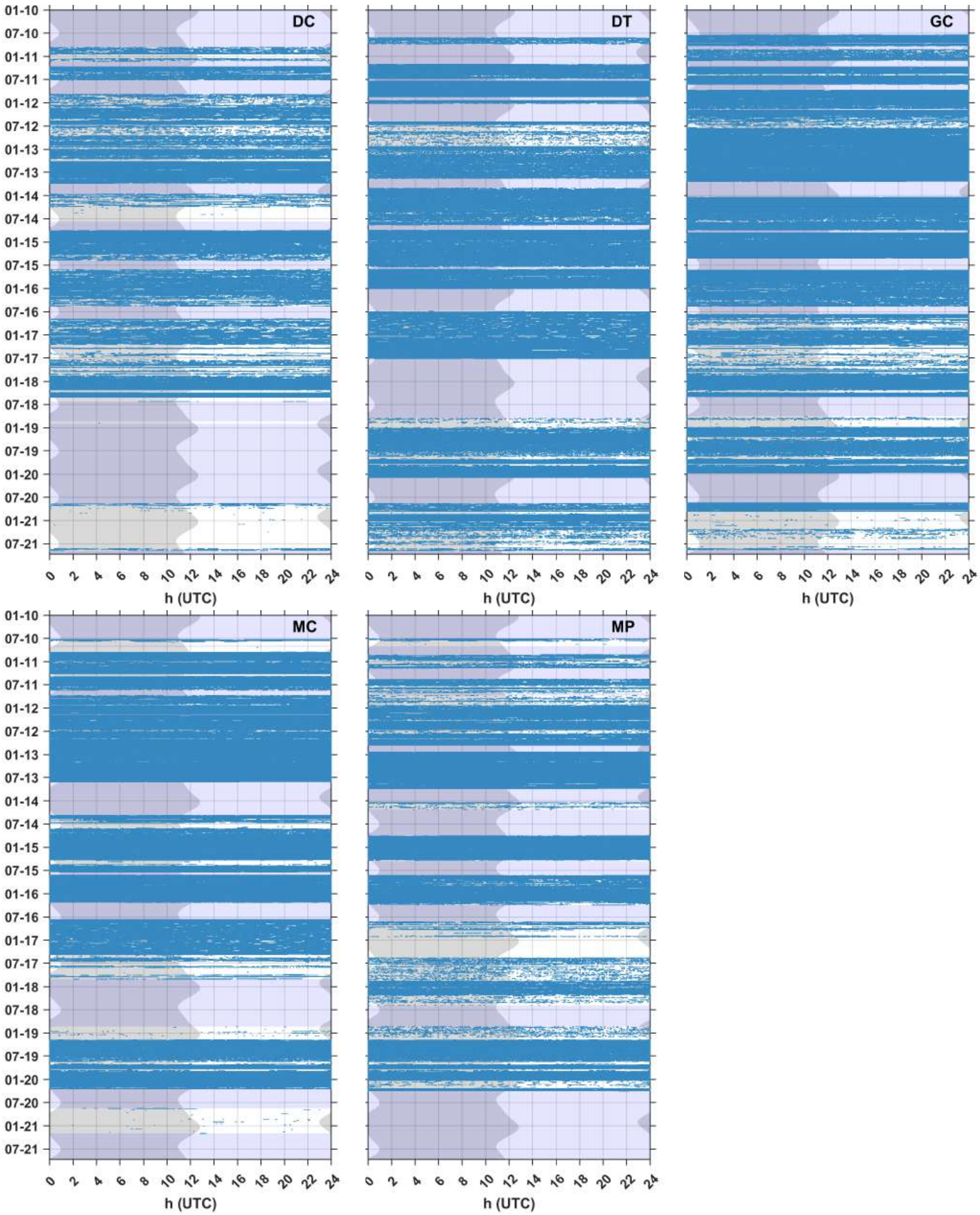

Figure 119: Airgun detections in five-minute bins (blue bars) at historical sites DC, DT, GC, MC, and MP. Shaded blue sections represent periods with no recording effort.

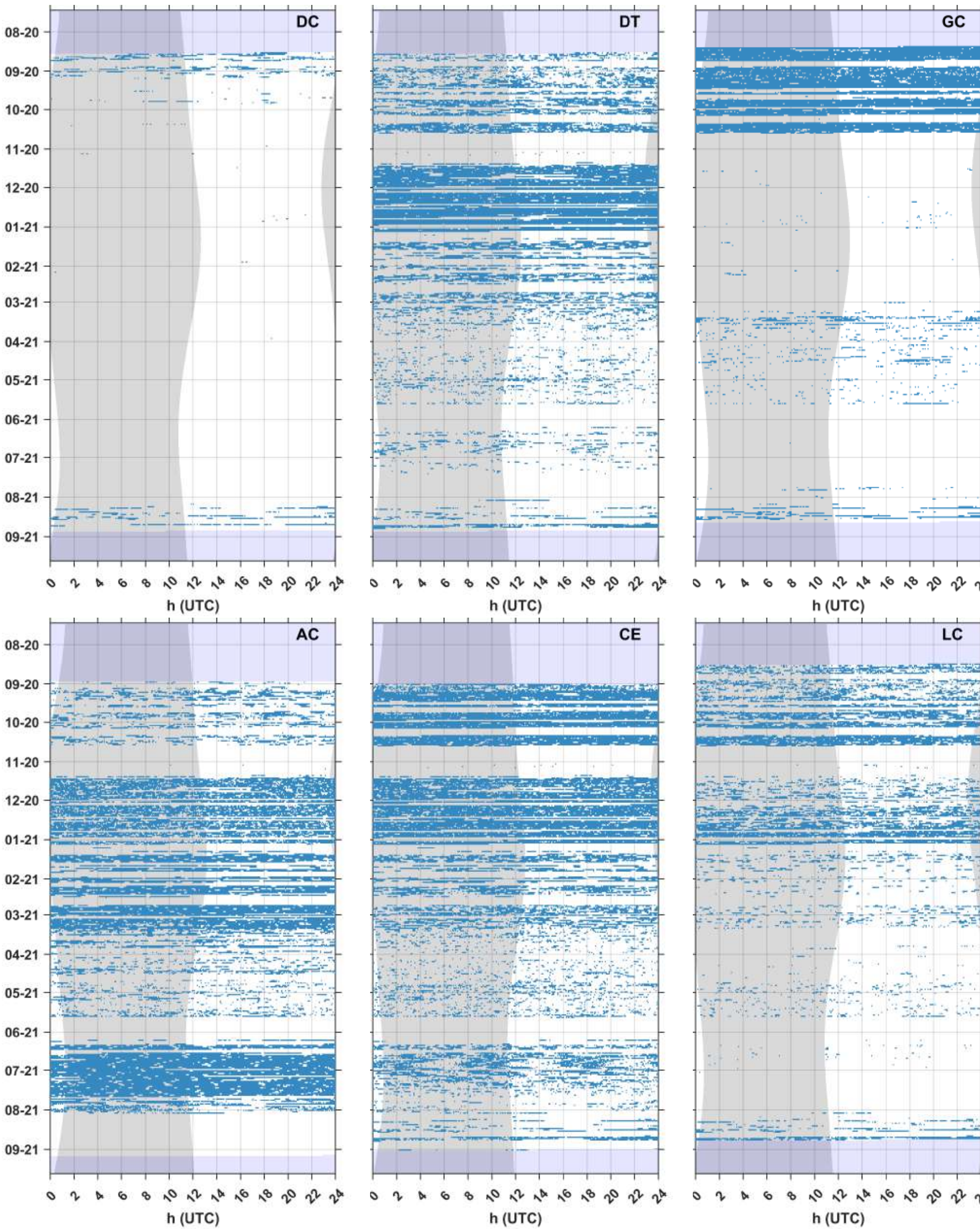

Figure 120: Airgun detections in five-minute bins (blue bars) at one-year sites DC, DT, GC, AC, CE, and LC. Shaded blue sections represent periods with no recording effort.

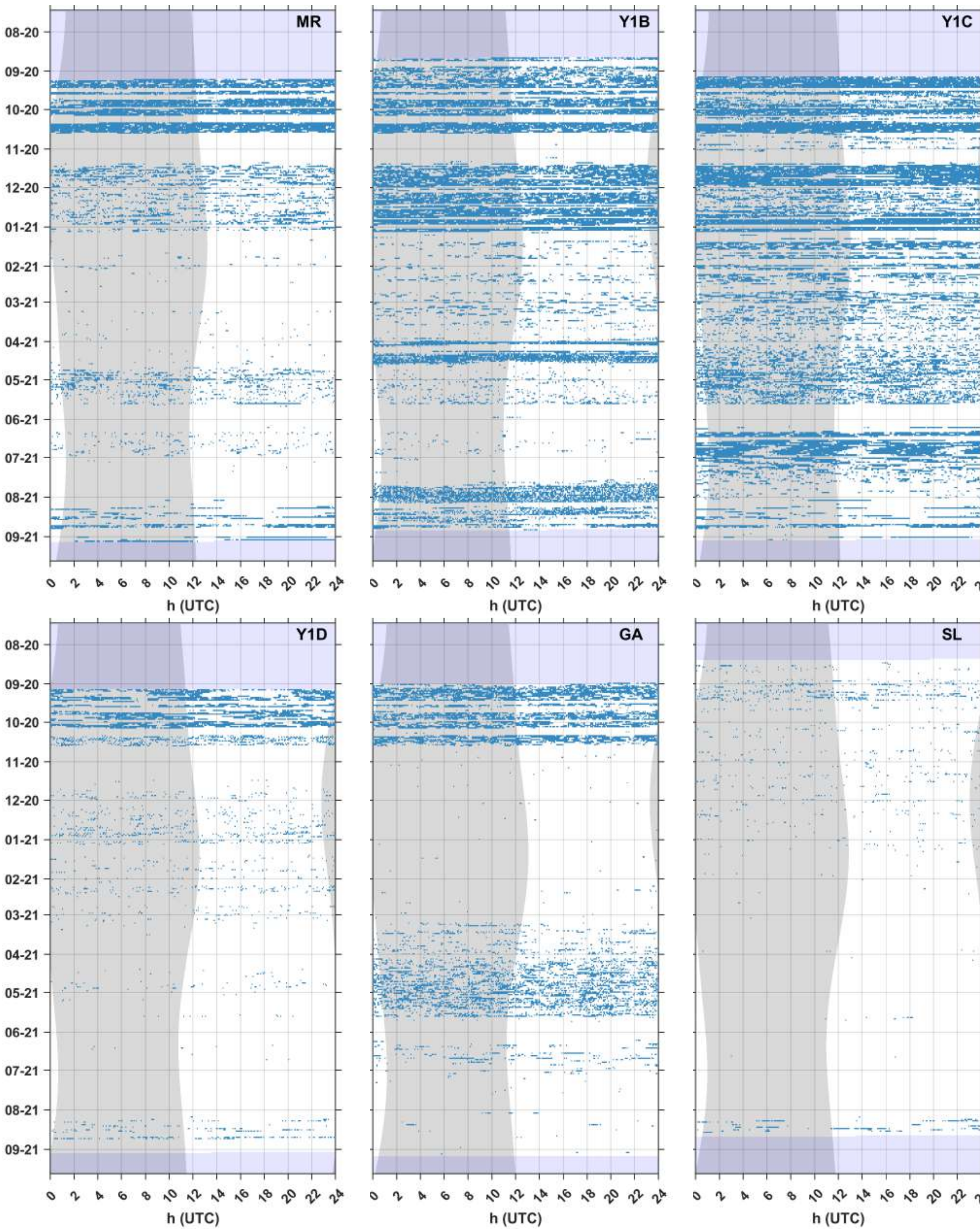

Figure 121: Airgun detections in five-minute bins (blue bars) at one-year sites MR, Y1B, Y1C, Y1D, GA, and SL. Shaded blue sections represent periods with no recording effort.

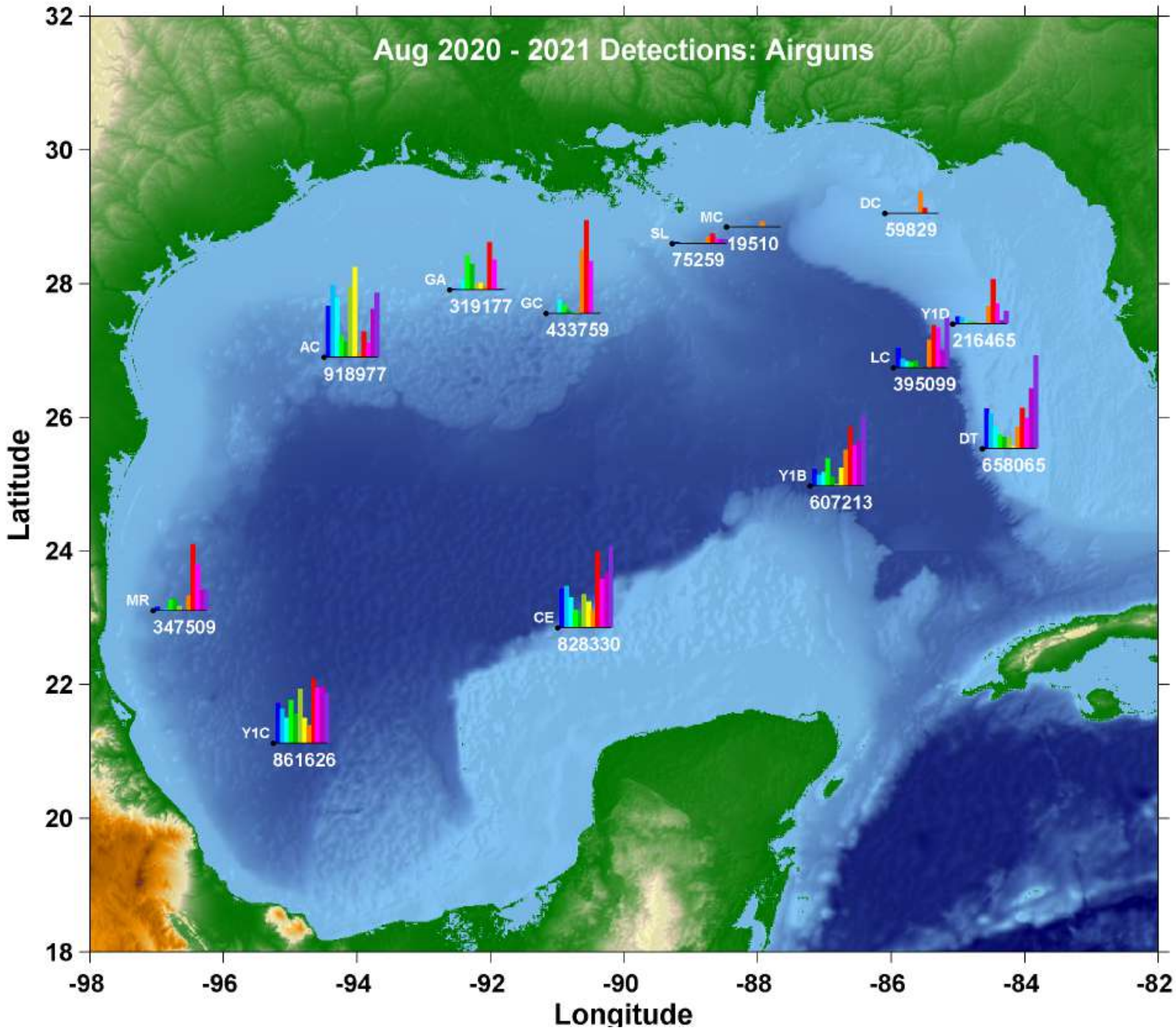

Figure 122: Airgun detections per month per HARP site from 2020-2021. Values under bars represent airgun detections per year. Note: The MC site results are from the 4-channel HARP and only have 6 months of recordings with no data from March to July. Site GA had data missing in July, and site SL had data missing in March and April.

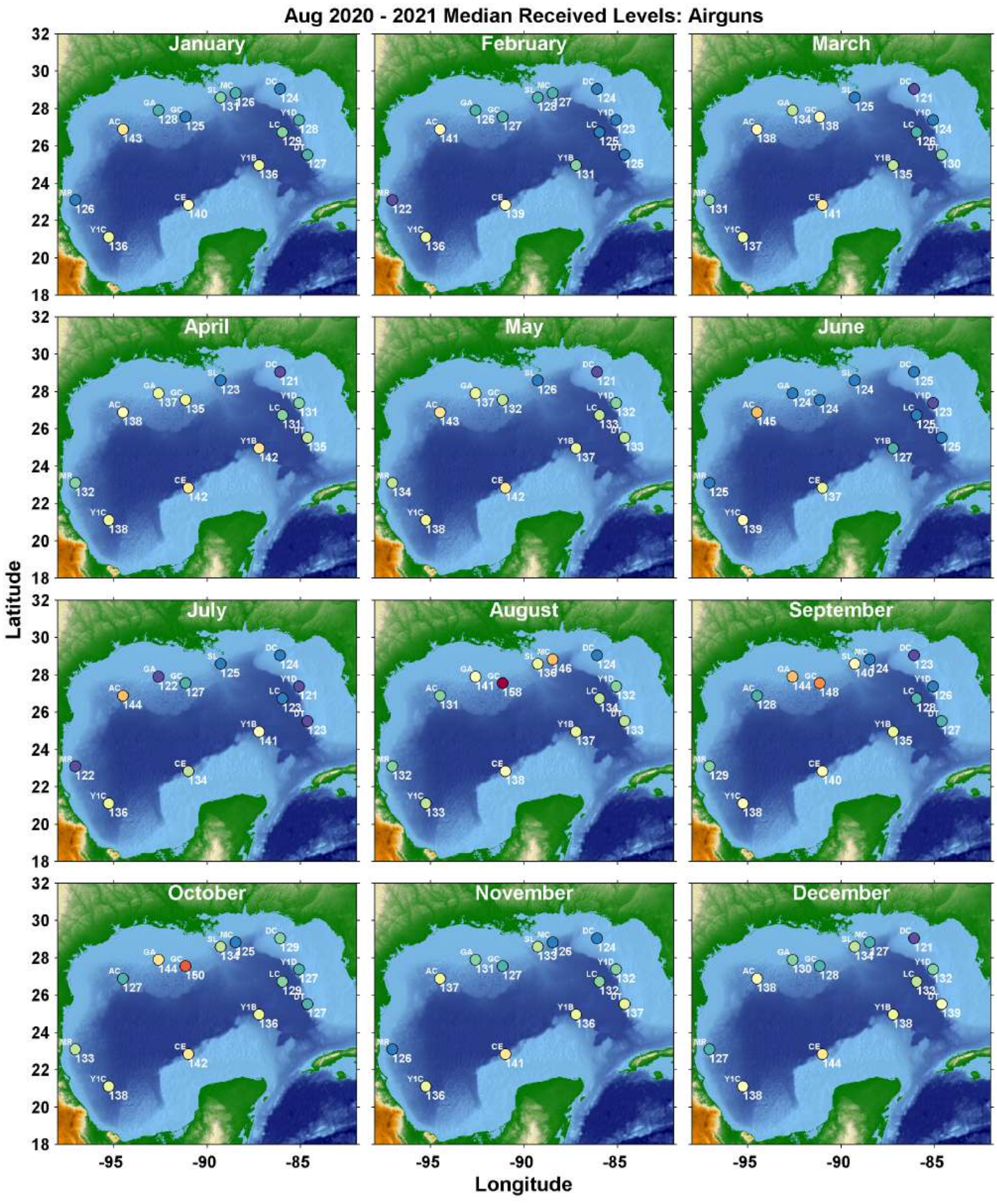

Figure 123: Median RLs for all airgun detections with ppRLs of at least 120 dB detected from 2020-2021.

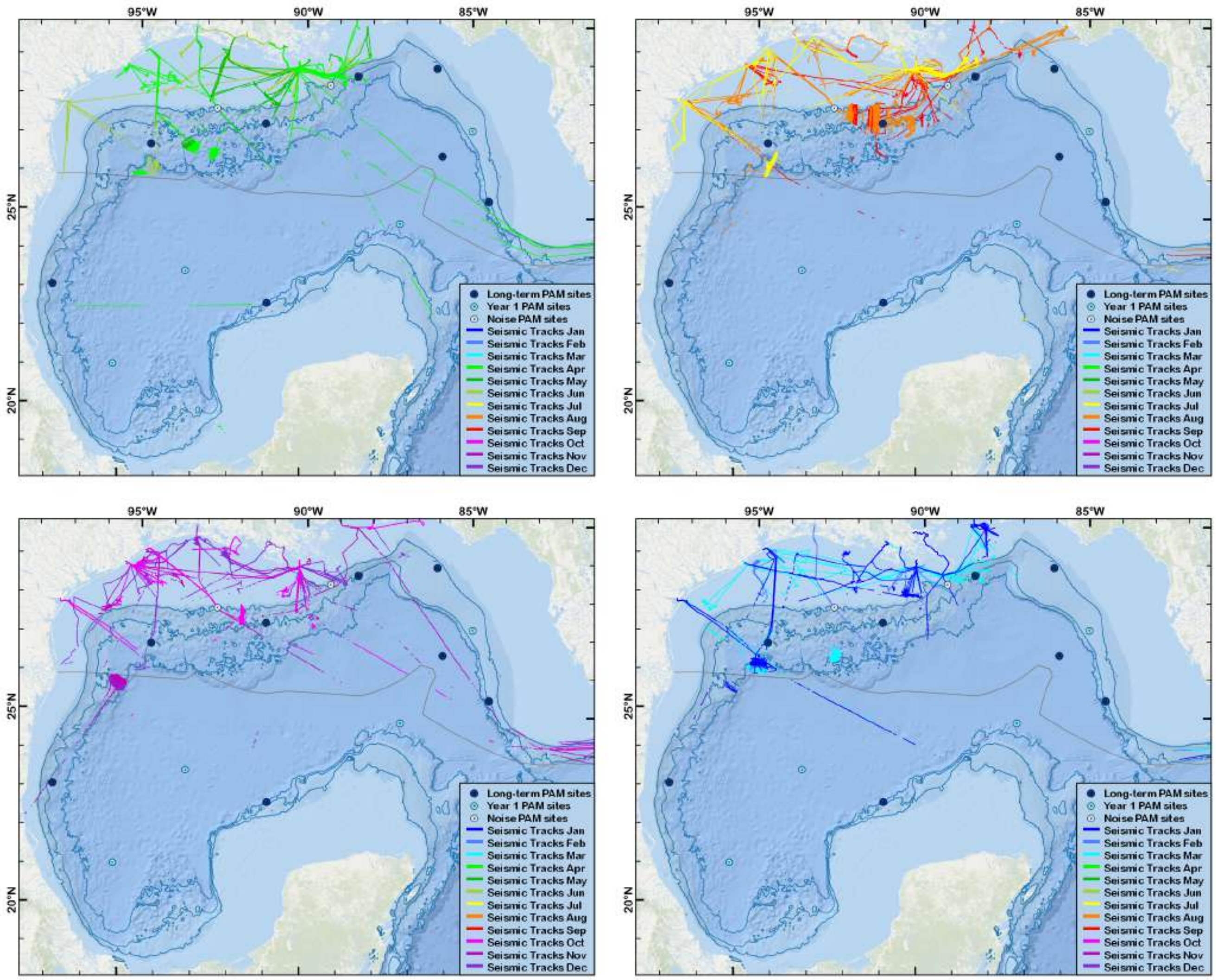

Figure 124: Vessel tracks (from MarineCadastre AIS data) for ships that conduct seismic airgun surveys) for the August 2020-2021 period, by season: Spring (Top Left), Summer (Top Right), Autumn (Bottom Left), and Winter (Bottom Right). Areas with dense track lines are presumed to be indicative of airgun survey activity.

5 Future Steps

Data results included in this report include the preliminary marine mammal occurrence and density estimates, and ambient and anthropogenic noise analyses from the 2010-2020 historic HARP data and the 2020-2021 LISTEN GoMex data. Data collection and analyses for this 2020-2024 passive acoustic monitoring program are ongoing, and future annual reports and manuscripts for peer-review will include preliminary marine mammal occurrence and density estimates for each year of data collected, along with more in-depth analyses of long-term density trends, spatio-temporal occurrence patterns, and predictive spatially-explicit models of marine mammal density related to environmental drivers.

Future work will include analyses of baleen whale call presence and finer taxonomic resolution of odontocete echolocation clicks. Future analyses of shipping activity and associated noise will include estimation of false positive rates from the automated detector, estimation of received levels of ships at each site (following removal of periods with airgun detections), and estimation of ship detection distances.

6 Acknowledgments

Ashley Cook, Bruce Thayre, Eva Hildalgo-Pla, Gania Figueroa, Itzel Carballo, John Hurwitz, Kieran Lenssen, Kristen Rosier, Natalie Posdaljian, Ryan Pierson, Sean Wiggins, and Vanessa ZoBell assisted with building, deploying and recovering of HARPs. Erin O'Neill, Diego Majewski, and Shelby Bloom processed the acoustic data. Vanessa ZoBell, Alba Solsana Berga, Jenny Trickey and Kieran Lenssen assisted with data analysis. Captain Tad Berkey and the crew of the R/V Pelican made the field work possible. Len Thomas assisted with the LISTEN GoMex survey design. Laura Engleby, Jason Gedamke, and Leila Hatch advised on shipping lane locations for the noise-focused HARP sites.

7 Funding Sources

Funding for the LISTEN GoMex program is provided by NOAA's RESTORE Science Program, the *Deepwater Horizon* Restoration Open Ocean Marine Mammal Trustee Implementation Group, and the Office of Naval Research Task Force Ocean. Funding for historic HARP data leveraged by the LISTEN GoMex program were provided by the *Deepwater Horizon* Natural Resource Damage Assessment program, the Gulf of Mexico Research Initiative through C-IMAGE at USF (Steve Murawski and Sheryl Gilbert), and NOAA NMFS' Office of Science and Technology (Mridula Srinivasan), NOAA's Southeast Regional Office (Laura Engleby).

Acoustic data collection at three long-term sites (MR, CE, LC), four short-term sites (Y1A, Y1B, Y1C, Y1D) and two tracking sites (MC-4CH-1, MC-4CH-2) over the 2020-2021 period, marine mammal occurrence analyses in these recordings, and all marine mammal density analyses from historic and 2020-2021 recordings were funded as part of the "Assessing long-term trends and processes driving variability in cetacean density throughout the Gulf of Mexico using passive acoustic monitoring and habitat modeling" project under federal funding opportunity Grant No. NOAA-NOS-NCCOS-2019-2005608 from the National Oceanic and Atmospheric Administration's RESTORE Science Program through the Gulf Coast Restoration Trust Fund to the NOAA Southeast Fisheries Science Center.

Acoustic data collection at five long-term sites (AC, GC, MC, DC, DT) and two noise-focused sites (GA, SL) over the 2020-2021 period, marine mammal occurrence analyses in these recordings, and all ambient and anthropogenic noise analyses from historic and 2020-2021 recordings were funded by the *Deepwater Horizon* Open Ocean Trustee Implementation Group's *"Reduce Impacts of Anthropogenic Noise on Cetaceans"* project to restore natural resources injured by the 2010 Deepwater Horizon oil spill in the Gulf of Mexico.

Ship-time aboard the R/V Pelican for HARP deployment and servicing cruises in August 2020 and August 2021, HARP equipment upgrades, and airgun detection algorithm development were funded under the Office of Naval Research Task Force Ocean (Robert Headrick).

References

Au, Whitlow WL (1993). *The sonar of dolphins*. Springer Science & Business Media.

Audoly, Christian and Valentin Meyer (2017). "Measurement of radiated noise from surface ships–Influence of the sea surface reflection coefficient on the Lloyd's mirror effect". In: *Proceedings of ACOUSTICS*. Vol. 19. 22.

Baumann-Pickering, Simone et al. (2013). "Species-specific beaked whale echolocation signals". In: *The Journal of the Acoustical Society of America* 134.3, pp. 2293–2301.

Baumann-Pickering, Simone et al. (2014). "Spatio-temporal patterns of beaked whale echolocation signals in the North Pacific". In: *PloS one* 9.1, e86072.

Blackman, Donna K et al. (2004). "Testing low/very low frequency acoustic sources for basin-wide propagation in the Indian Ocean". In: *The journal of the acoustical society of America* 116.4, pp. 2057–2066.

Cohen, Rebecca E et al. (2022). "Identification of western North Atlantic odontocete echolocation click types using machine learning and spatiotemporal correlates". In: *PloS one* 17.3, e0264988.

Cox, Henry (2004). "Navy Applications of High-Frequency Acoustics". In: *AIP Conference Proceedings*. Vol. 728. 1. American Institute of Physics, pp. 449–455.

Everest, F Alton, Robert W Young, and Martin W Johnson (1948). "Acoustical characteristics of noise produced by snapping shrimp". In: *The Journal of the Acoustical Society of America* 20.2, pp. 137–142.

Frasier, Kaitlin E et al. (2016). "Delphinid echolocation click detection probability on near-seafloor sensors". In: *The Journal of the Acoustical Society of America* 140.3, pp. 1918–1930.

Frasier, Kaitlin E et al. (2017). "Automated classification of dolphin echolocation click types from the Gulf of Mexico". In: *PLoS computational biology* 13.12, e1005823.

Frasier, Kaitlin Emily (2015). *Density estimation of delphinids using passive acoustics: A case study in the Gulf of Mexico*. University of California, San Diego.

Gassmann, Martin, Sean M Wiggins, and John A Hildebrand (2017). "Deep-water measurements of container ship radiated noise signatures and directionality". In: *The journal of the acoustical society of America* 142.3, pp. 1563–1574.

Gillespie, Douglas et al. (2009). “Field recordings of Gervais’ beaked whales Mesoplodon europaeus from the Bahamas”. In: *The Journal of the Acoustical Society of America* 125.5, pp. 3428–3433.
Goold, John C and Sarah E Jones (1995). “Time and frequency domain characteristics of sperm whale clicks”. In: *The Journal of the Acoustical Society of America* 98.3, pp. 1279–1291.
Hildebrand, John A (2009). “Anthropogenic and natural sources of ambient noise in the ocean”. In: *Marine Ecology Progress Series* 395, pp. 5–20.
Hildebrand, John A et al. (2015). “Passive acoustic monitoring of beaked whale densities in the Gulf of Mexico”. In: *Scientific reports* 5.1, pp. 1–15.
Hildebrand, John A et al. (2019). “Assessing seasonality and density from passive acoustic monitoring of signals presumed to be from pygmy and dwarf sperm whales in the Gulf of Mexico”. In: *Frontiers in Marine Science* 6, p. 66.
Johnson, Mark et al. (2004). “Beaked whales echolocate on prey”. In: *Proceedings of the Royal Society of London. Series B: Biological Sciences* 271.suppl_6, S383–S386.
Leu, Amanda A et al. (2022). “Echolocation click discrimination for three killer whale ecotypes in the Northeastern Pacific”. In: *The Journal of the Acoustical Society of America* 151.5, pp. 3197–3206.
Madsen, PT et al. (2002). “Sperm whale sound production studied with ultrasound time/depth-recording tags”. In: *Journal of Experimental Biology* 205.13, pp. 1899–1906.
Marques, Tiago A et al. (2009). “Estimating cetacean population density using fixed passive acoustic sensors: An example with Blainville’s beaked whales”. In: *The Journal of the Acoustical Society of America* 125.4, pp. 1982–1994.
McKenna, Megan F et al. (2012). “Underwater radiated noise from modern commercial ships”. In: *The Journal of the Acoustical Society of America* 131.1, pp. 92–103.
Møhl, Bertel et al. (2003). “The monopulsed nature of sperm whale clicks”. In: *The Journal of the Acoustical Society of America* 114.2, pp. 1143–1154.
Roch, Marie A et al. (2011). “Classification of echolocation clicks from odontocetes in the Southern California Bight”. In: *The Journal of the Acoustical Society of America* 129.1, pp. 467–475.
Soldevilla, Melissa S et al. (2017). “Geographic variation in Risso’s dolphin echolocation click spectra”. In: *The Journal of the Acoustical Society of America* 142.2, pp. 599–617.
Solsona Berga, Alba (2019). “Advancement of methods for passive acoustic monitoring: a framework for the study of deep-diving cetacean”. In: *Universitat Politècnica de Catalunya*.
Solsona-Berga, Alba et al. (2020). “DetEdit: A graphical user interface for annotating and editing events detected in long-term acoustic monitoring data”. In: *PLoS computational biology* 16.1, e1007598.
Solsona-Berga, Alba et al. (2022). “Echolocation repetition rate as a proxy to monitor population structure and dynamics of sperm whales”. In: *Remote Sensing in Ecology and Conservation*.
Watwood, Stephanie L et al. (2006). “Deep-diving foraging behaviour of sperm whales (Physeter macrocephalus)”. In: *Journal of Animal Ecology* 75.3, pp. 814–825.

Welch, Peter (1967). “The use of fast Fourier transform for the estimation of power spectra: a method based on time averaging over short, modified periodograms”. In: *IEEE Transactions on audio and electroacoustics* 15.2, pp. 70–73.

Wiggins, Sean M and John A Hildebrand (2007). “High-frequency Acoustic Recording Package (HARP) for broad-band, long-term marine mammal monitoring”. In: *2007 Symposium on Underwater Technology and Workshop on Scientific Use of Submarine Cables and Related Technologies*. IEEE, pp. 551–557.

Wiggins, Sean M et al. (2016). “Gulf of Mexico low-frequency ocean soundscape impacted by airguns”. In: *The Journal of the Acoustical Society of America* 140.1, pp. 176–183.

Zimmer, Walter MX et al. (2005). “Echolocation clicks of free-ranging Cuvier’s beaked whales (Ziphius cavirostris)”. In: *The Journal of the Acoustical Society of America* 117.6, pp. 3919–3927.